8-2019

Design and Synthesis of Stable Aminyl and Nitroxide Radical Precursors

Joshua Bryan Lovell
University of Nebraska - Lincoln, jblovell@huskers.unl.edu

DESIGN AND SYNTHESIS OF STABLE AMINYL AND NITROXIDE RADICAL PRECURSORS

by

Joshua Bryan Lovell

A THESIS

Presented to the Faculty of

The Graduate College at the University of Nebraska

In Partial Fulfillment of Requirements

For the Degree of Master of Science

Major: Chemistry

Under the Supervision of Professor Andrzej Rajca

Lincoln, Nebraska

August, 2019

DESIGN AND SYNTHESIS OF STABLE AMINYL AND NITROXIDE RADICAL PRECURSORS

Joshua Bryan Lovell, M.S.

University of Nebraska, 2019

Advisor: Andrzej Rajca

Aminyl diradicals with sterically-hindered *tert*-butyl groups have yet to be fully investigated for their increased stability due to their difficulty in synthesis. The first chapter of this thesis details design and synthesis towards sterically-hindered aminyl radical and diradical precursors.

Structural features effecting nitroxide radical stability have been well investigated except for the impact on the ring-size of stability of nitroxides towards reduction by ascorbate. Two 7-membered nitroxides derived from TEMPONE and TEMPOL have been synthesized and characterized. The alcohol nitroxide shows increased stability towards reduction by ascorbate compared to the corresponding TEMPOL, while the other nitroxide shows decreased stability compared to TEMPONE. Efforts towards nitroxide radicals with larger sized rings are also detailed.

Dedication

To my wonderful wife SaraAnne and our children, Annabelle and Henry, who bring so much joy and curiosity to our world.

Acknowledgement

Throughout my time at UNL I have had the pleasure of encountering many people who have supported my journey and development as a person and scientist. I have gained many great things in my life now because of my time here.

First and foremost, I'd like to thank Prof. Rajca for inspiring and fostering a passion for a deeper understanding of organic chemistry and the importance of sharing this passion and knowledge with others. I also express gratitude to both Suchada and Prof. Rajca for their continued guidance, support, advice and friendship.

I'd like to thank my additional committee members of Prof. Dussault and Prof. Griep, both of which have always been available to advise and whom I've had the privilege of taking courses that I enjoyed and positively impacted my growth as a scientist.

I also have great appreciation for the many teachers I've had the honor of learning from and the privilege to teach other students alongside with them, it's the passion of professors as teachers that motivates students to pursue discovery. Specifically, I had the pleasure of teaching closely with Profs. Hartung, Kautz, Kingsbury, Takacs, Dussault, McCune, and Rajca, all of whom show unique styles of teaching but an underlying determination to reach and inspire students to fulfill their curiosity and reach their full potential. Thank you also to the wonderful support staff (Dr. Martha Morton, Kurt Wulser, Sara Gaylor-Basiaga, Peg Bergmeyer, Darrel Kinnan, and Robert Wilson) who

supported my learning as a student and continued to support me as I attempted to connect and teach my own students.

Specifically, I would like to thank Drs. Prezemek Boratyński, Ying Wang, Hui Zhang, Arnon Olankitwanit, Nolan Gallagher, and Joseph Paletta for their support, assistance and friendship.

I would like to recognize Scott Pettibone, Ben Wymore and Kiel Neumann, whose friendship I gained at UNL and for the many lunches, intramural sports, and other time spent outside of Hamilton Hall to maintain levity.

I want to thank my family for all their support, balance and humor throughout this journey. To Annabelle and Henry, thank you for helping me know that the troubles and stress of life evaporate when holding you or seeing your bright smiles and laughs! Lastly, I want to thank my incredible wife for her love, support, drive to balance work and family, and the gift of our two wonderful kids.

Table of Contents

CHAPTER 1 – AMINYL DIRADICALS

1.1 Introduction

Organic radicals and polyradicals consist of molecules containing unpaired electrons, providing a class of compounds that exhibit unique characteristics and uses spanning many disciplines. Many of these compounds exhibit high reactivity and are generally short-lived. Investigations of fundamental principles of novel organic radicals continue, while practical applications towards organic magnetism, sensors, switches, spin labels, catalysis, and biomedicine including contrast agents for magnetic resonance imaging continues to be developed. There are many classes of different organic radicals including triphenylmethyl (trityl) radicals, triplet carbenes, nitrenes and the relatively stable and well-studied nitroxide radicals. This chapter will focus on efforts toward the design and synthesis of stabilized triplet ground-state aminyl diradicals.

1.1.1 Background on Diradicals

Interest in organic radicals grew following Gomberg's[1] groundbreaking discovery in 1900 of the triphenylmethyl radical (**1**), the first stable carbon-based radical. The stability for this first of its kind compound is derived from the propeller-twisting of the phenyl rings imposing large steric hindrance near the α-carbon yet allowing moderate enough twist-angle for significant delocalization of spin density into the phenyl rings. Experimentally, a benzene solution of triphenylmethyl radical at room temperature under inert atmosphere exists in equilibrium favoring its quinoid[2] dimer (**2**) 99% vs. 1% of the radical species as shown in Figure A-1.

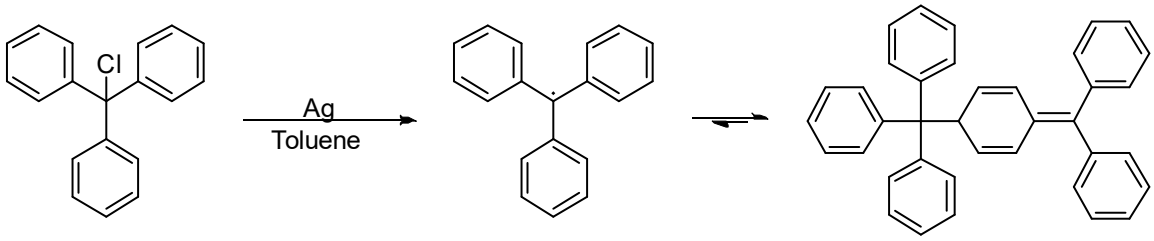

1 **2**

Figure A-1. Synthesis of triphenylmethyl radical (1) and equilibrium with its dimer (2) at room temperature in benzene.

The term diradical or biradical refer to molecules that contain two unpaired electrons. Specifically, according to the *IUPAC Compendium of Chemical Terminology*, diradicals are molecular species with two unpaired electrons that have a significant dipole-dipole interaction to produce a singlet and triplet spin state.[3] Diradicals can be categorized as either localized or delocalized; where delocalized diradicals can be further differentiated as Kekulé or non- Kekulé molecules. Several well-written reviews exist on diradicals[4-5] and polyradicals[6-8].

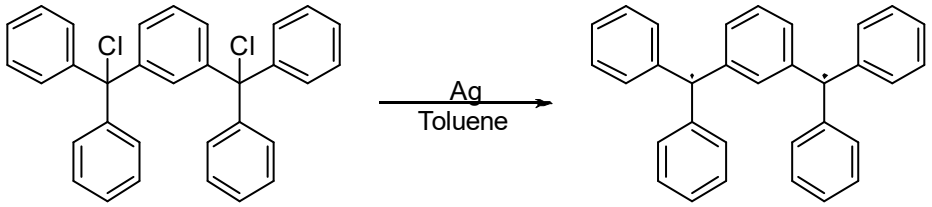

4 **3**

Figure A-2. Synthesis of Schlenk's diradical (3).

The first diradical was reported in 1915.[9] Schlenk's diradical (**3**) was prepared similarly to Gomberg's radical via metal reduction of the dichloride (**4**) as seen in Figure A-2. Several other diradicals based upon the Schlenk diradical have been synthesized and studied.[10]

In the past, our research group prepared several derivatives of Schlenk's diradical.[11] The stability of Schlenk's diradical was improved upon by introduction of alkyl groups at the *para*-position relative to the triarylmethyl radical site. These alkyl-substituted radicals were quite stable at room temperature and isolable as solids. A few of the structures (**5a-c**) synthesized including a planarized diradical (**6**) are shown in Figure A-3.

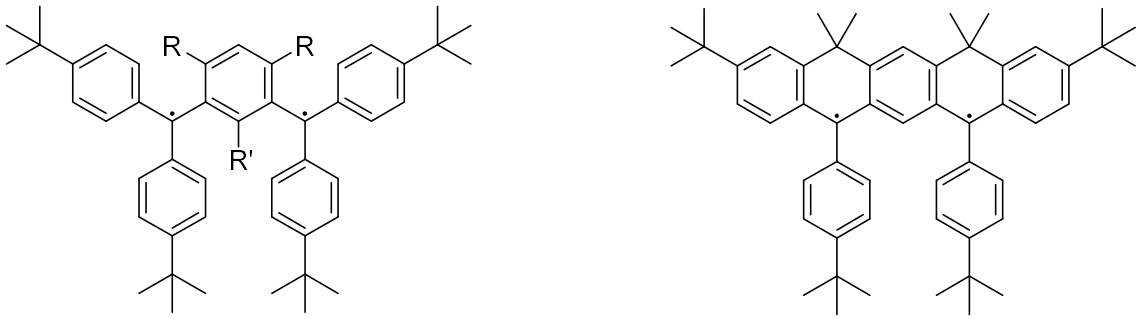

R = R' = H; *S* = 1
R = R' = Me; *S* = 0
R = Me, *i*-Pr, R' = H; *S* = 1

5a-c

S = 1

6

Figure A-3. Alkyl-substituted Schlenk Diradical derivatives (5-6).

The quantum-mechanical basis for organic radicals and their properties is that each electron has a spin (an intrinsic angular momentum), which is assigned a spin quantum number of S = ½, correlating with the magnitude of the spin angular momentum. Since an electron is a spinning charge, it creates a small magnetic field where the magnetic moment ($\boldsymbol{\mu_e}$) is proportional to the spin angular momentum (**S**) as seen in Equation 1.

$$\mu_e = g_e \mu_B S \qquad \textbf{(Equation 1)}$$

g_e is the g factor, which is 2.0023 for a free electron; μ_B is the Bohr magneton = $(-e)h/4\pi m_e$ = -9.274 x 10^{-24} J•T^{-1}, where m_e is the mass of an electron and e is the charge of an electron; and h is Planck's constant = 6.626 x 10^{-34} J•s.

There are two states for the spin of an electron, α or β. In the presence of an external magnetic field (**B**), the electron spin's magnetic moment will either align itself in the same (parallel, α spin) or opposite (antiparallel, β spin) direction relative to **B**. Each magnetic spin quantum number (m_s) equals ½ (for α spin) or –½ (for β spin). The interaction between the external field and the magnetic moment of the electron spin results in *Zeeman interaction*; the splitting of the spin energy level into two different levels (Zeeman's effect) as shown in Figure A-4.

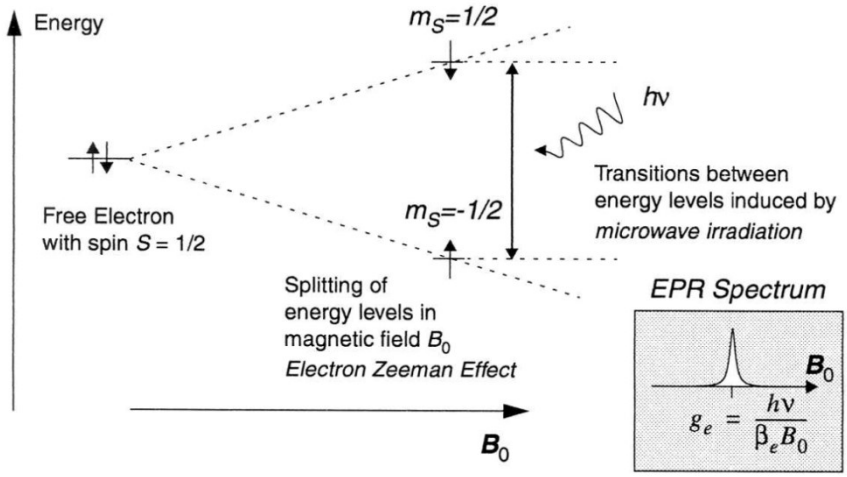

Figure A-4. Illustration of Zeeman Effect for *S* = 1/2 radical.[12]

The energy of the interaction between the electron spin and the external field is shown by $E = m_s g_e \mu_e B$ where g_e is the g factor, which is 2.0023 for a free electron; μ_B is the Bohr magneton = -9.274 x 10^{-24} J•T^{-1}; and B is the strength of the applied magnetic

field. This results in a Zeeman energy difference between the two energy levels (E_α and E_β) given by $\Delta E = E_\alpha - E_\beta = g_e \mu_e B$. A phenomenon known as electron spin resonance (ESR) occurs when a frequency (ν) matches the energy separation between the two energy levels, resulting in an absorption causing a transition between the two energy levels. This absorption can be experimentally monitored and converted to a spectrum by electron paramagnetic resonance (EPR) spectroscopy, also sometimes referred to as ESR spectroscopy.

According to the multiplicity rule $2S + 1$, the spin multiplicity of a radical containing one unpaired electron ($S = ½$, $m_s = ½$ or -½) is 2, indicating that there are two magnetic spin quantum number (m_s) energy sublevels (Zeeman figure). In a more general case of a diradical or polyradical, containing two or more unpaired electrons, the spin quantum number, $S \geq 1$, is possible for some of the electronic states; the multiplicity, $2S + 1$, represents the number of the $m_s = S, S - 1, \ldots, -S$.[4]

1.1.2 Background on High-spin Diradicals

According to the rules of spin multiplicity, in the case of the two-electron system, the total spin, S, can be either $S = 1$ (triplet) or $S = 0$ (singlet). A triplet ($S = 1$) ground state diradical yields an exchange coupling that is ferromagnetic; while a singlet ($S = 0$) ground state gives antiferromagnetic exchange coupling. The strength of the exchange coupling is proportional to the energy difference between the singlet and triplet ground states ($\Delta E_{ST} = E_S - E_T$). A positive value of ΔE_{ST} results if the triplet ground state is lower in energy than the singlet ground as exhibited in Figure A-1.

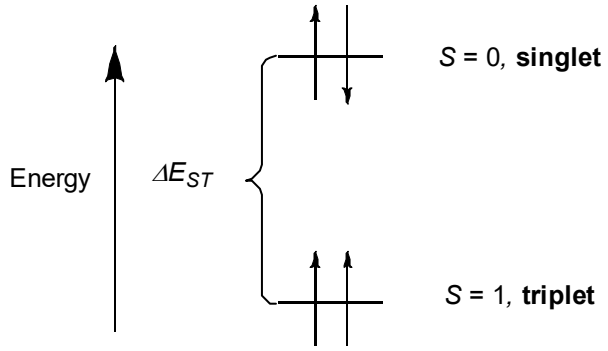

Figure A-1. Illustration of energy difference between singlet-triplet states for ferromagnetic coupling.

The preference between ferromagnetic or antiferromagnetic coupling in non-Kekulé diradicals can be determined by examining the non-bonding molecular orbitals (NBMOs). A non-Kekulé structure is defined as a fully conjugated hydrocarbon structures that contain at least two atoms that are not π-bonded.[13] As an example, we can examine the simple contrasting cases of trimethylenemethane (TMM)[14-15] and tetramethylenemethane (TME). TMM is a non-Kekulé diradical, where its unpaired electrons are located in singly occupied NBMO's. These NBMO's are non-disjoint meaning their atomic spin densities have at least an atom in common, resulting in a triplet ground state as illustrated in Figure A-2.

On the other hand, examination of the NBMO's in TME, which is also a non-Kekulé diradical, shows that the NBMO's are disjoint, indicating there is no spin density on any atoms in common. Thus, TME has a singlet ground state as seen in Figure A-2. These two simple cases illustrate how topology (or connectivity) of the molecule is indicative of either ferromagnetic or antiferromagnetic coupling.[6,8]

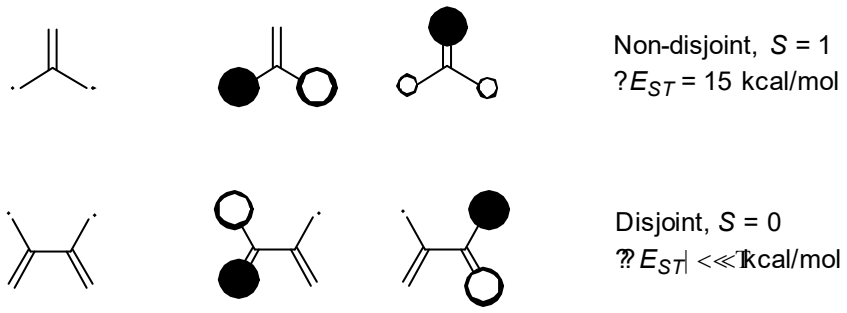

Figure A-2. Non-Kekulé radicals based on TMM and TME.

From this simple case of TMM and TME, additional ferromagnetic coupling units (fCU) and antiferromagnetic coupling units (aCU) can be described. The 1,3-phenylene (*m*-xylyene) unit is a good example of a frequently used fCU, with ΔE_{ST} significantly greater than thermal energy (RT) at ambient temperature; although if the π-conjugation between the radical and the fCU are perturbed by twisting, smaller ΔE_{ST} result. The alternating use of fCU's connected to radical sites allow for polymers with large values of S.[16]

1.1.3 Background on Aminyl Radicals

An aminyl radical is a neutral nitrogen-centered radical that has two bonded substituent groups, an unpaired electron, and a non-bonding pair of electrons. The substituents bonded to the nitrogen atom could be hydrogen, alkyl, phenyl, or heteroatoms; whichever is attached plays a significant role in radical stability, its electronic structure and properties. The ground state of the aminyl radical is predicted to have a planar structure where its electronic configuration (i.e. where the unpaired electron on the nitrogen atom is found) could be in the $2p_z$ orbital (π-type radical) or in sp^2 orbital (σ-type radical) as shown in Figure A-1.

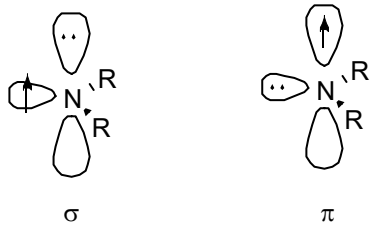

Figure A-1. Illustration of possible electronic configurations of the aminyl radical ground state.

Aminyl radicals have shown little attention since diphenylaminyl, the first aminyl radical reported in 1911.[17] It was formed upon the homolysis of tetraphenylhydrazine through UV irradiation or heating to 100 °C as exhibited in Figure A-2. The challenge with aminyl radicals is that many are short-lived, highly reactive species; they readily undergo radical reaction pathways such as dimerization and hydrogen atom abstraction. As an example of their reactivity, upon flash photolysis of tetraphenylhydrazine (**7**) in benzene solution at room temperature; the diphenylaminyl radical (**8**) was quenched with a second-order rate constant of 2.5 x 10^7 L•mol^{-1}•sec^{-1}.[18]

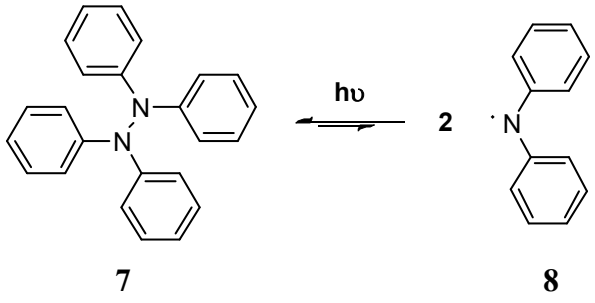

Figure A-2. Homolysis of tetraphenylhydrazine to form diphenylaminyl radical (8).

Most reported aminyl radicals are generally not isolable at room temperature. However, with better understanding of their decomposition pathways, aminyl radicals can be designed in order to understand different factors affecting stability. A basic understanding of the resonance structures of the diphenylaminyl radical show that the

unpaired electron can be delocalized into the two phenyl rings, specifically at the *ortho* and *para* positions as illustrated in Figure A-3. These simplified resonance structures indicate a large positive spin density at the sites, indicating potential reactive sites. In this simple case, without significant steric shielding around these reactive positions, the radicals may undergo bond-forming reactions, such as dimerization through σ-bond formation.

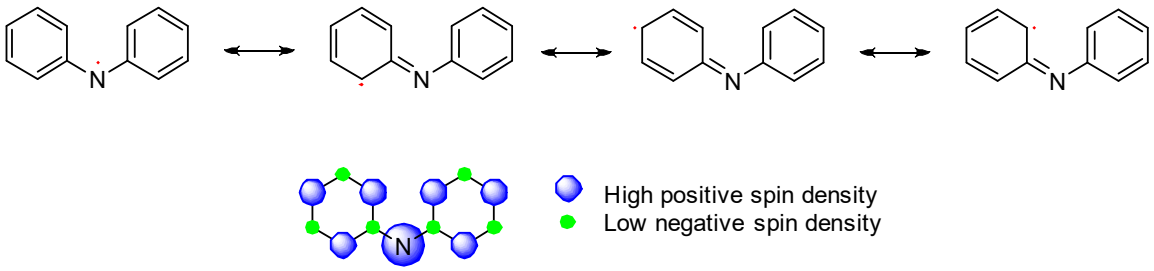

Figure A-3. Resonance structures and spin density map for diphenylaminyl radical (8).

With the understanding for the need to stabilize the radical by shielding these reactive sites, Neugebauer and co-workers[19-20] modified the diphenylaminyl radical in two ways in 1971. First, to increase resonance stability they chose the more planar carbazole framework. Next, *tert*-butyl groups were introduced at positions on the phenyl rings that showed large positive spin densities from delocalization of the aminyl radical into the phenyl rings. The *tert*-butyl groups work two-fold in stabilizing these sites through hyperconjugation and preventing dimerization due to their steric bulk. With this design, 1,3,6,8-tetra-*tert*-butylcarbazole aminyl radical (**9**) was successfully synthesized by oxidation of the lithium salt of the carbazole amine (**10**) in benzene with iodine and isolated as blue-black crystals as seen in Figure A-4.

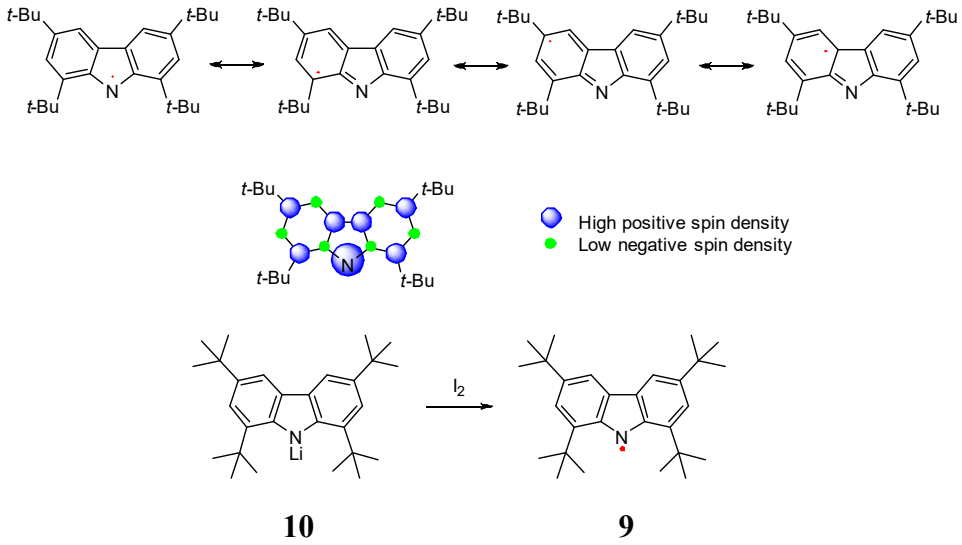

10 **9**

Figure A-4. Resonance, spin density map and synthesis for 1,3,6,8-tetra-*tert*-butylcarbazole aminyl radical (9).

In 1974, Ballester and co-workers[21] synthesized and isolated the air-stable perchlorodiphenylaminyl radical (**11**) by two different methods as exhibited in Figure A-5: oxidation of decachlorodiphenylamine (**12**) using alkaline aqueous solution of potassium ferricyanide or silver (II) oxide; or dechlorination of perchloro-*N*-phenylcyclohexan-2,5-dienimine (**13**) using silver (Ag^0). The *ortho*-chlorines on the aryl rings shield the radical site from reaction.

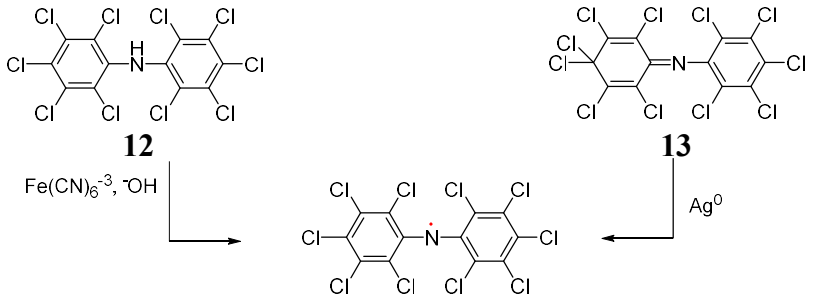

12 **13**

11

Figure A-5. Different reactions for the formation of perchlorodiphenylaminyl radical (11).

1.1.4 Background on Aminyl Diradicals

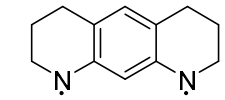

ΔE_{ST} = +13.5 kcal/mol

Figure A-1. Calculated ΔEST for m-xylylene aminyl diradicals (14).

As already discussed above, the *m*-phenylene motif has shown promising success as a ferromagnetic coupling unit. Previous work[22-23] shows that *m*-xylylene has a triplet ground state 9.6 ± 0.2 kcal•mol^{-1} (ΔE_{ST}) lower in energy than the singlet state. This value is much greater than the thermal energy at room temperature which is ~0.6 kcal•mol^{-1}. Aminyl radicals connected through a *m*-xylylene fCU's have been predicted to have a strong preference for the triplet ground state and calculated to have large ΔE_{ST} of 13.5 kcal/mol for molecule **14** shown in Figure A-1.[24-25]

Platz and colleagues photolyzed 2,4,6-trifluoro-1,3-diazidobenzene (**15**) and characterized at 77 K the first nitrogen centered diradical (**16**) in 1989 as shown in Figure A-2. [26]

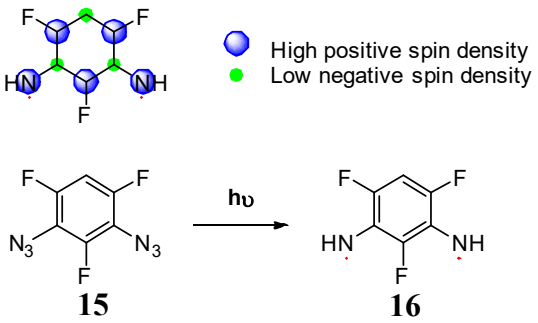

Figure A-2. Spin density map and synthesis for Platz diradical (16).

The second example wasn't synthesized until 2007, when Rajca and co-workers[27] synthesized radical (**17**) by deprotonation of the diamine precursor (**18**) with *n*-BuLi, followed by oxidation of the resulting dianion with iodine. The aminyl diradical consists of five linearly-fused six-membered rings (diazapentacene derivative), utilizing the *meta*-phenylene-coupling unit as its core and a (4-*tert*-butylphenyl) pendant *ortho* to both aminyl radical sites as seen in

Figure **A-3**. The diradical is stabilized with bulky substituents at sites of significant spin density without interfering with the planar geometry for spin delocalization; planarity is suggested by the X-ray crystal structure of diamine precursor **18**. The EPR spectra (X-band) of the aminyl diradical **17** in a 2-MeTHF matrix at 133 K showed transitions for $|\Delta\mu_s| = 1$ and $|\Delta\mu_s| = 2$. Superconducting Quantum Interference Device (SQUID) magnetic studies for the diradical in the THF matrix established a triplet

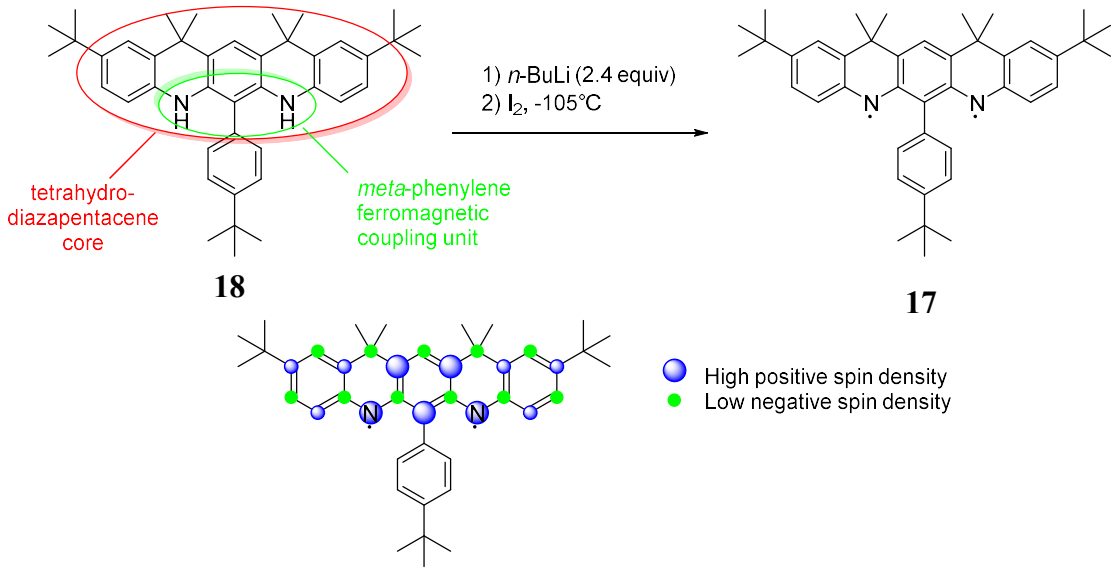

Figure A-3. Design, synthesis, and spin density map for 17.

ground state ($S = 1$). SQUID magnetometry also provided a measurement for the lower limit for the singlet-triplet energy gap (ΔE_{ST}) for **17** $\geq$ 0.4 kcal•mol^{-1}. The aminyl diradical in 2-MeTHF is persistent at around -100 °C and inert to dry oxygen at around -108 °C (165 K).

In 2010, Rajca and co-workers[28] further modified the diazapentacene derivative by introducing additional pendants at all free *ortho* positions relative to the aminyl radical sites shown in Figure A-4**,** synthesizing aminyl diradicals (**19**) and (**20**) from diamine precursors using the same deprotonation/oxidation sequence as before. In the case of aminyl diradical **20**, the additional sterically hindered *tert*-undecylphenyl pendants at the *ortho*-positions in regard to the aminyl radical, not only improved the persistence

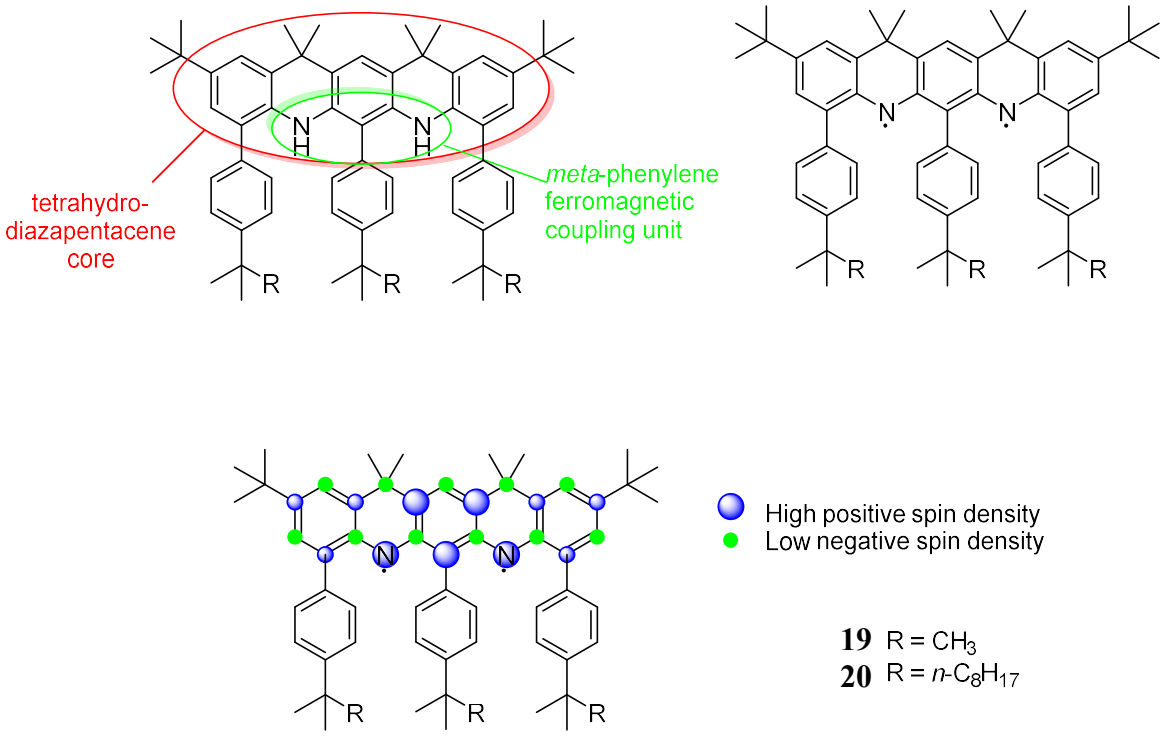

Figure A-4. Design and spin density map for aminyl diradicals 19 and 20.

of the radical by stabilizing sites of significant spin density, but also improved its solubility in organic solvents. The EPR spectra (X-band) of the aminyl diradical **20** in a 2-MeTHF matrix at 132 K showed both $|\Delta\mu_S| = 1$ and $|\Delta\mu_S| = 2$ transitions, thus suggesting presence of triplet state. SQUID magnetic studies for the diradical **20** in the THF matrix established a triplet ground state ($S = 1$) and provided the lower limit of ΔE_{ST} ≥ 2 kcal•mol^{-1}, in agreement with DFT-computed value of $\Delta E_{ST} \approx 7$ kcal•mol^{-1} for radical **20**, using the UB3LYP/6-31(d) level of theory. Encouraged by the persistence of **20** in 2-MeTHF solution at, showing a half-life ($\tau_{1/2}$) of ≈ 3 h, they isolated the diradical. The concentration of isolated solid **20** under Ar atmosphere at room temperature decreased to 60% over five days. The aminyl diradical **20** in 2-MeTHF showed to be sensitive to excess of iodine and oxygen at -26 and -78 °C respectively.

Building on their past success, Rajca and colleagues continued to investigate stable aminyl diradicals based upon the aza-*m*-xylylene core framework with $\Delta E_{ST} \geq 10$ kcal•mol^{-1}. Based on calculations of model diradicals with $\Delta E_{ST} \approx 13.5$ kcal•mol^{-1} such as octahydropyridoquinoline (OHPQ) as seen in Figure A-1,[22] a planar derivative of the aza-*m*-xylylene with limited delocalization to maximize spin-spin interactions was needed to reach this objective. Rajca's lab[29-31] was able to report the successful synthesis and characterization of a series of sterically shielded planar aza-*m*-xylylene derivatives as shown in Figure A-5, owning triplet ground state comparable to *m*-xylylene. Diradical (**21**) is persistent for minutes in 2-MeTHF solution at room temperature with a ΔE_{ST} on the order of 10 kcal•mol^{-1}, showing a half-life ($\tau_{1/2}$) of about 600 s. The EPR spectra (X-band) of the aminyl diradical in a 2-MeTHF matrix at 132 K showed transitions for

$|\Delta\mu_S| = 1$ and $|\Delta\mu_S| = 2$. SQUID magnetic studies for the diradical in the THF matrix established a triplet ground state (S = 1) and provided a measurement for the lower limit of $\Delta E_{ST} > 0.8$ kcal•mol^{-1}, in agreement with DFT-computed value of $\Delta E_{ST} \approx 11.6$ kcal•mol^{-1}, using the UB3LYP/6-31G(d) level of theory. The aminyl diradical in 2-MeTHF showed to be sensitive to excess of iodine and oxygen at -115 and -105 °C respectively.

Diradical (**22**) showed a shorter half-life ($\tau_{1/2}$) of ≈ 19.64 min at 246 K. The faster decay compared to diradical **21** is likely due to intramolecular hydrogen abstraction from the benzylic methyl groups, followed by intermolecular hydrogen abstraction from 2-MeTHF solvent. The EPR spectra (X-band) of the aminyl diradical Y in a 2-MeTHF matrix at 132 K showed transitions for $|\Delta\mu_S| = 1$ and $|\Delta\mu_S| = 2$. SQUID magnetic studies for the diradical in the THF matrix established a triplet ground state (S = 1) and provided a measurement for the lower limit of $\Delta E_{ST} > 0.3$ kcal•mol^{-1}, compared with DFT-computed value of $\Delta E_{ST} \approx 10$ kcal•mol^{-1}, using the UB3LYP/6-31G(d) level of theory.

Diradical (**23**) showed a shorter half-life ($\tau_{1/2}$) of ≈ 80-250 s at 295 K, upon complete decay the resulting product was not just starting diamine, but a mixture with a byproduct that suggests an additional pathway of decay of diradical resulting in shorter half-life. The EPR spectra (X-band) of the aminyl diradical in a 2-MeTHF matrix at 132 K showed transitions for $|\Delta\mu_S| = 1$ and $|\Delta\mu_S| = 2$. SQUID magnetic studies for the diradical in the THF matrix established a triplet ground state (S = 1) and provided a measurement for the lower limit of $\Delta E_{ST} > 1.6$ kcal•mol^{-1}, in agreement with DFT-

computed value of $\Delta E_{ST} \approx 14$ kcal•mol^{-1}, using the UB3LYP/6-31G(d) level of theory. The improved ΔE_{ST} for diradical based on the six-membered ring (**23**) vs. the analogous five-membered ring (**21**) is presumably due to slightly increased delocalization of spin density into the *m*-phenylene.

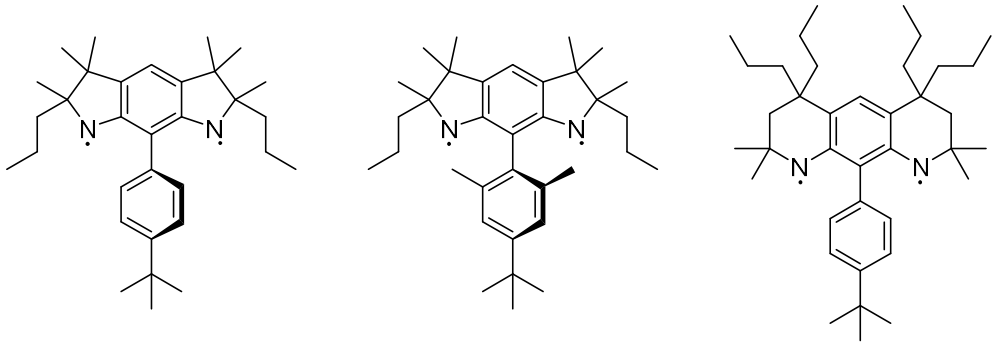

21 **22** **23**

Figure A-5. Aminyl diradicals 21, 22, 23.

1.2 Results and Discussion

The objective of our project was to improve upon the stability of aminyl diradical frameworks based upon aza-*m*-phenylene framework already utilized in our lab. The main tactic to achieve this goal was to design and synthesize molecules where we placed bulky *tert*-butyl (or other groups of equivalent steric bulk) adjacent (or *ortho*-) to the carbons attached to the aminyl radical sites; effectively replacing the *tert*-undecylphenyl pendants on aminyl diradicals already successfully made by our group. Thus, increasing the steric bulk around the radical sites would inhibit radical decomposition with the potential to create a ($S = 1$) triplet ground state diaminyl radical with a large singlet-triplet gap (ΔE_{ST}), persistent at room temperature, and more resistant to decomposition by oxygen.

The inherent difficulty in these synthetic targets is that introduction of the bulky *tert*-butyl groups meant to suppress reactions near the radical site; would also hinder synthetic methods towards our targets. All of our overall initial retrosynthetic strategies as seen in Scheme 1.1 are based upon past successful forays towards less-substituted diazapentaacene-derivative (**24)** generated by a Friedel-Crafts-like ring closure of the product (**25)** of Buchwald-Hartwig couplings between a core diamine fragment (**26)** and two terminal halogen-substituted coupling partners (**27)**.

Scheme 1.1. Retrosynthesis for diaminyl radical precursors (24)

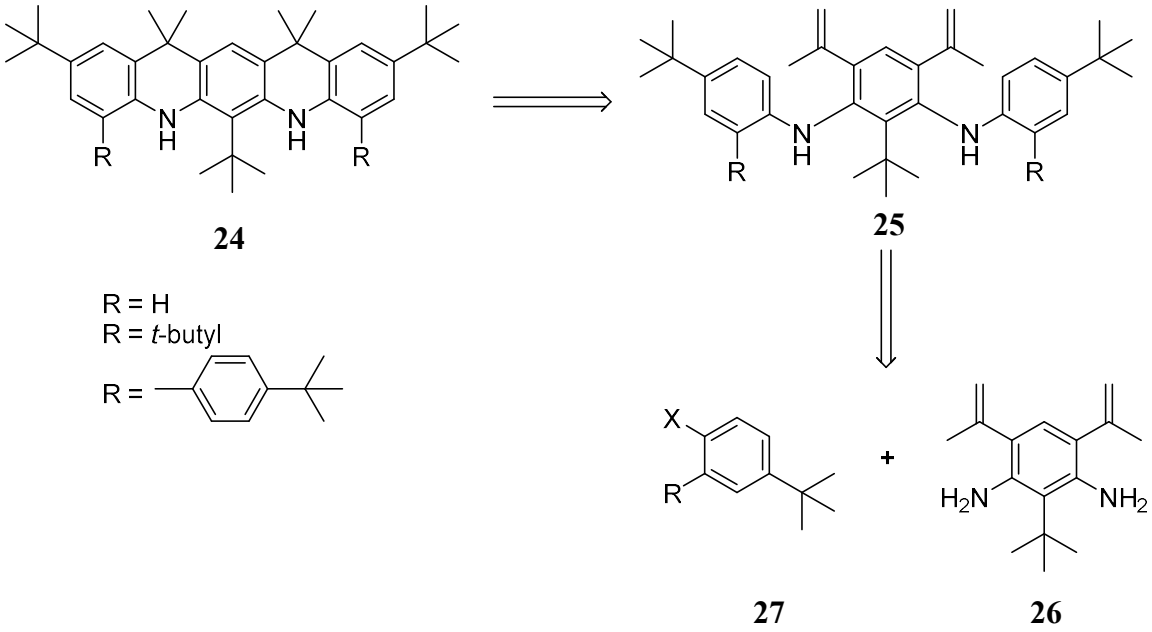

24 **25** **27** **26**

Synthetic strategies towards the core diamine evolved as we encountered synthetic difficulties along our original paths and will be discussed further below. But the overall end game remained the same for coupling of the core and periphery fragments through a Buchwald-Hartwig coupling reaction.

1.2.1 Synthesis of the Buchwald-Hartwig Halogen Coupling Partners

Our first objective was to synthesize the terminal ends of the diazapentaacene-derivative in order to couple with our diamine core building blocks as seen in the retrosynthetic disconnection in Scheme 1.1. There were three terminal targets of interest, one with a hydrogen in the R position, one with a *tert*-butyl group in the R position and another where there was a halogen allowing for future Suzuki coupling at the R position.

1-bromo-2,4-di-(*tert*-butyl)benzene (**28**) was obtained following a literature procedure[32] via bromination of 1,3-di-(*tert*-butyl)benzene (**29**) using Br_2 and trimethyl phosphate as seen in Scheme 1.2 below.

Scheme 1.2. Synthesis of 1-bromo-2,4-di-(*tert*-butyl)benzene (28).

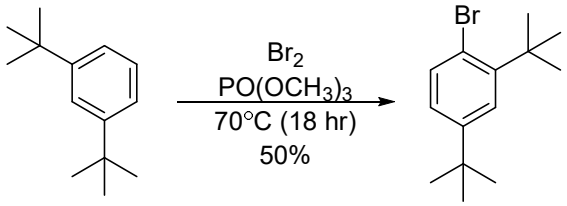

29 **28**

The terminal fragment with a halogen instead of a *tert*-butyl group allowing for the addition of various pendants via Suzuki reactions was synthesized over three steps from 1-bromo-4-(*tert*-butyl)benzene (**30**) via a series of literature reactions[33] as seen in Scheme 1.3. Nitration of the commercially available starting material to 1-bromo-4-(*tert*-butyl)-2-nitrobenzene (**31**) followed by reduction to the amine (**32**) resulted in two high yielding steps. The resulting amine was subjected to a Sandmeyer reaction to generate 1-bromo-4-(*tert*-butyl)-2-iodobenzene (**33**) in moderate yield.

Scheme 1.3. Synthesis of 33.

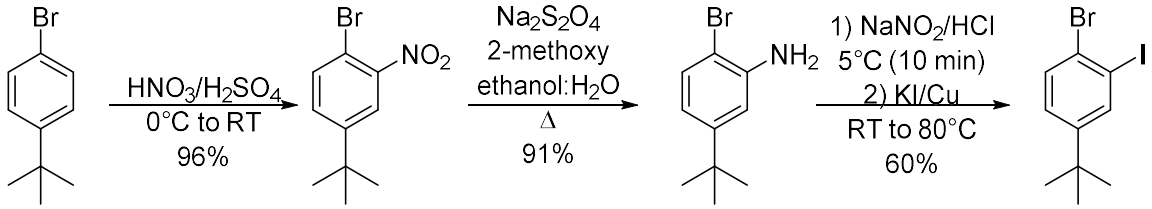

30 **31** **32** **33**

These reactions provide a valuable series of similar functional group transformation[34] for other *tert*-butyl substituted benzene compounds that may be useful for the synthesis of amine coupling precursors towards the synthesis of highly substituted mono-aminyl radical.

1.2.2 Original Synthetic Path towards Diamine Coupling Precursor

Our initial strategy to synthesize the *tert*-butyl-aza-phenylene core was based upon the commercially available, already highly functionalized musk ketone (**34**). As seen in Scheme 1.4, from this starting material we envisioned a series of seven functional group transformations that would yield the *tert*-butyl substituted diamine Buchwald-Hartwig coupling precursor.

Scheme 1.4. Retrosynthesis of diamine core (35).

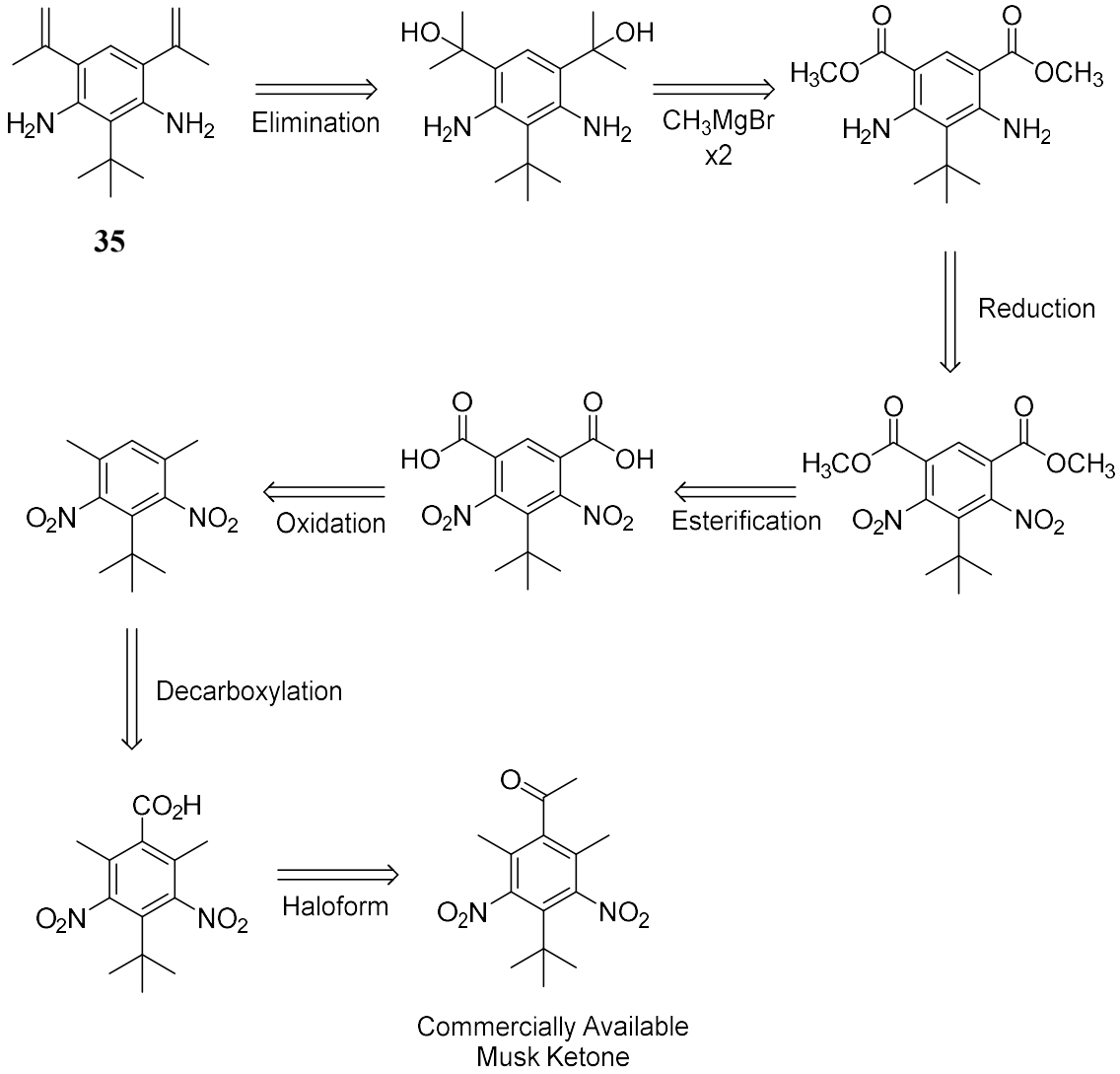

Our synthesis towards **35** is shown in Scheme 1.5. We attempted several variations of the haloform reaction on **34**, until we found a method[35] that was successful in the transformation of the methyl ketone to a carboxylic acid (**36**), which then underwent Cu-catalyzed decarboxylation to (**37**).[36] Subjecting the remaining methyl groups to oxidation with $KMnO_4$ giving the dicarboxylic acid (**38**) followed by acid-catalyzed esterification yielded the methyl ester (**39**).

Scheme 1.5. Attempted synthesis of 44.

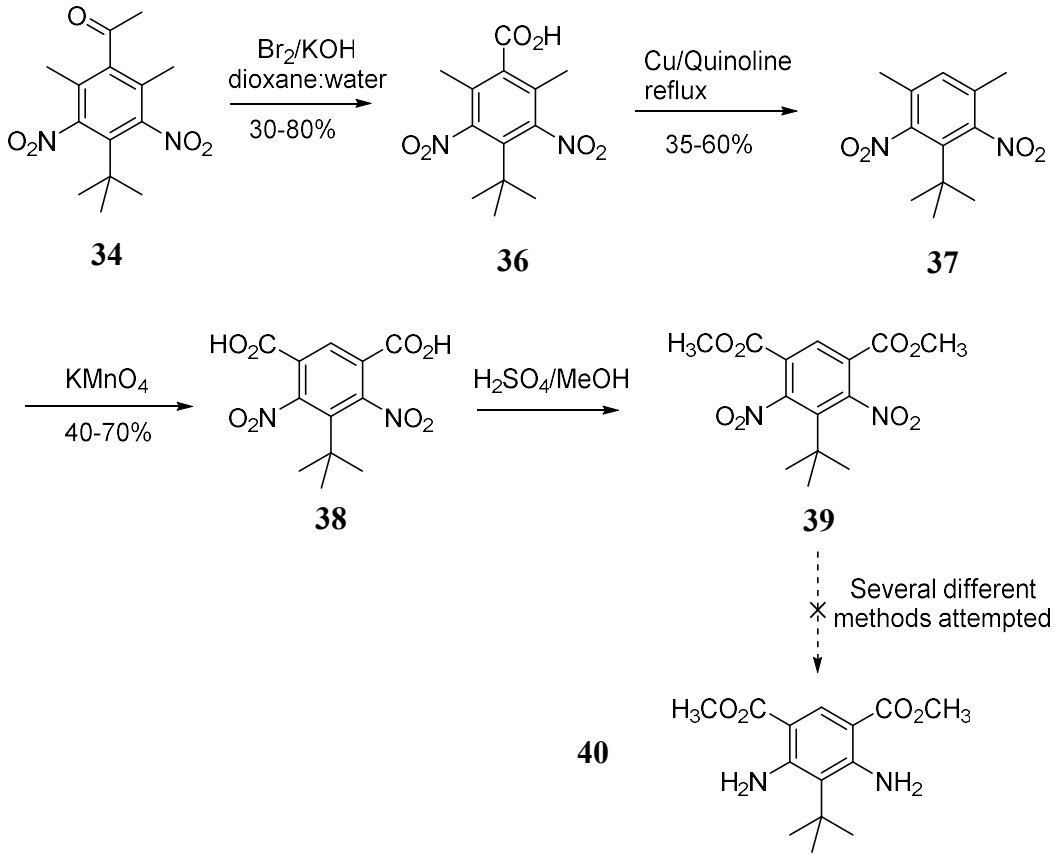

The reduction of the two nitro groups to amines yielding the diester-diamine (**40**) proved to be non-trivial as after multiple attempts using several different methods failed (Fe/Acetic Acid[37]; 10% Pd/C, Ammonium Formate[38]; 10% Pd/C, H_2; $SnCl_2 \cdot 2H_2O$[39]; $Na_2S_2O_4$; Raney Ni[40]). We even tried some of the reactions (Fe/Acetic Acid; 10% Pd/C, Ammonium Formate; 10% Pd/C, H_2) using a simpler test molecule (methyl-2-nitrobenzoate, representing a similar *ortho*-nitro-ester motif) with clean complete conversion without purification to methyl-2-aminobenzoate.

Reaching an impasse and considering that maybe congestion around the nitro group on the substrate were inhibiting the reaction, we investigated the reduction of the

less sterically hindered 2-(*tert*-butyl)-1,3-dinitro-benzene. While, we found a very successful reduction method[40] (as discussed in the next section) it did not translate to the reduction of dimethyl-5-(*tert*-butyl)-4,6-dinitroisophthate.

1.2.3 Synthesis of 2,6-diamino-*tert*-butyl benzene

To investigate reductions of simpler dinitro-benzene compounds, we synthesized 4-(*tert*-butyl)-3,5-dinitro-benzoic acid (**41**) via nitration of 1,4-*tert*-butyl benzoic acid (**42**). After having varied success with traditional decarboxylation, we tried a more recent catalytic Cu_2O decarboxylation[41] protocol using bathophenanthroline ligand in NMP:Quinoline to give 2,6-dinitro-*tert*-butyl benzene (**43**) with better consistency and moderate yield; which was then subjected to reduction with Raney Ni and hydrogen gas to cleanly give 2,6-diamino-*tert*-butyl benzene (**44**) as shown in Scheme 1.6 in almost quantitative yield. [40]

Scheme 1.6. Synthesis of 44.

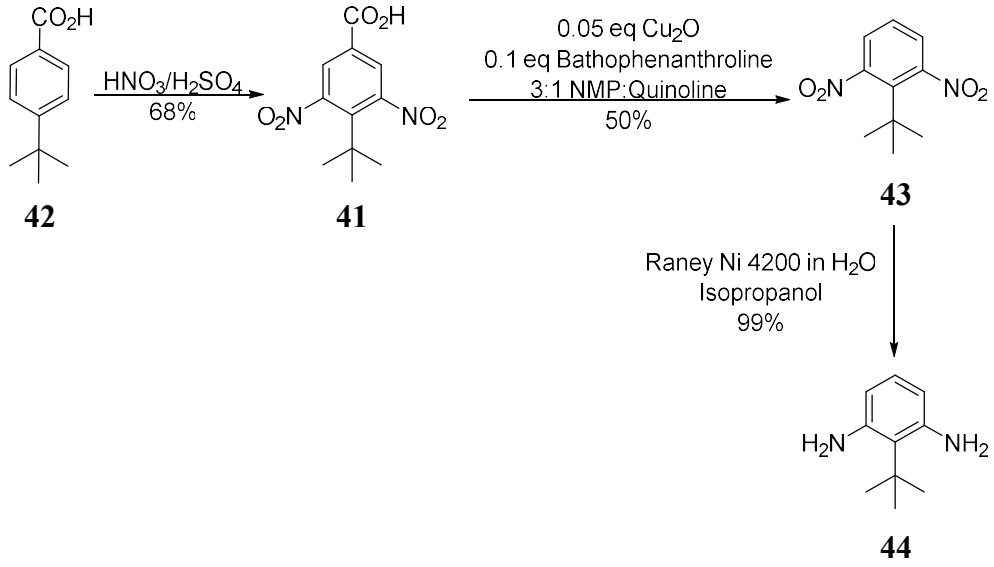

42 **41** **43** **44**

1.2.4 Modified Synthesis based upon Isatin Intermediate

With good success in generating **44** and unable to translate that method to the reduction of **39**, we reevaluated our synthetic strategy towards the diamine core. With 2,6-diamino-*tert*-butyl benzene in hand we began to investigate transformations that would lead to carbon-addition adjacent to the amine and the ability to transform to an ester. After further literature review (both new[42] and old[43]) show a plethora of possible reactions towards and from isatin structure. Specifically, we envisioned the versatile isatin motif as a potential entry into our *tert*-butyl-diamine-diene core[44], while also providing divergent routes to other *tert*-butyl diamine structures of interest to our group[45-46] as seen in Scheme 1.7.

Scheme 1.7. Retrosynthetic strategies towards 47.

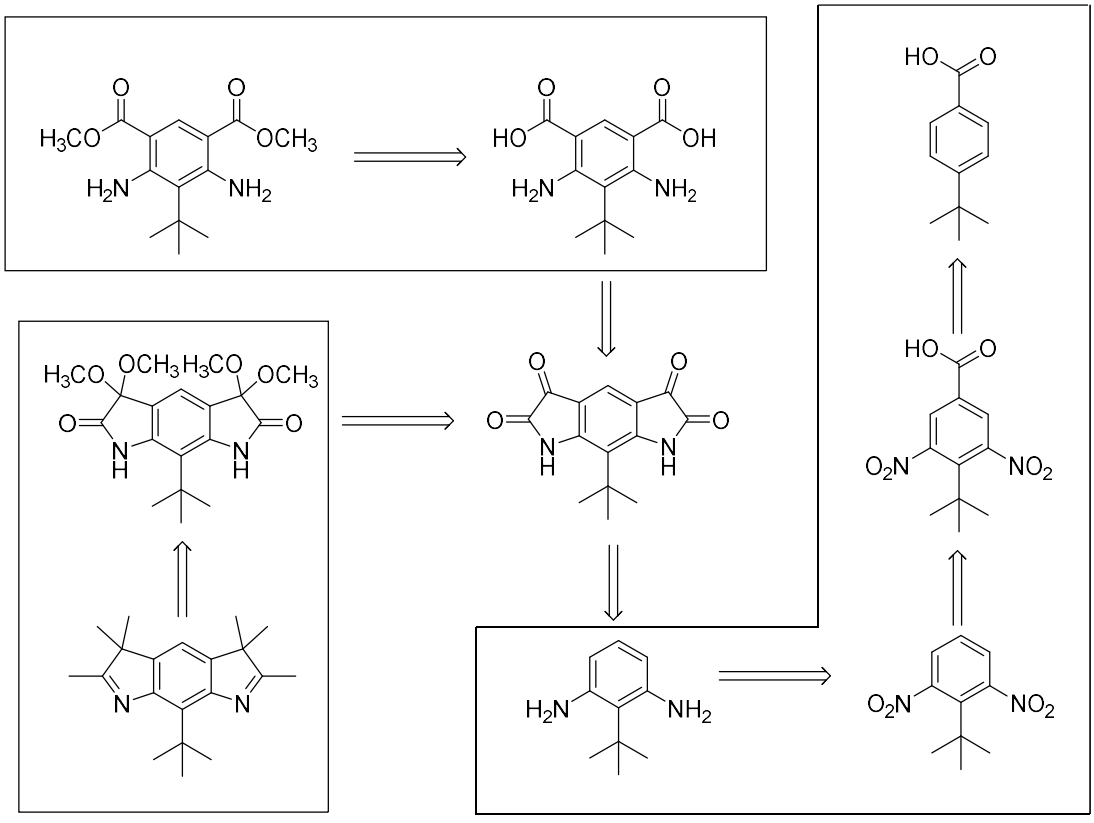

While, more traditional isatin synthetic routes[47] (i.e. Sandmeyer isatin synthesis using chloral hydrate and hydroxylamine) appear to work well on a single amine; it proved difficult on diamines (we also failed to convert a test compound of 2,6-diaminotoluene) resulting in an inseparable mixture of compounds. An efficient and clean step-wise alternative[48] based upon amide coupling of a protected acid-chloride (**45**) (that we generated) followed by deprotection-condensation cleanly gave the diisatin precursor (**46**) in moderate yield as shown in Scheme 1.8. This then underwent acid-catalyzed EAS to give the diisatin target material (**47**) in 65% yield.

Scheme 1.8. Synthesis of 47.

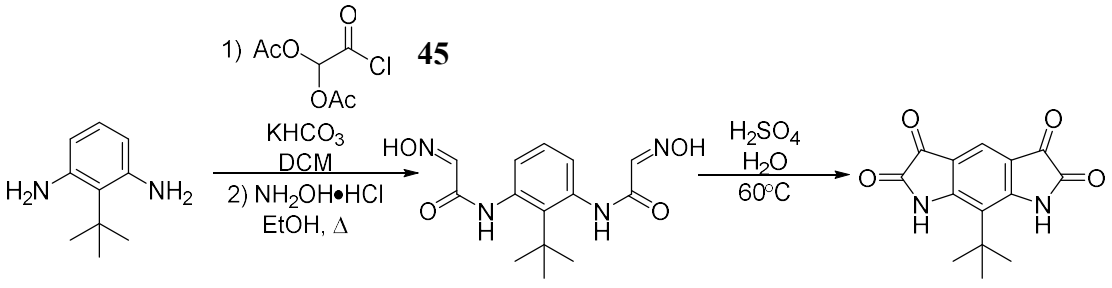

44 **46** **47**

1.2.5 From Diisatin to Diamine Core for Buchwald-Hartwig Coupling

From the **47** our synthetic strategy diverged to provide proposed routes to two different diaminyl radical precursors. In order to obtain the Buchwald-Hartwig coupling precursor per our original plan, the isatin was oxidized and then hydrolyzed with H_2O_2 under basic conditions[49] to yield the dicarboxylic acid-diamine (**48**), which was esterified with TMS-diazomethane to the diester-diamine[50-51] (**49**) as you can see in Scheme 1.9. This method for esterification was chosen as attempts to use H_2SO_4 and methanol

resulted in esterification but also loss of *tert*-butyl group as it was now strongly electronically activated via the two amine groups *ortho* to its position.

Scheme 1.9. Attempted synthesis of 50.

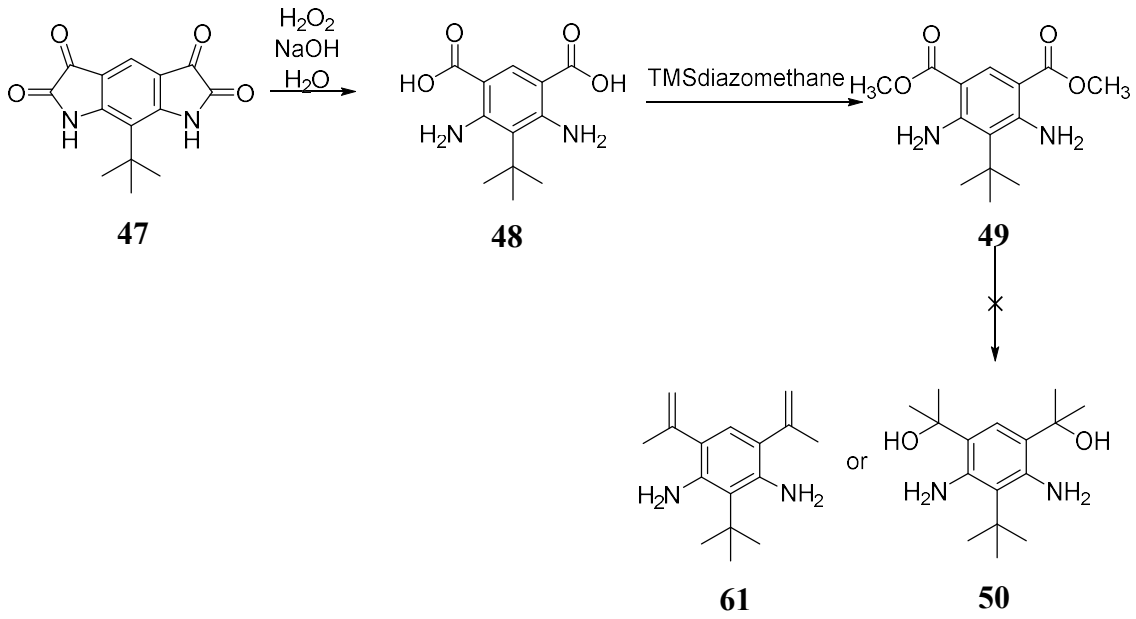

47 **48** **49** **61** **50**

Originally, we attempted to subject the diester-diamine to exhaustive Grignard addition as our initial strategy indicated to give the diol diamine (**50**), however we were unable to achieve consistent results as it appears the alcohol was readily eliminated on one side of the molecule and not the other and we kept obtaining complex mixtures of products.

With that difficulty we attempted to try the Buchwald-Hartwig coupling on the diester-diamine. Using methods that had previously worked in out lab for unhindered Buchwald-Hartwig couplings we attempted to couple the diester-diamine with 4-bromo-*tert*-butylbenzene without success using tri(*tert*-butyl)phosphine and $Pd_2(dba)_3$ and either

Cs_2CO_3 or *t*-BuONa. The diamine appears to be too sterically hindered to allow this ligand and system to succeed.

It is at this point where this project currently stands. As will be discussed in next section, investigations into potentially better ligand systems may allow for this reaction to succeed and this project be continued. On the other hand, we were successful in creating novel *tert*-butyl diamine substituted benzene systems and applying known chemistry to both diaminobenzene systems and sterically hindered aniline systems. These routes and compounds should allow for further investigation of various systems composed with similar connectivity.

1.2.6 Buchwald-Hartwig Coupling of Sterically Hindered Systems

Early in our work we made several attempts at the Buchwald-Hartwig coupling of 2,4,6-tri(*tert*-butyl)aniline (**51**) with a 1,5-dibromo-2,4-di(prop-1-en-2-yl)benzene (**52**) as shown in Scheme 1.10 without success.

Scheme 1.10. Attempted Buchwald-Hartwig Coupling.

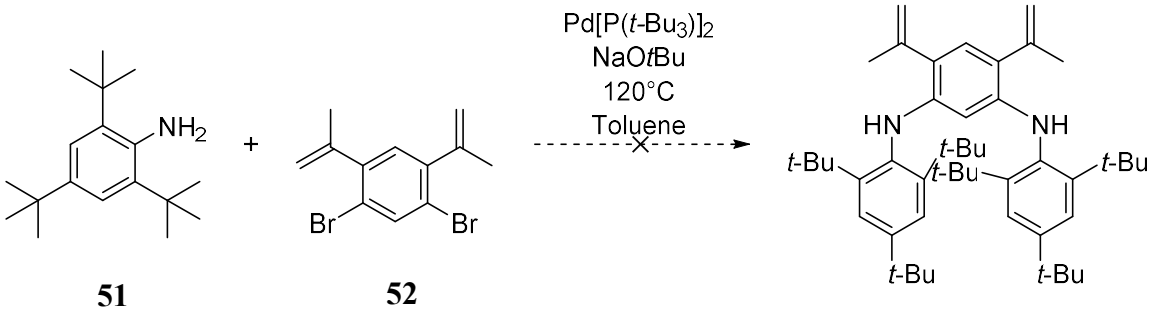

51 **52**

Once we obtained dimethyl 4,6-diamino-5-(*tert*-butyl)isophthalate (**49**) we also made several attempts at coupling it with 4-*tert*-butyl-bromobenzene without any success. We also attempted the Buchwald-Hartwig coupling on our *tert*-butyl diisatin

with 4-*tert*-butyl-bromobenzene without success. Both these examples are shown in Scheme 1.11.

Scheme 1.11. Attempted Buchwald-Hartwig Couplings.

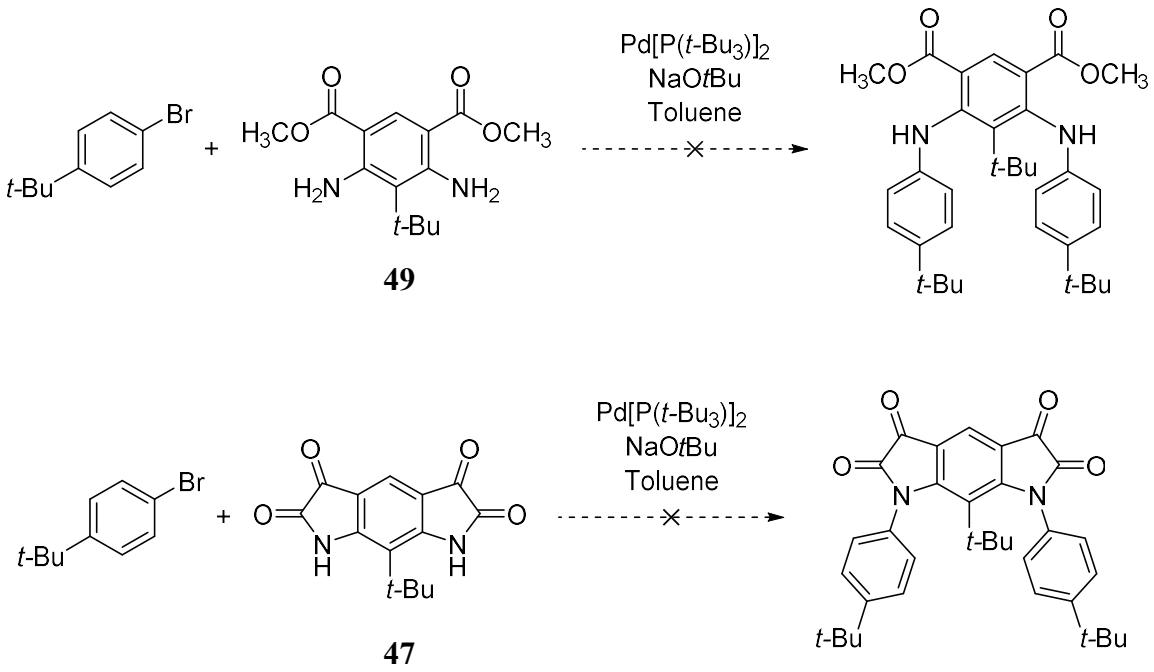

A review of the literature shows no successful examples of Buchwald-Hartwig coupling between compounds bearing *tert*-butyl groups *ortho*- to both the amine or halogen site. The closest example, as shown in Scheme 1.12, is the successful coupling of isopropyl groups *ortho*- to both the amine and halogen (and 2-*tert*-butylaniline with 1-bromo-2,4,6-triisopropyl-benzene) by Shaunnesey and co-workers[52] using trineopentylphospine (TnPP), a ligand that is currently commercially unavailable. Feeling that this may provide a solution to our problem and confirming with the author that such examples had yet to be attempted (rather than not reported because they failed), we decided to undertake an investigation of this ligand for sterically hindered systems like our own.

Scheme 1.12. Successful examples Buchwald-Hartwig reactions using TnPP ligand.

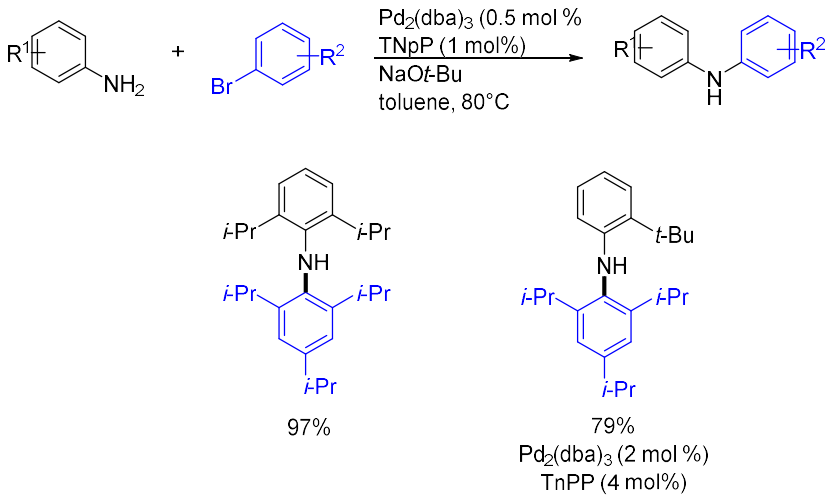

The original literature procedure[53] for the synthesis of TnPP (**53**) proved to be very difficult resulting in poor recovery and poor reproducibility; it didn't give a yield for their recovery of TnPP. After several attempts to synthesize this ligand in our lab using the original paper, we did so with great success by applying a modified literature procedure used in the synthesis of other trialkylphosphines as described in Scheme 1.13.[54] Using a CuI-mediated Grignard addition to phosphous trichloride resulted in greatly increased conversion, increasing purity and allowing for more facile purification via recrystallization versus distillation as previously reported. This resulted in greatly improved yield (60.1%) compared to the previous reported methods (34.6%).

As an investigation into the ability to couple sterically-hindered Buchwald-Hartwig coupling partners, we devised a strategy towards the synthesis of a sterically-hindered dihydroacridine-based monoaminyl radical precursor (**54**) as part of our summer visiting undergraduate research program as seen in Scheme 1.14. While unable to complete the project over the summer, following the literature procedure[52] we were able

Scheme 1.13. Previous and current attempts at synthesis of TnPP (53).

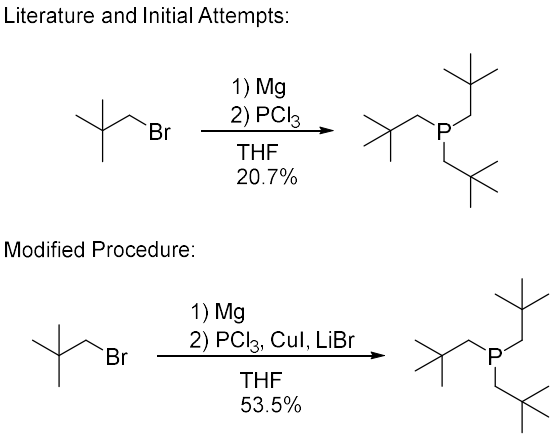

to show successful coupling of 2-*tert*-butyl-iodobenzene (**55**) with 2-*tert*-butyl aniline (**56**), and of 2,5-*tert*-butyl-bromobenzene (**57**) with 2,5-*tert*-butyl aniline (**58**). Amines **59** and **60** are the first known examples of successful Buchwald-Hartwig couplings between two partners with *tert*-butyl groups adjacent to the halide and amine on both coupling partners. The ability to use the TnPP ligand for such previously difficult hindered systems is a great step forward for the synthesis and investigation of similar hindered systems.

This success showed that anilines *ortho*- to *tert*-butyl groups can successfully be coupled to other sterically hindered Buchwald-Hartwig coupling partners. This should allow our original project to go forward and open the door for others to make additional sterically hindered couplings to access other products of interest.

Scheme 1.14. Attempted synthesis towards 54.

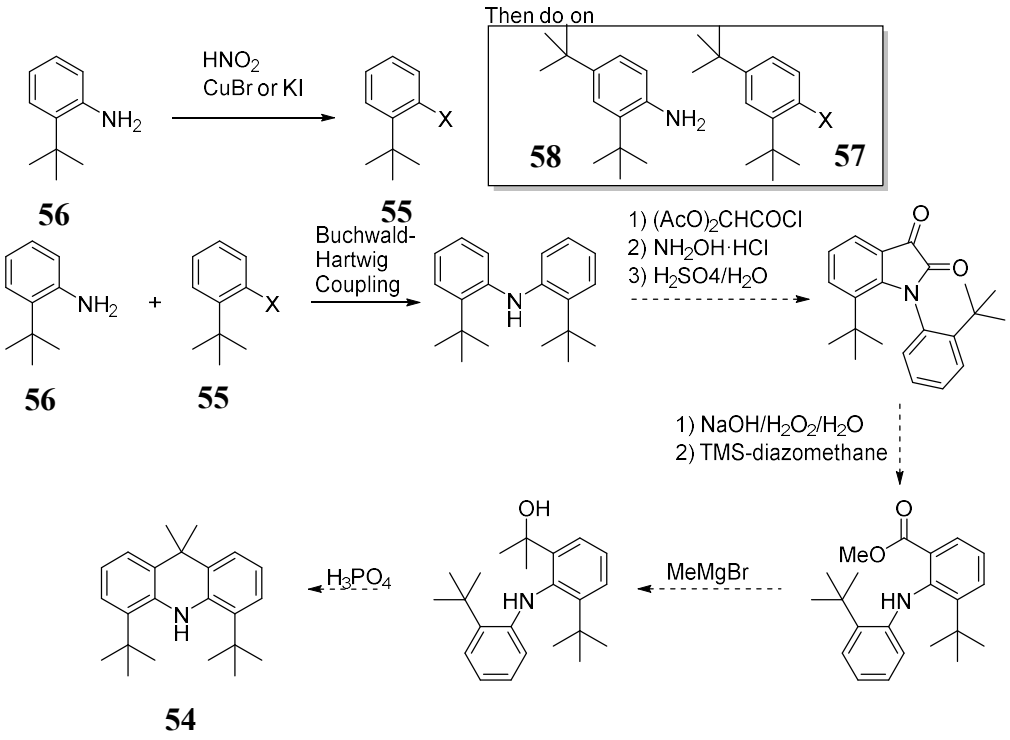

1.2.7 Attempts towards *tert*-butyl substituted Aza-*m*-phenylene Targets

As briefly discussed before, we felt the isatin motif may provide a unique route towards other diaminyl radical structures of interest to our group. Based on literature examples[45] and their proposed reaction mechanism as reproduced in Scheme 1.15, we hoped to obtain (**61**) from exhaustive Grignard alkylation, but attempts to do so were unsuccessful. We were unable to duplicate the literature reaction results on the simple isatin molecule either. Having past success with allyl Grignard additions when alkyl Grignard's had failed, we also made attempts of allylation of the diisatin using allyl Grignard and another method using a Samarium-mediated Barbier reaction. [55-56] Additionally, due to the extended amide resonance structure of diisatin, we also

attempted an alkylation using methyl lithium in the presence of $TiCl_4$ on *N*-methyl isatin.[57,58] We did not have success with these reactions on the diisatin molecule.

Scheme 1.15. Proposed mechanism for alkylation of isatin.

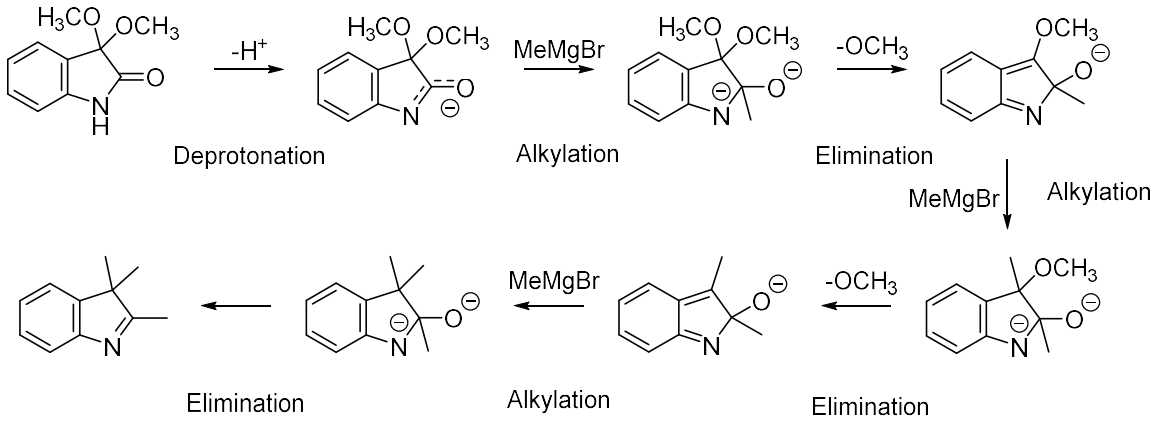

We did briefly investigate some alternative reactions in order to selectively deoxygenate the ketone of isatin to oxindole using a Wolff-Kishner reaction and then attempt alkylation of the enolate of the amide as shown in the figure below. Attempts to deoxygenate ketone of diisatin were unsuccessful, leading to an unidentifiable mix of products.[59-61]

This compound may be accessible through two other proposed routes which we have yet to investigate. One route is based on getting to an alkylated indolinone derivative, our group[30] and others have had success with exhaustive alkylation of amide species with different organometallic alkylation methods which will be discussed further in Section 1.2.9. The synthesis towards 7-*tert*-butyl-3,3-dimethyl-2-indolinone (**62**) has already been reported as shown in Scheme 1.16.[62] It would be possible to extend this same synthesis to both sides of 2,6-diamino-*tert*-butyl benzene (**44**) as a starting material,

giving us an intermediate that we could continue reaction of the amide as shown in Scheme 1.17. We did not have a chance to explore this possibility though.

Scheme 1.16. Literature synthesis of 62.

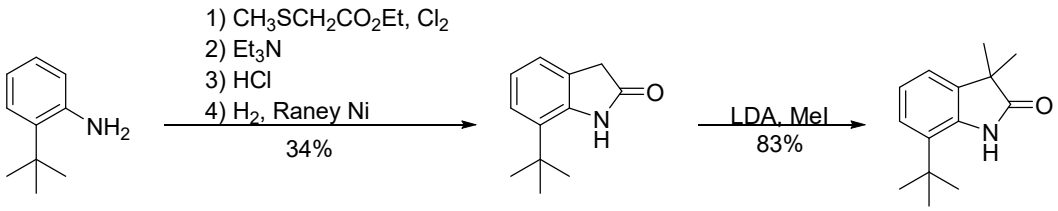

Scheme 1.17. Application of synthesis on 44.

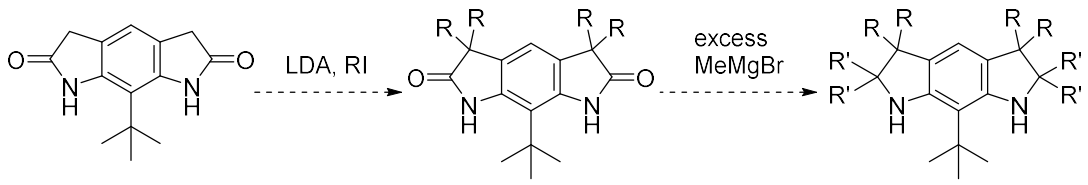

This synthesis is based upon a unique key step, a [2,3] rearrangement—cyclization reaction, whose mechanism is shown in Scheme 1.18. It proceeds by a reaction between chlorine and ethyl(methylthio)acetate followed by addition of the aniline generating a azasulfonium salt. Reaction of the salt with triethylamine forms an ylid, which then undergoes the [2,3] rearrangement bonding the (methylthio)acetate group *ortho*- to the amine. Oxindole is formed upon acid-catalyzed ring closure and desulfurization with Raney nickel. Dialkylation with LDA/MeI gives 7-*tert*-butyl-3,3-dimethyl-2-indolinone.

Scheme 1.18. Mechanism for [2,3] rearrangement-cyclization.

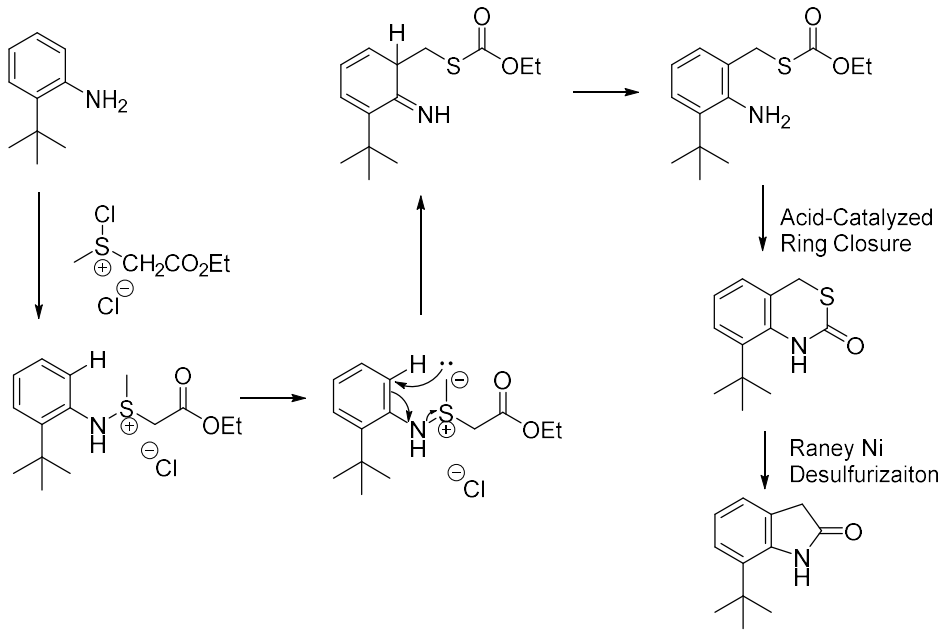

Additionally, an alternative route is envisioned in Scheme 1.19 based on previous success with other substrates.[29] An example synthesis on one side of the molecule is showed for 2-*tert*-butyl aniline (**56**), but may also apply to 2,6-diamino-*tert*-butyl benzene (**44**). The starting aniline would be converted to the diazonium salt, followed by reduction to the hydrazine with $SnCl_2$. A modified-Fischer indole synthesis with isobutryaldehyde in acetic acid gives the alkylated indole.[63] Exhaustive Grignard alkylation of the indolenine could be performed as in the past. However, there is an interesting literature example with allylation of the indolenine to the substituted indoline, followed by oxidation of the indoline to the nitrone. The nitrone could then be subjected to another allylation, which gives the di-allylated indoline upon workup. [64-65]

Scheme 1.19. Alternative Synthesis (shown on one side of core).

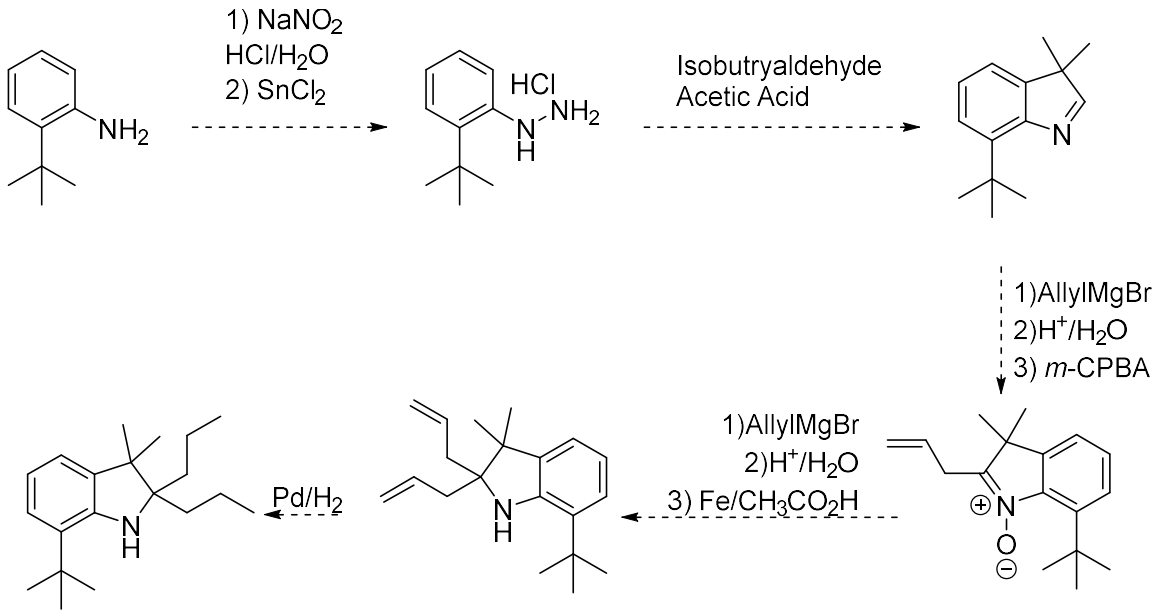

1.2.8 Synthetic Strategies towards OHPQ-based Aminyl Radical Precursors

Octahydropyridoquinoline (OHPQ)-based aminyl radicals are another class of aminyl radicals that are of interest to our group. An alternative path towards them beginning with 2,6-diamino-*tert*-butyl benzene, following a series of reactions performed in the literature[62] on 2-*tert*-butyl aniline as shown in Scheme 1.20. This simple set of reactions is essentially an amide formation between a protected amine and acyl chloride, followed by a 6-endo-*trig* ring closure via a Friedel-Craft-like electrophilic aromatic substitution.

Scheme 1.20. Literature example of potential intermediate towards OHPQ molecule.

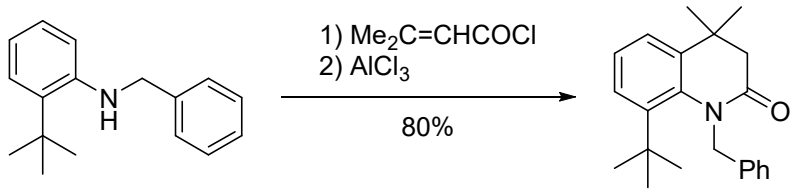

The literature notes that in the absence of the *N*-benzyl protecting group, cyclization was accompanied by loss of the *tert*-butyl group. Looking deeper into the manuscript, they didn't explicitly say whether they isolated the amide cyclization precursor or not. Based on our past experience with 2,6-diamino-*tert*-butyl benzene and its similar compounds, it's possible that the *tert*-butyl group could be lost under strongly acidic conditions, as previously discussed in Section 1.2.5. It's also possible their acylation procedure was too harsh, as it did not have a base to neutralize the HCl produced from the reaction. We've had past success with a similar acylation of 2,6-diamino-*tert*-butyl benzene towards the di-isatin precursor by adding K_2CO_3 as described in Section 0. Additionally, due to the weaker electron donating ability of the amide vs. the free amine, we successfully closed the isatin ring using acidic conditions via an electrophilic aromatic substitution mechanism. It would be reasonable to assume that this reaction would be possible without protection on the diamine.

Nonetheless if needed, the resulting deprotection of the amide followed by exhaustive addition of allyl Grignard would give a product of unique interest to our group and similar to other intermediates synthesized previously by our group, but with the more sterically shielding *tert*-butyl group at the core. An example of the synthesis applied from 2,6-diamino-*tert*-butyl benzene (**44**) is shown in Scheme 1.21.

Scheme 1.21. Literature synthesis applied to 44.

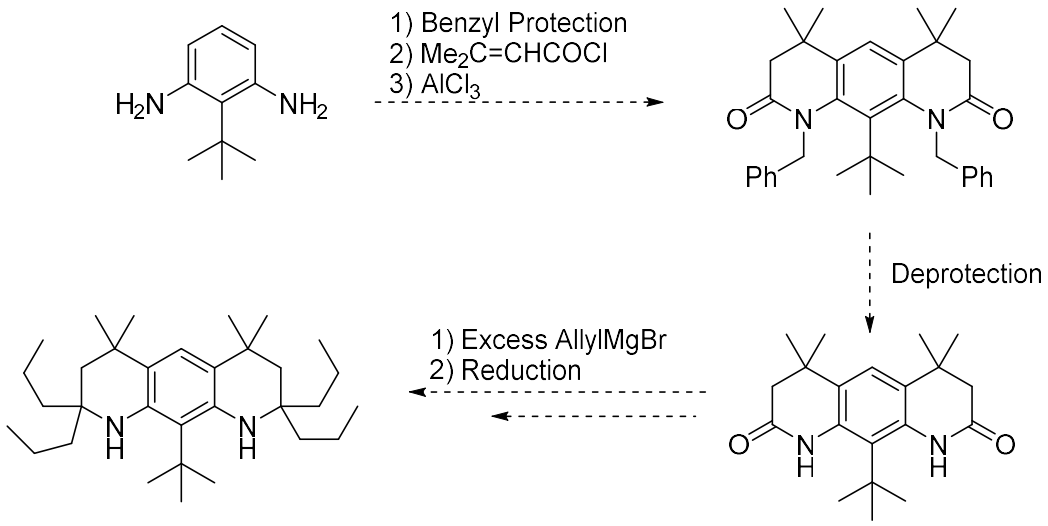

1.2.9 Methods towards Construction of Quaternary Carbons

Fundamental to the synthetic strategy towards our amine precursors are methods[57] to construct quaternary centers to provide stability at labile positions within the molecule. Currently and previously, our group has been able to establish a quaternary site by acid-catalyzed Friedel-Crafts-like alkylation of a substituted alkene onto another aromatic ring. This method proves difficult though on molecules where there is a *tert*-butyl group in an electronically activated position (i.e. *ortho* to two amine groups) and the *tert*-butyl groups serves as a better leaving group than hydrogen for the alkylation. Thus, the loss of the *tert*-butyl group in this step negates the work of installing it earlier in the synthesis.

Examples of alkylation of various functional groups giving quaternary carbons exist in the literature[57], but are usually driven by unique structural features. Amides and lactams, for example have shown promise as substrates for geminal dialkylation or diallylation of the carbonyl oxygen through Grignard addition to activated amides;[66]

allylboration;[67-68] thioamide intermediates using Lawesson reagent and organometallics;[69] or organotitanium reagents.[70-72]

The driving force for the reaction is the generation of a stabilized iminium ion intermediates as seen in Scheme 1.22. Other carbonyl types that have been shown to undergo dialkyl substitution are ketones[73-74] and acid chlorides[75-76] using pyrophoric solutions of trimethylaluminum or methyltitanium chloride reagents.

Scheme 1.22. Proposed mechanism of dialkylation of carbonyls.[57]

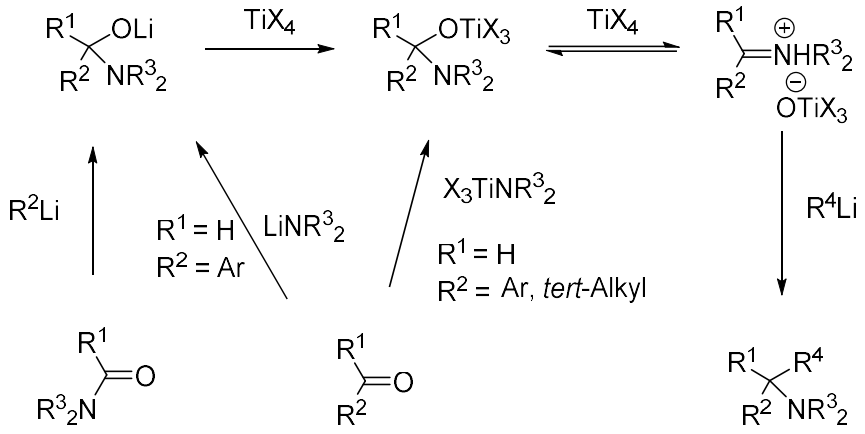

Our group[30] has had some limited success in the diallylation of diketones using excess amounts of allyl Grignard, with difficult purifications and yields around 20%. This also necessitates a subsequent hydrogenation with yields around 86 to 95%. Other avenues may be more attractive.

1.2.9.1 Alkylation of Trifluoromethyl Groups using Grignard Reagents

Another functional group that shows promise in exhaustive alkylation to the quaternary carbon is aromatic trifluoromethyl groups. Several different papers from the

Strekowski group in the 1994 and 1997 have shown different outcomes of the Grignard alkylation of 2- and 4-trifluoromethylaniline depending upon substitution of the aniline; solvent choice; and choice of Grignard. In some cases, Grignard addition leads to the reaction of the trifluoromethyl group to a substituted vinyl group, the authors proposed mechanism is shown in Scheme 1.23.[77] This provides a possible synthon for late-stage functionalization of the trifluoromethyl group.

Scheme 1.23. Proposed mechanism for Grignard addition to 2-(trifluoromethyl)anilines.[77]

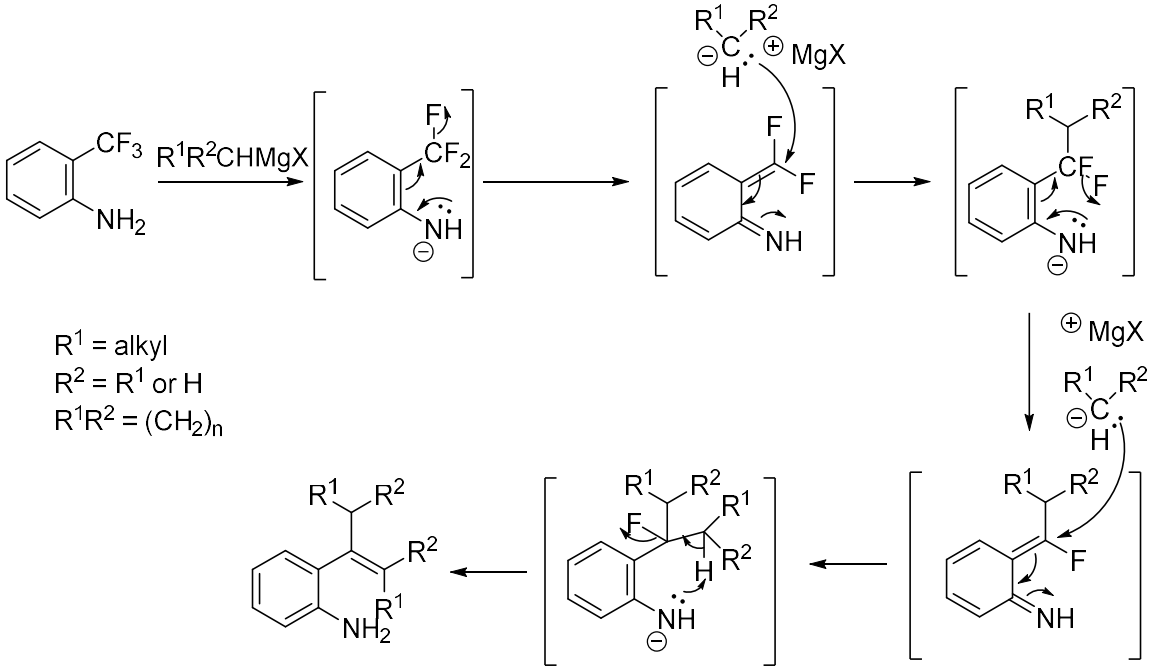

In these papers they reported the reaction of *ortho*-substituted trifluoromethyl anilines with primary and secondary alkyl Grignards resulted in their respective 1-alkenyl anilines. Of note, their reaction conditions used mostly RMgCl Grignard's in diethyl ether including (*iso*-propyl, *iso*-butyl, *n*-butyl, cyclopentyl, and cyclohexyl). We were interested in creating a substituted-vinyl group adjacent to the amine using methyl

Grignard. When we attempted to use their conditions with 3.0 M MeMgBr in Et_2O on 2-(trifluoromethyl)aniline (**63**) as a test reaction, we clearly saw the predominant product as 2-(*tert*-butyl)aniline in the crude ^1H NMR as shown in Figure A-1 and Figure A-2. The aromatic region of proton NMR for the crude reaction mixture is shown in blue, the crude shows a predominant spectra corresponding with 2-(*tert*-butyl)aniline (**56**) which is shown in red. The alkyl region is represented the same way in Figure A-2. This was contrary to what we expected (but similar to results they reported for 4-(trifluoromethyl)anilines), we also attempted the reaction with CuI added as a modifier and performed the reaction in THF to see if there were any noticeable solvent effects (as the authors suggested in the Grignard reaction of 4-(trifluoromethyl)aniline), in which case we did not observe any additional products. One possible explanation is that the difference between the methyl group (which they did not use) and the cyclohexyl, isopropyl, and *n*-butyl groups is significant enough to hinder the addition of the last Grignard species, allowing the intramolecular amine-assisted elimination to predominate.

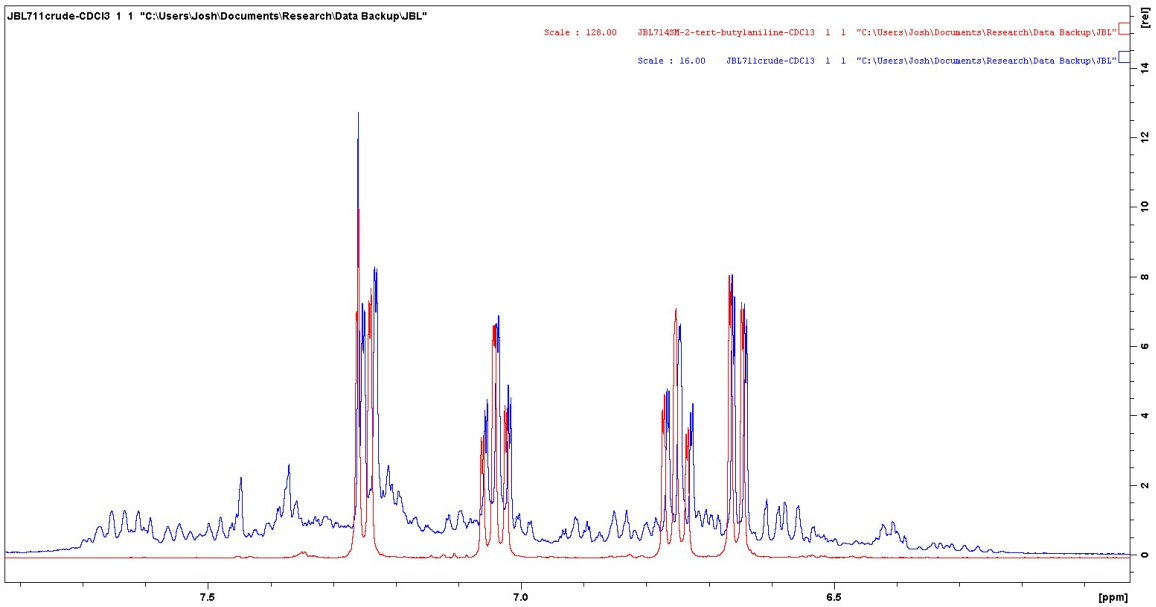

Figure A-1. Aromatic region of ^{1}H NMR for JBL711crude (blue) and 2-*(tert*-butyl)aniline (red).

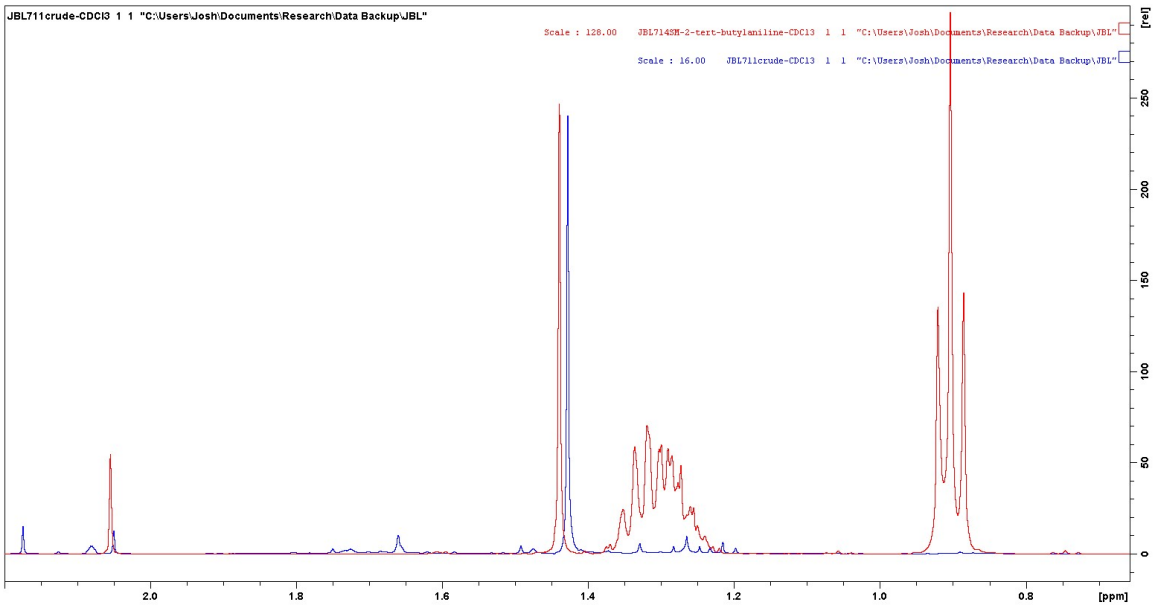

Figure A-2. Alkyl region of ^{1}H NMR for JBL711crude (blue) and 2-(tert-butyl)aniline (red).

In the case of 4-(trifluoromethyl)aniline, the authors reported the Grignard reaction of the trifluoromethyl group provides for transformation to trialkyl-substituted group, via the mechanism proposed in Scheme 1.24.[78] If able to control the outcomes

efficiently, either of the reaction pathways would be of great value in the synthesis of sterically-hindered amines. Without the position of the amine adjacent to the trifluoromethyl group, it can't facilitate the elimination after the addition of the second equivalent of alkyl Grignard of the mechanism in Scheme 1.23 to generate the alkene. In the *para*- position the resulting final intermediate can be attacked by another equivalent of Grignard or another nucleophilic molecule (possibly another aniline molecule); the authors note the observation of these alternate product pathways for alkyl Grignard's in THF but not in Et_2O. The authors also note that when using more nucleophilic Grignard reagents such as allyl or benzyl Grignard that the tri-substituted products still dominate in both THF and Et_2O.

Scheme 1.24. Proposed mechanism for Grignard addition to 4-(trifluoromethyl)anilines.[78]

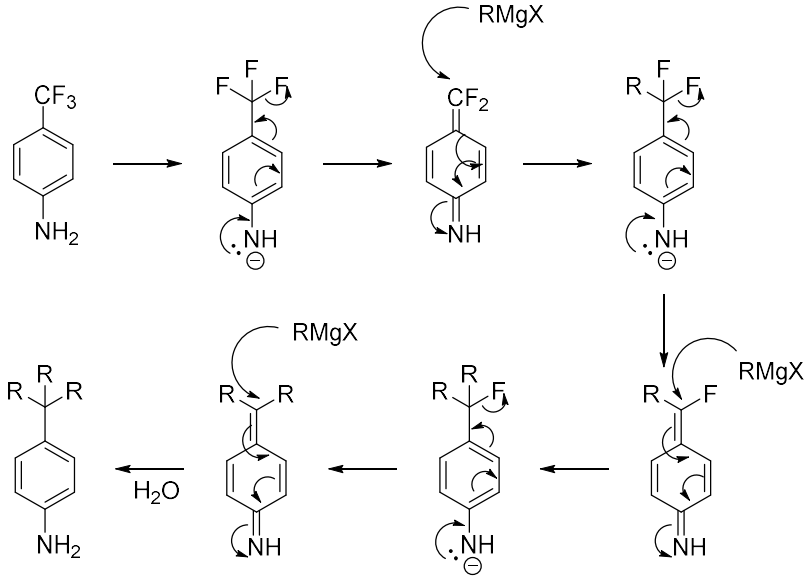

Observing that the addition of methyl Grignard to 2-(trifluoromethyl)aniline actually resulted in the *tert*-butyl product we attempted a Hail Mary reaction on a small

amount of (**64**) that had been previously synthesized and saved by our group, as seen in Scheme 1.25. Crude NMR of this reaction mixture showed a clear mixture of SM and the alkene product as shown in

Figure A-3 and Figure A-4. 2-D COSY NMR of the reaction mixture showed clear coupling between the two alkene protons with the methyl group as seen in Figure A-5. Processing of the ^{1}H NMR to remove the background starting material clearly shows the alkene product (**65**). None of the *tert*-butyl product was observed. We also attempted allylation of the same compound using allyl Grignard to see if the increased nucleophilicity of the allyl group vs. the alkyl group would favor tri-allylation. The NMR was inconclusive; however preliminary ESI of this reaction does show a mass that matches that of the tri-alkylated product.

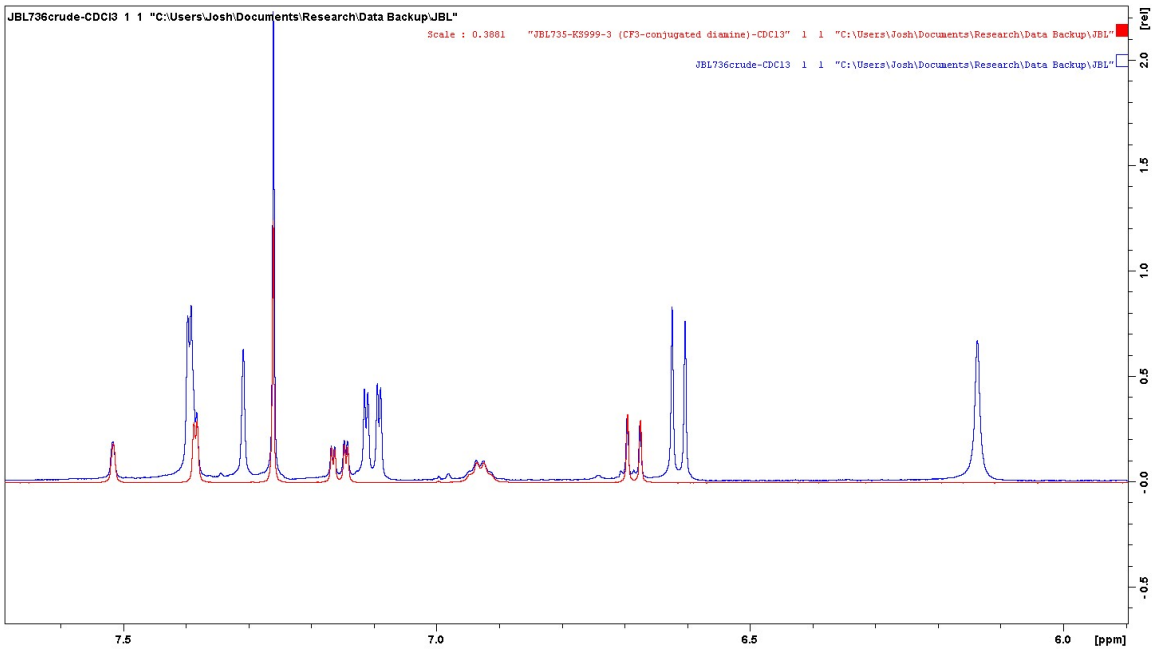

Figure A-3. Aromatic region of ^{1}H NMR of JBL 736crude (blue) and SM (red).

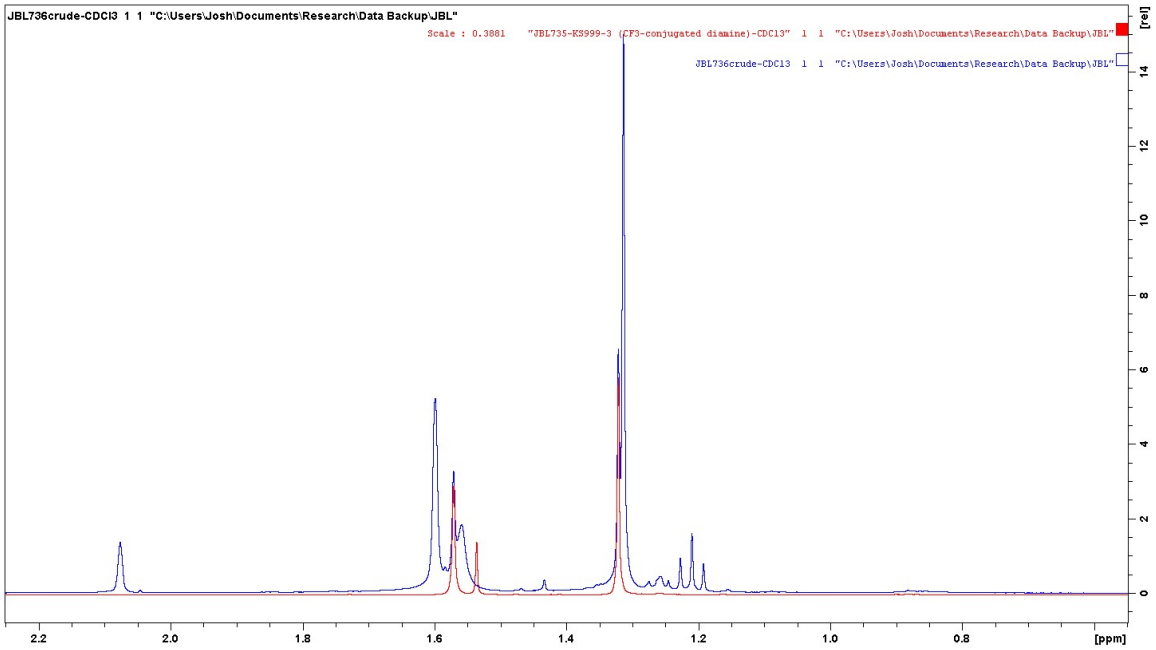

Figure A-4. Alkyl region of 1H NMR of JBL 736crude (blue) and SM (red).

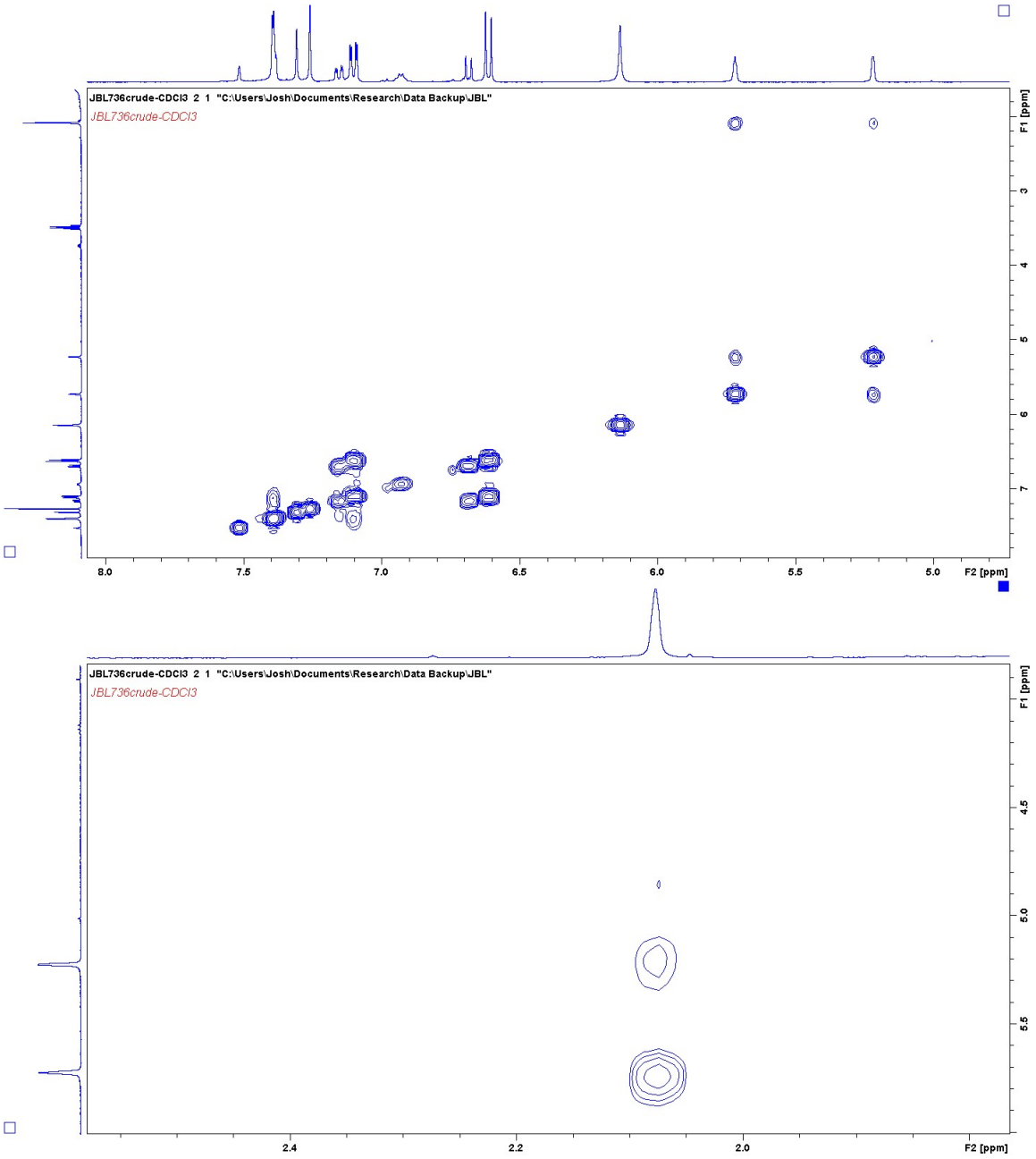

Figure A-5. 2-D COSY showing alkene coupling in JBL736crude.

Scheme 1.25. Attempts of Exhaustive Grignard alkylation and allylation on 64.

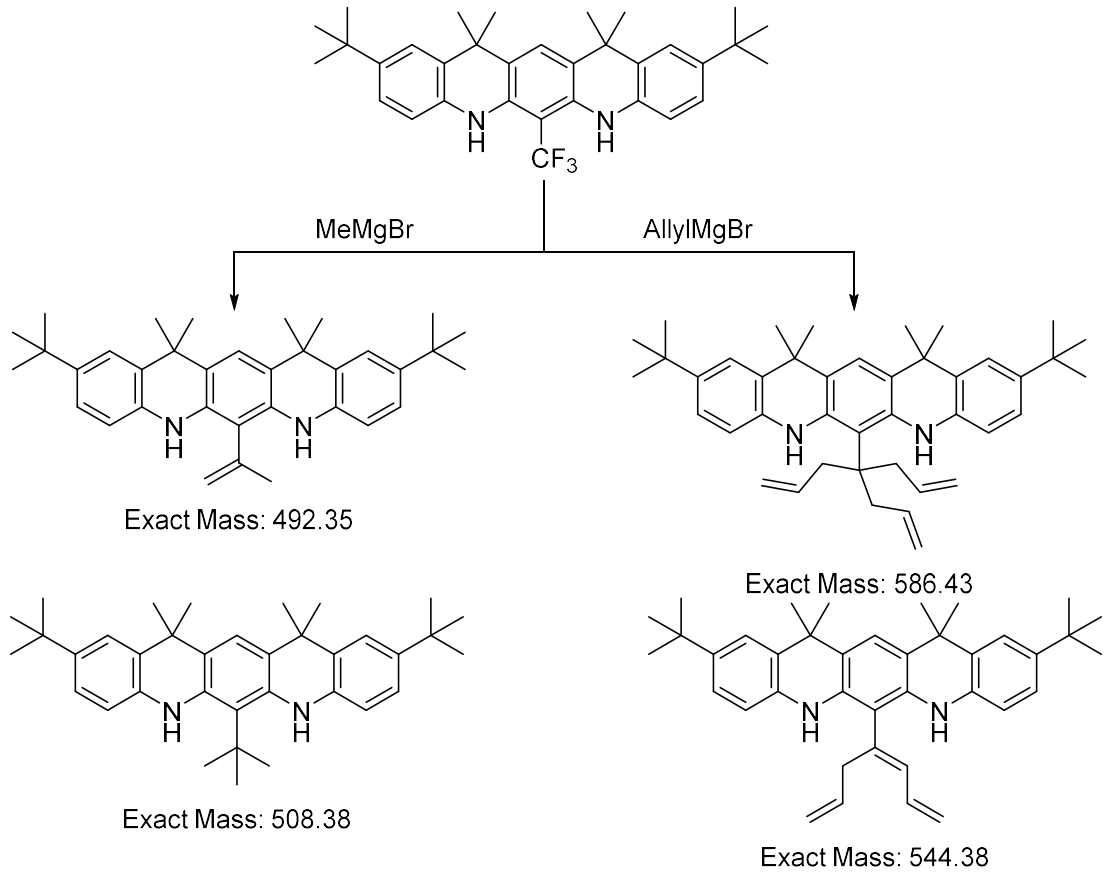

1.2.9.2 Alkylation of Trifluoromethyl Groups with Organoaluminum Reagents

Another group has also shown promising alkylation's of trifluoromethyl groups using trimethyl aluminum.[79] The mechanism is quite different from the Grignard process above, but provides several potentially interesting and useful outcomes. A proposed reaction mechanism is shown in Scheme 1.26, as we can see it proceeds via a carbocation intermediate that could undergo E_1, Friedel-Crafts-like alkylation, or exhaustive alkylation. If these pathways were optimized, each outcome could be useful in synthesis of aza-*m*-phenylene ring systems and steric protection of each radical site. An example of potential methods using trialkyl aluminum reagents to achieve multiple synthetic goals is shown in Scheme 1.27 and Scheme 1.28.

Scheme 1.26. Literature example of outcomes of $AlMe_3$ addition.[79]

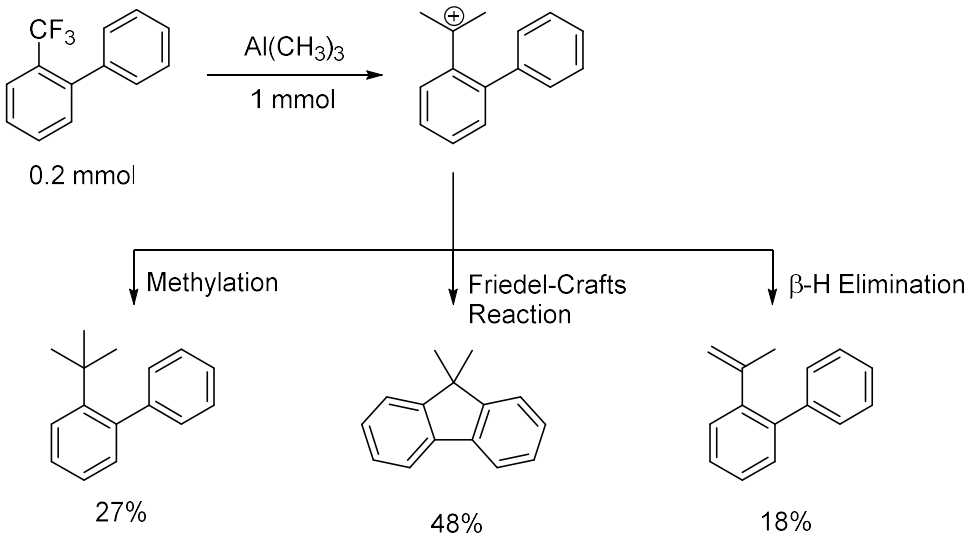

As part of our investigation of Grignard reactions towards trifluoromethyl anilines, we also attempted alkylation of compound **64** with trimethyl aluminum in Toluene:DCE, in this case compared to the ESI for the alkylation with methyl Grignard, the mass corresponding to the *tert*-butyl alkylated product is seen along with a mix of alkene by product.

Scheme 1.27. Reaction of $AlMe_3$ with 64.

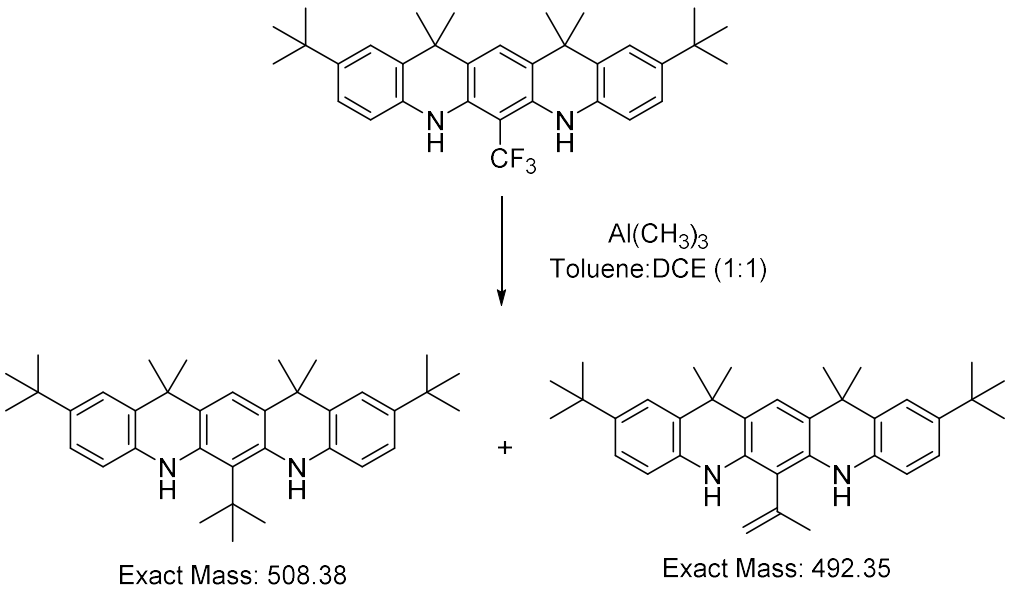

1.2.9.3 Perdeuterated-Alkylation of Aromatic Trifluoromethyl Groups

These methods towards exhaustive alkylation of the trifluoromethyl group also provides potential entry into perdeuterated *tert*-butyl groups as steric protecting groups adjacent to aminyl radical sites. If methods using alkyl Grignard's prove successful, using perdeuterated alkyl Grignard sources should translate. Alternatively, methods to make perdeuterated trimethyl aluminum already exist[80], and would also allow for possible synthesis of perdeuterated *tert*-alkyl protecting groups. This may prove very interesting in the study of organic radicals, allowing further investigation[81] into the kinetic isotope effect on stability for sterically protected aminyl radicals. This ultimately could be another feasible method to improve organic radical stability.

Scheme 1.28. Application of $AlMe_3$ as *tert*-butyl synthons towards sterically-hindered diamines of interest to our group.

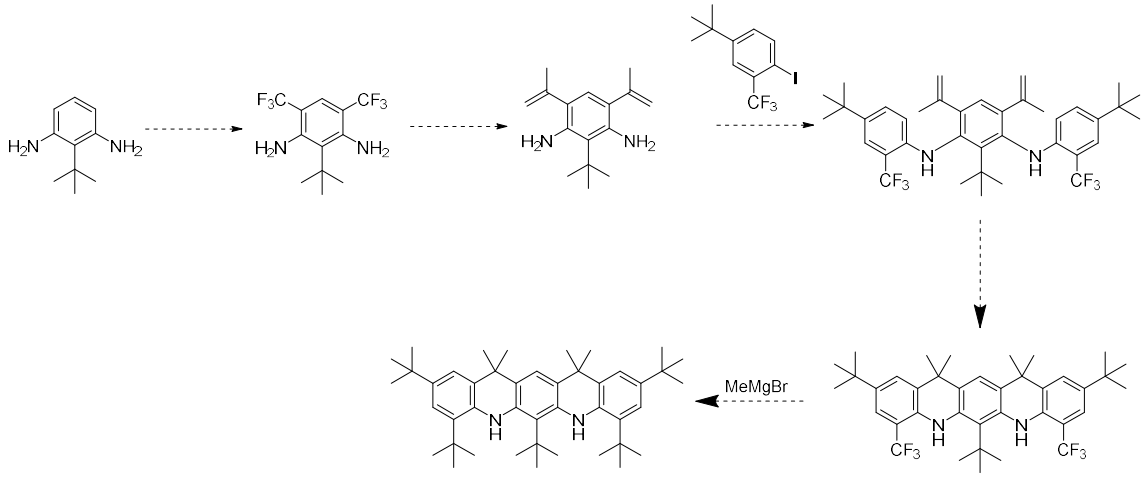

The successful late-stage substitution of *tert*-alkyl groups for trifluoromethyl groups would have several benefits over current strategies. First, since introducing the bulky *tert*-alkyl groups late in the synthesis would not hinder as many synthetic steps; potentially increasing yield or even allowing reactions that were previously not possible with the *tert*-butyl groups already on the molecule, i.e. loss of *tert*-butyl group under acidic conditions or coupling reactions that may be impossible due to the steric hindrance (or comparison-sake, the A-value for $–C(CH_3)_3$ [4.9 kcal/mol][82] is almost twice that of $–CF_3$ [2.4-2.5 kcal/mol][83] or $–CH(CH_3)_2$ [2.21 kcal/mol][84], both of which have many more successful examples of Buchwald-Hartwig coupling). Second, using trifluoromethyl may reduce the number of synthetic steps towards ring closing of the aza-*m*-phenylene ring system; you can go from the trifluoromethyl group to a closed-ring potentially in one-step, while current methods employed from a carboxylic acid group require four steps including esterification, Grignard alkylation, elimination of the resulting alcohol, and finally ring closure of the alkene. Lastly, it allows the introduction

of perdeuterated alkyl groups late in the synthesis, which makes it more cost-effective and versatile, compared to introducing perdeuterated groups early in the synthesis.

1.2.9.4 Trifluoromethylation of Aromatic Amines

In order to take advantage of transformations of the trifluoromethyl group, we need a reliable method to install them onto the aromatic ring. The use of expensive trifluoromethylation reagents such as Umemoto[85] and Togni reagents proved unreliable. We even attempted synthesis of Umemoto reagent with poor yield and purity.[86] We were only able to recover 103 mg of product in 8.7% yield (MKK137/152).

Ultimately, we did have some success using a literature procedure using CF_3I in the presence of Fe(II), H_2O_2, and DMSO,[87] a cheaper and more reliable method in our hands. This protocol is essentially a Minisci-type reaction that has found recent success in some large-scale pharmaceutical trifluoromethylations.[88-89] The mechanism for this reaction is shown in Scheme 1.29, it is a radical process beginning with Fe^{2+} decomposition of H_2O_2 to generate a highly reactive hydroxyl radical, which then indiscriminately adds to DMSO to generate a radical adduct of DMSO (the excess of DMSO as solvent minimizes indiscriminate unwanted side reactions of the very reactive hydroxyl radical). This adduct undergoes a rapid β-scission that eliminates a methyl radical which selectively reacts with the alkyl halide (in our case CF_3I) to give the stabilized CF_3 radical which then does a radical addition to the aromatic ring, with the product forming upon reaction of the radical with Fe(III).[90-91] In practice, we found the gaseous CF_3I easier to handle and store as an adduct complexed with DMSO.[92] Without

time to explore this further in depth, this seemed to be a promising method for future trifluoromethylation needs in our lab.

Scheme 1.29. Radical steps of CF_3 addition to aromatic rings.

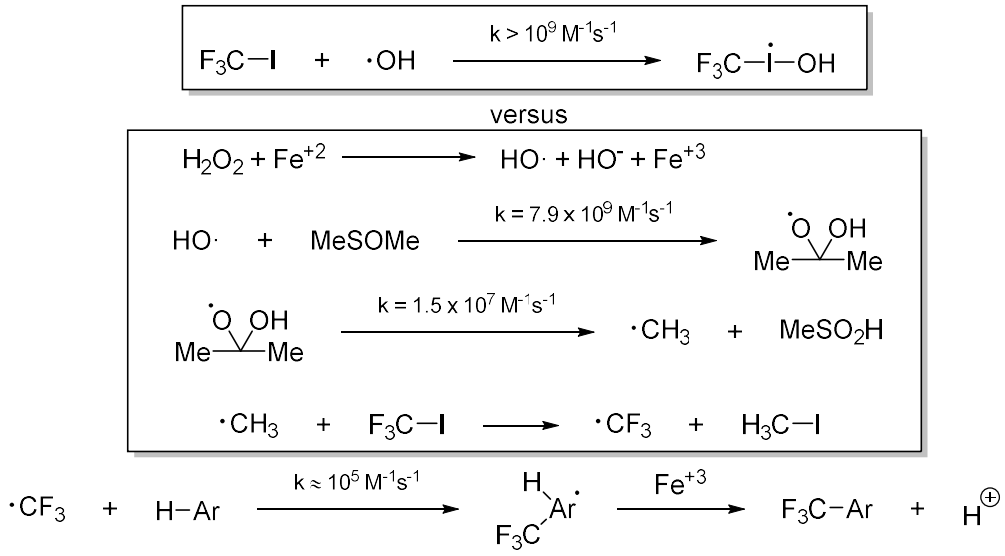

1.3 Conclusion

Although the ultimate objective of this project has not yet been realized in the synthesis and characterization of either of the aminyl diradical targets, we were able to establish several different methods that can be used to complete the project in the future. Additionally, we made several other valuable contributions creating several novel compounds and improving synthetic methods towards sterically-hindered target molecules.

Specifically, to our knowledge there are no other reports of any synthetic targets using a *tert*-butyl diamine or successfully creating the di-isatin motif and the additional reactions from isatin. Successful synthetic paths towards these compounds may allow investigation of compounds with similar motifs in other areas of chemistry.

Additionally, we were able to show expanded scope of the Buchwald-Hartwig reaction using TnPP as a ligand using more hindered coupling partners than previously reported. Further, we were able to develop a modified procedure for the convenient and facile synthesis and purification of TnPP, potentially improving the availability or its synthesis by other groups.

We were also able to expand on the previous investigation of Grignard reactions with trifluoromethylaniline compounds and show a better understanding for which reaction pathway was preferred forming the trialkylated or alkene product. Better understandings of methods that lead to quaternary carbons are important in the synthesis of many molecules.

1.4 Experimental Section

General procedures and materials

For large scale reactions, all solvents were freshly distilled, e.g., benzene and toluene (from sodium), ether and THF (from sodium benzophenone), or alternatively obtained from solvent purification system. Per-deuterated solvents for NMR spectroscopy were obtained from Cambridge Isotope Laboratories. All other commercially available chemicals were obtained from either Aldrich or Acros, unless indicated otherwise. Column chromatography (0–20 psig pressure) was carried out on silica gel or silica gel or deactivated silica gel (typically 3% triethylamine in pentane). Analytical and preparative TLC plates (Analtech silica plates, tapered with a preadsorbent zone) were typically deactivated with 3% triethylamine in pentane immediately before use. Standard

techniques for synthesis under inert atmosphere, using Schlenk glassware and gloveboxes (Vacuum Atmospheres), were employed.

NMR spectroscopy

NMR spectra were obtained with a Bruker spectrometer (^{1}H, 300, 400, 600 and 700 MHz) using chloroform-*d* ($CDCl_3$), benzene-d_6 (C_6D_6), dimethyl sulfoxide-d_6 (DMSO-d_6) and acetone-d_6 as solvent. The chemical shift references were as follows: (^{1}H) chloroform-*d* 7.26 ppm; (^{13}C) chloroform-*d*, 77.00 ppm (chloroform-*d*), (^{1}H) benzene-d_6, 7.15 ppm; (^{13}C) benzene-d_6, 128.39 ppm; (^{1}H) DMSO-d_6, 2.50 ppm; (^{13}C) DMSO-d_6, 39.50 ppm; (^{1}H) acetone-d_5, 2.05 ppm; (^{13}C) acetone-d_5, 29.92 ppm (acetone-*d*6). Typical 1D FID was subjected to exponential multiplication with a line broadening exponent (LB) of 0.3 Hz (for ^{1}H) and 1.0 – 2.0 Hz (for ^{13}C). For selected spectra, smaller (or negative) values of LB and additional Gaussian multiplication (GB) were used, to resolve closely spaced resonances, as indicated in the spectral data summaries. IR spectra were obtained using a Nicolet Avatar 360 FT-IR instrument, equipped with an ATR sampling accessory (Spectra Tech, Inc.). A few drops of the compound in CH_2Cl_2 were applied to the surface of a ZnSe ATR plate horizontal parallelogram (45°, Wilmad). After the solvent evaporated, the spectrum was acquired (2-cm^{-1} resolution).

Mass spectrometry

EI and ESI MS analyses were carried out at the Nebraska Center for Mass Spectrometry.

1.4.1 Synthesis of Buchwald-Hartwig Halogen Coupling Partners

1-bromo-2,4-di-(tert-butyl)benzene (28)

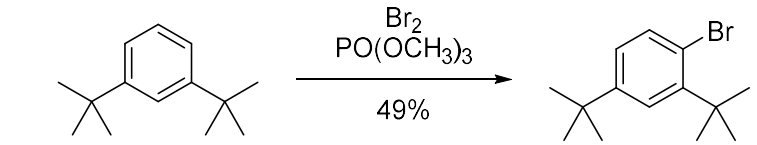

Molecular Weight: 190.33 Molecular Weight: 269.23

Run	SM (g/mmol)	Br_2 (Total) (mL/mmol)	$PO(OCH_3)_3$ (mL)	TM (g)	Yield (%)	TM label
JBL103	0.1096 / 0.5768	0.1051 / 0.6578	1.58	0.140	89.7	JBL107crude
JBL107	1.5775 / 8.302	1.9 / 11.8	23.25	1.10	49.2	JBL110crude

JBL107: Following a literature[32] procedure, 1,3-di-(*tert*-butyl)benzene (1.5 g, 8.302 mmol, 1 equiv) was dissolved in trimethyl phosphate (8.25 mL) and was heated at 70°C and stirred. A solution of Br_2 (1.9 g, 11.8 mmol, 1.25 equiv) was dissolved in trimethyl phosphate (15 mL) and added to the above solution in two portions (4.5 g, 0 hours) and (0.5 g, 6 hours later). The reaction was stirred overnight at 70°C. The reaction mixture was extracted with hexane and then washed with Na_2SO_3 and brine and then dried on $MgSO_4$. The solvent was then evaporated, and the crude product was obtained as an oil (1.1002 g, 49.2%). ^{1}H NMR (400 MHz, $CDCl_3$, JBL108crude): δ 7.489 (d, 8.3 Hz, 1H), 7.466 (d, 2.5 Hz, 1H), 7.046 (dd, 8.3 Hz, 2.5 Hz, 1H), 1.302 (s, 9H).

1-bromo-4-(tert-butyl)-2-nitrobenzene (31)

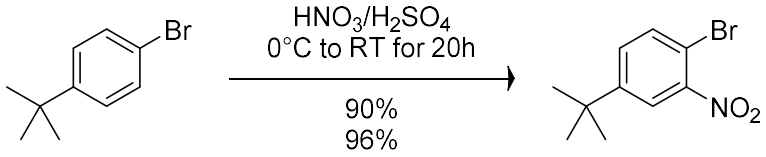

Molecular Weight: 213.12 Molecular Weight: 258.12

Run	SM (g/mmol)	HNO_3 (mL)	H_2SO_4 (mL)	TM (g)	Yield (%)	TM label
JBL102	1.22 / 5.73	0.55	0.78	1.340	90.5	JBL102crude
JBL105	5.09 / 23.9	2.3	3.2	5.904	95.8	JBL105crude

JBL105: Following a literature[33] procedure, sulfuric acid (3.2 mL, 2.5 equiv) was slowly added to nitric acid (2.3 mL, 1.5 equiv) at 0°C. The aqua regia mixture was carefully added to 1-bromo-4-(*tert*-butyl)-benzene (**1**) (5.09 g, 23.9 mmol, 1 equiv) at 10°C and allowed to warm to ambient temperature for 20 hours while stirring. The reaction mixture was diluted with H_2O and then extracted with Et_2O and dried with $MgSO_4$. The crude compound (5.9 g, 95.8%) was obtained after evaporation of the organic solvent. ^{1}H NMR (400 MHz, $CDCl_3$, JBL105crude): δ 7.828 (d, 2.3 Hz, 1H), 7.638 (d, 8.5 Hz, 1H), 7.442 (dd, 8.5 Hz, 2.3 Hz, 1H), 1.338 (s, 9H).

2-bromo-5-(tert-butyl)aniline (32)

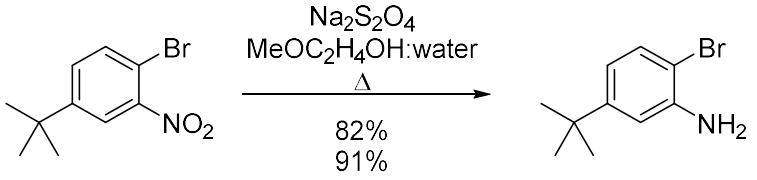

Molecular Weight: 258.12 Molecular Weight: 228.13

Run	SM (g/mmol)	$Na_2S_2O_4$ (g/mmol)	2-methoxyethanol (mL)	H_2O (mL)	TM (g)	Yield (%)	TM label
JBL104	1.01 / 3.91	2.51 / 14.39	6[a]	6	0.743	30	JBL108crude
JBL106	0.743 / 2.88	2.47 /14.19	6[b]	6	0.538	81.9	JBL108crude
JBL108	5.90 / 22.87	14.64 / 84.08	35	35	4.77	91.5	JBL108crude

[a] 1:1:2 ratio of 1,2-dimethoxyethane:Ethylene Glycol:Water; NMR and GC showed only 30% conversion
[a] Continued reduction of JBL104 in 1:1 ratio of 2-methoxyethanol:water

JBL108: Modifying a literature[33] procedure, **31** (5.90 g, 22.87 mmol, 1 equiv) was dissolved in solution of 2-methoxyethanol/water (1:1, 70 mL total volume) and refluxed with stirring for 6 hours after the addition of $Na_2S_2O_4$ (14.62 g, 84.08 mmol, 3.67 equiv). A solution of HCl and H_2O (1:1, 60 mL total volume) was added to the reaction flask and refluxed for 15 minutes. The reaction mixture was then poured into ice water (50 mL) and solid Na_2CO_3 was added until basic. The product was extracted with Et_2O (75 mL) and dried over $MgSO_4$. The crude compound (4.77g, 91.5%) was obtained after evaporation of the organic solvents. ^{1}H NMR (400 MHz, $CDCl_3$, JBL108crude): δ 7.305 (d, 8.4 Hz, 1H), 6.789 (d, 2.3 Hz, 1H), 6.657 (dd, 8.4 Hz, 2.3 Hz, 1H), 1.264 (s, 9H).

1-bromo-4-(tert-butyl)-2-iodobenzene (33)

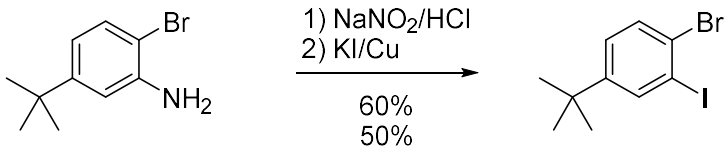

Molecular Weight: 228.13 Molecular Weight: 339.01

Run	SM (g/mmol)	$NaNO_2$ (g/mmol)	KI (g/mmol)	H_2O (mL)	HCl (conc.) (mL)	TM (g)	Yield (%)	TM label
JBL109	1.01 / 4.44	0.333 / 4.83	1.09 / 6.56	7.88	1.65	0.892	59.5	JBL109cr
JBL110	3.35 / 14.63	1.18 / 17.10	4.89 / 29.42	26.2	5.5	2.51	50.6	JBL110cr

JBL109: Following a literature[33] procedure, **32** (1.01 g, 4.44 mmol, 1 equiv) was dissolved in H_2O:HCl (6.875 mL:1.65ml), and then a solution of $NaNO_2$ (0.3325 g, 4.83 mmol, 1.1 equiv in 1 mL H_2O) was added dropwise at 5°C and stirred for 10 minutes. A solution of KI (1.09 g, 6.56 mmol, 1.5 equiv in 1.675 mL H_2O) and spatula tip of copper powder was added and stirred for 15 minutes without cooling, then for 15 minutes at 50°C and 80°C. The solution was cooled to 0°C and a solution of sodium sulfite (5%, 5 mL) was added. The organic layer was separated and the aqueous layer extracted with Et_2O (25 mL, 3 times). The combined organic solvents were then dried with $MgSO_4$ and then evaporated, yielding the crude product (0.892 g, 59.5%). ^{1}H NMR (400 MHz, $CDCl_3$, JBL108crude): δ 7.841 (d, 2.3 Hz, 1H), 7.515 (d, 8.4 Hz, 1H), 7.216 (dd, 8.4 Hz, 2.3 Hz, 1H), 1.281 (s, 9H).

1.4.2 Synthesis from Musk Ketone towards Diamine core

Musk Ketone Starting Material (34)

^{1}H NMR (400 MHz, $CDCl_3$, JBL113SM): δ 2.5011 (s, 3H), 2.1047 (s, 6H), 1.4413 (s, 9H). ^{13}C NMR (400 MHz, $CDCl_3$, JBL113SM): δ 203.68, 150.61, 143.32, 132.17, 126.98, 37.54, 32.29, 30.44, 14.99.

4-(tert-butyl)-2,6-dimethyl-3,5-dinitrobenzoic acid (36)

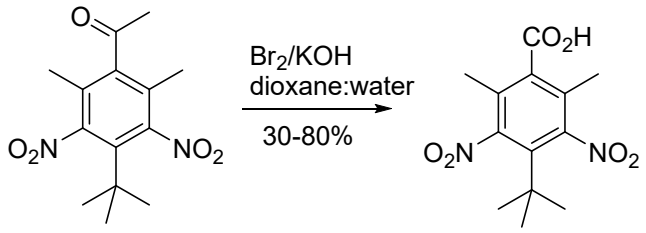

Molecular Weight: 294.31 Molecular Weight: 296.28

Run	SM (g)	KOH (g)	Br_2 (mL)	Dioxane (mL)	H_2O (mL)	TM (g)	Yield (%)	TM label
JBL115	0.694	3.00[1]	1.2	10	4	0.3171	45.3	JBL115c1
JBL122	0.994	4.44	1.3	36	17	0.8459	84.0	JBL122cr
JBL123	3.586	15.29	4.6	126	60	1.7803	49.3	JBL123cr
JBL125	10.33	43.06	13	150	170	6.2471	60.1	JBL125cr
JBL128	20	86	26	300	340	13.184	65.5	JBL125cr
JBL137	40	172	52	500	640	12.558	31.6	JBL142c1
JBL142	40	172	52	600	640			
JBL146	40	172	52	600	640	12.284	30.5	JBL146c1

JBL142: Br_2 (52 mL, 1.008 mol, 7.4 equiv) was carefully added to a solution at 0°C of KOH (172 g, 3.064 mol, 22.55 equiv) dissolved in H_2O (640 mL) and stirred. Musk ketone (40 g, 135.9 mmol, 1 equiv) was dissolved in dioxane (600 mL) and then added to the KOH/Br_2 solution. The reaction sat for 1 hour stirring and then was refluxed

for 6 hours. Na_2SO_3 (6 g) was added to the reaction after cooling on ice. The reaction mixture was washed with Et_2O (5 x 100 mL) and the aqueous extract was then acidified with HCl at 0°C. The solution was allowed to precipitate out and was collected via vacuum filtration, yielding yellow-orange solid that also contained inorganic salts. A continuous extraction using a Soxhlet apparatus was performed to extract the product from the solids with toluene (200 mL). After running for 12 hours and then sitting overnight, the organic solid was collected via vacuum filtration and then rinsed with hexane to remove the orange color, leaving a yellow solid (12.5583 g, 31.6%). Filtrate was saved and combined with JBL137 residue for further possible extraction. ^{1}H NMR (400 MHz, $CDCl_3$, JBL115recrystallized): δ 9.250 (br, 1H), 2.272 (s, 6H), 1.454 (s, 9H). ^{13}C NMR (400 MHz, $CDCl_3$, JBL115recrystallized): δ 171.0, 150.5, 134.6, 133.6, 129.3, 37.7, 30.4, 15.9.

3-(tert-butyl)-1,5-dimethyl-2,4-dinitrobenzene (37)

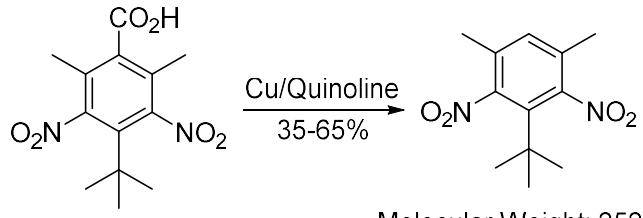

Molecular Weight: 296.28 Molecular Weight: 252.27

Run	SM (g)	Cu (g)	Quinoline (mL)	TM (g)	Yield (%)	TM label
JBL124	0.2124	0.1	2	0.2135	100	JBL129crude
JBL129	1.5678	0.7662	10	0.8459	65.4	JBL129crude
JBL131	5.9997	3.0	40	2.787	54.6*	JBL131column1
JBL143	12.5583	6.25	84	4.546	42.5	JBL143crude

JBL149	12.284	5.351	84	4.01	38.3	JBL149crude

JBL131: Preheated sand bath to 200°C. **36** (JBL126crop1, 5.9997 g, 20.25 mmol) and Cu powder (3.0 g, 47.21 mmol, 2.33 equiv) were added to quinoline (40 mL) in a round bottom flask with stirring and then heated to reflux (~240°C) for 4 hours. The solution was then extracted with diethyl ether (3 x 50 mL). The organic extract was then washed with HCl (2 M, 5 x 50 mL) and then washed with NaOH (2 M, 2 x 50 mL). The extract was then dried with $NaSO_4$ and then the solvent was evaporated leaving a yellow solid (3.6004 g, 70.5%). The solid was purified via column chromatography (20:1 Hexane/Ethyl Acetate) yielding a white solid (2.7870 g, 54.6%). ^{1}H NMR (400 MHz, $CDCl_3$, JBL143crude): δ 7.139 (s, 1H), 2.230 (s, 6H), 1.440 (s, 9H). ^{13}C NMR (400 MHz, $CDCl_3$, JBL143crude): δ 150.4, 132.2, 132.2, 132.2, 37.5, 30.6, 18.2.

5-(tert-butyl)-4,6-dinitroisophthalic acid (38)

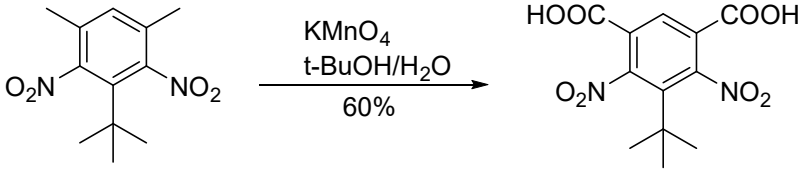

Molecular Weight: 252.27 Molecular Weight: 312.23

Run	SM (g)	$KMnO_4$ (g)	t-BuOH/H_2O (1:1) (mL)	TM (g)	Yield (%)	TM label
JBL139	0.1099	0.266	0.77	0.0142	10.4	JBL139crude
JBL140	0.5	1.33	3.85	0.3912	60.6	JBL140crude
JBL141	1.5351	4.08	11.82	0.7967	41.9	JBL141crude
JBL145	4.546	24.12	35	3.1758	56.4	JBL145crude
JBL151	4.2644	21.75	34	3.5356	67.0	JBL151crude

JBL151: An oil bath was preheated to 90°C. **37** (JBL149crude and JBL150recovered, 4.264 g, 16.90 mmol) was suspended in a solution of H_2O/t-BuOH

(1:1, 34 mL) and stirred. First equivalent of $KMnO_4$ (7.25 g, 45.9 mmol, 2.72 equiv) was added to the suspension and then placed in the oil bath to reflux for two hours. The reaction was then cooled to room temperature and the second equivalent of $KMnO_4$ (7.25 g, 45.9 mmol, 2.72 equiv) was added to the reaction mixture and refluxed for another hour. The reaction was again cooled to room temperature and the final equivalent of $KMnO_4$ (7.25 g, 45.9 mmol, 2.72 equiv) was added to the reaction mixture. The reaction was then put back in the oil bath and refluxed for 17 hours. After being cooled to room temperature it was filtered through a glass funnel and the filtrate was the acidified to pH of 2 with HCl (conc.). The precipitate was extracted with diethyl ether (4 x 30 mL) and then washed with H_2O (2 x 10 mL). The organic solvent was then dried with $NaSO_4$ and evaporated yielding a yellow solid, which was then dried over vacuum (3.5356 g, 67.0%). NMR of JBL151crude showed a 3:1 ratio of dicarboxylic acid to monocarboxylic acid product. ^1H NMR (400 MHz, $CDCl_3$, JBL139crude): δ 8.057 (s, 1H), 1.189 (s, 9H).

Dimethyl 5-(tert-butyl)-4,6-dinitroisophthalate (39)

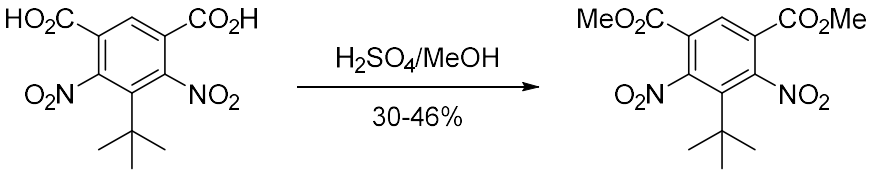

Molecular Weight: 312.23 Molecular Weight: 340.29

Run	SM (g)	H_2SO_4 (mL)	MeOH (mL)	TM (g)	Yield (%)	TM label
JBL154	0.5013	0.4	6	0.1655	30	JBL154crude
JBL155	0.1799	0.35	4	0.0820	41.8	JBL155crude
JBL156	3.0495	4.0	40	1.454	43.7	JBL159col2frac2
JBL158	0.1071	0.14	3	0.0513	43.9	JBL158crude

JBL165	3.4716	4.5	50	1.754	46.3	JBl165crude

JBL156: **38** (JBL145, 3.0495 g, 9.767 mmol) was suspended in MeOH (40 mL) and stirred. H_2SO_4 (conc, 4 mL, 69.10 mmol, 7.07 equiv) was carefully added to the solution. The solution was then refluxed under N_2 for 48 hours. The solution was cooled to room temperature and then extracted with $CHCl_3$ (60 mL) and ice H_2O (50 mL). The resulting aqueous solution was extracted once more with $CHCl_3$ (60 mL) and the organic extracts were combined and then washed with cold saturated $NaHCO_3$ (50 mL). The aqueous phase was extracted with Et_2O (3 x 20 mL). All the organic phases were combined, dried with $NaSO_4$ and evaporated yielding a yellow solid that was dried further under vacuum (2.4 g, 72.2%). The aqueous washes were combined and acidified with conc. HCl and extracted with Et_2O (4 x 20 mL). The organic phase was then dried with $NaSO_4$ and evaporated recovering the starting material (0.224 g). The target material was purified via column chromatography (100% Benzene) to recover two fractions the first fraction was the precursor to the starting material (0.0284 g) and the second fraction was a combination of the mono and diester products (1.757 g). A second column (1:1 Benzene:Hexane) was able to separate the mono and diester products, with the second fraction yielding the diester (1.454 g, 43.7%) and the first fraction the monoester (0.226 g) after evaporation and drying under vacuum. ^{1}H NMR (400 MHz, $CDCl_3$, JBL159colfrac2): δ 8.193 (s, 1H), 3.823 (s, 6H), 1.379 (s, 9H). ^{1}H NMR (400 MHz, acetone-d_6, JBL159colfrac2-acetone): δ 8.358 (s, 1H), 3.929 (s, 6H), 1.496 (s, 9H).

1.4.3 Synthesis towards 2-(*tert*-butyl)-1,3-diamino-benzene

4-(tert-butyl)-3,5-dinitro-benzoic acid (41)

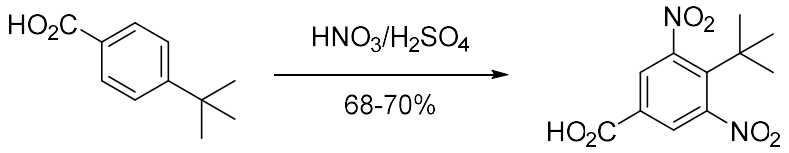

Molecular Weight: 178.23 Molecular Weight: 268.23

Run	SM (g)	HNO_3 (mL)	H_2SO_4 (mL)	TM (g)	Yield (%)	TM label
JBL199*	Recrystallization of compound from AO3_83 in MeOH					JBL199bulkrecrystcr1
JBL209	52.21	52	104	53.13	68	JBL209recrystcrop1+2
JBL321	50.18	50	100	54.2	70	JBL321recrystcrop1+2

*JBL199: Recrystallization in methanol of crude product previously synthesized by Dr. Arnon Olankitwanit of our lab (AO3_83).

JBL321: Fuming HNO_3 (50 mL) was added to 4-*tert*-butyl benzoic acid (52.21 g, 0.293 mol) with good stirring. Once dissolved the reaction was cooled to 0°C in ice bath, causing some precipitation. Fuming H_2SO_4 (100 mL) was then slowly added to the reaction mixture dropwise via an addition funnel at 0°C, causing more precipitation and stirring stopped due to solid formation. Once the addition of H_2SO_4 was completed the reaction was then heated at 80° C for 3 hours. After the heating period, the reaction was cooled to room temperature and poured on to ice (500 mL). The solid yellow precipitate was collected via suction filtration. The solid was then recrystallized from methanol and dried under vacuum. Resulting solid is a mixture of target material and 4-(*tert*-butyl)-3-nitro-benzoic acid as a minor product. ^{1}H NMR (400 MHz, acetone-d_6, JBL199bulkrecrystcrop1): δ 8.288 (s, 2H), 1.509 (s, 9H). ^{1}H NMR of 4-(*tert*-butyl)-3-

nitro-benzoic acid (400 MHz, acetone-d_6, JBL199bulkrecrystcrop1): δ 8.150 (dd, J = 8.4 Hz, 2 Hz, 1H), 8.021 (d, J = 2 Hz, 1H), 7.876 (d, J = 8.4 Hz, 1H), 1.435 (s, 9H).

2-(tert-butyl)-1,3-dinitrobenzene (43)

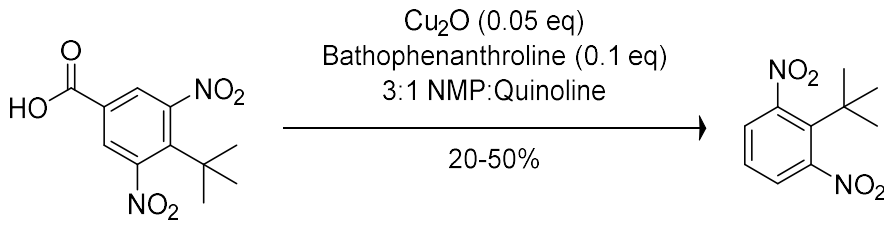

Molecular Weight: 268.23

Molecular Weight: 224.22

Run	SM (g)	Cu_2O (mg)	1,10-phenanthroline (mg)	Quinoline :NMP (mL/mL)	TM (g)	Yield (%)	TM label
JBL195	1.003	0.55	0	6	N/A	N/A	JBL195crude
JBL197	0.268	7.15	18	0.5 / 1.5	0.0449	20.2	JBL197colfrac2
JBL203	1.010	26.7	67.14	2 / 5.8	0.171	20.2	JBL203colfrac2
					0.1605	7.61	JBL203colfrac1
JBL204	1.1	30	68.02	2 / 5.8	N/A	N/A	JBL204crude
JBL207	5	267	671.4	30 / 10	1.7427	41.6	JBL207colfrac2
JBL213a	9.99	545	1330	55 / 20	N/A	N/A	JBL213frac1
JBL213b	10.03	541	1310	55 / 20	N/A	N/A	JBL213frac2

Run	SM (g)	Cu_2O (mg)	Bathoph-enanthr-oline (mg)	3:1 NMP: Quinoline (mL)	Time (hrs)	TM (g)	Yield (%)	TM label
JBL224	1.0022	29.3	0	7.5	22	N/A	N/A	JBL224crude
JBL225[a]	1.0052	41	123.4	7.5	64	0.3073	18	JBL226colfrac2
JBL226	1.0024	41	136.7	7.5	64			
JBL228[b-c]	3.0049	102.5	374	22.5	72	0.8503	34	JBL228colfrac3

JBL231	5.000	213	602.9	37.5	96	1.459	35	JBL231colfrac2
JBL239	3.332	100	400	25	120	2.370	33	JBL247colfrac2
JBL247	5.2265	270	668	37.5				
JBL325[d]	5.150	500	600	40	120	6.921	52	JBL333colfrac2-4cr1
JBL333[d]	10.51	1	1.2	80				JBL333colfrac3-cr2

[a] Previous runs before JBL225 used phenanthroline rather than bathophenanthroline
[b] All runs before JBL228 were worked up with 5 M HCl solution and extracted repeatedly with copious amounts of diethyl ether instead of silica plug with DCM.
[c] JBL228 was worked up the same as previous reactions, but the aqueous layer was also extracted with DCM improving the separation abilities.
[d] Combined JBL325 and JBL333 together and extracted with diethyl ether, then with ethyl acetate, and then with DCM. Combined all organic fractions and evaporated, leaving a brown oil. Then purified with established column conditions and then recrystallized mixed fractions from ethyl acetate/pentane.

Note regarding starting material purity: Must be recrystallized from methanol before use, dinitration side-product (from previous reaction) with one nitro group ortho to carboxylic acid is more reactive to decarboxylation and elutes at same R_f as target material. Mononitrated side-product is allowable as it is less reactive and has much different R_f than target compound allowing purification.

JBL231: Based on methods developed by Gooßen[41], **41 (**JBL199crop1, 5.0237 g, 18.74 mmol), bathophenanthroline (602.9 mg, 1.814 mmol, 0.0968 equiv) and Cu_2O (213 mg, 1.489 mmol, 0.07946 equiv) were combined in a 100 mL RBF with stir bar, and sealed with a septum. The flask was then evacuated and then filled with N_2 for a series of 5 cycles.

N-methyl-2-pyrrolidone (NMP, 30 mL) and freshly distilled quinolone (10 mL) were added via syringe to a two-neck flask that had been sealed with septum and had been purged via three vacuum-N_2 flush cycles. The combined solution was then

degassed with three freeze-pump-thaw cycles. This 3:1 solution of NMP:Quinoline (37.5 mL) was then added to the above reaction flask via syringe.

The reaction flask was filled with N_2 and a balloon of N_2 was placed on the flask. The mixture was vigorously stirred and heated between 170° and 185° C for 96 hours. The solution was cooled to room temperature.

Once cooled the reaction mixture was added to dry silica until slurry formed. This slurry was added to a silica plug and eluted with DCM to remove NMP and Quinoline. The initial fraction was collected with the target material. This solution was evaporated and the resulting residue was subjected to another silica column (20% Ethyl Acetate:Hexane) resulting in 3 fractions. The second fraction containing the TM was evaporated and dried under vacuum (1.459 g, 35%). ^{1}H NMR (400 MHz, acetone-d_6, JBL231colfrac2): δ 7.824 (d, J = 8 Hz, 2H), 7.714 (t, J = 8 Hz, 1H), 1.475 (s, 9H).

2-(tert-butyl)-1,3-diaminobenzene (44)

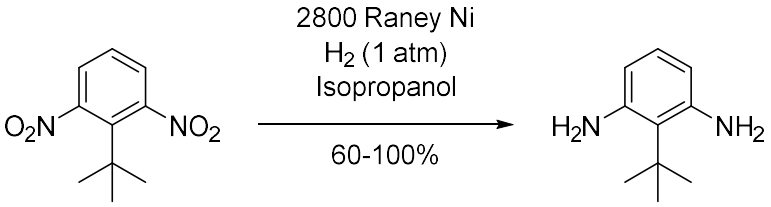

Molecular Weight: 224.22

Molecular Weight: 164.25

Run	SM (g)	Raney 2800 Ni in H_2O (mL)	H_2 approx. (mL)	Isopropanol (mL)	Time (hrs)	TM (g)	Yield (%)	TM label
JBL217	0.0216	0.5	50	2	48	N/A	N/A	JBL217crude
JBL219	0.0400	0.2	50	2	24	N/A	N/A	JBL219crude
JBL220	0.1544	0.8	50	8	36	114.4	100	JBL220crude

JBL230	0.3072	1.6	100	16	36	0.2552	100	JBL230crude
JBL241	1.459	7.6	1000	55	72	1.001	91.8	JBL241crude
JBL251	3.398	17	2500	120	72	2.442	98.0	JBL251crude
JBL341A	2.366	15	2000	80	72	1.380	79	JBL341crude
JBL341B	1.893	10	1500	60	72	1.684	62	JBL341recrystcrop1+2
JBL341C	1.822	10	1500	60	72			

JBL220: Based on a modified literature[40] procedure, Raney Nickel 2800 in H_2O was added to a suspension of **43** (JBL215colfrac3wash, 154.4 mg, 0.689 mmol) in isopropanol with stir bar in a 50 mL RBF. The flask was sealed with septum and evacuated and flushed with N_2 three times. The flask was then evacuated one last time before charging with H_2 via balloon, the balloon was recharged and placed on the flask. The reaction was then stirred for 36 hours. The reaction mixture was then passed over Celite on a glass frit funnel with isopropanol and then ethyl acetate to remove the nickel (water was used to keep the nickel wet). The filtrate was then evaporated and dissolved in ethyl acetate and washed with saturated NaCl solution. The organic layers were combined, dried with Na_2SO_4, evaporated and dried under vacuum to yield (114.4 mg, 100%). ^{1}H NMR (400 MHz, acetone-d_6, JBL341recrystcrop1): δ 6.590 (t, J = 7.8 Hz, 1H), 6.044 (d, J = 7.8 Hz, 1H), 4.158 (br, 4H), 1.563 (s, 9H).

1.4.4 Synthesis towards *tert*-Butyl Diisatin

N,N'-(2-(tert-butyl)-1,3-phenylene)bis(2-(hydroxyimino)acetamide)(46)

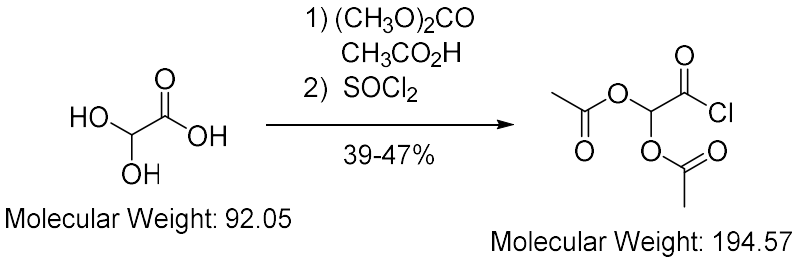

Run	SM (g)	Acetic Anhydride (mL)	Acetic Acid (mL)	DCM (mL)	Thionyl Chloride (mL)	TM (g)	Yield (%)	TM label
JBL249	15.483	104.6	23.9	50	26.85	6.4389	39.1	JBL249distill
JBL259	15.483	105	24	50	27	7.64	46.7	JBL259distill

JBL259: Based on a literature[48] procedure, a mixture of 50% w/w aqueous glyoxylic acid (15.48 g), acetic anhydride (105 mL) and glacial acetic acid (24 mL) were heated under reflux for 2 hours, and the solvents were removed on a rotary evaporator. The mixture was then azeotropically evaporated with toluene resulting in a residual oil which was dissolved in a mixture of dichloromethane (50 mL) and $SOCl_2$ (27 mL) and heated under gentle reflux for 30 minutes. The volatiles were removed with water aspirator and then dichloromethane (35 mL) was added to the mixture and then removed on a rotary evaporator to remove any remaining volatiles. The residue was distilled under vacuum to give a clear liquid (6.44 g, 39%). This was subsequently used in the addition to the *tert*-butyl diamine.

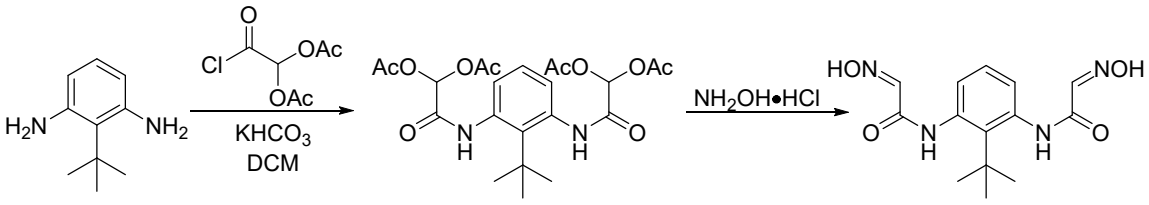

Molecular Weight: 164.25

Molecular Weight: 306.32

Run	SM (g)	(45) (g)	$KHCO_3$ (g)	DCM (mL)	$NH_2OH \cdot HCl$ (g)	2:1 EtOH: H_2O (mL)	TM (g)	Yield (%)	TM label
JBL250	0.301	0.976	1.945	15	1.3615	15	0.178	32	JBL250crude
JBL254	1.21	3.88	7.78	60	5.446	60	1.221	54	JBL254crude
JBL261	1.232	3.88	7.78	60	5.446	60	0.958	42	JBL261crude
JBL342	0.95	3.4	6.11	45	4.28	45	1.124	64	JBL342crude
JBL353	1.051	4	6.5	50	4.5	50	0.755	41	JBL353crude

JBL254: Modifying the literature[48] method, **44** (JBL251crude, 1.21 g, 7.37 mmol) and potassium bicarbonate (7.78 g, 73.7 mmol, 10 equiv.) were combined in a RBF with stir bar and then was dissolved in dichloromethane (40 mL) and then cooled to -10° C in a salt water bath. A solution of **45** (JBL249distill, 3.88 g, 19.16 mmol, 2.6 equiv.) in dichloromethane (20 mL) was added dropwise to the reaction mixture at -10° C. After the addition is completed, the mixture was allowed to warm to room temperature and stirred for 1.5 hours. The solvent was evaporated on the rotary evaporator leaving a white solid of the crude tetraacetate intermediate.

Without any purification, a solution of hydroxylamine-hydrochloride (1.3615 g, 73.7 mmol, 10 equiv.) in ethanol:water (2:1, 60 mL) was added to the intermediate. This solution was stirred and heated to reflux for 2 hours and then cooled to room temperature. The solution was concentrated on rotary evaporator, causing precipitation of a white solid. More water was added to the solution to incite further precipitation and cooled in

ice bath. A white solid (1.221 g, 54%) was collected via vacuum filtration, washed with cold water and dried under vacuum. ^{1}H NMR (400 MHz, acetone-d_6, JBL250crudetetraacetate): 9.096 (s, 2H), 7.142-7.254 m 3H), 7.016 (s, 2H), 2.169 (s, 12H), 1.513 (s, 9H). ^{1}H NMR (400 MHz, acetone-d_6, JBL353crude): δ 11.367 (br, 2H), 8.779 (s, 2H). 7.559 (s, 2H), 7.331 (d, J = 7.87 Hz, 2H), 7.203 (t, J = 7.87, 1H), 1.510 (s, 9H).

8-(tert-butyl)pyrrolo[3,2-f]indole-2,3,5,6(1H,7H)-tetraone (47)

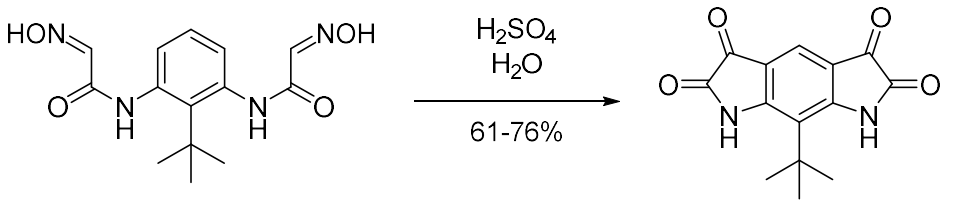

Molecular Weight: 306.32

Molecular Weight: 272.26

Run	SM (g)	Conc. H_2SO_4 (mL)	H_2O (mL)	TM (g)	Yield (%)	TM label
JBL252	0.1467	3.5	0.5	0.0862	66.1	JBL252crude
JBL255	1.221	14	2	0.715	65.4	JBL254crude
JBL262	0.9579	14	2	0.5274	61.5	JBL262crude
JBL347	1.1107	14	2	0.7303	72.9	JBL347crude
JBL360	0.870	14	2	0.590	76	JBL360crude

JBL252: Warmed a solution of concentrated H_2SO_4 (3.5 mL) and water (0.5 mL) to 60° in oil bath with stirring. Then added **46** (JBL250crude, 146.7 mg, 0.4824 mmol) slowly to the solution with good stirring, causing the solution to turn orange. The color deepened and the reaction was stirred for 30 minutes at 65-75°. The mixture was cooled to room temperature and then poured onto ice, producing an orange precipitate (86.2 mg, 66.1%) that was collected via vacuum filtration on a glass frit funnel and dried under

vacuum. ^{1}H NMR (400 MHz, DMSO-d_6, JBL360crude): δ 10.736 (s, 2H), 7.524 (s, 1H), 1.451 (s, 9H).

1.4.5 Synthesis towards diamine-diester core

4,6-Diamino-5-(tert-butyl)isophthalic acid (48)

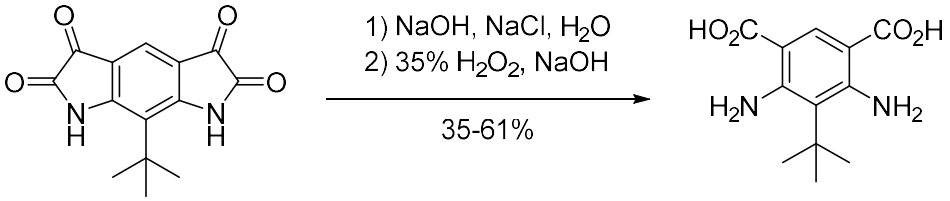

Run	SM (mg)	NaOH (mg)	NaCl (mg)	H_2O (mL)	35% H_2O_2 (mL)	NaOH (mg)	TM (mg)	Yield (%)	TM label
JBL256	98.8	134	96	2.25	0.11	113	45.2	49	JBL256crude
JBL265	410	537	384	13	0.45	452	230	61	JBL265crude
JBL349	710	1000	700	22	6.8	270	227	35	JBL349crude

JBL265: Following a literature[49] procedure, **47** (JBL255crude, 410 mg, 1.49 mmol), NaOH (537 mg, 13.4 mmol, 9.01 equiv.) and NaCl (384 mg, 6.57 mmol, 4.41 equiv.) were suspended in water (7 mL) and stirred for 2 hours and then cooled to 0°C in an ice bath. Then a solution of H_2O_2 (35% w/w H_2O, 0.45 mL) and NaOH (452 mg, 11.3 mmol, 7.59 equiv.) in water (1.5 mL) was added dropwise to the reaction at 0°C. After addition was completed the solution was stirred overnight. The pH was adjusted to 3-4 with glacial acetic acid and the solid precipitate was collected via vacuum filtration, washed with cold water, and dried under vacuum to yield (230 mg, 61%). ^{1}H NMR (400 MHz, DMSO-d_6, JBL265crude): δ 12.007 (br, 2H), 8.370 (s, 1H), 7.138 (br, 4H), 1.501 (s, 9H).

Dimethyl 4,6-diamino-5-(tert-butyl)isophthalate (49).

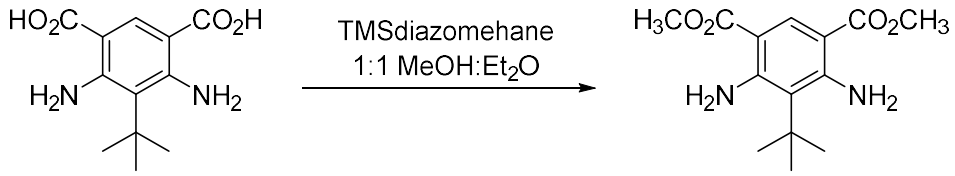

Run	SM (mg)	MeOH:Et_2O (1:1) (mL)	TMSdiazomethane (2.0 M in Et_2O) (mL)	TM (mg)	Yield (%)	TM label
JBL271	54.2	3	0.27	35.1	63	JBL271crude
JBL275	172.8	7	0.9	62.4	33	JBL265crude
JBL352	225	9	1.35	120	49	JBL352w-up

JBL271: Following a literature[50] procedure **48** (JBL265crude, 54.2 mg, 0.215 mmol) was dissolved in methanol/diethyl ether (1:1, 3 mL) and cooled to 0°C with good stirring. While at 0°C, a solution of (trimethylsilyl)diazomethane (2.0 M in diethyl ether, 0.27 mL) was added dropwise to the reaction solution until the evolution of N_2 bubbles ceased. The reaction was stirred for two hours at room temperature. Then the reaction mixture was concentrated on the rotary evaporator. The residue was dissolved in diethyl ether and extracted with NaOH (1 M, 2 x 5 mL). The organic fractions were combined, dried with Na_2SO_4, evaporated and dried under vacuum to yield (35.1 mg, 63%). ^{1}H NMR (400 MHz, acetone-d_6, JBL271crude): δ 8.520 (s, 1H), 7.127 (br, 4H), 3.775 (s, 6H); 1.623 (s, 9H). ^{1}H NMR (400 MHz, DMSO-d_6, JBL271crude): δ 8.376 (s, 1H), 7.090 (br, 4H), 3.725 (s, 6H), 1.502 (s, 9H).

1.4.6 Attempts and Successful Buchwald-Hartwig Couplings

Examples of unsuccessful Buchwald-Hartwig Coupling attempts

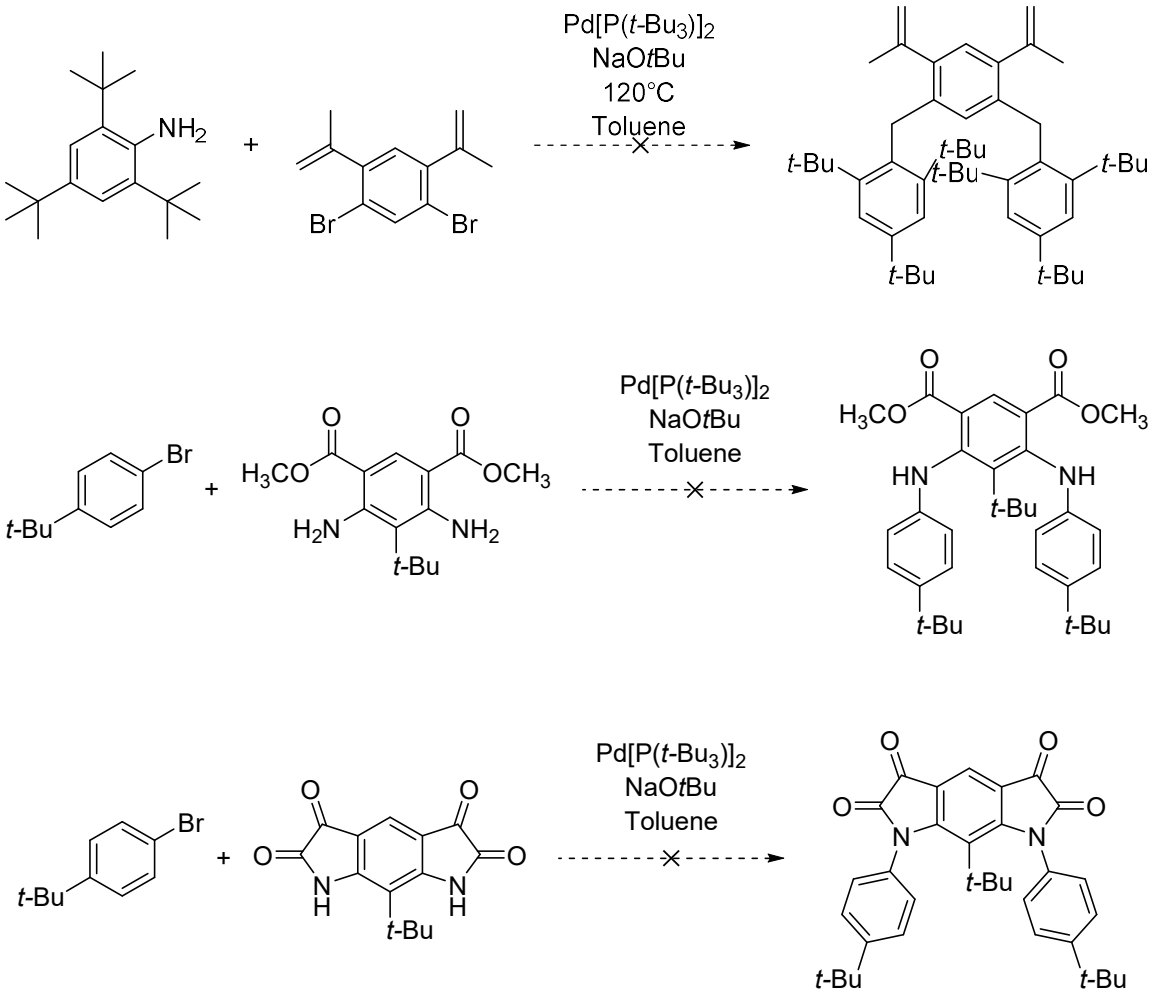

Trineopentylphosphine (53)

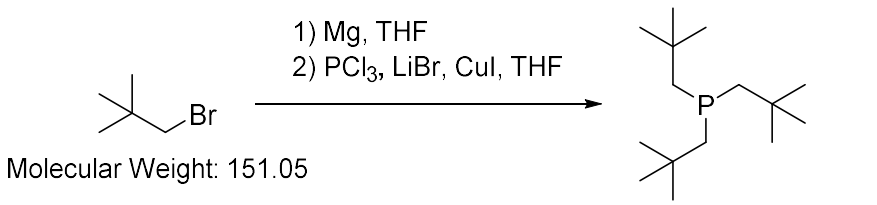

Molecular Weight: 151.05

Molecular Weight: 244.40

Run	SM (g)	Mg (g)	THF (mL)	LiBr (g)	CuI (g)	PCl_3 (mL)	TM (g)	Yield (%)	TM label
MKK112	11.2	1.99	31	0	0	1.55	0.91	20.3	MKK116disfrac2
JBL701	21	3.9	165	0.68	0.7	3.4	5.73	60.1	JBL702recc1+2

JBL701: Modifying a literature[54] procedure, LiBr and CuI were added to a 500-mL RBF equipped with a reflux condenser, addition funnel, and stir bar. The apparatus was sealed and evacuated overnight and then backfilled with Ar.

Mg turnings (freshly scratched with mortar and pestle under N_2 in a glovebag) was added to a separate 250-mL RBF under N_2 in a glovebag and sealed. The flask was then evacuated and heated with a heat gun. Once cooled, the flask was then backfilled with Ar and I_2 (one crystal) was added under Ar. The flask was flushed with Ar and then heated to sublime the I_2 with stirring. THF (10 mL) was added and allowed to stir until clear. A few drops of neopentylbromide was added and the solution became cloudy; the flask was then sonicated and then the solution was heated to boiling with a heat gun. Heat was removed and a few more drops of neopentylbromide was added and the reaction began boiling vigorously, turning the solution a deep purple/black color. The remaining neopentylbromide was dissolved in THF (60 mL) and added over 50 minutes to maintain reflux. THF (30 mL) was added to the flask and the reaction was refluxed for 2 hours.

THF (50 mL) was added to the reaction apparatus with LiBr and CuI and stirring began. The black neopentyl magnesium bromide solution from the 250-mL RBF was transferred via cannula under Ar to the sealed addition funnel of the reaction apparatus. PCl_3 () was then added via syringe the RBF portion of the reaction apparatus with the LiBr and CuI with stirring. The resulting yellow solution was cooled to -20°C. The neopentyl magnesium bromide solution in the addition funnel was then slowly added to the cooled stirred yellow solution dropwise over 1 hour. After the completion of addition, the resulting solution turned cloudy brown and stirred at -20°C for 1 hour. The solution was allowed to warm to room temperature and stirred for 12 hours. The reaction was an orange slurry and an aliquot of the reaction was taken and ^{31}P NMR showed a 81% concentration of the trineopentylphosphine product.

The reaction mixture was transferred to a 500-mL RBF and rotovapped to remove THF. Diethyl ether (300 mL) was then added to the flask followed by NH_4Cl solution (saturated, 150 mL) and stirred until most of the solid dissolved. The organic and aqueous layers were then separated via extraction. The organic layer was washed with NH_4Cl solution (saturated, 100 mL); then NH_4OH solution (concentrated, 3 x 25 mL) to remove any Cu species; then H_2O (30 mL); followed lastly by brine (50 mL). The organic layer was dried with $MgSO_4$, decanted and evaporated. ^{31}P NMR of the crude material showed 78% purity.

The crude material was recrystallized from hot ethanol and then cooled to room temperature and placed in the freezer overnight. The beige solid was collected over frit funnel. The beige solid was recrystallized once more from hot ethanol. The mother

liquor also was subjected to recrystallization. After combining pure crops from several recrystallizations, a white solid powder was obtained (5.73 g, 60.1%). ^{1}H NMR (400 MHz, $CDCl_3$, JBL702recryst2crop2): δ 1.349 (d, 6H), 0.982 (s, 9H). ^{31}P NMR (400 MHz, $CDCl_3$, JBL702recryst2crop2): δ 57.124.

Bis(2-(tert-butyl)phenyl)amine (59)

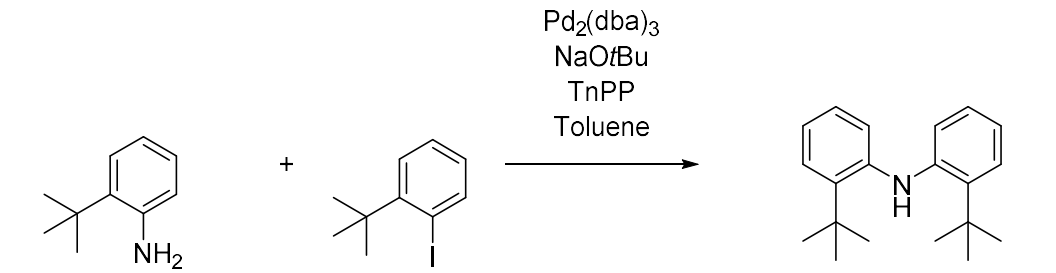

Molecular Weight: 149.24

Molecular Weight: 260.12

Molecular Weight: 281.44

Run	2-*t*-bu-iodo-benzene (mg)	2-*t*-bu-aniline (mg)	$Pd_2(dba)_3$ (mg)	NaO*t*Bu (mg)	TnPP (mg)	Tol-uene (mL)	TM (mg)	Yield (%)	TM label
MKK117	21	18	9.98	14.0	4.9	0.2	7.6	33.3	MKK119colfrac3
MKK121	42	36	18.2	28.8	10.6	0.4	N/A	N/A	MKK122crude
MKK131	260	179	112.6	144	60.5	2	235	83.5	MKK155colf1-2

MKK131: Modifying a literature[5254] procedure, 2-(*tert*-butyl)iodobenzene (260 mg, 1 mmol) and 2-(*tert*-butyl)aniline (179 mg, 1.2 mmol, 1.2 equiv.) were transferred to the same vial with DCM and then sealed with septum. The DCM was evaporated off with N_2 flow. Toluene (distilled and dried) was transferred via syringe to the vial under N_2.

$Pd_2(dba)_3$ (112.6 mg, 0.123 mmol, 0.12 equiv.) and NaO*t*Bu (144.2 mg, 1.5 mmol, 1.5 equiv.) and trineopenylphosphine (60.5 mg, 0.248 mmol, 0.248 equiv.) was added to Schlenk vessel with a stir bar in a glovebag under N_2. The Schlenk was transferred to the vacuum line and evacuated and filled with N_2 three times. The solution of the combined starting materials dissolved in toluene in the vial was then transferred via syringe under N_2 to the Schlenk vessel. The reaction was stirred and heated at 100 °C for

96 hours. The reaction mixture was then cooled to room temperature and transferred with EtOAc (3 x 5 mL) to run through a silica plug with EtOAc (15 mL). The resulting filtrate was evaporated giving an orange-brown oil. The crude was purified via column chromatography (silica, 100% pentane) to give an orange solid (235 mg, 83.5%). ^{1}H NMR (400 MHz, $CDCl_3$, MKK155colfrac1-2): δ 7.470 (d, J = 7.8, 2H), 7.154 (m, 2H), 6.988-7.026 (m, 4H), 5.508 (s, 1H), 1.573 (s, 18H).

Bis(2,5-di-(tert-butyl)phenyl)amine (60

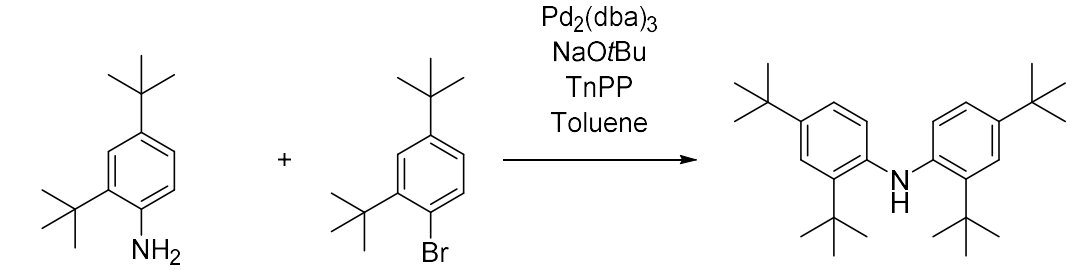

Molecular Weight: 205.35

Molecular Weight: 269.23

Molecular Weight: 393.66

Run	2,5-di-*t*-bu-bromo-benzene (mg)	2,5-di-*t*-bu-aniline (mg)	$Pd_2(dba)_3$ (mg)	NaO*t*Bu (mg)	TnPP (mg)	Tol-uene (mL)	TM (mg)	Yield (%)	TM label
MKK123	21.7	24.64	9.8	14.8	4.9	0.2	18.5	58.4	MKK124pTLCfr2
MKK129	43.5	49.3	17.7	29.6	9.7	0.4	27.8	43.7	MKK138colf1-2
MKK144	273.5	230	66.4	145	36	2	N/A	N/A	MKK153colf2-2.5

MKK123: Modifying a literature[52,54] procedure, 2-5-di(*tert*-butyl)bromobenzene (43.5 mg, 0.1614 mmol) and 2,5-di(*tert*-butyl)aniline (49.3 mg, 0.24 mmol, 1.4 equiv.) were transferred to the same vial with DCM and then sealed with septum. The DCM was evaporated off with N_2 flow. Toluene (distilled and dried) was transferred via syringe to the vial under N_2.

$Pd_2(dba)_3$ (17.67 mg, 0.0193 mmol, 0.12 equiv.) and NaO*t*Bu (29.6 mg, 0.308 mmol, 1.5 equiv.) and trineopentylphospine (9.73 mg, 0.0398 mmol, 0.247 equiv.) was added to Schlenk vessel with a stir bar in a glove bag under N_2. The Schlenk was transferred to the vacuum line and evacuated and filled with N_2 three times. The solution of the combined starting materials dissolved in toluene in the vial was then transferred via syringe under N_2 to the Schlenk vessel. The reaction was stirred and heated at 100 °C for 96 hours. The reaction mixture was then cooled to room temperature and transferred with EtOAc (3 x 5 mL) to run through a silica plug with EtOAc (15 mL). The resulting filtrate was evaporated giving an orange-brown oil. The crude was purified via column chromatography (silica, 100% pentane) to give an orange solid (27.8 mg, 43.7%). ^{1}H NMR (400 MHz, $CDCl_3$, MKK124pTLCfrac2): δ 7.391 (d, J = 2.2, 2H), 7.391 (dd, J_1 = 2.2, J_2 = 8.4, 2H), 6.860 (d, J = 8.4, 2H), 5.259 (s, 1H), 1.484 (s, 18H), 1.312 (s, 18H). ^{13}C NMR (400 MHz, $CDCl_3$, MKK124pTLCfrac2): δ 144.64, 141.51, 139.43, 123.70, 123.61, 122.52, 34.88, 34.53, 31.73, 30.76.

1.5 References

[1] Gomberg, M. J. An Instance of Trivalent Carbon: Triphenylmethyl. *J. Am. Chem. Soc.,* **1900**, *22*, 757-771.

[2] Lankamp, H.; Nauta, W. T.; MacLean, C. A New Interpretation of the Monomer-Dimer Equilibrium of Triphenylmethyl- and Alkyl-Substituted-Diphenyl Methyl Radicals in Solution. *Tetrahedron Lett.*, **1968**, *9*, 249-254.

[3] *IUPAC Compendium of Chemical Terminology*, release 2.3.2; International Union of Pure and Applied Chemistry (IUPAC): Research Triangle Park, NC, 2012; pp. 427.

[4] Borden, W. T. Diradicals – A Fifty Year Fascination. In *The Foundations of Physical Organic Chemistry: Fifty Years of the James Flack Norris Award;* Strom, E. T., Mainz, V. V., Eds.; ACS Symposium Series 1209; American Chemical Society: Washington, DC, 2015; pp. 251-303 and references therein.

[5] Abe, M. Diradicals. *Chem. Rev.,* **2013**, *113*, 7011-7088 and references therein.

[6] Rajca, A. The Physical Organic Chemistry of Very High-Spin Polyradicals. *Adv. Phys. Org. Chem.,* **2005**, *40*, 153-199.

[7] Gallagher, N.; Olankitwanit, A.; Rajca, A. High-Spin Organic Molecules. *J. Org. Chem.,* **2015**, *80*, 1291-1298.

[8] Rajca, A. Organic Diradicals and Polyradicals: From Spin Coupling to Magnetism?, *Chem. Rev.,* **1994**, *94*, 871-893.

[9] Schlenk, W.; Brauns, M. Zur Frage der Metachinoide. *Chem. Ber.,* **1915**, *48*, 661-669.

[10] Rajca, A.; Rajca, S. Alkyl-Substituted Schlenk Hydrocarbon Diradicals with Triplet and Singlet Ground States in Frozen Solutions. *J. Chem. Soc. Perkins 2,* **1998**, 1077-1082.

[11] Rajca, A.; Utamapanya, S. π-Conjugated systems with unique electronic structure: a case of planarized 1,3-connected polyarylmethyl carbodianion and stable triplet hydrocarbon diradical. *J. Org. Chem.,* **1992**, *57*, 1760-1767.

[12] Reproduced from http://www.epr.ethz.ch/education/basic-concepts-of-epr/one-elect--in-the-magn--field/zeeman.html

[13] Dewar, M. J. S. *The molecular orbital theory of organic chemistry*. McGraw-Hill: New York, 1969; pp. 232.

[14] Dowd, P. Trimethylenemethane. *J. Am. Chem. Soc.,* **1966**, *88*, 2587-2589.

[15] Dowd, P. Trimethylenemethane. *Acc. Chem. Res.,* **1972**, *5*, 242-248.

[16] Ovchinnikov, A. A. Multiplicity of the Ground State of the Large Alternant Organic Molecules with Conjugated Bonds (Do Organic Ferromagnetics Exist?). *Theor. Chim. Acta,* **1978**, *47*, 297-304.

[17] Wieland, H. Tetraphenylhydrazin und Hexaphenylathan. *Liebigs Ann. Chem.*, **1911**, *381*, 200-216.

[18] Shida, T.; Kira, A. Optical and Electron Spin Resonance Studies on Photolyzed and Radiolyzed Tetraphenylhydrazine and Related Compounds. *J. Phys. Chem.,* **1969**, *73*, 4315-4320.

[19] Neugebauer, F. A.; Fischer, H. l,3,6,8-Tetra-*tert*-butyl-9-carbazyl: A Crystalline Monomeric Aminyl Radical. *Angew. Chem. Int. Ed.,* **1971**, *10*, 732–733.

[20] Neugebauer, F. A.; Fischer, H.; Bamberger, S; Smith, H. O. Aminyle, 6. tert.-Butyl-substituierte 9-Carbazolyl-Radikale, Carbazol-Radikalkationen und Carbazol-9-oxyl-Radikale. *Chem. Ber.,* **1972**, *105*, 2694–2713.

[21] Ballester, M.; Castaner, J.; Olivella, S. Syntheses and Isolation of the Perchlodiphenylaminyl, An Exceptionally Stable Radical. *Tetrahedron Lett.,* **1974**, 615–616.

[22] Neuhaus, P.; Grote, D.; Sander, W. Matrix Isolation, Spectroscopic Characterization, and Photoisomerization of *m*-Xylylene. *J. Am. Chem. Soc.,* **2008**, *130*, 2993–3000.

[23] Noodleman, L. Valence Bond Description of Antiferromagnetic Coupling in Transition Metal Dimers. *J. Chem. Phys.,* **1981**, *74*, 5737-5744.

[24] Amiri, S.; Schreiner, P. R. Non-Kekulé *N*-Substituted *m*-Phenylenes: *N*-Centered Diradicals versus Zwitterions. *J. Phys. Chem. A,* **2009**, *113*, 11750-11757.

[25] Migirdicyan, E.; Baudet, J. Electron spectra of *o*- and *m*-xylylenes and their methylated derivatives. Experimental and theoretical study. *J. Am. Chem. Soc.,* **1975**, *97*, 7400-7404.

[26] Haider, K.; Soundararajan, N.; Shaffer, M.; Platz, M. S. EPR Spectroscopy of a Diaza Derivative of *Meta*-xylylene. *Tetrahedron Lett.,* **1989**, *30*, 1225-1228.

[27] Rajca; A.; Shiraishi, K.; Pink, M.; Rajca, S. Triplet (S = 1) Ground State Aminyl Diradical. *J. Am. Chem. Soc.,* **2007**, *129*, 7232.

[28] Boratynski, P. J.; Pink, M.; Rajca, S.; Rajca, A. Isolation of the Triplet Ground State Aminyl Diradical. *Angew. Chem., Int. Ed.,* **2010**, *49*, 5459.

[29] Rajca, A.; Olankitwanit, A.; Rajca, S. Triplet Ground State Derivative of Aza-*m*-xylylene Diradical with Large Singlet—Triplet Energy Gap. *J. Am. Chem. Soc.,* **2011**, *133*, 4750.

[30] Olankitwanit, A.; Pink, M.; Rajca, S.; Rajca, A. Synthesis of Aza-m-Xylylene Diradicals with Large Singlet–Triplet Energy Gap and Statistical Analyses of Their EPR Spectra. *J. Am. Chem. Soc.,* **2014**, *136*, 14277-14288.

[31] Olankitwanit, A.; Rajca, S.; Rajca, A. Aza-m-Xylylene Diradical with Increased Steric Protection of the Aminyl Radicals. *J. Org. Chem.*, **2015**, *80*, 5035-5044.

[32] Komen, C. M. D.; Bickelhaupt, F. Easy Preparation of 1,3-Di-*tert*-butylbenzene and Some Derivatives Thereof. *Syn. Commun.*, **1996**, *26*, 1693-1697.

[33] Wegner, H. A.; Reisch, H.; Rauch, K.; Demeter, A.; Zachariasse, K. A.; Meijere, A.; Scott, L. T. Oligoindenopyrenes: A New Class of Polycyclic Aromatics. *J. Org. Chem.*, **2006**, *71*, 9080-9087.

[34] De Koning, A. J. Derivatives of *m*-di-*tert*-butylbenzene. Part VI. The Preparation of Miscellaneous Halogenated Compounds. R*ecl. Trav. Chim. Pays-Bas,* **1981**, 100, 421-425.

[35] Edwards, J. D.; Cashaw, J. L. Orientation in Aromatic Substitution. I. 1,2-Dimethoxy-3-isopropylbenzene and 3,5-Dimethylanisole. *J. Am. Chem. Soc.,* **1956**, *78*, 3821-3824.

[36] Trost, B. M.; Kinson, P. L. Organocopper Chemistry. Decarboxylation of a Benzhydryl Carboxylic Acid. *J. Org. Chem.,* **1972**, *37*, 1273-1275.

[37] Owsley, D. C.; Bloomfield, J. J. The Reduction of Nitroarenes with Iron/Acetic Acid. *Synthesis*, **1977**, *1*, 119-121.

[38] Ram, S.; Ehrenkaufer, R. E. A General Procedure for Mild and Rapid Reduction of Aliphatic and Aromatic Nitro Compounds using Ammonium Formate as a Catalytic Hydrogen Transfer Agent. *Tetrahedron Lett.*, **1984**, *25*, 3415-3418.

[39] Bellamy, F. D.; Ou, K. Selective Reduction of Aromatic Nitro Compounds with Stannous Chloride in Non Acidic and Non Aqueous Medium. *Tetrahedron Lett.*, **1984**, *25*, 839-842.

[40] Hoefnagel, A. J.; Nunnink, A. J.; Van Veen, A; Verkade, P. E.; Wepster, B. M. The Nitration of 2-Nitro-1,4-di-*t*-butylbenzene: Synthesis of the Three Dinitro-1,4-di-*t*-butylbenzenes and Some Related Compounds. R*ecl. Trav. Chim. Pays-Bas*, **1969**, *88*, 386-397.

[41] Gooßen, L. J.; Thiel, W. R.; Rodríguez, N.; Linder, C.; Melzer, B. Copper-Catalyzed Protodecarboxylation of Aromatic Carboxylic Acids. *Adv. Synth. Catal.*, **2007**, *349*, 2241-2246.

[42] Da Silva, J. F. M.; Garden, S. J.; Pinto, A. C. The Chemistry of Isatins: A Review from 1975-1999. *J. Braz. Chem. Soc.,* **2001**, *12*, 273-324.

[43] Sumpter, W. C. The Chemistry of Isatin. *Chem. Rev.,* **1944**, *34,* 393-434.

[44] Yamamoto, G.; Koseki, A.; Sugita, J.; Mochida, H.; Minoura, M. Deamination of 1-Alkyl-9-aminomethyltriptycenes. Participation of a Neighboring 1-Alkyl Substituent. *Bull. Chem. Soc. Jpn.,* **2006**, *79*, 1585-1600.

[45] Wenkert, E.; Hudlický, T. Reactions of Isatin Dimethyl Ketal and Its Ethyl Imino Ether with Methyllithium. *Synth. Commun.,* **1977**, *7*, 541-547.

[46] Pinder, J. L.; Weinreb, S. M. Preliminary Feasibility Studies on Total Synthesis of the Unusual Marine Bryozoan Alkaloids Chartellamide A and B. *Tetrahedron Lett.,* **2003**, *44*, 4141-4143.

[47] Demerson, C. A.; Humber, L. G.; Phillipp, A. H. Etodolic acid and related compounds. Chemistry and antiinflammatory actions of some potent di- and trisubstituted 1,3,4,9-tetrahydropyrano[3,4-b]indole-1-acetic acids. *J. Med. Chem.*, **1976**, *19*, 391-395.

[48] Rewcastle, G. W.; Sutherland, H. S.; Weir, C. A.; Black burn, A. G.; Denny, W. A. An Improved Synthesis of Isonitrosoacetanilides. *Tetrahedron Lett.,* **2005**, *46*, 8719-8721.

[49] Montoya-Pelaez, P. J.; Uh, Y.-S.; Lata, C.; Thompson, M. P.; Lemieux, R. P.; Crudden, C. M. The Synthesis and Resolution of 2,2‘-, 4,4‘-, and 6,6‘-Substituted Chiral Biphenyl Derivatives for Application in the Preparation of Chiral Materials. *J. Org. Chem.,* **2006**, *71*, 5921-5929

[50] Hashimoto, N.; Aoyama, T.; Shioiri, T. New Methods and Reagents in Organic Synthesis. 14. A Simple Efficient Preparation of Methyl Esters with Trimethylsilyldiazomethane ($TMSCHN_2$) and Its Application to Gas Chromatographic Analysis of Fatty Acids. *Chem. Pharm. Bull.*, **1981**, *29*, 1475-1478.

[51] Tipparju, S. K.; Joyasawal, S.; Pieroni, M.; Kaiser, M.; Brun, R.; Kozikowski, A. P. In Pursuit of Natural Product Leads: Synthesis and Biological Evaluation of 2-[3-hydroxy-2-[(3-hydroxypyridine-2-carbonyl)amino]phenyl]benzoxazole-4-carboxylic acid (A-33853) and Its Analogues: Discovery of *N*-(2-Benzoxazol-2-ylphenyl)benzamides as Novel Antileishmanial Chemotypes. *J. Med. Chem.,* **2008**, *51*, 7344-7347. SI

[52] Raders, S. M.; Moore, J. N.; Parks, J. K.; Miller, A. D.; Leißing, T. M.; Kelley, S. P.; Rogers, R. D.; Shaughnessy, K. H. Trineopentylphosphine: A Conformationally Flexible Ligand for the Coupling of Sterically Demanding Substrates in the Buchwald–Hartwig Amination and Suzuki–Miyaura Reaction. *J. Org. Chem.,* **2013**, *78*, 4649-4664.

[53] King, R. B.; Cloyd, Jr., J.C.; Reimann, R. H. Poly(tertiary Phosphines and Arsines). XIII. Neopentyl Poly(tertiary Phosphines). *J. Org. Chem.,* **1976**, *41*, 972-977.

[54] Rampf, F.; Militzer, H.-C. Process for Preparing Tertiary Phosphines. U.S. Patent 7,847,126 B2. Dec. 7, 2010.

[55] Negoro, N.; Yanada, R.; Okaniwa, M.; Yanada, K.; Fujita, T. Diastereoselective Allylation of optically Active Imines with Metallic Samarium. *Syn. Lett.*, **1998**, *55*, 13947-13956.

[56] Basu, M. K.; Banik, B. K. Samarium-mediated Barbier Reaction of Carbonyl Compounds. *Tet. Lett.*, **2001**, *42*, 187-189.

[57] Seebach, D. Generation of Secondary, Tertiary, and Quaternary Centers by Geminal Disubstitution of Carbonyl Oxygens. *Angew. Chem.,* **2011**, *50*, 96-101 and references therein.

[58] Denton, S. M.; Wood, A. A Modified Bouveault Reaction for the Preparation of α,α-Dimethylamines from Amides. *Syn. Lett.*, **1999**, 55-56.

[59] Zuidema, D. R.; Williams, S. L.; Wert, K. J.; Bosma, K. J.; Smith, A. L.; Mebane, R. C. Deoxygenation of Aromatic Ketones using Transfer Hydrogenolysis with Raney Nickel in 2-Propanol. *Syn. Commun.*, **2011**, *41*, 2927-2931.

[60] Maier, W. F.; Bergmann, K.; Bleicher, W.; Schleyer, P. v. R. Heterogenous Deoxygenation of Ketones. *Tetrahedron Lett.*, **1981**, *22*, 4227-4230.

[61] Mitchell, R. H.; Lai, Y.-H. The Neutral Deoxygenation (Reduction) of Aryl Carbonyl Compounds with Raney-Nickel. An Alternative to the Clemmenson, Wolf Kishner or Mozingo (Thioketal) Reductions. *Tetrahedron Lett.*, **1980**, *21*, 2637-2638.

[62] Janusz, J. M.; Young, P. A.; Scherz, M. W.; Enzweiler, K.; Wu, L. I.; Gan, L.; Pikul, S.; McDow-Dunham, K. L.; Johnson, C. R.; Senanayake, C. B.; Kellstein, D. E.; Green, S. A.; Tulich, J. L.; Rosario-Jansen, T.; Magrisson, I. J.; Wehmeyer, K. R.; Kuhlenbeck, D. L.; Eichhold, T. H.; Dobson, R. L. M. New Cyclooxygenase-2/5-Lipoxygenase Inhibitors. 2. 7-*tert*-Butyl-2,3-dihydro-3,3-dimethylbenzofuran Derivatives as Gastrointestinal Safe Anti-inflammatory and Analgesic Agents: Variations of the Dihydrobenzofuran Ring. *J. Med. Chem.*, **1998**, *41*, 1124-1137.

[63] Cheng, D.-J.; Tian, S.-K. A Highly Enantioselective Catalytic Mannich Reaction of Indolenines with Ketones. *Adv. Syn. & Cat.*, **2013**, *355*, SI.

[64] Dopp, D.; Greci, L.; Nour-el-Din, A. M. Indolenine Oxides, VIII. Reaction of 5,7-di-*tert*-butyl-3,3-dimethyl-3*H*-indole-1-Oxide with Grignard Reagents. —A New Stable Aminyl Oxide (Nitroxide). *Chem. Ber.*, **1983**, *116*, 2049-2057.

[65] Letcher, R. M; Sin, D. W. M.; Cheung, K.-K. Oxazolo[3,2-*a*]indoles, Pyrrolo- and Azepino-[1,2-*a*]indoles from 3*H*-indole 1-oxides and Acetylenecarboxylic Esters by Skeletal Rearrangements. J. *Chem. Soc. Perkin Trans. I*, **1993**, 939-944.

[66] Xiao, K.-J.; Luo, J.-M.; Ye, K.Y.; Wang, Y.; Huang, P.-Q. Direct, One-pot Sequential Reductive Alkylation of Lactams/Amides with Grignard and Organolithium Reagents through Lactam/Amide Activation. *Angew. Chem.*, **2010**, *49*, 3037-3040.

[67] Bubnov, Y. N.; Pastukhov, F. V.; Yampolsky, I.; Ignatenko, A. V. A Convenient Synthesis of 2,2-Diallylated Nitrogen Heterocycles by Allylboration of Lactams. *Eur. J. Org. Chem., **2000**, 1503-1505.*

[68] Nieczypor, P.; Mol, J. C.; Bespalova, N. B.; Bubnov, Y. N. Synthesis of Nitrogen-Containing Spiro Compounds from Lactams by Allylboration and Subsequent Ring-Closing Metathesis. *Eur. J. Org. Chem.*, **2004**, 812-819.

[69] Agosti, A.; Britto, S.; Renaud, P. An Efficient Method to Convert Lactams and Amides into 2,2,-Dialkylated Amines. *Org. Lett.*, **2008**, *10*, 1417-1420.

[70] Reetz, M. T. Organotitanium Reagents in Organic Synthesis a Simple Means to Adjust Reactivity and Selectivity of Carbanions. In *Synthetic and Structural Problems*; Boschke, F. L., Ed.; Topics in Current Chemistry, Vol. 106; Springer: Berlin, 1982, 1-54.

[71] Reetz, M. T. In *Organotitanium Reagents in Organic Synthesis;* Reactivity and Structure: Concepts in Organic Chemistry, Vol. 24; Springer, Berlin, 1986.

[72] Schiess, M. Anwendung von Titanderivaten in der organischen Synthese neue Varianten der Mannich- und der Passerini-Reaktion. Ph. D. Dissertation, ETH Zurich, 1986.

[73] Meisters, A.; Mole, T. Exhaustive *C*-methylation of Ketones by Trimethyl Aluminum. *Aust. J. Chem.*, **1974**, *27*, 1655-1663.

[74] Jeffery, E. A.; Meisters, A.; Mole, T. Nickel-catalysed Methylation of Ketones by Trimethylaluminium. *Aust. J. Chem.,* **1974**, *27*, 2569-2476.

[75] Reetz, M. T.; Westermann, J.; Steinbach, R. Direct Geminal Dimethylation of Ketones Using Dimethyltitanium Dichloride. *J. Chem. Soc. Chem. Comm.,* **1981**, 237-239.

[76] Reetz, M. T.; Westermann, J.; Kyung S.-H. Direct Geminal Dimethylation of Ketones and Exhaustive Methylation of Carboxylic Acid Chlorides Using Dichlorodimethyltitanium. *Chem. Ber.,* **1985**, *118*, 1050-1057.

[77] Hojjat, M.; Kiselyov, A. S.; Strekowski, L. An Activated Trifluoromethyl Group as a Novel Synthon for a Substituted Vinyl Function: Facile Synthesis of 2-(Substituted 1-Alkenyl)Anilines. *Synth. Commun.* **1994**, *24*, 267-272.

[78] Lin, S.-Y.; Hojjat, M.; Strekowski, L. A Facile Synthesis of 4-(Trialkylmethyl)anilines by the Reaction of 4-(Trifluoromethyl)aniline with Grignard Reagents. *Synth. Commun.* **1997**, *27*, 1975-1980.

[79] Terao, J.; Nakamura, M.; Kambe, N. Non-catalytic Conversion of C—F Bonds of Benzotrifluorides to C—C Bonds using Organoaluminium Reagents. *Chem. Commun.*, **2009**, 6011-6013.

[80] Kaleta, J.; Tarábek, J.; Akdag, A.; Pohl, R.; Michl, J. The 16 $CB_{11}(CH_3)_n(CD_3)_{12-n}$• Radicals with 5-Fold Substitution Symmetry: Spin Density Distribution in $CB_{11}Me_{12}$•. *Inorg. Chem.,* **2012**, *51*, 10819-10824, SI28-29.

[81] Wang, Y.; Olankitwanit, A.; Rajca, A; Rajca, S. Intramolecular Hydrogen Atom Transfer in Aminyl Radical at Room Temperature with Large Kinetic Isotope Effect. *J. Am. Chem. Soc.*, **2017**, *139*, 7144-7147.

[82] Manoharan, M.; Eliel, E. L. Conformation, in solution, of c-4-t-butyl-1-phenyl-c-1-(N-piperidyl)cyclohexane hydrochloride. The conformational energy of t-butyl. *Tet. Lett.,* **1984**, *25*, 3267-3268.

[83] Della, E. W. Conformational Analysis. Trifluoromethyl Group. *J. Am. Chem. Soc.*, **1967**, *89*, 5221-5224.

[84] Booth, H.; Everett, J. R. The experimental determination of the conformational free energy, enthalpy, and entropy differences for alkyl groups in alkylcyclohexanes by low temperature carbon-13 magnetic resonance spectroscopy. *J. Chem. Soc. Perkin 2*, **1980**, 255-259.

[85] Umemoto, T.; Ishihara, S. Efective Methods for Preparing *S*-(trifluoromethyl)dibenzothiphenium Salts. *J. Fluor. Chem.*, **1999**, *98*, 75-81.

[86] Macé, Y.; Raymondeau, B.; Pradet, C.; Blazejewski, J.-C.; Magnier, E. Benchmark and Solvent-Free Preparation of Sulfonium Salt Based Electrophilic Trifluoromethylating Reagents. *Eur. J. Org. Chem.,* **2009**, *9*, 1390-1397.

[87] Kino, T.; Nagase, Y.; Ohtsuka, Y.; Yamamoto, K.; Uraguchi, D.; Tokuhisa, K.; Yamakawa, T. Trifluoromethylation of Various Aromatic Compounds by CF_3I in the Presence of Fe(II) Compound, H_2O_2 and Dimethylsulfoxide *J. Fluorine Chem.,* **2010**, *131*, 98-105.

[88] Monteiro, J. L.; Carneiro, P. F.; Elsner, P.; Roberge, D. M.; Wuts, P. G. M.; Kurjan, K. C.; Gutmann, B.; Kappe, C. O. Continuous Flow Homolytic Aromatic Substitution with Electrophilic Radicals: A Fast and Scalable Protocol for Trifluoromethylation. *Chem. Eur. J.,* **2017**, *23*, 176-186.

[89] Uraguchi, D.; Yamamoto, K.; Ohtsuka, Y.; Tokuhisa, K.; Yamakawa, T. Catalytic Trifluoromethylation of Uracil to 5-Trifluoromethyluracil by Use of CF_3I and its Industrial Applications. *Appl. Catal. A,* **2008**, *342*, 137-143.

[90] Minisci, F.; Vismara, E.; Fontana, F. Homolytic Alkylation of Protonated Heteroaromatic Bases by Alkyl Iodides, Hydrogen Peroxide, and Dimethyl Sulfoxide. *J. Org. Chem.,* **1989**, *54*, 5224-5227.

[91] Bravo, A.; Bjørsvik, H.-R.; Fontana, F.; Liguori, L.; Mele, A.; Minisci, F. New Methods of Free-Radical Perfluoroalkylation of Aromatics and Alkenes. Absolute Rate Constants and Partial Rate Factors for the Homolytic Aromatic Substitution by *n*-Perfluorobutyl Radical. *J. Org. Chem.*, **1997**, *62*, 7128-7136.

[92] Sladojevich, F.; McNeill, E.; Börgel, J.; Zheng, S.-L.; Ritter, T. Condensed-Phase, Halogen-Bonded CF_3I and C_2F_5I Adducts for Perfluoroalkylation Reactions. *Angew. Chem.*, **2015**, *54*, 3712-3716SI.

CHAPTER 2 – EFFECT OF RING SIZE ON THE STABILITY OF NITROXIDE RADICALS

2.1 Introduction

Nitroxide radicals are a class of stable organic radicals that have found application in many areas of chemistry, materials[1], and biomedicine[2]. The basis for success in these applications of nitroxide radicals are their stability, paramagnetic properties, and redox properties at ambient temperatures. Much effort has been done to tune these properties for these unique applications.

2.1.1 Background and Properties of Nitroxide Radicals

The inorganic compound, commonly referred to as Fremy's salt (potassium nitrosulfonate) was the first nitroxide discovered in 1845.[3] Over 50 years later, Piloty and Schwerin reported in 1901 the first organic nitroxide radical, an alkyl/iminyl nitroxide named porphyrexide, originally thought to be the corresponding oxoammonium.[4] In 1959, over a half century later, Lebedev reported the synthesis of the first *gem*-dialkyl nitroxide, 2,2,6,6-tetramethylpiperidine-1-oxy radical (TEMPO).[5] This stable nitroxide consisting of *gem*-dimethyl six-membered heterocyclic ring is the structural basis for many commonly used nitroxides today. All of these compounds can be seen in Figure A-1.

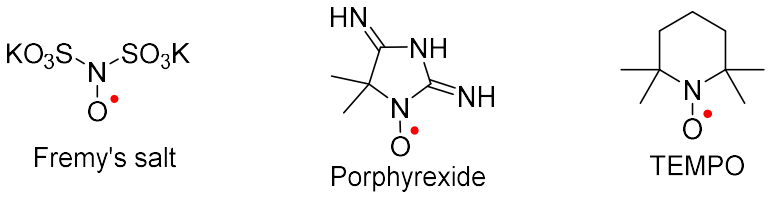

Figure A-1. Early Nitroxide Radicals

A nitroxide radical is generally an oxygen-centered radical bonded to a nitrogen atom with two R groups attached. Two resonance structures exist as seen in Figure A-2: a neutral resonance form with the radical located on the oxygen; and another zwitterionic structure with the radical on the nitrogen atom. In reality, combining the resonance structure of the nitroxide shows that the unpaired electron is shared between both the nitrogen and oxygen atom and thus is delocalized over the N—O bond. This resonance effect is one of the main reasons for the inherent stability of nitroxide radicals over other free radicals species.

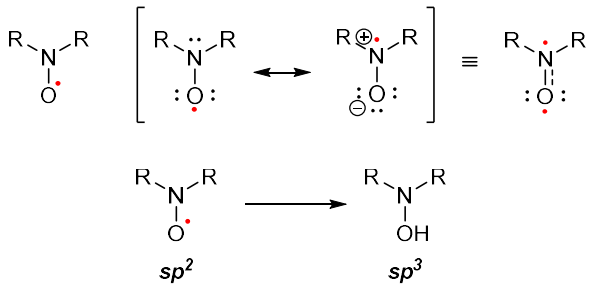

Figure A-2. Nitroxide resonance structures and hybridization.

This three-electron bond exhibits some physical properties that support the nitrogen atom exhibiting sp^2 nature. In particular, the N—O bond length of TEMPOL[6] is 1.26 Å; compared to 1.48 Å for the sp^3 hybridized *N*-methylhydroxylamine[7] and 1.19 Å for the sp^2 hybridized oxoammonium salt of TEMPO[8]. Further, the IR spectrums of the same set of molecules follow the same trend for the stretches of the N—O bond;

hydroxylamine[9] (926 cm^{-1}), TEMPOL[10-11] (1371 cm^{-1}), and the TEMPO oxoammonium salt (1602 cm^{-1}). The comparisons of these properties seem to indicate that the nitrogen atom in nitroxide has significant sp^2 character.

2.1.2 Applications and Limitations of Nitroxide Radicals

The ability of nitroxides to undergo both oxidation (to the oxoammonium ion) and reduction (to the hydroxylamine) make them valuable redox agents. Additionally, controlling nitroxide reactivity with other radicals to form alkoxyamines offers another path of reactivity to utilize. Each of these reactivity pathways, as shown in Scheme 2.1, offers different areas of chemistry a versatile class of molecules that can be tuned for their unique applications.

Nitroxides have found practical application in several areas of research. In regard to biological applications[12] they are one of the most used spin labels in biomolecular EPR research,[13] show great value as biological antioxidants,[14] provide information regarding the redox status of tissues,[15-17] measure hydroxyl radical generation,[18] and measure cerebral pO_2,[19-21] and recent advances include the use of nitroxide polymers for tumor detection using MRI.[22] In other fields, nitroxide and nitroxide polymers show great promise and utility in catalysis and synthesis, energy storage and other high-tech applications.[23]

Scheme 2.1. Oxidation, reduction and radical scavenging reactions of nitroxide.

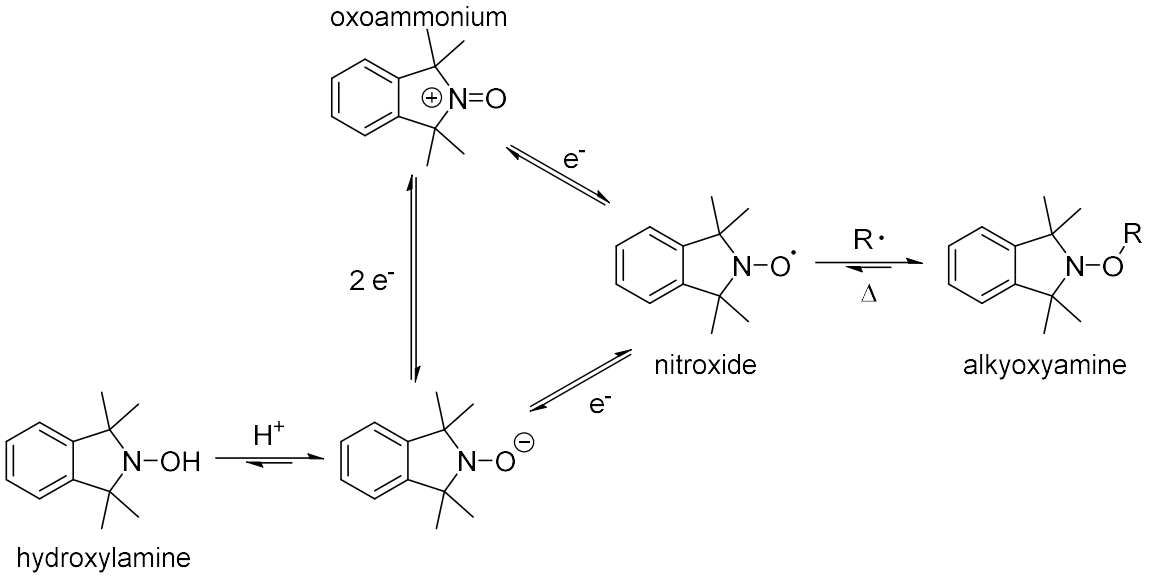

2.1.3 Decomposition and Reactions of Nitroxides

While nitroxide radicals have a lower reactivity than many other radical types, they are not immune to decomposition or other reactions that destroy the radical species. Among the various pathways of reaction, include dimerization between two radicals, hydrogen atom abstraction, and single electron transfers. *In vivo*, and of more practical concern is the reduction of nitroxide radicals by enzyme-based processes and antioxidants such as ascorbate.

2.1.3.1 Decomposition Pathways of Nitroxide Radicals

One potential decomposition pathway for nitroxide radicals is through an equilibrium dimerization resulting in the formation of a NO—ON bond from two nitroxide radicals as seen in Scheme 2.2; a endothermic process of ~28 kcal•mol^{-1}.[24]

However, the nitroxide radical gains resonance stability of ~32 kcal•mol^{-1}, offering more stability than the endothermicity of the dimerization process.

Scheme 2.2. Dimerization of nitroxide radicals.

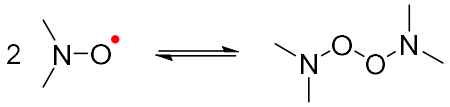

If the nitroxide possesses a α-hydrogen adjacent to the nitrogen atom then the dimerization product may undergo disproportionation. This process may occur via two different pathways; single electron transfer followed by deprotonation or through a direct hydrogen atom transfer. Both pathways can be seen in Scheme 2.3. Most nitroxide radicals are designed without α-hydrogens in order to avoid this process. The design of α-hydrogen substituted nitroxides is beyond the scope of this discussion but is well described in this excellent article.[25]

Scheme 2.3. Disproportionation of Nitroxides.

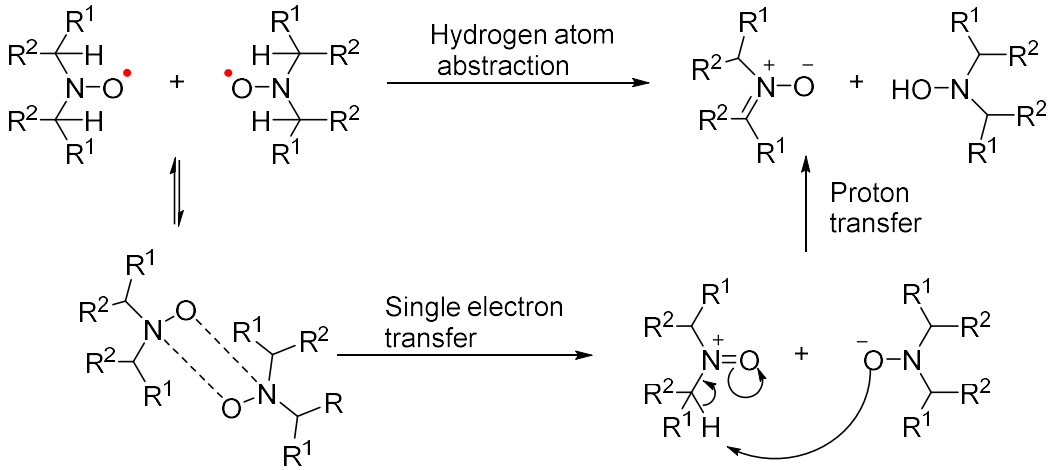

2.1.3.2 Reduction of Nitroxides by Ascorbate

For most applications, reduction of the nitroxide to the hydroxylamine limits its utility. The predominant reduction mechanism of concern for nitroxides is by ascorbate, better known as Vitamin C and shown in Figure A-1 and the rate of reduction by ascorbate is commonly reported for nitroxide radicals with biological applications. To determine the reduction rate of radicals, an experiment is performed using a solution of nitroxide and a 10- to 100-fold excess of ascorbate in buffer and monitoring the disappearance of radical by EPR. Determination of the rate constant can be made from the early stage of the reduction profile.

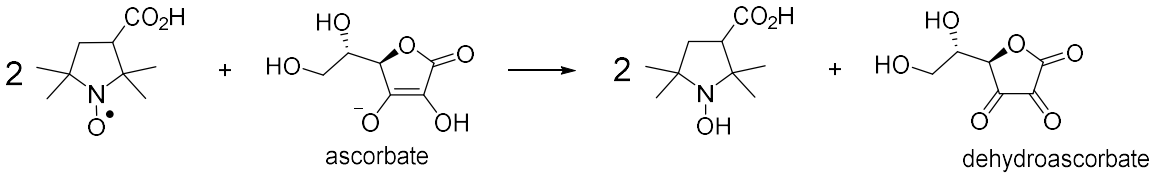

Figure A-1. Reduction of PROXYL with Ascorbate.

While the reaction in Figure A-1 seems simple enough, the actual process is much more complex, involving several intermediates and equilibria[26-27]. A study[28] investigating its full scope resulted in the set of reaction equations in Scheme 2.4 with reaction rates shown for PROXYL where known.

Examining the decay profile of nitroxides in a solution of ascorbate shows a fast-initial reduction followed by a *quasi*-equilibrium period, which points towards incomplete conversion to the hydroxylamine. No other products are known from the reduction of nitroxide to hydroxylamine, indicating that the hydroxylamine is undergoing oxidation back to the nitroxide.

Scheme 2.4. Equilibrium processes in the reduction of nitroxides by ascorbate.

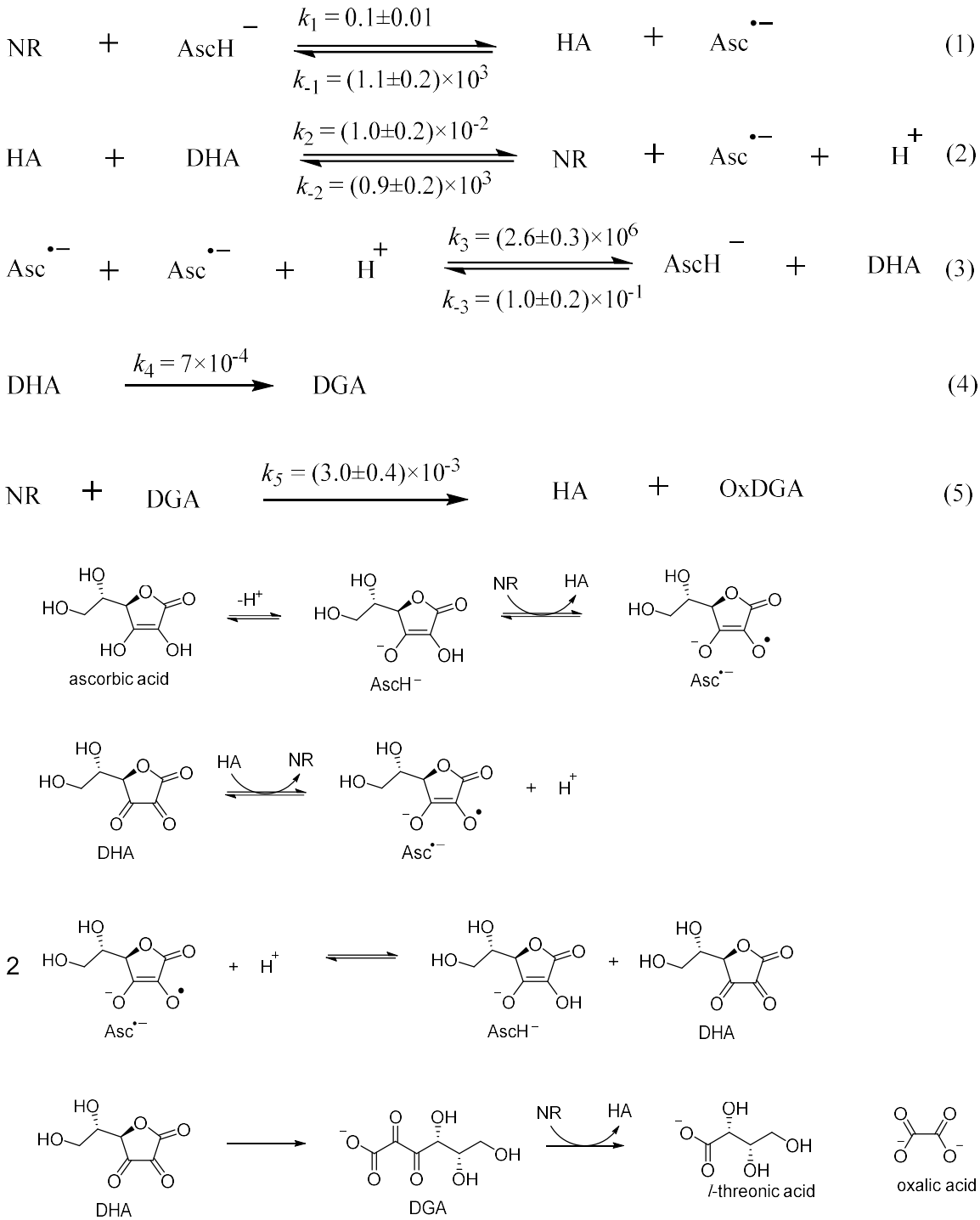

There are two potential oxidant species to react with hydroxylamine: the ascorbate radical or dehydroascorbate (DHA). The ascorbate radical is formed by one-electron oxidation of ascorbate, and DHA is formed by two-electron oxidation and proton loss of ascorbate. Other studies, determined that the ascorbate radical was responsible for the oxidation of the hydroxylamine, the detail of this extrapolation is explained well in my colleagues dissertation.[29]

This equilibrium between the nitroxide and hydroxylamine can be shifted by the presence of reduced glutathione (GSH). GSH does not react with nitroxides at relevant concentrations,[30] but does reduce ascorbate radical with a rate constant of 10 $M^{-1}s^{-1}$. Instead GSH reduces the ascorbate radical to ascorbate, decreasing the ascorbate radical in solution, inhibiting the oxidation of hydroxylamine to nitroxide. This does allow a more direct measurement of k_1 and the profile of concentration over time. More accurately reflecting the conditions seen in the biological system is important especially considering the concentration of glutathione (1.2 mM)[31] and ascorbate (~75 μM)[32-33] in whole blood.

2.1.4 Factors Impacting Resistance to Reduction of Nitroxide Radical

TEMPO provides a good basis for a relatively stable nitroxide radical. It is a cyclic nitroxide, has quaternary carbons adjacent to the nitrogen atom meaning no α-hydrogens, and the methyl groups provide steric bulk around the radical site. The TEMPO molecule is a great starting point for investigation of permutations and changes to its structural features and comparison of the effect on molecular properties, reactivity

and function. Of particular importance to our research is the effect on relative rates of reduction by ascorbate of nitroxide to hydroxylamine.

Rajca and co-workers[34-35] have already shown how increasing the size of the groups around the radical site can impact the stability of the nitroxide radical, specifically regarding decreased rates of reduction by ascorbate. They showed that when comparing groups of different sizes, the smaller group (methyl) had a faster rate of reduction compared to larger (ethyl or cyclohexyl) groups. Further, the tetra-ethyl was better than the larger *spiro*-cyclohexyl groups because the tetra-ethyl is not restricted by the limited number of ring conformations. Other examples showing similar steric effects by other groups have also been noted.[36-38]

Another property that has shown to have significant effect on the stability of the nitroxide radical towards reduction by ascorbate is the polarity of the groups adjacent to the nitroxide radical.[37, 39-40] Using a series of tetracarboxylate pyrroline nitroxides, Rajca and co-workers[41-42] were able to demonstrate that electron withdrawing groups adjacent to the nitroxide radical accelerate its reduction in the presence of ascorbate/GSH. This work established good correlation between both reduction rates and electrochemical potentials of nitroxide radicals with field/inductive parameters of their substituents.

Lastly, and least understood is how the ring size of cyclic nitroxide radicals effects their stability and the rate of reduction by ascorbate.[40] There are many different examples of 5 or 6-membered ring nitroxide radicals; and the trend shows that 5-

membered ring systems are more stable than 6-membered ring, and in regards to reduction by ascorbate are reduced 100-fold slower.

There are two prevailing thoughts for these results: 1) Six-membered rings may adopt conformations that facilitate approach of the radical site by reducing agents;[40] and 2) a comparison of the ring strain in the nitroxide radical vs. its reduced form. Cyclohexyl rings are optimal sp^3 ring system as all bond angles are ideal; in the sp^2 system that the nitroxide radical requires, ring strain is increased as ideal bond angles become strained. Reduction of the nitroxide to the hydroxylamine would relieve this ring strain as it becomes sp^3 hybridized. A similar trend is observed in the reduction of cyclic ketones to alcohols, although it has been extended to a series of 3-14 membered ring systems and better described by the term I-strain, which will be discussed in more detail in the next section.

2.1.5 I-Strain

Strain energy changes as rings transform from sp^2 to sp^3 hybridization or vice versa are termed "I-strain" (for internal strain) as proposed by Brown and co-workers in 1951.[43] I-strain is composed of the combination between angle and eclipsing strain differences in ring transformations, with eclipsing strain becoming more predominant in medium sized rings versus the obvious angle strain evident in 3 to 4 membered rings. [44] For medium sized rings, as further explained by Eliel and Wilen, "eclipsing strain is important in all but the six-membered ring, which is nearly perfectly staggered in the chair conformation. Since eclipsing is more serious for saturated than for unsaturated

ring carbon atoms, the $sp^3 \rightarrow sp^2$ change will be favored and the $sp^2 \rightarrow sp^3$ change disfavored for five –membered and medium-sized rings."[45]

As discussed previously, the reduction of nitroxides by ascorbate is a process where the coordination number of the nitrogen atom in the ring goes from three to four, as it transforms from a sp^2 hybridization of the nitroxide radical to the sp^3 hybridization of the hydroxylamine. Based on the observations that "relative small differences in internal strain can have very large effects upon the rates and equilibria of reactions of these ring compounds"[43] and applying the same rationale centered on the change in coordination number during the reaction resulting in increased I-Strain, we hypothesize that a similar trend would be observed in different-sized ring nitroxides.

This effect could exacerbate in the case of nitroxides, since gem-dialkyl groups stabilize adjacent to the nitroxide on the ring. It would not be difficult to suppose that the eclipsing strain component of the I-Strain becoming larger as more alkyl groups substitute for the hydrogen. The methyl groups are sterically more demanding than the hydrogen; in the conformational analysis of butane, the energy for the hydrogen-hydrogen eclipsing interaction[46] is 2.9 kcal/mol versus the hydrogen-methyl eclipsing interaction[45] of 3.4 kcal/mol. This would be an additive energy strain of 0.5 kcal/mol for each methyl-hydrogen eclipsing interaction.

Scheme 2.5. Reduction of Cycloanones

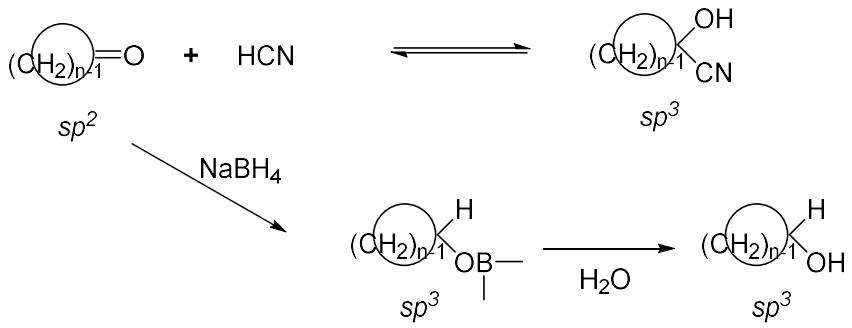

Table 2.1. Predictions and Observations on I Strain on Cycloanones[45]

Ring Size	*Prediction for* $sp^3 \rightarrow sp^2$	*Reaction A* [a]	*Reaction B* [b]
Acyclic	--	1.00	1.00
3	Facile	--	--
4	Facile	--	581
5	Difficult	3.33	15.4
6	Facile	70.	355
7	Difficult	0.54	2.25
8	Difficult	0.081	0.172
9	Difficult	0.041	0.070
10	Difficult	Small	0.0291
11	Difficult	0.063	0.0518
12	Difficult	0.226	0.401
13	Difficult	0.269	0.427
14[c]	--	1.17	--

[a] *Equilibrium constants for cyanohydrin formation (Prelog and Kobelt, 1949; Wheeler and Granell de Rodriguez, 1964).*
[b] *Relative rates of reduction of cycloanones with sodium borohydride (Brown and Ichikawa, 1957).*
[c] *The 14-membered and larger rings have negligible I strain. In fact, where rates or equilibrium constants have been measured, they are within less than a factor of 2 of those of acyclic analogues.*

2.1.6 The relationship between Nitroxides and Alkoxyamines

While the focus of our research has been towards increasingly more stable nitroxide species an understanding of alkoxyamines and their association with nitroxides gives an added perspective on factors that contribute to nitroxide stability or even allow chemistry where nitroxides are generated *in vivo* from non-radical surrogates.

Alkoxyamines are essentially alkyl substituted hydroxylamines. From our understanding one of the primary products in the decomposition of nitroxides, and particularly in the reduction of nitroxide by ascorbate is hydroxylamine. The reverse reaction is essentially a H—ON bond homolysis, and in the case of alkoxyamine a C—ON bond homolysis. Just as we can modify the structure of the nitroxide to influence the resistance to this reaction, in the case of alkoxyamine the reaction can be further controlled via structural features on the alkyl side of the C—O bond.

Scheme 2.6. Homolysis of alkoxyamine into nitroxide and alkyl radical.

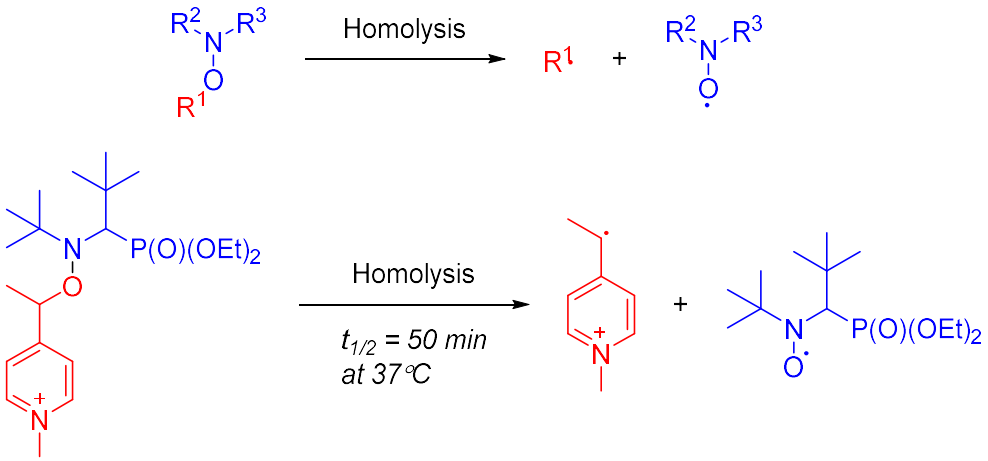

Alkoxyamines have found application in several areas of chemistry including their role in nitroxide mediated polymerization (NMP), in tin-free radical chemistry, catalysis and synthesis, and recently applications towards their use in biological systems.[47] There are several examples of tuning alkoxyamines for spontaneous homolysis into the alkyl radical and nitroxide at ambient or relevant biological or reaction temperatures. One such application is towards a 'theranostic' (therapeutic and diagnostic) agent. This alkoxyamine spontaneously undergoes homolysis with a half-life of 50 minutes at 37°C as shown in Scheme 2.6. The alkyl radical has toxic effect on

cells, while the nitroxide fragment offers a way to monitor the progress of the reaction as a molecular probe. [48]

2.1.6.1 Factors effecting C-ON Homolysis

Various effects of the structure of both the alkyl and nitroxyl fragment on C—ON bond homolysis have been investigated. Some of the effects are based in the same principles that have been discovered that effect the reduction of nitroxides with ascorbate to hydroxylamine. [49] The various effects are too numerous to go into detail and is already well-reviewed, but Figure A-1 illustrates what and how changes on the alkyl and nitroxide fragments of the alkoxyamine effect the rate of homolysis.

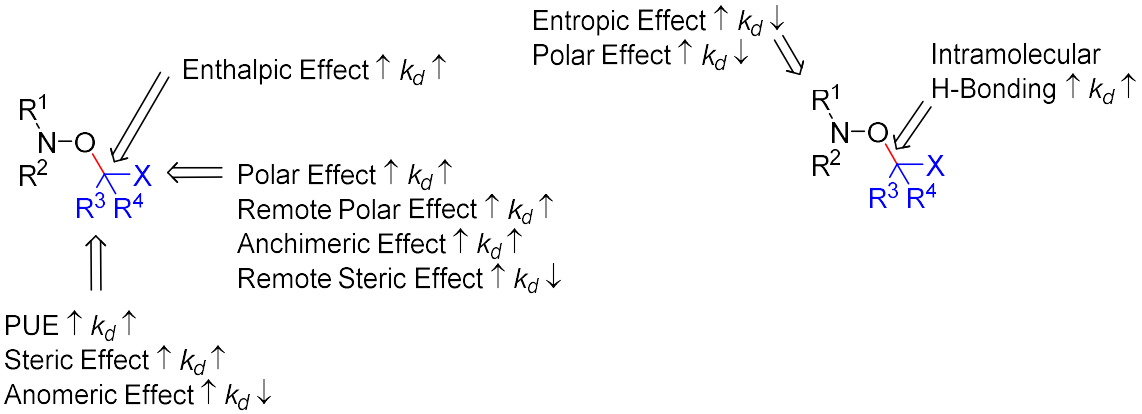

Figure A-1. Illustration of how different structural changes to the alkoxyamine effect the rate of homolysis.

2.1.6.2 Alkoxyamines as surrogates for nitroxide release *in vivo*

An interesting potential application of alkoxyamine in biological systems is the potential to use it as a theranostic agent,[50] meaning it serves a therapeutic and diagnostic purpose. Specifically, alkoxyamine compounds could be designed to undergo homolytic cleavage at room temperature, generating an alkyl radical and a nitroxide radical as

shown in Figure A-1. The alkyl radical could be used to perform protein and lipid modifications or address ROS/AO imbalance, while the nitroxide could serve as a diagnostic tool using electron paramagnetic imaging (EPRI)[51] or Overhauser-enhanced magnetic resonance (OMRI)[52].

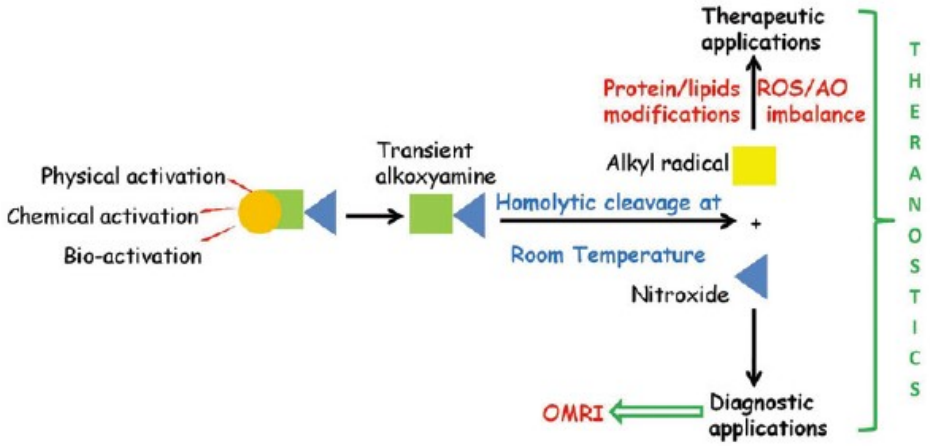

Figure A-1. Illustration of Alkoxyamine triggered homolysis as a Theranostic Agent.[50]

The half-life and E_a for C—ON bond homolysis can be altered by being triggered by protonation[53] and other chemical modification[54]. Figure A-2 shows the range that different chemical triggers at the pyridine nitrogen affect the half-life and E_a for C—ON bond homolysis.

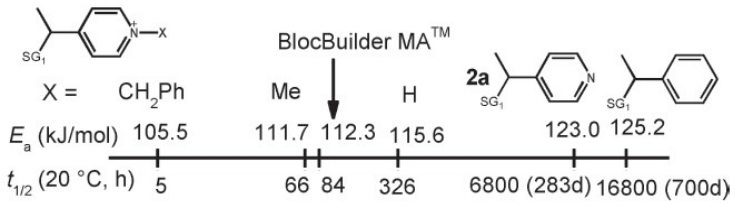

Figure A-2. Half-life and *Ea* of different chemical triggering of alkoxyamines.[54]

2.1.6.3 Living Radical Polymerization and ring size.

Alkoxyamines are important mediators in stable free radical polymerizations and nitroxide-mediate polymerizations. The control of the polymerization reaction is derived based on the reversible formation of the latent alkoxyamine from the corresponding nitroxide and the radical of the growing chain polymer. This ensures a low concentration of free radicals throughout the polymerization process, minimizing termination of the polymerization via radical dimerization or disproportionation. These processes are controlled through the persistent radical effect, which is well reviewed.[55] While not on face directly related to nitroxide stability, work in other areas focused on understanding the homolysis of alkoxyamines into nitroxides may provide some important insight into nitroxide stability.

Research into alkoxyamines has shown that the reactivity of the alkoxyamines can be tuned via the structure of the nitroxides. Further, there seems to be good correlation between increasing alkoxyamine C—ON bond homolysis rates and the stability of the resulting nitroxide product. Obviously, other factors contribute to the rate of C—ON bond homolysis in alkoxyamines but increasing nitroxide stability should increase the rate of C—ON bond homolysis.

In fact, the rate C—ON bond homolysis of 7- and 8-membered ring alkoxyamines has been determined.[56-57] The authors compared both a ketone and alcohol series of 6, 7, and 8-membered alkoxyamines as seen in Table 2.2; in the ketone series ring enlargement from 6 to 7-membered alkoxyamines reduced the activation energy for C—ON bond homolysis, producing a 4-fold increase in rate constant. Going from 7 to 8-membered

rings didn't produce much change, this agreed with their observations regarding slow polymerization with the 6-membered ring, and very similar conversion with 7 and 8-membered alkoxyamines.

Table 2.2. Structure and C-ON bond homolysis rate (M^{-1} s^{-1}) of six-, seven-, and eight-membered alkoxyamine ketones and alcohols.

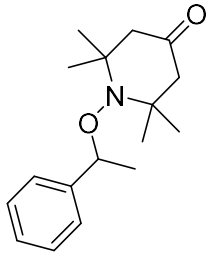	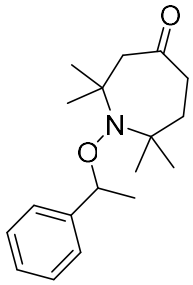	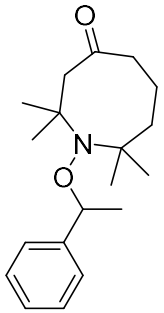	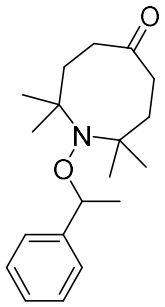
5.7×10^{-4}	2.0×10^{-3}	1.1×10^{-3}	1.7×10^{-3}
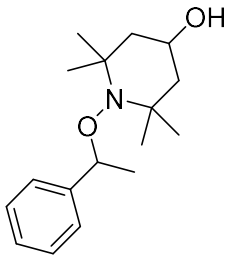	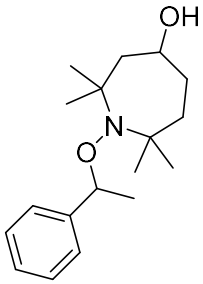	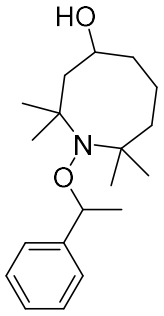	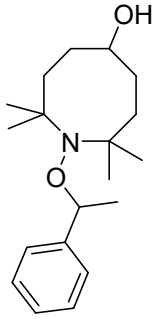
3.3×10^{-3}	2.7×10^{-2}	7.4×10^{-3}	1.3×10^{-2}

Enlargement from the 6- to the 7-membered ring in the alcohol series showed an even greater effect on the rate of C-ON bond homolysis. The 7-membered ring underwent homolysis 14-times faster than the 6-membered ring. Again though, the 8-membered ring was faster than the 6-membered ring, but slightly slower than the 7-membered alcohol alkoxyamine.

2.2 Results and Discussion

Based on the experimental data regarding I-strain in the reduction of cycloanones and the potential for its explanation in the homolytic cleavage of alkoxyamine of varying ring sizes into their respective nitroxide radicals a more direct investigation on the reduction of nitroxide radicals of varying ring sizes seemed logical.

The objective of our project is to synthesize nitroxide radicals of varying ring size to investigate its effect on the reduction of nitroxide radical by ascorbate. Our hypothesis is that the rate of reduction of nitroxide radical by ascorbate will follow the same pattern previously observed and reported for the reduction of cycloanones by sodium borohydride, as both involve a transition from a sp^2 to sp^3 hybridization state and would have similar effects on rate. Realizing even a portion of the potential 3500-fold increase in stabilization from the 6-membered to the 10-membered ring nitroxide would be a significant tool in the design of stable nitroxide radicals.

2.2.1 Original Synthetic Strategy

Our original strategy was based upon what we thought would be a trivial alkylation of the enolate generated from 2,2,6,6-tetramethylpiperidinone (**66**). From this keto-ester (**67**) we would again generate the enolate then alkylate with an alkyl dihalide and then proceed to do the ring expansion via a radical Dowd-Beckwith ring enlargement. You can see our original retrosynthetic scheme in Scheme 2.7 below.

Scheme 2.7. Original Synthetic Scheme towards ring-enlarged nitroxides.

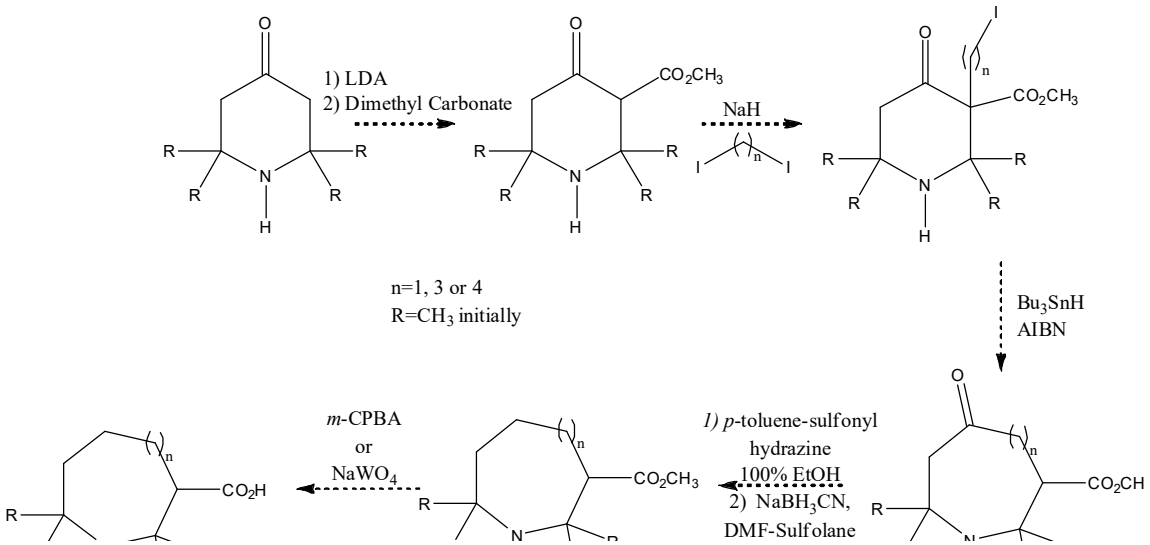

This route proved unsuitable from the beginning. We presumed that upon deprotonation of the α-hydrogen adjacent to the ketone, the generated enolate would then easily do a nucleophilic attack of an acyl chloride or dialkyl carbonate.[58] This reaction and many others trying to add different electrophiles to this position failed. We began to suspect the methyl groups provided enough steric hindrance to prevent the enolate anion from approaching a suitable electrophile. In review of the reported reactions of 2,2,6,6-tetramethylpiperidinone, there were very few examples with addition of an electrophile next to the carbonyl.[59-61]

To rule out the free amine as an acid/base reaction partner we also attempted reactions on the methyl carbamate protected 2,2,6,6-tetramethylpiperidinone[62], although this protecting group addition proved to be low yielding and inefficient as it used excess 2,2,6,6-tetramethylpiperidinone as a sacrificial base. Also, attempts of alkylation of the protected amine by generating the enolate with different bases (including NaH, LDA,

NaOMe, potassium phenoxide) and reacting with different electrophiles such as CO_2, chloromethylformate or dimethyl carbonate failed.

This initial failure forced us to look at different positions on the 2,2,6,6-tetramethylpiperidinone that may be less sterically hindered, allowing attack. Steric hindrance on the carbons adjacent to the ketone left us looking for a reaction that occurred at the carbonyl position to avoid the steric problems at the adjacent sites. We found several examples[63-64] of a literature reaction[65-67] using $BF_3 \cdot OEt_2$ and ethyl diazoacetate that generated not only a 6 to 7 membered ring expansion, but simultaneously incorporated a β-keto-ester functional group allowing us a framework to go forward and attempt future ring expansions to 8 and 10 membered rings using the Dowd-Beckwith radical conditions originally planned.

Additionally, there was a similar example[57] of a $BF_3 \cdot OEt_2$ mediated expansion using (TMS)-diazomethane on 2,2,6,6-tetraethylpiperdinone towards the synthesis of 7- and 8-membered ring alkoxyamines as shown in Scheme 2.8. We attempted this reaction on 2,2,6,6-tetramethylpiperdinone (as the synthesis of 2,2,6,6-tetraethylpiperdinone is tedious) resulting in one-carbon ring expansion to the silyl enol ether but attempts to remove the silyl enol ether failed. In hindsight, based on obtaining pure 7-membered ketone-amine via other routes, the amine probably was too volatile for the conditions necessary to remove the silyl enol ether, while the authors most likely had less volatility issues with 2,2,7,7-tetraethylazepan-4-one.

Scheme 2.8. Literature ring-expansion reaction.

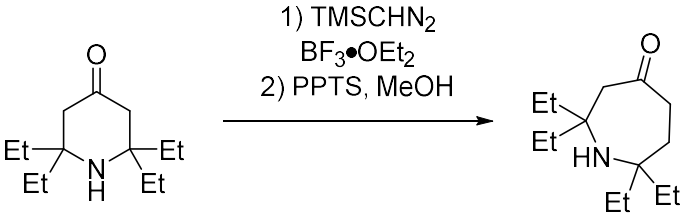

2.2.2 Synthesis towards 7 and 8-membered ring Nitroxide Radicals using $BF_3 \cdot OEt_2$-mediated ring expansion

Scheme 2.9. Mechanism of $BF_3 \cdot OEt_2$ mediated ring expansion with ethyl diazoacetate.

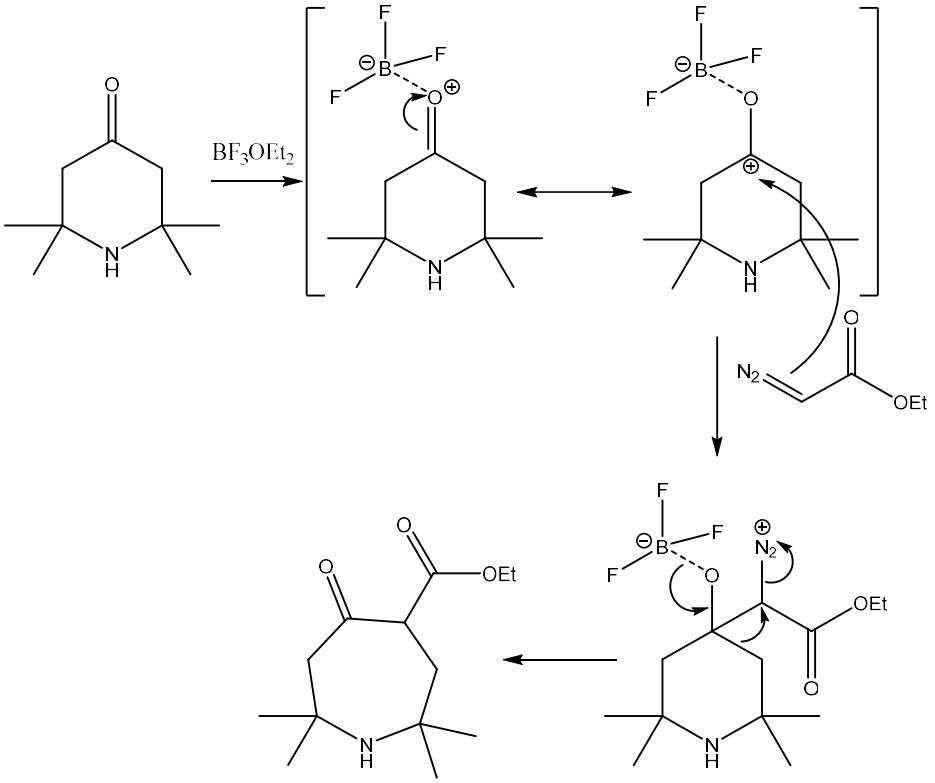

This reaction was based upon the addition of ethyl diazoacetate dropwise at low temperature to the $BF_3 \cdot OEt_2$ activated 2,2,6,6-tetramethylpiperidinone. The mechanism for the reaction is shown in Scheme 2.9. The $BF_3 \cdot OEt_2$ behaves as a Lewis acid activating the carbonyl for nucleophilic attack by the ethyl diazoacetate. This

intermediate then undergoes rearrangement and extrusion of N_2 generates the ring expanded β-keto ester (**68**).

The actual synthesis towards 7-membered ketone and amine is shown in Scheme 2.10. The crude 7-membered β-keto-ester was unable to be purified while maintaining a reproducible and sufficient yield as it essentially behaved as a zwitterion with the pK_a's of the protonated amine and the keto-ester being so similar. Thus, we carried the crude β-keto-ester directly into the decarboxylation step. Of note, the 7-membered β-keto-ester was observed via NMR in $CDCl_3$ to be predominantly in an enol form vs. the keto form. There are other examples in the literature[68] of the enol form being favored in other 7-membered β-keto-ester systems.

Scheme 2.10. Synthesis of nitroxide radicals 70 and 71.

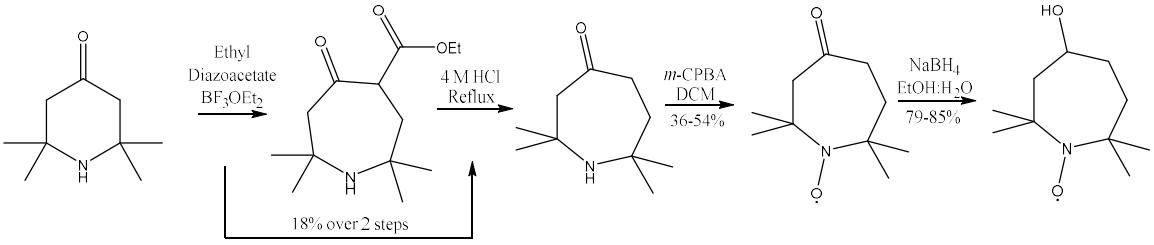

The crude β-keto-ester then underwent decarboxylation generating a very oily 7-membered ring amine (**69**). This oil was purified via precipitation of the protonated amine in an ethereal HCl solution, followed by recrystallization of the protonated amine. The protonated amine was susceptible to E_1 elimination at the amine, as shown in Scheme 2.11, if heated as it generates a tertiary carbocation upon opening that forms an enone, so it required careful handling. The purified amine salt was then deprotonated and extracted into to give the free amine.

Scheme 2.11. Mechanism for E_1 elimination product from 69.

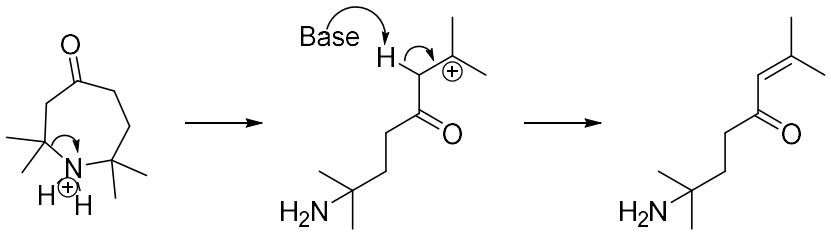

Subjecting the free amine to *m*CPBA generated the 7-membered ring ketone nitroxide (**70**). After purification via column, a portion was reduced using $NaBH_4$ to generate the 7-membered ring alcohol nitroxide (**71**), which was also purified via column chromatography.

Attempts to first reduce the ketone to the alcohol (**72**) were successful, but upon oxidation of the amine to the nitroxide with *m*CPBA the alcohol was also reoxidized to the ketone nitroxide (**70**). This is outcome is supported by previous literature examples[69] on the oxidation of six-membered 4-hydroxy-2,2,6,6-tertramethylpiperidine, and where nitroxides are commonly used as oxidation catalysts for the oxidation of alcohols.[70-71]

2.2.2.1 Comparison of 7-membered Ring Nitroxides to existing Nitroxides

Successful generation of **70** and **71** as seen in the EPR's in Figure A-1 gave us our first opportunity to compare 7-membered ring nitroxides rates of reduction to existing nitroxides like TEMPONE, TEMPOL, PROXYL and other more stabilized nitroxides generated by our lab[34] to establish a magnitude on the stabilization effect due to nitroxide ring size, if any. Table 2.3 compares the rates of reduction by ascorbate of these new and known nitroxides.

Figure A-1. EPR (X-band) spectrum of 70 (2.0 mM) (Left) and 71 (2.0 mM) (Right) in $CHCl_3$ used for spin concentration determination.

Table 2.3. Structure and reduction rate (M^{-1} s^{-1}) of piperidine, piperidinone, and pyrrolidine nitroxides.[a]

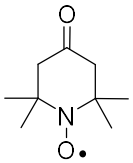 6.32 ± 0.01	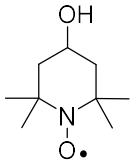 5.6 ± 0.2	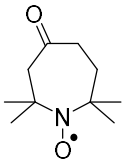 26.4 ± 0.65	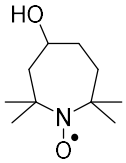 0.278[b]	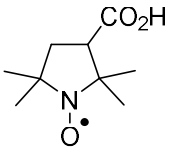 0.063 ± 0.002
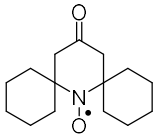 3.2 ± 0.2	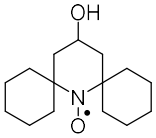 2.57 ± 0.03			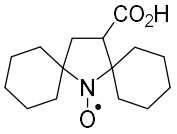 0.031 ± 0.003
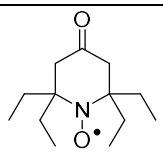 0.044 ± 0.002	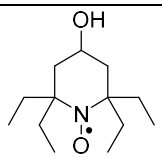 0.039 ± 0.003			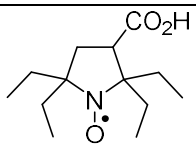 ≤0.001

[a] Mean ± two standard deviations from at least three measurements.
[b] The result of one measurement.

Table 2.3 also shows trends for the significant factors already well understood in nitroxide structural features affecting resistance to reduction by ascorbate.[34] Specifically, by comparing the different shielding groups (ie. methyl-, ethyl-, and spiro-cyclohexyl-) around the nitroxide

In the case of the **71** compared to the 6-membered nitroxide TEMPOL (**73**), there appears to be some stabilization evident by the decreased rate of reduction by ascorbate. **71** has a stabilization factor of about 20 compared to the 6-membered TEMPOL; if expecting to realize the full stabilization seen in I-strain examples in Table 2.1, we should see stabilization by around a factor of 130-160. The I-strain model would also predict the 7-membered nitroxide would be more stable than their 5-membered counterpart. Since the functional group is changing from an alcohol to a carboxylic acid in addition to the ring size, we are unable to make a comparison to the 5 membered rings correcting for the functional group change.

However, when compared to the 6-membered nitroxide TEMPONE (**74**), the **70** unexpectedly has an accelerated rate of reduction in the presence of ascorbate by about a factor of 4. The **70** is less stabilized than the TEMPONE counterpart. This is contrary to rate measurements for known nitroxides where is only a minor difference in the rate of reduction of the ketone- vs. alcohol-functionalized nitroxides across the methyl-, ethyl-, and spiro-cyclohexyl-shielded nitroxide.

The first initial observation from these results is that full realization of the stabilization observed in the reduction of cycloanones of various ring sizes was not

observed for the reduction of nitroxides of various by ascorbate. This may be rationalized by the fact the nitroxide is not fully sp^2-hybridized. This is supported by other experimental measurements of the N—O bond; as previously discussed in the Section 2.1.1. Specifically, the measured bond length of TEMPOL[72] is 1.26 Å; compared to 1.48 Å for the sp^3 hybridized *N*-methylhydroxylamine[73] and 1.19 Å for the sp^2 hybridized oxoammonium salt of TEMPO[74]. Further, the IR spectrums follow the same trend for the N—O bond; hydroxylamine[9] (926 cm^{-1}), TEMPOL[10-11] (1371 cm^{-1}), and the TEMPO oxoammonium salt (1602 cm^{-1}). Since the rehybridization of the N—O bond as the nitroxide is reduced by ascorbate to hydroxylamine never has full sp^2 character, the expected magnitude should be less.

The second observation is the fact the 7-membered ketone had a result that was opposite of what was expected and observed in the reduction of cycloanones. The first rationale for this deviation from what is observed for the reduction of cycloanones is that the ketone-nitroxide system introduces an additional sp^2 center into the ring system. This additional center would cause different possible conformations compared to the alcohol nitroxide system. Some of these conformations may allow the carbonyl to interact with the nitroxide, thus activating it towards reduction by ascorbate. In fact, as previously presented in the C—ON bond homolysis of alkoxyamines, alkoxyamine ketones underwent homolysis slower than the reduced alcohol series. The effect of the carbonyl on the nitroxide may be explained by looking at some physical measurements observed in some simple medium-sized heterocycles that are explained via transannular interaction between the amine and the carbonyl. We will discuss this more fully in Section 2.2.2.3,

as some additional experimental observations regarding 8-membered rings may also be explained by the same reasons.

2.2.2.2 BF_3•OEt_2 Ring Expansion of 7 to 8-membered

As mentioned before, attempts to duplicate the success of the one-carbon ring expansion with diazoacetate and BF_3•OEt_2 to go from the 7-membered to 8-membered proved difficult. After obtaining the 7-membered keto-amine, we successfully attempted the BF_3•OEt_2 mediated ring expansion, although were unable to purify the keto-ester (**75**) as it was behaving as a zwitterion making purification difficult (as we also saw with the 7-membered keto-ester amine). Attempts to decarboxylate the crude material (as was done for the 7-membered ring) to purify the ketone-amine failed.

Literature example shows that the free amine in 5-azacyclooctanone is in a position favorable to attack the carbonyl readily reacting to form 1,8-dehydropyrrolizidine resulting in an enamine upon elimination.[75] We observed similar products in our attempts to decarboxylate the 8-membered keto-ester amine. When evaluating the crude material via ESI-MS the predominant peaks were masses matching the proposed structures shown in Figure A-1. The crude NMR also shows a mixture of unknown compounds and a failure to generate the amine of interest.

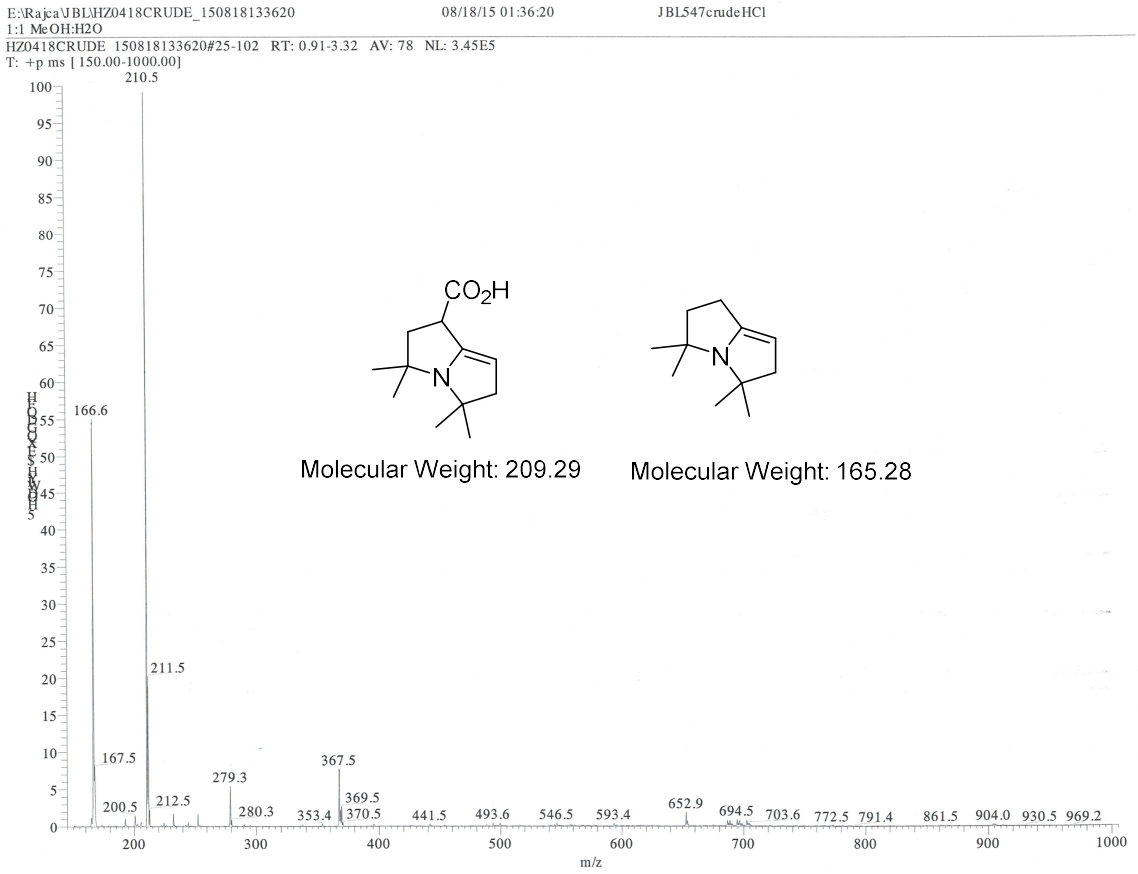

Figure A-1. ESI of attempted decarboxylation of 75 and proposed structure of products.

Understanding that the free amine and keto-ester were making purification difficult and knowing that if attempting a radical Dowd-Beckwith ring expansion on a cyclic amine (literature attempts of the ring expansion on N-heterocycles required a protecting group[76-77]) it would need an amine-protecting group, we explored placing a protecting group on the 2,2,6,6-tetramethylpiperidinone starting material.

We successfully and ultimately improved upon a literature protection strategy[78] installing a benzyl carbamate protecting group onto 2,2,6,6-tetramethylpiperidinone using K_2CO_3 and benzyl chloroformate in THF. The reported literature yield was 15% for the

protected compound (**76**) and we were able to improve this to over 26%, we were also able to perform the reaction on much larger scale (25x). The literature procedure omitted K_2CO_3, essentially using 2,2,6,6-tetramethylpiperidinone as a sacrificial base to neutralize the HCl produced by the reaction. By adding K_2CO_3 to neutralize the HCl produced, we were able to make the 2,2,6,6-tetramethylpiperidinone the limiting reagent rather than benzyl chloroformate.

Scheme 2.12. Synthetic Scheme towards 8-membered ring nitroxides.

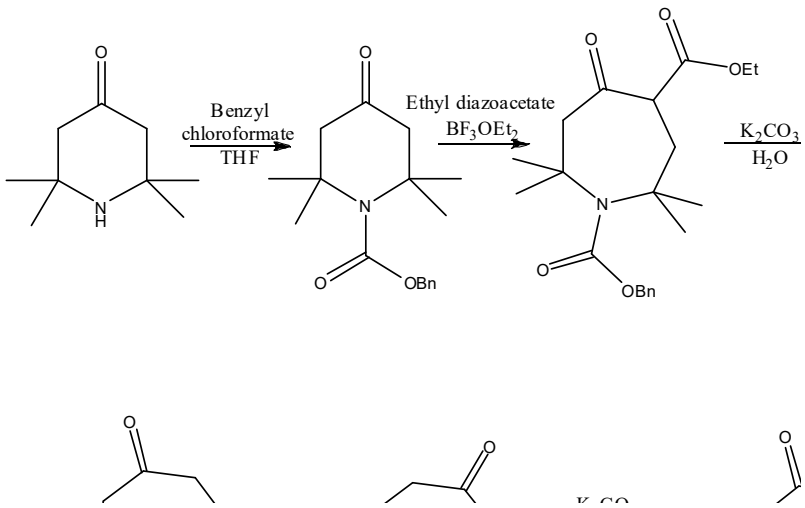

From the benzyl carbamate protected 2,2,6,6-tetramethylpiperidinone (**77**) we were able to better control the BF_3•OEt_2 ring expansion reaction and greatly improve its

reproducibility and purity (up to 60% and consistently able to isolate pure material) of the protected keto-ester (**78**), even having successful reaction on larger scale.

2.2.2.3 Conformational Interactions of Medium-sized Rings

Transannular interaction between the amine and carbonyl has been observed and studied in medium sized *aza*-cycloanones[79-82] (particularly 8-membered, but it's been postulated to explain behavior in some unique 7-membered azepanones). The lower spectral shifts in IR observed indicate the electrons in the nonbonding orbital of the nitrogen atom are in a conformation able to interact with the antibonding π orbital of the carbonyl, resulting in partial if not full electron transfer and a carbonyl with decreased double bond character. Additional physical measurements result in a δ5-10 ppm shift for ^{13}C NMR of the carbonyl peak of 8-membered amino ketones vs. cyclooctanone.[83-85] The evidence of this transannular interaction in these systems and similar observations in the physical properties and reaction outcomes of the compounds we've been investigating suggest transannular interaction may explain some of our observations.

2.2.3 Synthesis towards 8 and 10-membered Ring Nitroxide Precursors using Dowd Beckwith Radical Ring Expansion

Having obtained the protected 7-membered keto-ester, deprotonation to generate the keto-enolate with Cs_2CO_3 followed by alkylation with either diiodomethane or diiodopropane gave us the alkyl halogen precursors (**79** and **80**) needed for the radical ring expansion as seen in Scheme 2.13. Both alkylations occurred in good yield and were easily purified via column chromatography.

Scheme 2.13. Alkylation followed by Ring expansion of 78.

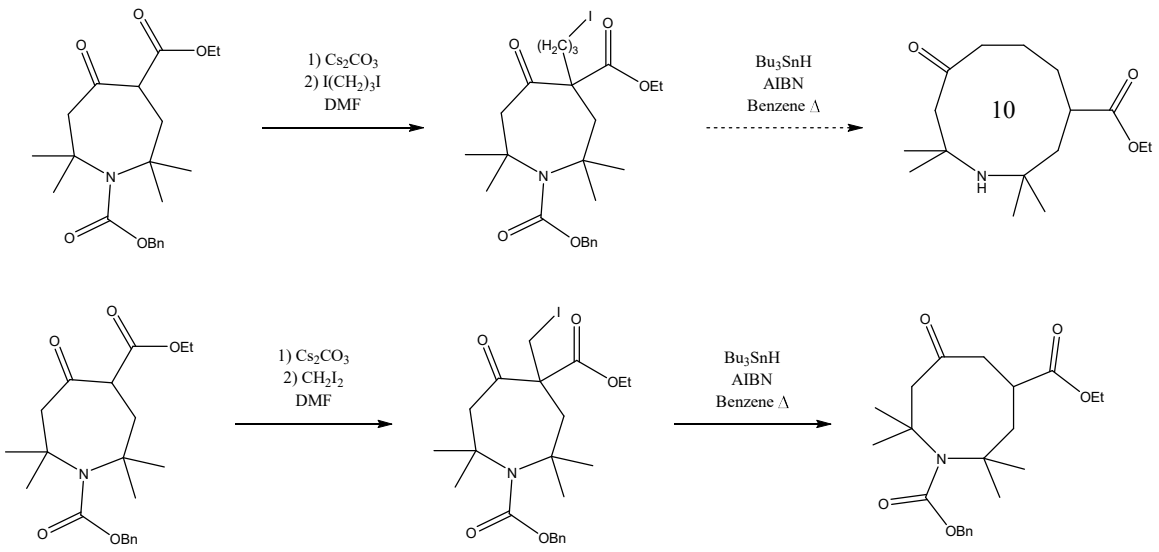

2.2.3.1 Dowd-Beckwith Radical Ring Expansion

Originally, we felt that the Dowd-Beckwith radical ring expansion[86-89] would prove a useful synthetic tool allowing us access to expanded ring products as precursors for nitroxide radicals. We based our original retrosynthetic design upon this reaction as previously discussed, as it provided access from the 6-membered starting material to 7, 9 and 10-membered rings just by varying the alkyl chain length. Obviously, when we were unable to generate the require starting 6-membered keto-ester, we had to modify our synthetic strategy to use the **78** as the starting point for Dowd-Beckwith ring expansion.

This radical reaction begins with an initiation step by thermal decomposition of AIBN forming two 2-cyanoprop-2-yl radicals, which readily reacts with Bu_3SnH generating a radical $Bu_3Sn\cdot$ species. The propagation step is based on generation of a carbon-centered radical from homolytic abstraction of the halogen from an alkyl halide

chain with the radical $Bu_3Sn\cdot$ species, the generated radical then attacks the carbonyl group via a 3, 5 or 6-*exo-trig* (depending on the substrate chain length) ring cyclization. The resulting alkoxy radical undergoes bond scission of the ring to yield a radical at a position stabilized by an ester substituent. A mechanism of the reaction along with an alternate competing pathway is shown in Scheme 2.14.

Scheme 2.14. Mechanism and factors controlling Dowd-Beckwith Ring Expansion.

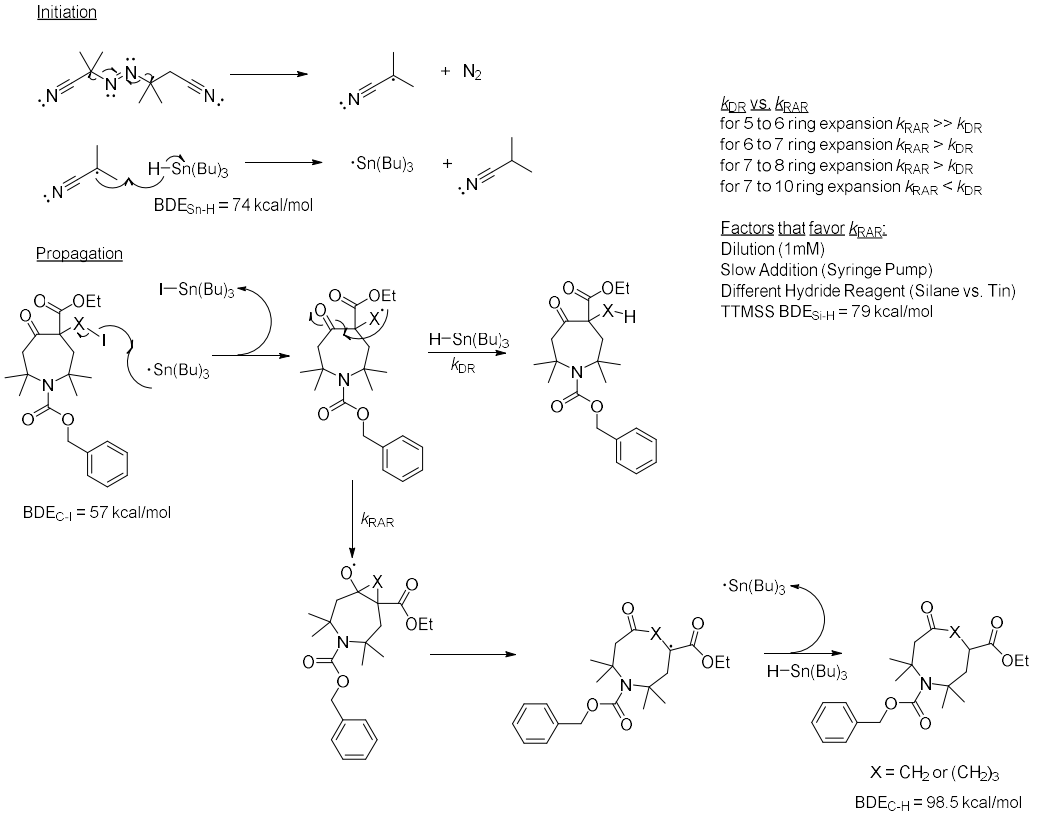

However, as Scheme 2.14 shows, a common observed side product of the reaction is the direct reduction of the alkyl halide to the alkane. Once the carbon centered radical is generated, there is a competition between the rates of reaction for the ring expansion product vs. direct reduction by Bu_3SnH. Some experimental factors that can be used to favor k_{RAR} over k_{DR} include: dilute reaction conditions (~1 mM) to minimize excess

$SnBu_3H$ available to react; and controlled, slow addition of Bu_3SnH via syringe pump. Alternative solutions suggested by the literature include using a different hydride reagent such as TTMSS, which is a silane that has a larger H—Si BDE of 79 kcal/mol vs. H—Sn BDE of 74 kcal/mol, which could slow the termination step resulting in the direct reduction product by the reaction of the alkyl radical with the hydride reagent.[90] We also briefly explored a Zn-mediated radical reaction without success.[91]

Another issue already noted in the literature, is this reaction has been attempted on protected amines but depending on the protecting group had mixed results due to alternative pathways including 1,5-hydrogen atom transfer from the benzyl protecting group from the initial radical. Upon replacing the benzyl group with a trityl group (eliminating the hydrogen atom source) the ring expansion reaction became predominant.[76-77] To avoid this potential issue via the 1,5-hydrogen atom transfer, we used a benzyl carbamate protecting group which moved the possible hydrogen atom being abstracted farther away.

After varying success, the reaction proved more reliable and reproducible using distilled benzene thoroughly degassed with a series of freeze-pump thaw cycles and controlled slow addition of Bu_3SnH using a syringe pump under Ar atmosphere. Another initial difficulty was the removal of organotin impurities, however a literature procedure[92] using traditional flash column chromatography using a modified stationary phase composed of 10% finely ground K_2CO_3 with silica gel proved to offer substantial improvement in the ease of purification and in purity of compounds.

We were able to isolate the intended 8-member ring expanded product (**81**) as shown in Figure A-1, but it had a predominant side product (**82**) as discussed in the next subsection. We were able to obtain a sample pure enough for structural analysis via ^{1}H, ^{13}C, $^{1}H—^{1}H$ COSY, $^{1}H—^{13}C$ HSQC, and $^{1}H—^{13}C$ HMBC NMR. The ^{1}H NMR in Figure A-2 shows chemical shifts expected for the **81** with 4 distinct CH_3 groups, and distinct multiplets for each of the hydrogens on the ring. Additionally the $^{1}H—^{1}H$ COSY confirms the suspected couplings as indicated in Figure A-3, showing: coupling between the hydrogens on the isolated CH_2 adjacent to the ketone with themselves (circled in red); coupling between the CH_2 adjacent to the quaternary C attached to the amine with themselves (circled in blue) along with those hydrogens coupling with tertiary CH where the ester attaches (shown in orange); it also shows coupling between the multiplet around δ3.0 ppm (which is in fact two different CH signals as confirmed by $^{1}H—^{13}C$ HSQC) with both two different CH_2 groups (circled in orange and green); and finally the obvious coupling of the ethyl group of the ester is evident.

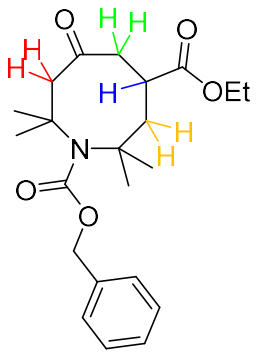

Figure A-1. Proposed structure for Compound 81

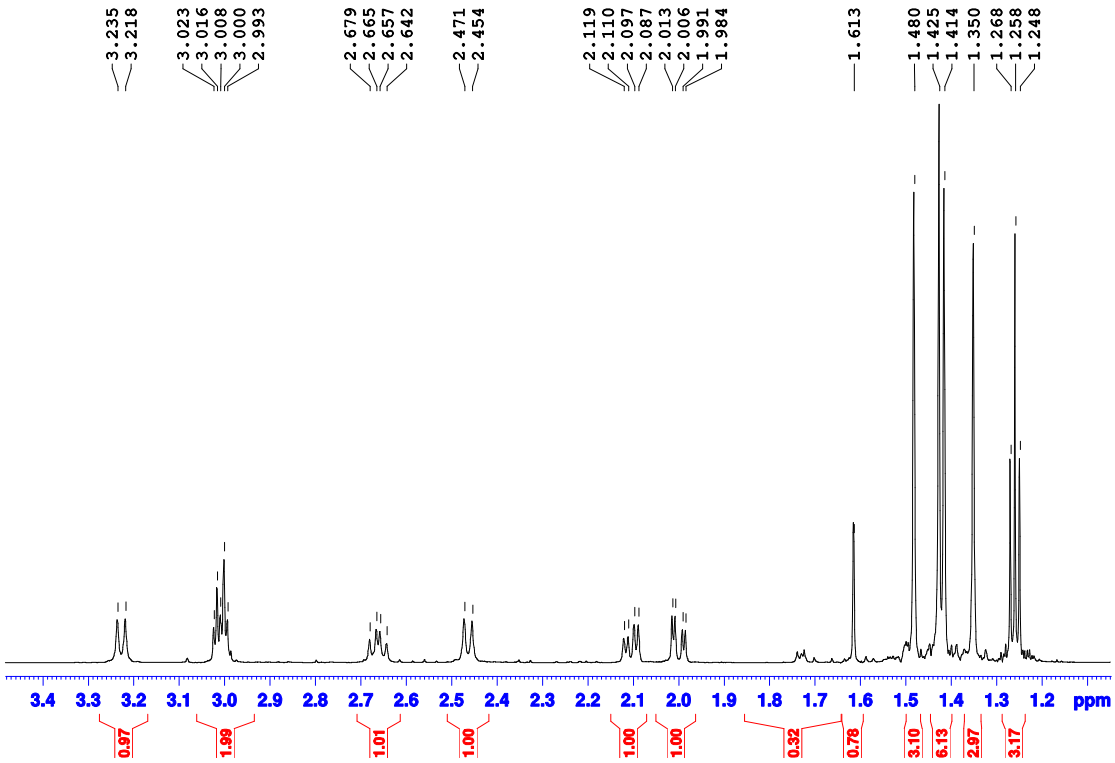

Figure A-2. ^{1}H NMR for 81.

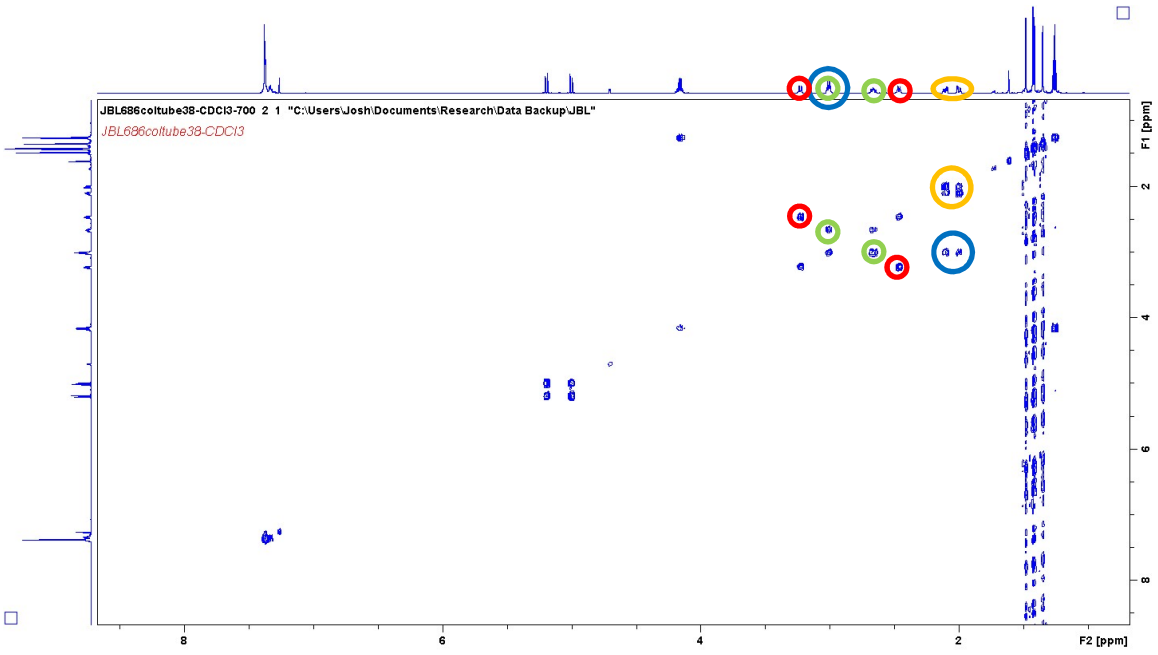

Figure A-3. ^{1}H—^{1}H COSY for compound 81. **Key couplings for structural identification are circled.**

The ^{13}C confirms 20 different resonances, which matches with what is expected and matches chemicals shifts for the carbonyls of the ketone, the benzylic ester and the ethyl ester. As mentioned before the $^{1}H—^{13}C$ HSQC in Figure A-4 confirmed the presence of overlapping C—H peaks in the proton NMR, one assigned to the tertiary CH where the ester attaches, and the other a hydrogen that is part of a CH_2 group between the ketone and the tertiary carbon where the ester attaches. The $^{1}H—^{13}C$ HSQC also confirms which protons are on shared carbons as expected.

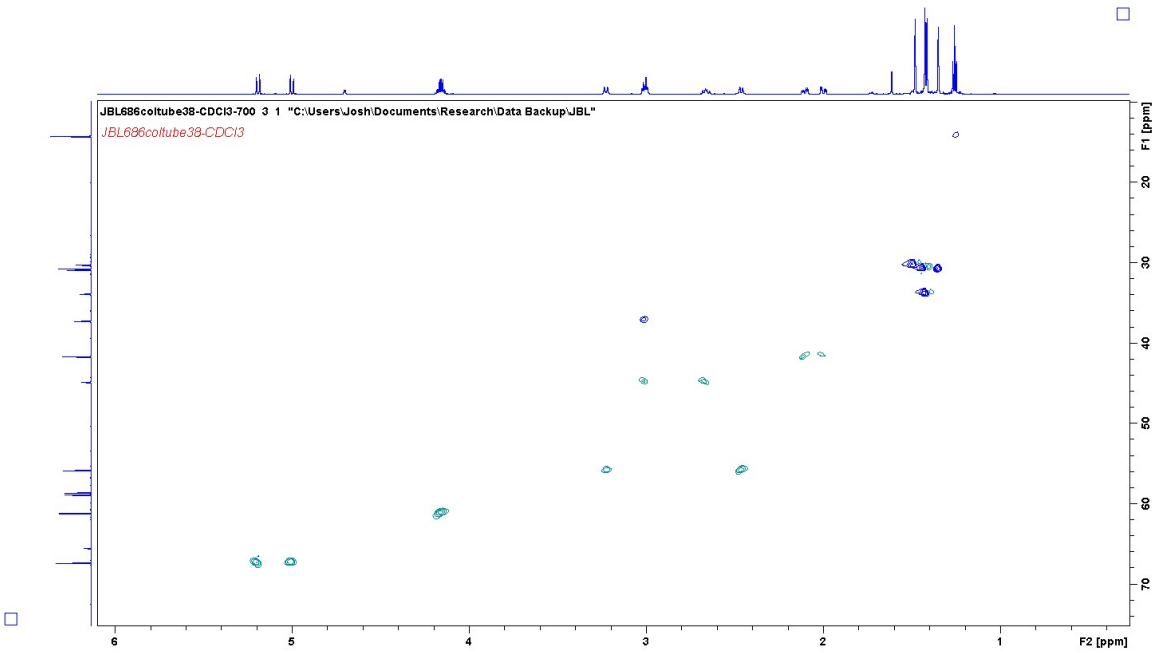

Figure A-4. $^{1}H—^{13}C$ HSQC for compound 81**.**

Finally, the $^{1}H—^{13}C$ HMBC seen in Figure A-5 with the $^{1}H—^{13}C$ HSQC overlaid, and zoomed in Figure A-6, and zoomed in the carbonyl region in Figure A-7. The HMBC zoomed in the carbonyl region shows 2- to 3-through bond coupling between the carbonyl and the expected hydrogens (both CH_2 groups adjacent to the ketone, and with the tertiary CH three bonds away); the carbonyl of the ester shows coupling with the

expected hydrogens (only on CH_2 adjacent to the ketone, the CH_2 adjacent to the quaternary C, and the tertiary CH where the ester is attached). The coupling of the tertiary CH where the ester attaches with both carbonyl groups is in line for our proposed structure.

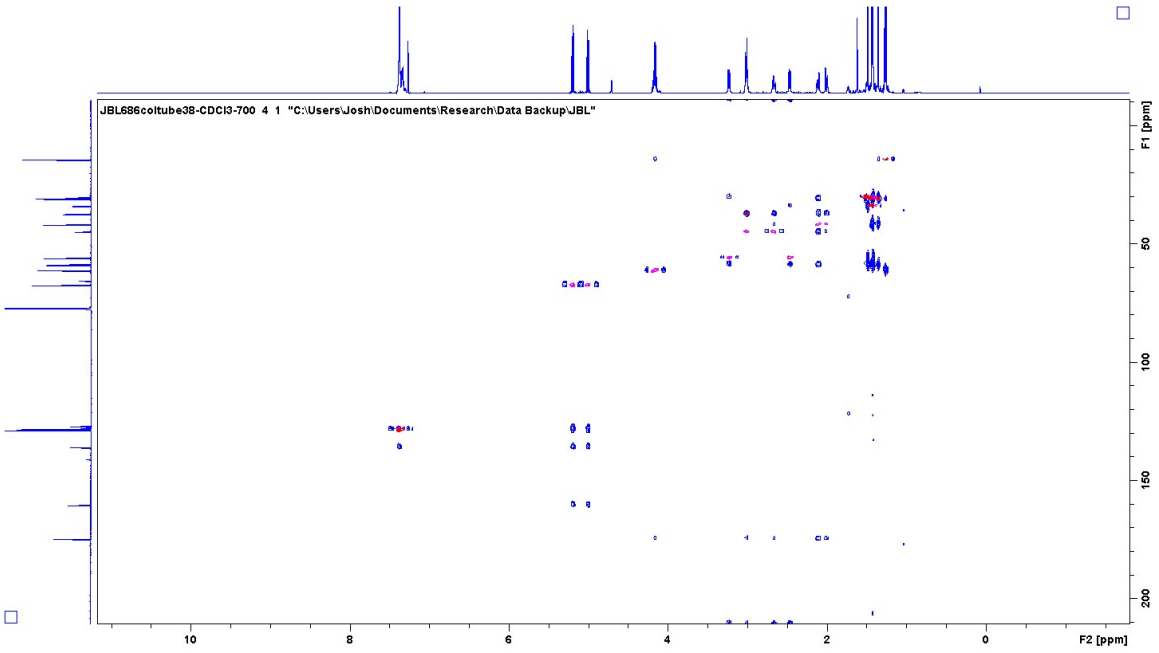

Figure A-5. ^{1}H—^{13}C HMBC with ^{1}H—^{13}C HSQC overlaid for compound 81**.**

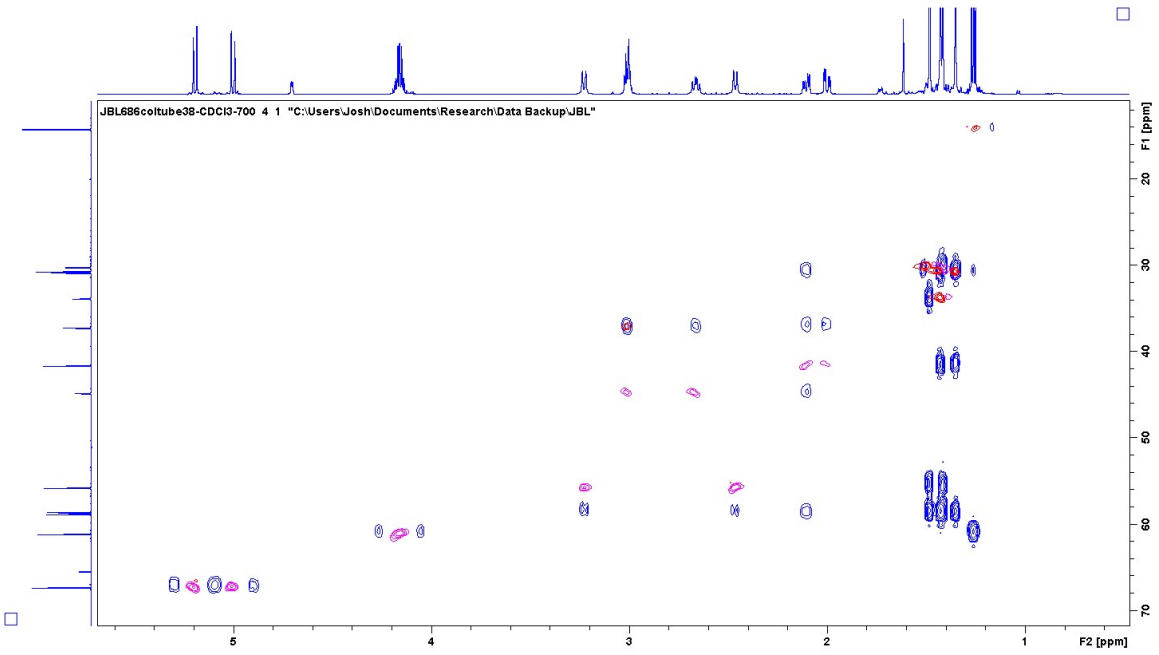

Figure A-6. Zoomed $^{1}H—^{13}C$ HMBC with $^{1}H—^{13}C$ HSQC overlaid for compound 81**.**

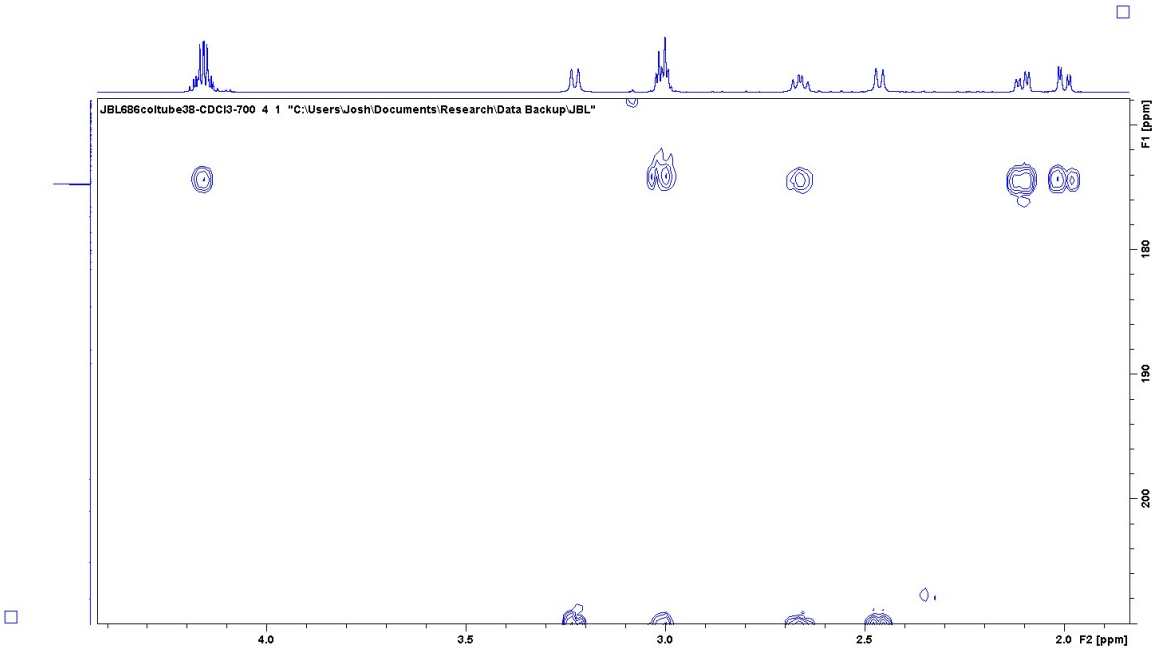

Figure A-7. Zoomed $^{1}H—^{13}C$ HMBC (carbonyl region) for compound 81**.**

2.2.3.2 Alternate Outcomes of Radical Ring Expansion

While having some success with the radical ring expansion towards the 8-membered ring, it also gave some unprecedented side products not reported or characterized before in the literature as shown in Figure A-1. Two diastereomers resulted from ring contraction through an alternative rearrangement pathway in almost equal conversion as the target material.

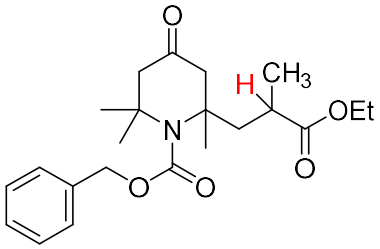

Figure A-1. Proposed structure for contracted ring product 82**.**

A sample sufficiently pure of one of the diastereomers was confirmed via NMR experiments including ^{1}H, ^{13}C, $^{1}H—^{1}H$ COSY, $^{1}H—^{13}C$ HSQC, $^{1}H—^{13}C$ HMBC and $^{1}H—^{15}N$ HMBC, giving conclusive proof of the structure. The ^{1}H NMR in Figure A-2 shows chemical shifts expected for the **82** with 4 distinct CH_3 groups (a potential 5^{th} CH_3 group at around 1.57 has no ^{13}C coupling via $^{1}H—^{13}C$ HSQC and is an impurity of either a byproduct or H_2O), with the CH_3 around 1.06 showing as a doublet. This is an unexpected coupling for our proposed target compound and is indicative of being adjacent to a carbon with one hydrogen attached. Specifically, the coupling of the hydrogen adjacent to the ester (highlighted in red) and the methyl is confirmed by the $^{1}H—^{1}H$ COSY NMR as seen in Figure A-3, as it shows coupling with the CH_2 and the CH_3 group.

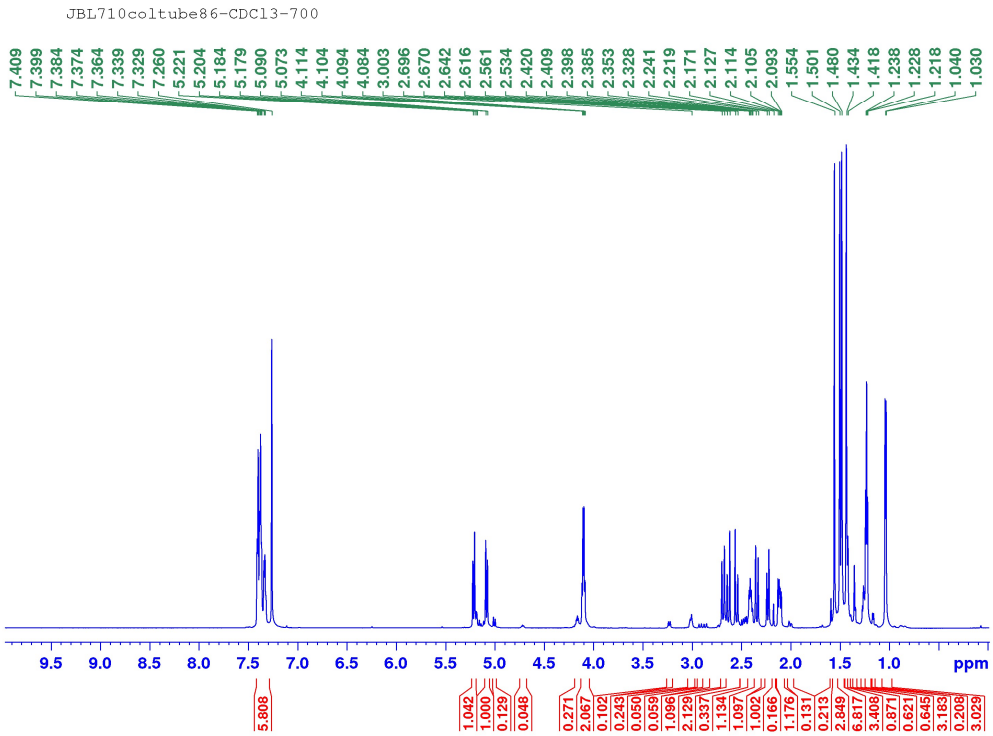

Figure A-2. ^{1}H NMR and zoomed ^{1}H NMR for compound 82**.**

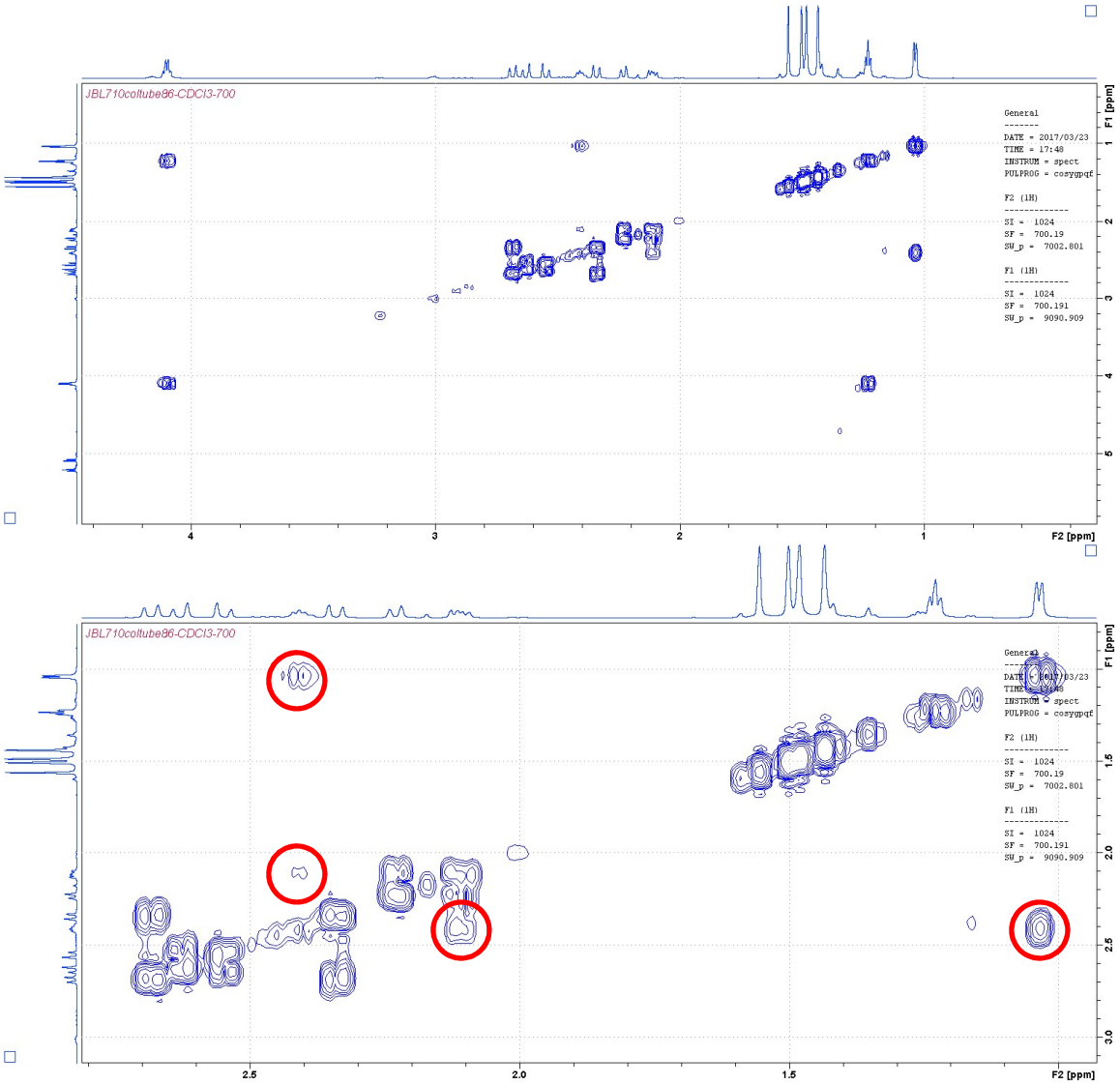

Figure A-3. ^{1}H—^{1}H COSY and zoomed ^{1}H—^{1}H COSY for compound 82. Key couplings for structural identification are circled in red.

The ^{13}C confirms 20 different resonances, which matches with what is expected and matches chemicals shifts for the carbonyls of the ketone, the benzylic ester and the ethyl ester. The ^{1}H—^{13}C HSQC in Figure A-4 was able to identify the substitution of each of the carbons and shows which carbons have multiple proton peaks.

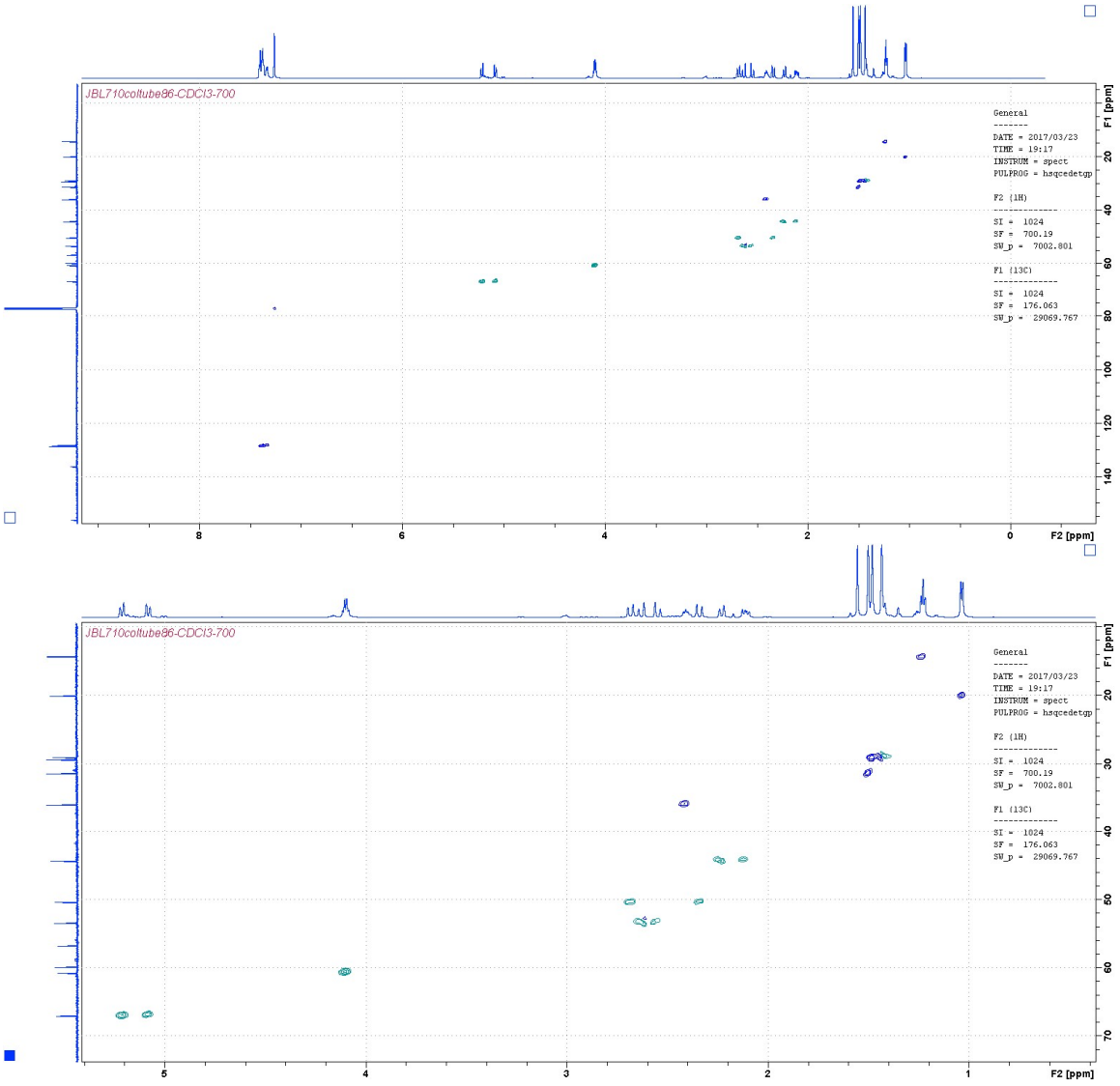

Figure A-4. $^{1}H—^{13}C$ HSQC and zoomed $^{1}H—^{13}C$ HSQC for compound 82.

The $^{1}H—^{13}C$ HMBC seen in Figure A-5 showed 2 to 3-through bond coupling of the tertiary hydrogen only with the ester carbon and not with the ketone carbon. It also showed the same coupling of the ester with the CH_3 and CH_2 group adjacent to the CH indicating an isolated chain, with no other coupling of the ester with any other hydrogen's outside the alkyl portion of the ester itself.

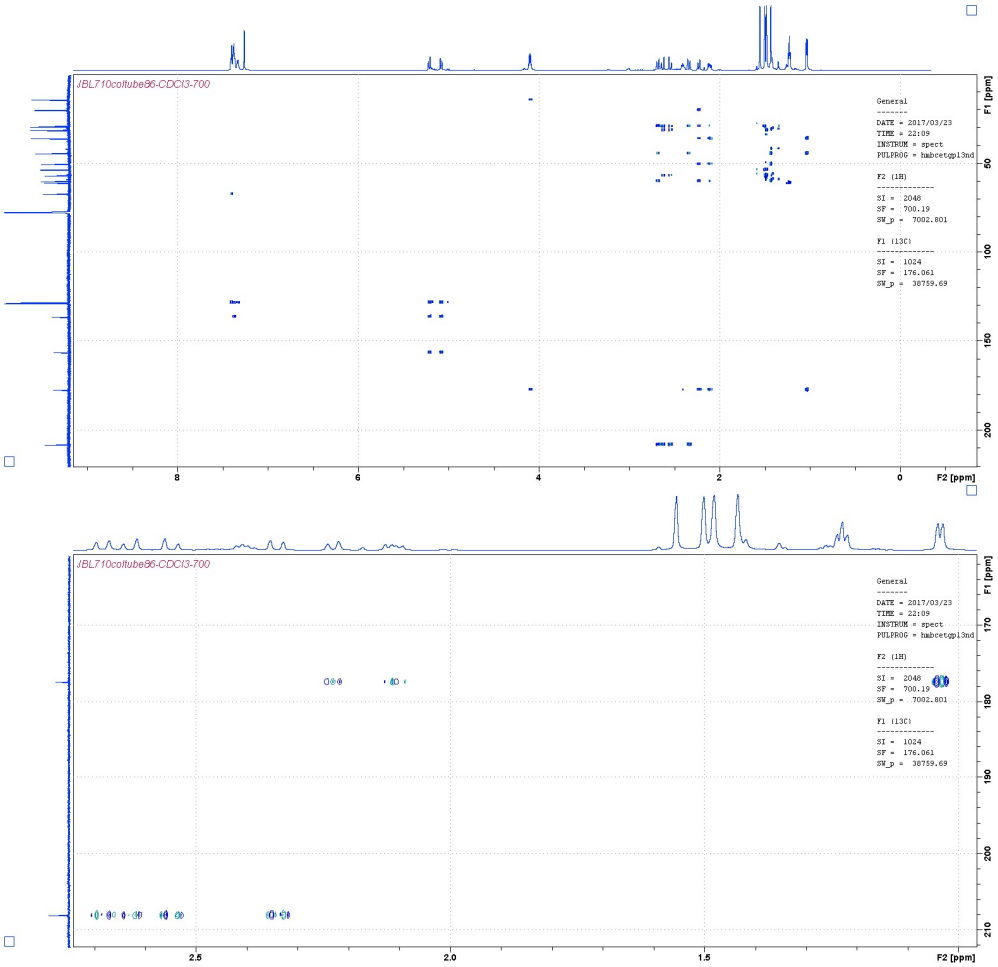

Figure A-5. ^{1}H—^{13}C HMBC and zoomed ^{1}H—^{13}C HMBC (carbonyl region) for compound 82**.**

Finally, the ^{1}H—^{15}N HMBC shown in Figure A-6, confirms which hydrogens have 2 to 3-through bond coupling with the N atom, which are the three CH_3 groups, the two CH_2 groups adjacent to the ketone and only the CH_2 group starting the alkyl chain with the CH, CH_3 and ester. The ^{15}N chemical shift of 81.0 for the amine in **82** is observed in the ^{1}H—^{15}N HMBC NMR.

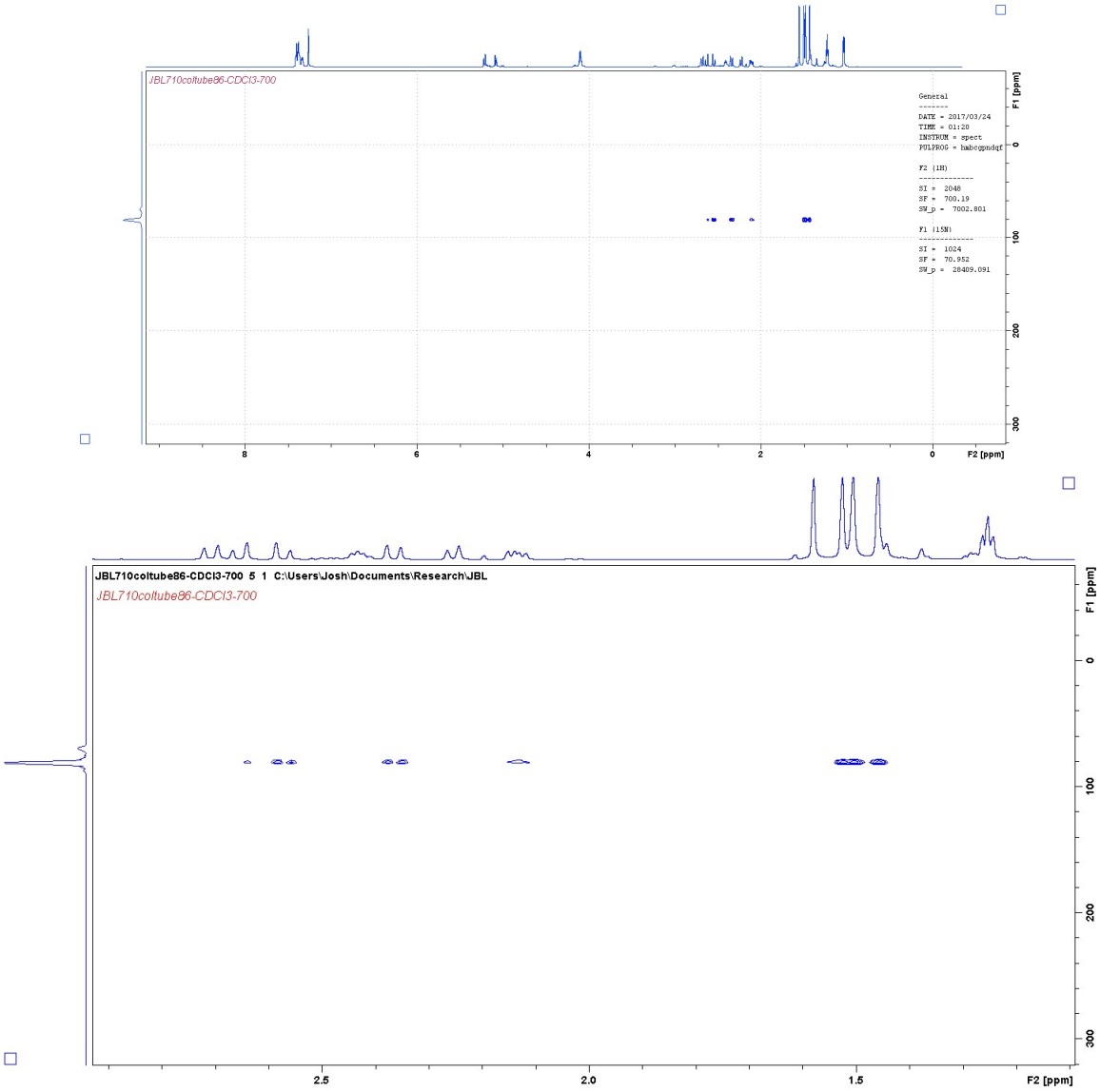

Figure A-6. ^{1}H—^{15}N HMBC for compound 82**.**

A mechanism and rationale for its basis is shown in Scheme 2.15. If follows that once the radical is generated it has three different plausible reaction paths: it can undergo direct reduction to the alkane; undergo the desired 1,3-radical cyclization; or as proposed could undergo a 1,5-hydrogen transfer. The hydrogen on the methyl group is in a position where 1,5-hydrogen transfer is competitive for the 1,3-radical cyclization. Once the 1,5-hydrogen transfer takes place, a 1,5-radical cyclization between the radical and

the carbonyl is proposed. Once, this cyclization takes place, a tertiary radical stabilized by an ester is formed giving the one-carbon ring contraction product.

Scheme 2.15. Proposed mechanism for ring expansion vs. ring contraction.

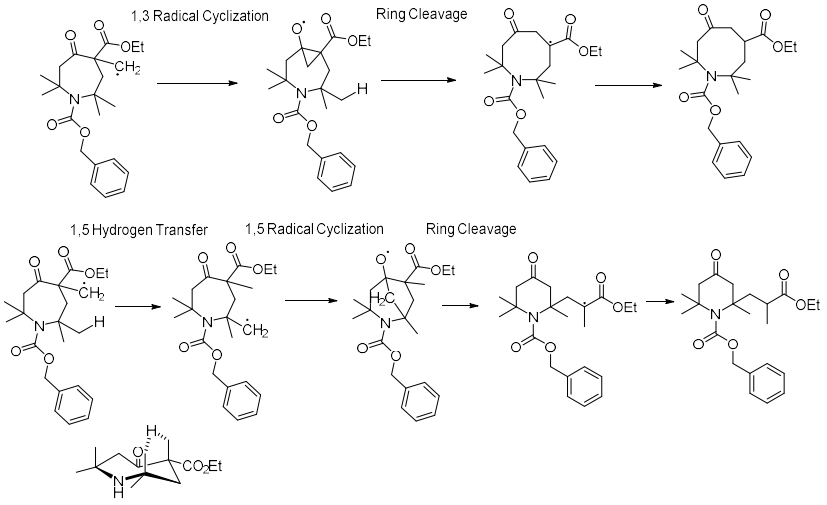

Additionally, the 7 to 10 membered radical ring expansion was attempted as examples of 1-, 3- or 4-carbon Dowd-Beckwith ring expansions have been shown. These attempts resulted in a diastereomeric mixture (**83**) of a one-carbon ring expansion from the 7- to 8-membered ring with an ethyl group attached to the carbon now incorporated into the ring as proposed in Figure A-7. This is another previously unreported rearrangement. These were the only products other than early iterations of the reaction that generated some direct reduction products before optimization. These diastereomers were further resolved via pTLC to give a sample sufficiently enriched with one diastereomer over the other for structural confirmation using ^{1}H, ^{13}C and 2-D NMR experiments including ^{1}H—^{1}H COSY, ^{1}H—^{13}C HSQC, ^{1}H—^{13}C HMBC and ^{1}H—^{15}N HSQC.

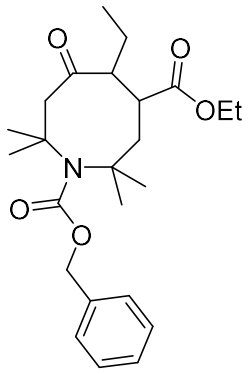

Figure A-7. Proposed structure of compound 83.

First, the chemical shifts for the ^{1}H and ^{13}C NMR are very similar to what we see for compound **81**, with the only difference being the replacement of hydrogen with an ethyl group. Specifically, the ^{1}H NMR and ^{1}H—^{1}H COSY clearly shows two different ethyl substituents, one part of the ester based on chemical shifts and the other an unknown part of the molecule. Analysis of the ^{1}H—^{13}C HSQC show there are two different proton peaks that appear on tertiary carbons (the peak at 2.388 shows as a singlet; the peak at 2.683 a triplet). The ^{1}H—^{1}H COSY experiment confirms that coupling between the hydrogen adjacent to the ester and the CH_2 group next to the quaternary carbon connected to the amine. What is interesting is that the tertiary hydrogen near the ketone appears as a singlet, when coupling is expected between both the attached ethyl group and the neighboring proton adjacent to the ester. The ^{1}H—^{13}C HMBC shows that the singlet proton has 2- to 3-through bond coupling to both the ketone and ester carbonyl groups, while the triplet single proton does not show through bond coupling to the ketone and only the ester. Additionally, they also show through-bond coupling to each other.

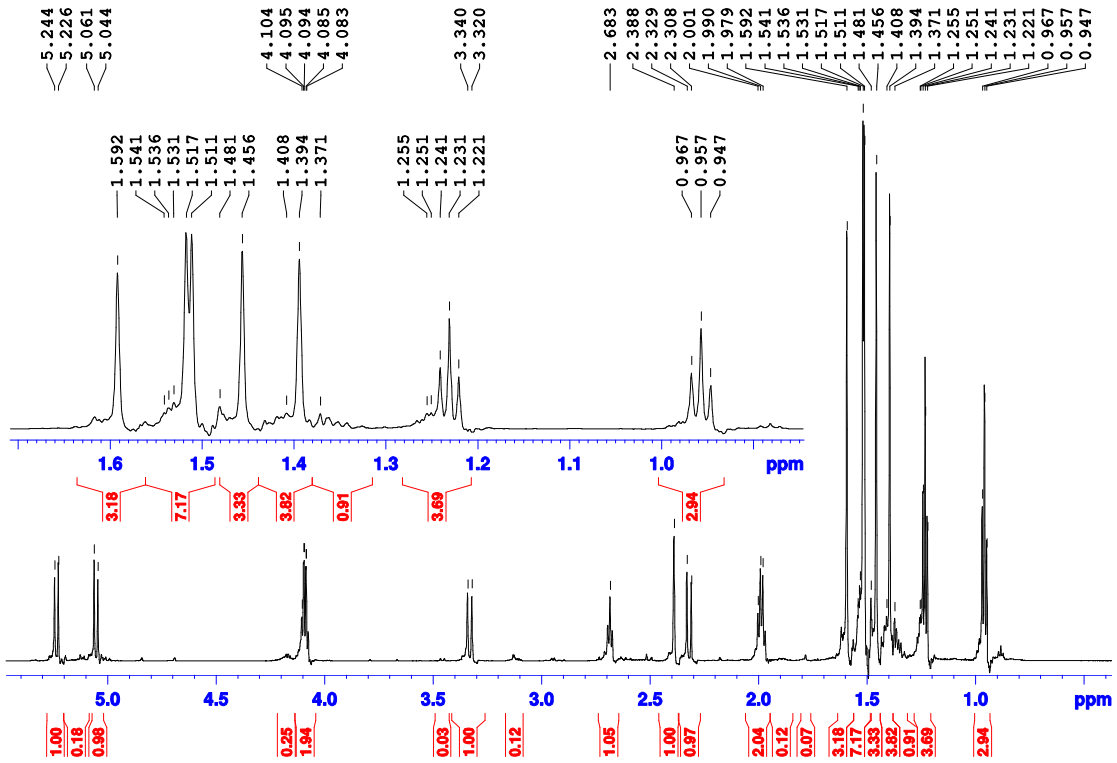

Figure A-8. ^{1}H NMR and zoomed ^{1}H NMR for compound 83.

Figure A-9. ^{1}H—^{13}C HSQC and zoomed ^{1}H—^{13}C HSQC for compound 83.

A mechanism and rationale for the formation of **83** is shown in Scheme 2.16. If follows that once the radical is generated it has three different pathways for reaction: the previously discussed 1,5 radical cyclization leading to the 3-carbon ring expansion; direct

reduction; or a third pathway via a 1,3 hydrogen-atom transfer, giving a radical that then can proceed via a 1,3-radical cyclization to the 8-membered ring.

Scheme 2.16. Proposed mechanism for formation of 83.

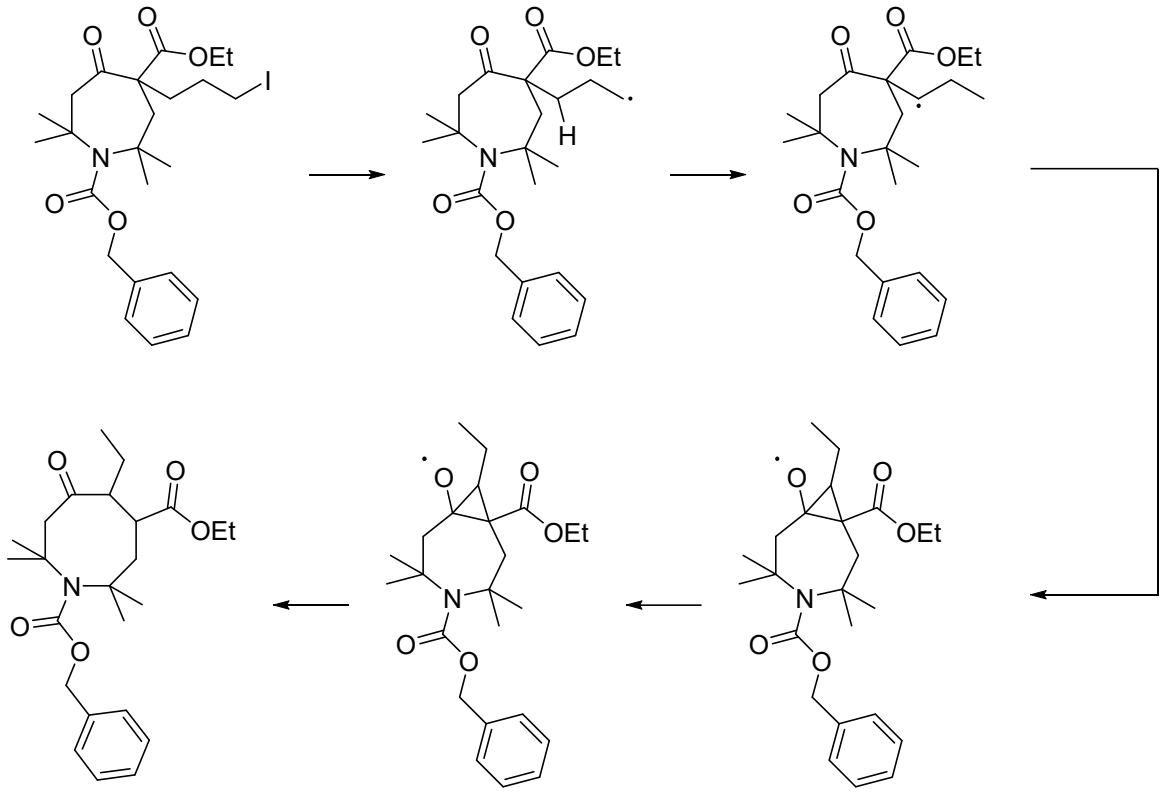

2.2.4 Alternative Approach towards Larger Ring Frameworks

One last approach that we tried included a pK_a driven reaction where the reaction was driven by the formation of a thermodynamically favored β-keto-ester stabilized enolate with a pK_a around 11 to 13. This strategy has successfully been used towards the synthesis of (-)-muscone, via an intramolecular aldol condensation of the 7-membered β-keto ester followed by retro aldol cleavage giving the expansion to the 10-membered ring.[93] The proposed mechanism of this method towards **84** is shown in Scheme 2.17.

Scheme 2.17. Proposed mechanism for 3-carbon nucleophilic ring expansion to 84.

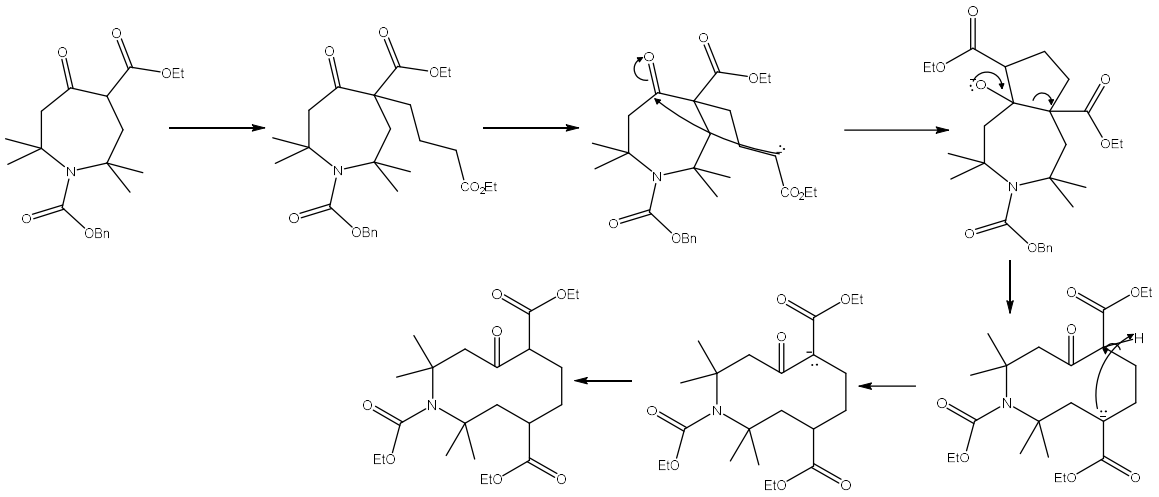

We briefly explored this avenue by synthesizing **85** and then attempting the three-carbon ring expansion, we were unsuccessful but unable to fully explore whether it may be a feasible method.

2.3 Conclusions

We achieved some success towards our initial project goals in generating and characterizing the 7-membered ring nitroxide radicals **70** and **71** and comparing their rates of reduction by ascorbate to existing compounds. Based on the additional data points of these 7-membered rings, our initial theory that I-strain may play a role in nitroxide stability is still possible, although the magnitude not quite as strong as we originally thought. It appears that other structural features and conformations may play a greater role in nitroxide stability as we observed the unforeseen destabilization of the 7-membered ketone compared to the alcohol towards reduction by ascorbate. Without being able to generate enough 8-membered nitroxide to subject to reduction and characterization, it's difficult to determine the true impact of I-strain on stability. Future

endeavors towards 8-, 9- and 10-membered nitroxide alcohols would provide a nice series evaluating the impact of I-strain in the future.

Overall, the ring expanded nitroxide project proved much more challenging than originally thought. We underestimated the limitations of doing chemistry around the ketone of the 2,2,6,6-tetramethylpiperidinone and the complexities surrounding the ring conformations of later expanded rings introduced new challenges with each iteration. We did gain some valuable experience how to handle these types of compounds and improved reaction efficiency as we became more familiar with the reactions.

While some of the reactions did provide for some unique outcomes, it was interesting and potentially useful to understand how and why these previously unreported alternate reaction pathway products predominated and, in some cases, we were able to mitigate their formation by modifying reaction conditions. Great satisfaction can still be found in discovering and identifying a structure or pathway for an unexpected reaction product through application of fundamental organic chemistry principles and old-fashioned problem-solving.

2.4 Experimental Section

2.4.1 Synthesis of 7-membered keto-nitroxide

2,2,7,7-tetramethylazepan-4-one (69)

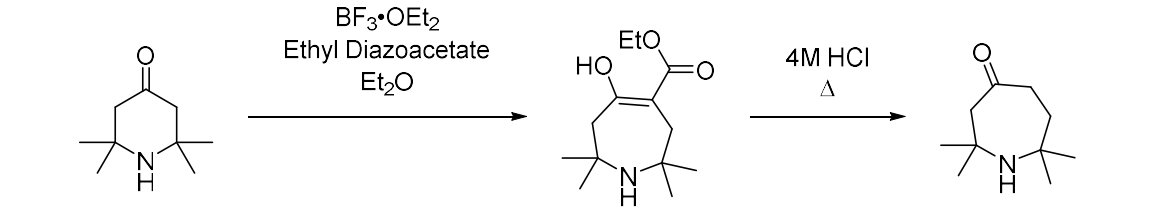

Run	SM (g)	$BF_3 \cdot OEt_2$ (mL)	Ethyl Diazoacetate (g)	Et_2O (mL)	TM (g)	Yield (%)	TM label
JBL514	1.0	2.98	1.033	26	0.313	20	JBL514solid
					0.97	62.1	JBL514filtrateextract
JBL518	3.0	9.0	3.1	90	1.409	30.1	JBL518solid
JBL522	3.0	9.0	3.1	90	1.449	30.9	JBL522solid
JBL528	3.0	9.0	3.1	90	1.548	33	JBL528solid
JBL529	3.0	9.0	3.1	90	2.168	46.3	JBL529solid
JBL551	3.0	9.0	3.1	90	2.871	N/A	JBL551/552solid
JBL552	3.0	9.0	3.1	90	6.184	N/A	JBL551/552extract

Run	SM (g)	HCl (4 M) (mL)	TM (g)	Yield (%)	TM label
JBL447	.936.7	40	.409	62.2	JBL447colfrac5-8
JBL489	3.900	120	1.058	N/A	JBL489colfrac2-4
JBL520	0.970	30	0.249	30	JBL520HClrecryst3-crop1
JBL524	410	55	0.5176	43	JBL524HClrecryst-crop1
JBL525	1.449	55	0.523	43	JBL525HClrecryst-crop1

JBL531	2.168	70	0.3365	18.7	JBL531HClrecryst-crop1
JBL556	2.52	55	0.200	18.3[a]	JBL556HClrecryst-crop1+2
JBL557	6.18	130	1.253		JBL557HClrecryst-crop1-4

[a] Yield based on 2-steps from 2,2,6,6-tetramethylpiperidinone

JBL551/552 and 556/557: Distilled 2,2,6,6-tetramethylpiperidi-4-none (3.0 g, 19.35 mmoles) was put in 250 mL round bottom flask with stir bar and sealed with a septum. The flask was then evacuated and filled with N_2 three times. A N_2 balloon was placed on the flask. Dry diethyl ether (80 mL) was then transferred via syringe to the reaction flask. The flask was cooled to -10°C and BF_3•OEt_2 (9.0 mL, 72.9 mmol, 3.76 equiv.) was then slowly added via syringe, followed by dropwise addition of ethyl diazoacetate (3.1 g; 27.1 mmol; 1.4 equiv.) over ten minutes via syringe. The reaction warmed to room temperature after 1 hour and stirred overnight. A precipitate formed, and the solvent is decanted from it. The solid is washed sequentially with diethyl ether (50 mL), sat. $NaHCO_3$ solution (50 mL), and water (2 x 50 mL) (combining all the washes) and diethyl ether again (2 x 50 mL). The solid is pure enough for the next step. The combined washes are then separated. NaCl is added to saturate the aqueous solution, which is then extracted 3 times with EtOAc. The organic layers are all combined and dried with Na_2SO_4, filtered, and evaporated on the rotary evaporator, yielding an orange oil sufficiently pure for decarboxylation.

The oil (6.18 g) and solid (2.52 g) are separately suspended in 4M HCl (55 and 135 mL respectively) and refluxed for 16 hours. The solvent is then evaporated on the rotary evaporator, followed by azeotropic drying by adding toluene and evaporating on the

rotary evaporator four times. The HCl salt of the product is then recrystallized from acetone giving a yellow solid.

Note: In some cases, recrystallization was unsuccessful resulting in an oil. In this case the product can be purified by dissolving the HCl crude in 1 M NaOH solution and then extraction of the free amine with EtOAc three times. The organic layers are combined, dried with Na_2SO_4, filtered and evaporated. The brown oil is then dissolved in dry diethyl ether and acidified with dry HCl gas passed through Drierite generated by the addition of sulfuric acid into NaCl. The amine•HCl salt precipitates and collected via filtration. The solid is then recrystallized from acetone. Solid after recrystallization (1.45 g, 18.3% over two steps).

The free amine product is volatile, so the product is stored as the HCl salt. The free amine can quantitatively be generated immediately before subsequent reactions by dissolving in 1 M NaOH solution, adding NaCl to saturate the solution and extraction with EtOAc 4 times.

Intermediate Keto-Ester (**68**): ^{1}H NMR (400 MHz, $CDCl_3$, JBL555solidrecrystcrop2): δ 12.617 (s, 1H), 4.2539 (7, J = 7.1, 2H), 2.796 (br, 2H), 2.747 (s, 2H), 1.516 (s, 6H), 1.455 (s, 6H), 1.302 (7, J = 7.1, 3H). HR ESI-MS (methanol/water, JBL514solid) *m/z*: calculated for $^{12}C_{13}{}^{1}H_{24}{}^{14}N^{16}O_3$ $[M+H]^+$ calculated 242.1756, found 242.1744 (-5.0 ppm). HR ESI-MS (methanol/water, JBL514solid) *m/z*: calculated for $^{12}C_{13}{}^{1}H_{23}{}^{14}N^{16}O_3{}^{23}Na$ $[M+Na]^+$calculated 264.1576, found 264.1570 (-2.3 ppm).

Ketone Product: ^{1}H NMR (400 MHz, $CDCl_3$, JBL447colfrac5): δ 2.647 (s, 2H), 2.383 (t, J = 12.6, 2H), 1.924 (t, J = 12.6, 2H), 1.231 (s, 6H), 1.182 (s, 6H). ^{13}C NMR (400

MHz, $CDCl_3$, JBL489colfrac4-2): δ 211.7, 54.4, 53.3, 52.8, 39.2, 36.2, 32.8, 32.0. LR ESI-MS (JBL531recrystcrop1) *m/z* 170.3 $[M+H]^+$. HR EI-MS (JBL489colfrac4) *m/z*: calculated for $^{12}C_{10}{}^{1}H_{19}{}^{14}N^{16}O$ $[M]^+$ calculated 169.1467, found 169.1471 (2.6 ppm). IR: 3340.85 (N—H stretch), 1699.48 (C=O stretch). ^{1}H NMR (400 MHz, D_2O, JBL525HClrecrystcrop1): δ 3.002 (s, 2H), 2.763 (t, J = 12.6, 2H), 2.235 (t, J = 12.6, 2H), 1.484 (s, 12H).

2,2,7,7-tetramethylazepan-4-ol (72).

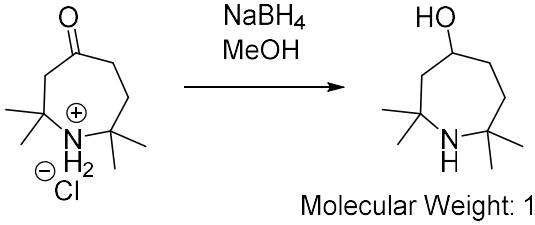

Molecular Weight: 171.28

Run	SM (mg)	$NaBH_4$ (mg)	H_2O: MeOH (1:1) (mL)	TM (mg)	Yield (%)	TM label
JBL430	17.0	12.4	2	10	70	JBL430w-up
JBL440	192.8	100	10	111	57	JBL440w-up
JBL448A	49.2	36	6	38.2	94	JBL448Aw-up
JBL448B	132	96	16	64.3	60	JBL448Bw-up

JBL448A: **69** (49.2 mg, 0.25 mmol) was dissolved in a solution of MeOH:H_2O (1:1, 16 mL) with stirring. $NaBH_4$ (36 mg, 0.95 mmol, 3.8 equiv.) was added to the solution and stirred for 3 hours. The solution was acidified with HCl and the solvent was evaporated. The residue was dissolved in sat. K_2CO_3 and then extracted into DCM. The organic layer was dried with $NaSO_4$ and then evaporated leaving a white residue (38.2 mg, 94%). ^{1}H NMR (400 MHz, $CDCl_3$, JBL448w-up): δ 3.925 (m, 1H), 1.736-1.831 (m, 4H), 1.604-1.637 (m, 2H), 1.228 (s, 3H), 1.173 (s, 3H), 1.144 (s, 6H). ^{1}H NMR (400

MHz, D_2O, JBL448CrudeHCl): δ 4.035 (m, 1H), 1.919-2.084 (m, 5H), 1.728-1.774 (m, 1H), 1.527 (s, 3H), 1.484 (s, 3H), 1.468 (s, 3H), 1.454 (s, 3H).

2,2,7,7-tetramethylazepan-4-one-N-oxyl radical (70)

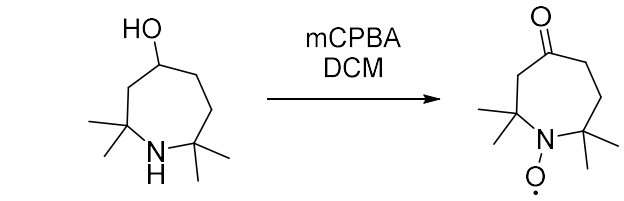

Molecular Weight: 171.28 Molecular Weight: 184.26

Run	SM (mg)	*m*-CPBA (mg)	DCM (mL)	TM (mg)	Yield (%)	TM label
JBL449A	10	42	1	2	18.5	JBL449colfrac4
JBL451	10	22	1.6	2.2	20.4	JBL451colfrac4
JBL462	60	180	3.5	40	62.5	JBL462crude

JBL462: **72** (60 mg, 0.350 mmol) was dissolved in DCM (7.5 mL) and cooled to 0°C with stirring in a RBF. Recrystallized *m*-CPBA (180 mg, 1.04 mmol, 2.97 equiv.) was dissolved in DCM (3.5 mL) and added dropwise to the RBF, the solution was stirred for 20 minutes at 0°C , before being allowed to warm up to room temperature over 2 hours. The solid was filtered off and washed with DCM. The filtrate was washed with sat. $NaHCO_3$ (3 x 20 mL), followed by sat. NaCl (20 mL). The organic layer was collected and dried over $NaSO_4$, filtered and evaporated giving an orange oil (40 mg, 62.5%). Product pure enough for next reaction

2,2,7,7-tetramethylazepan-4-one-N-oxyl radical (70)

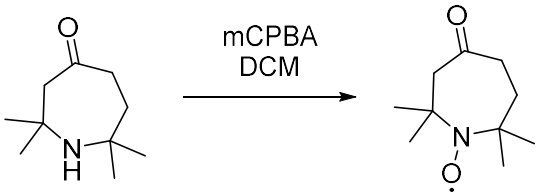

Molecular Weight: 169.27 Molecular Weight: 184.26

Run	SM (mg)	*m*-CPBA (mg)	DCM (mL)	TM (mg)	Yield (%)	Spin Concentration (%)	TM label
JBL457	10	22	1.4	4.6	42	NR	JBL457pTLCfrac2
JBL464	32	68	3.6	230	NR	NR	
JBL468	74	75.5	3.6	6	7.4	69	JBL468colfrac3
JBL474	162.5	343.1	7.5	62.9	36	105	JBL474colfrac2
JBL558	600	1287	28.125	350	53.5	NR	JBL558colfrac2

JBL558: **69** (600 mg, 3.545 mmol) was dissolved in DCM (7.5 mL) and cooled to 0°C with stirring in a RBF. Recrystallized *m*-CPBA (1.287 g, 7.46 mmol, 2.1 equiv.) was dissolved in DCM (20.65 mL) and added dropwise to the RBF, the solution was stirred for 20 minutes at 0°C , before being allowed to warm up to room temperature over 2 hours. The solid was filtered off and washed with DCM. The filtrate was washed with sat. $NaHCO_3$ (3 x 20 mL), followed by sat. NaCl (20 mL). The organic layer was collected and dried over $NaSO_4$, filtered and evaporated giving an orange oil. This was purified via column chromatography (0-15% EtOAc:pentane gradient). The combined fractions were evaporated leaving an orange solid (350 mg, 53.5%). R_f (25% EtOAc:pentane): 0.43. EPR (JBL474colfrac2, 1.20 mM in $CHCl_3$): spin concentration ~100%. HR EI-MS (JBL474colfrac3) *m/z*: calculated for $^{12}C_{10}{}^{1}H_{18}{}^{14}N^{16}O_2$ $[M]^+$ calculated 184.1338, found 184.1346 (4.6 ppm). IR: 1708.91 (C=O stretch).

2.4.2 Synthesis of 7-membered alcohol-nitroxide

2,2,7,7-tetramethylazepan-4-ol-N-oxyl radical (71)

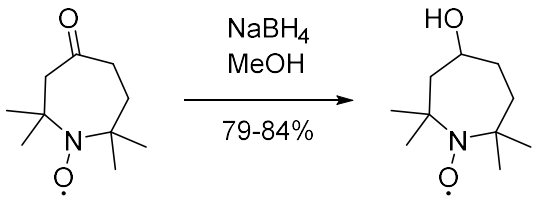

Molecular Weight: 184.26 Molecular Weight: 186.28

Run	SM (mg)	$NaBH_4$ (mg)	MeOH (mL)	TM (mg)	Yield (%)	Spin Concentration (%)	TM label
JBL470	40	32	4	8.9	13.7	64	JBL470colfrac2
JBL479	34	30	4	26	79	99	JBL470colfrac2
JBL559	40	32	4	34.4	85	NA	JBL559colfrac2

JBL479: **70** (34 mg, 0.184 mmol) was dissolved in MeOH (4 mL) and cooled to 0°C with stirring. $NaBH_4$ (30 mg, 0.811 mmol, 4 equiv.) was added to the solution and stirred for 3 hours. Solid $NaHCO_3$ was added until foaming stopped. The mixture was then filtered with cotton plug in a pipet with MeOH. The solvent was evaporated leaving an oil. This was purified via column chromatography (20-50% EtOAc:pentane gradient). The combined fractions were evaporated leaving an orange oil (26 mg, 79%). EPR (JBL479colfrac2, 1.24 mM in $CHCl_3$): spin concentration ~99%. HR EI-MS (JBL479colfrac2) *m/z*: calculated for $^{12}C_{10}{}^{1}H_{20}{}^{14}N^{16}O_2$ $[M]^+$ calculated 186.1494, found 186.1503 (4.8 ppm) IR: 3193.74 br (O—H stretch).

2.4.3 Ring expansion and alkylation's of protected 7-membered keto-ester amine

Benzyl 2,2,6,6-tetramethyl-4-oxopiperidine-1-carboxylate (77).

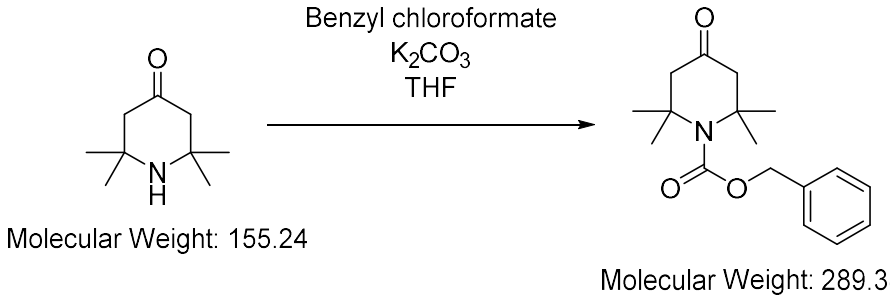

Molecular Weight: 155.24

Molecular Weight: 289.38

Run	SM (g)	Benzyl chloro-formate (mg)	K_2CO_3 (g)	THF (mL)	TM (mg)	Yield (%)	TM label
JBL571	10.6	4.88	0	70	1.42	14.4	JBL256crude
JBL577	14	40	25	100	6.77	26	JBL583colfrac6-7 JBL583colfrac2frac0-6
JBL653	28.4	70	70	200	11.8	22.3	JBL653colfrac8-12

JBL577: Distilled 2,2,6,6-tetramethylpiperidi-4-none (14 g, 90.2 mmol) and K_2CO_3 (25 g, 181 mmol, 2 equiv.) were placed in a 250-mL round bottom flask with stir bar and connected to a septum-sealed Claisen adaptor with a septum-sealed reflux condenser. The assembled apparatus was then evacuated and filled with N_2 before being placed under N_2 flow. Dry THF (100 mL) was then added via syringe and the solution was cooled to 0°C while stirring. Benzyl chloroformate (previously flushed with N_2 for twenty minutes) (40 mL, 270 mmol., 1.5 equiv.) was added via syringe over five minutes. After addition the solution was kept at 0°C for ten minutes, and then placed in a 70°C for 72 hours. The reaction was cooled to room temperature and then concentrated using the rotary evaporator. The residue was then dissolved in diethyl ether (200 mL) and then the

solids were removed via vacuum filtration, washing the solid with diethyl ether (3 x 100 mL). The filtrate was then washed sequentially with 0.1 M H_2SO_4, sat. $NaHCO_3$ solution and sat. NaCl solution. The organic layer was then dried with Na_2SO_4, filtered and then evaporated giving a yellow oil. The crude oil was purified via column chromatography (silica, 5-10% EtOAc:pentane gradient), the solvent was evaporated and then dried in vacuo giving an off-white solid (6.77 g, 26%). ^{1}H NMR (700 MHz, C*D*Cl_3, JBL571colfrac4): δ 7.328-7.400 (m, 5H), 5.165 (s, 2H), 2.588 (s, 4H), 1.485 (s, 12H). ^{13}C NMR (700 MHz, C*D*Cl_3, JBL571colfrac4): δ 208.1, 156.5, 136.5, 128.7, 128.4, 128.2, 66.9, 56.8, 53.5, 30.3.

1-Benzyl 4-ethyl 2,2,7,7-tetramethyl-5-oxoazepane-1,4-dicarboxylate (78)

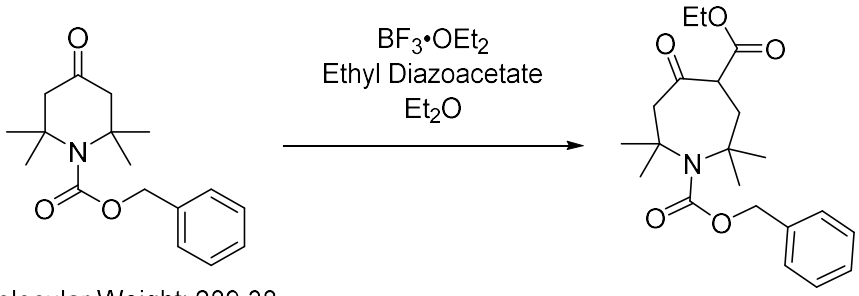

Molecular Weight: 289.38

Molecular Weight: 375.47

Run	SM (g)	$BF_3{\cdot}OEt_2$ (mL)	Ethyl Diazo-acetate (g)	Et_2O (mL)	TM (g)	Yield (%)	TM label
JBL593	0.210	0.373	0.350	4.0	0.107	39.5	JBL593colfrac2
JBL596	0.286	0.541	0.525	6.0	0.166	44.8	JBL596colfrac2
JBL602	1.05	1.865	1.740	20	0.385	53.5	JBL602colfrac2
JBL603	0.494	0.94	0.870	10	0.187	30	JBL603crude
JBL605	2.26	4.2	3.915	45	1.721	68.9	JBL605colffrac1-2

JBL660	5.00	9.375	8.75	100	2.9	44.6	JBL660colfrac6-8

JBL605: **77** (2.26 g, 7.82 mmol) was placed into a 100-mL RBF with stir bar and sealed with septum. It was then evacuated and filled with N_2 three times and placed under N_2 balloon. Dry diethyl ether (45 mL) was added to the flask via syringe. The solution was then cooled down to -30 ºC using a recirculating chiller. BF_3•OEt_2 (4.2 mL, 34.3 mmol, 4.4 equiv.) was then slowly added via syringe, followed by dropwise addition of ethyl diazoacetate (3.91 g; 34.3 mmol; 4.4 equiv.) over 15 minutes via syringe. The solution was stirred for 85 hours. The solution was warmed to above 0 ºC and sat. K_2CO_3 solution (50 mL) was added and the mixture was transferred to a separatory funnel. The organic layer was separated and washed with sat. K_2CO_3 solution (2 x 50 mL), followed by brine (2 x 50 mL), then dried with $NaSO_4$, decanted and evaporated. The oil was the purified via column chromatography (silica, 3% EtOAc:pentane) to give a white solid (1.721 g, 59%). ^{1}H NMR (700 MHz, $CDCl_3$, JBL605colfrac8) (enol form noted): δ 12.314 (s, 1H), 7.299-7.383 (m, 5H), 5.105 (s, 2H), 4.233 (q, J = 7.1, 2H), 2.710 (s, 2H), 2.649 (s, 2H), 1.512 (s, 6H), 1.453 (s, 6H) 1.302 (t, J = 7.1, 3H). ^{13}C NMR (700 MHz, $CDCl_3$, JBL605colfrac8): δ 173.3, 172.3, 158.5, 128.6, 128.5, 128.1, 97.7, 67.0, 60.9, 60.7, 59.0, 48.9, 40.1, 30.2, 30.0, 14.4. NMR is mixture of enol to keto (9:1) form of compound.

Benzyl 2,2,7,7-tetramethyl-5-oxoazepane-1-carboxylate (86)

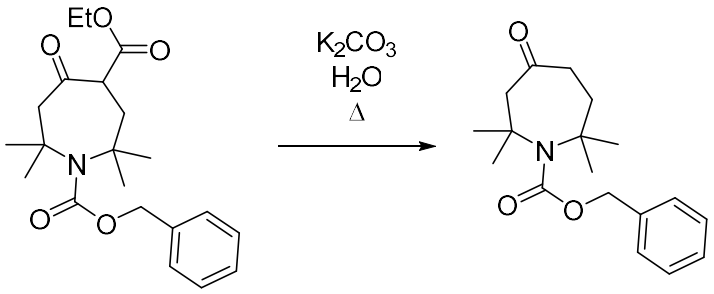

Molecular Weight: 375.47 Molecular Weight: 303.40

Run	SM (mg)	K_2CO_3 (mg)	H_2O (mL)	TM (mg)	Yield (%)	TM label
JBL598	74.5	110	3.0	39.5	65.8	JBL598colfrac2
JBL604	385	570	15.0	165	65.7	JBL604colfrac4
JBL609	705	1.04	30	268	44	JBL609colfrac14-18

JBL604: **78** (JBL602colfrac2, 385 mg, 1.02 mmol) was dissolved in H_2O (15 mL) with K_2CO_3 (570 mg, 4.1 mmol, 4 equiv.) and refluxed for 12 hours. The solution was then extracted with EtOAc (4 x 25 mL) and then dried over Na_2SO_4, decanted and evaporated. The crude oil was then purified via column chromatography (silica, 8% EtOAc:pentane), giving an oil (165 mg, 66%).

^{1}H NMR (700 MHz, C*D*Cl$_3$, JBL623coltube31): δ 7.318-7.385 (m, 5H), 5.096 (s, 2H), 2.798 (s, 2H), 2.491-2.509 (m, 2H), 2.049-2.066 (m, 2H), 1.494 (s, 6H), 1.467 (s, 6H),.^{13}C NMR (700 MHz, CDCl$_3$, JBL623coltube31): δ 210.5, 159.9, 136.2, 128.7, 128.5, 128.2, 67.3, 60.3, 58.4, 56.4, 39.2, 38.6, 31.4, 31.0.

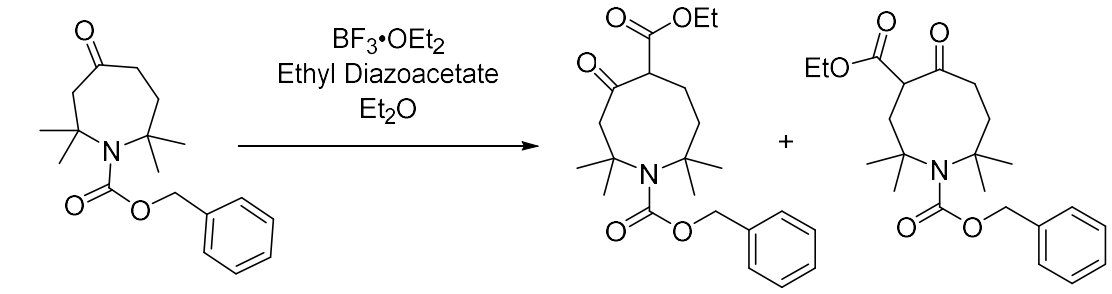

Molecular Weight: 303.40

Molecular Weight: 389.49

Run	SM (mg)	$BF_3 \cdot OEt_2$ (mL)	Ethyl Diazo-acetate (mg)	Et_2O (mL)	TM (mg)	Yield (%)	TM label
JBL606	198	0.396	368	4	23.0	10	JBL606colfrac2
					8.4	?	JBL606colfrac3

JBL606: **86** (198 mg, 0.651 mmol) was placed into a Schlenk with stir bar and sealed. It was then evacuated and filled with N_2 three times. Dry diethyl ether (3.5 mL) was added to the flask via syringe. The solution was then cooled down to -30 ºC using a recirculating chiller. BF_3•OEt_2 (0.396 mL, 3.23 mmol, 4.4 equiv.) was then slowly added via syringe, followed by dropwise addition of ethyl diazoacetate (368 mg; 3.23 mmol; 4.4 equiv.) over 5 minutes via syringe. The solution was stirred for 85 hours. The solution was warmed to above 0 ºC and sat. K_2CO_3 solution (5 mL) was added and the mixture was transferred to a separatory funnel. The organic layer was separated and washed with sat. K_2CO_3 solution (2 x 5 mL), followed by brine (2 x 5 mL), then dried with $NaSO_4$, decanted and evaporated. The oil was the purified via column chromatography (silica, 3% EtOAc:pentane) to give a clear oil (23.0 mg, 10%), there were also 2 other fractions of interest, but unable to determine structure. ^{1}H NMR (400 MHz, $CDCl_3$, JBL606colfrac2) (enol form noted): δ, 7.279-7.339 (m, 5H), 6.222 (s, 1H) 5.044 (s, 2H), 4.146 (q, J = 7.1, 2H), 2.917 (s, 2H), 2.351 (d, J = 6.6, 2H), 1.611 (d, J = 6.6, 2H) 1.410

(s, 6H), 1.268 (t, J = 7.1, 3H), 1.250 (s, 6H). ^{13}C NMR (400 MHz, $CDCl_3$, JBL606colfrac2): δ 169.1, 163.1, 155.0, 137.4, 128.5, 127.9, 127.8, 102.9, 76.0, 65.7, 60.2, 53.8, 43.6, 32.2, 26.8, 19.8, 14.4.

1-Benzyl 4-ethyl 4-(iodomethyl)-2,2,7,7-tetramethyl-5-oxoazepane-1,4-dicarboxylate (79)

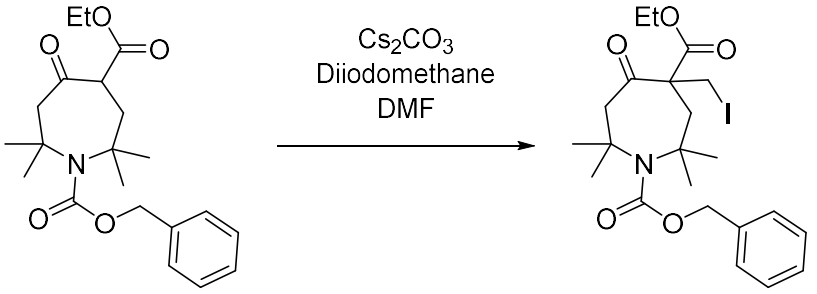

Molecular Weight: 375.47 Molecular Weight: 515.39

Run	SM (mg)	Cs_2CO_3 (g)	Diiodo-methane (mg)	DMF (mL)	TM (g)	Yield (%)	TM label
JBL642	44.0	0.040	0.0783	1	0.0296	49	JBL642colfrac2
JBL652	102.5	0.092	0.160	2.25	0.039	28	JBL643colfrac2
JBL664	1.20	1.10	2.140	27	1.235	75	JBL664colfrac2
JBL684	1.20	1.10	2.140	27	1.188	67	JBL684colfrac6
JBL729	0.200	0.191	0.333	5[a]	1.43	78	JBL730colfrac2-3
JBL730	1.144	1.10	1.4 g	25[a]			

[a] THF used instead to allow for easier work up vs. DMF extraction.

JBL664: Modifying a literature procedure[94], **78** (JBL660colfrac6-8, 200.0 mg; 0.533 mmol) was transferred to a Schlenk with a spin bar with $CHCl_3$, and then the $CHCl_3$ was evaporated with N_2. The Schlenk tube was then evacuated under high vacuum then filled with N_2 three times. DMF (distilled, 27 mL) was then transferred to the Schlenk via syringe under N_2. The solution was then cooled to 0°C, and then Cs_2CO_3 (dried under vacuum overnight, 1.1 g; 3.36 mmol; 1.05 equiv.) was added to the Schlenk

under N_2 with stirring. The suspension was stirred for 15 minutes at 0°C. Then diiodomethane (2.14 g; mmol; 2.35 equiv.) was added via syringe under N_2 to the stirred solution. The solution was then allowed to warm to room temperature and stirred for 24 hours.

The reaction mixture was transferred to a RBF with diethyl ether and evaporated. Heptane was then added to the RBF and then evaporated to try and remove DMF via azeotrope. The suspension was then diluted with water and placed in a separatory funnel and extracted with diethyl ether. The aqueous layer was then transferred into another separatory funnel with diethyl ether, leaving the previous diethyl ether layer in the preceding funnel. This same process was repeated for a total of 5 extractions. Water was then added to the first separatory funnel containing the first diethyl ether extract. The aqueous layer was then transferred to the remaining separatory funnels sequentially. This process was repeated 3 more times. Finally, all the organic layers were combined and dried with Na_2SO_4 and then evaporated. The crude material was then subjected to column chromatography (silica; 5% EtOAc:2.5%Et_2O:pentane) yielding the product as a clear oil (1.235 g; 75%). ^{1}H NMR (400 MHz, $CDCl_3$, JBL642colfrac2): δ 7.298-7.377 (m, 5H), 5.078 (d, J = 12.3, 1H), 5.004 (d, J = 12.3, 1H), 4.201 (q, J = 7.1, 2H), 3.659 (d, J = 10.1, 1H), 3.659 (d, J = 10.1, 1H), 3.460 (d, J = 10.1, 1H), 3.416 (d, J = 12.8, 1H), 2.591 (d, J = 15.2, 1H), 2.539 (d, J = 12.8, 1H), 2.199 (d, J = 15.2, 1H), 1.584 (s, 3H), 1.481 (s, 3H), 1.462 (s, 3H), 1.395 (s, 3H), 1.270 (t, J = 7.1, 3H). ^{13}C NMR (400 MHz, $CDCl_3$, JBL642colfrac2): δ 201.9, 169.4, 159.7, 135.9, 128.7, 128.5, 128.3, 67.5, 62.5, 62.0, 58.9, 57.9, 54.4, 46.8, 34.3, 31.2, 30.4, 30.3, 14.1, 9.5.

1-Benzyl 4-ethyl 4-(3-iodopropyl)-2,2,7,7-tetramethyl-5-oxoazepane-1,4-dicarboxylate (80)

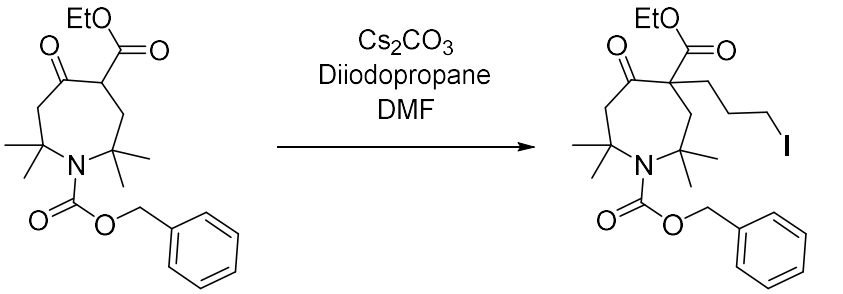

Molecular Weight: 375.47 Molecular Weight: 543.44

Run	SM (g)	Cs_2CO_3 (g)	1,3-Diiodo-propane (g)	DMF (mL)	TM (mg)	Yield (%)	TM label
JBL608	0.100	0.0912	0.197	2.25	33	28	JBL622colfrac2
JBL625	0.200	0.182	0.394	4.5	216	74.7	JBL627colfrac8
JBL641	0.1025	0.092	0.180	2.25	74	50	JBL651colfrac2
JBL665	1.20	1.10	2.36	27	1200	75	JBL664colfrac2
JBL685	1.20	1.10	2.36	27	760	47.5	JBL685colfrac4

JBL625: Modifying a literature procedure[94], **78** (JBL605, 200.0 mg; 0.533 mmol) was transferred to a Schlenk with a spin bar with $CHCl_3$, and then the $CHCl_3$ was evaporated with N_2. The Schlenk tube was then evacuated under high vacuum, then filled with N_2 three times. DMF (distilled, 4.5 mL) was then transferred to the Schlenk via syringe under N_2. The solution was then cooled to 0°C, and then Cs_2CO_3 (dried under vacuum overnight, 182 mg; 0.56 mmol; 1.05 equiv.) was added to the Schlenk under N_2 with stirring. The suspension was stirred for 15 minutes at 0°C. Then 1,3-diiodopropane was added via syringe under N_2 to the stirred solution. The solution was then allowed to warm to room temperature and stirred for 24 hours.

The reaction mixture was transferred to a RBF with diethyl ether and evaporated. Heptane was then added to the RBF and then evaporated to try and remove DMF via azeotrope. The suspension was then diluted with water and placed in a separatory funnel and extracted with diethyl ether. The aqueous layer was then transferred into another separatory funnel with diethyl ether, leaving the previous diethyl ether layer in the preceding funnel. This same process was repeated for a total of 5 extractions. Water was then added to the first separatory funnel containing the first diethyl ether extract. The aqueous layer was then, transferred to the remaining separatory funnels sequentially. This process was repeated 3 more times. Finally, all the organic layers were combined and dried with Na_2SO_4 and then evaporated. The crude material was then subjected to column chromatography (silica; 10% EtOAc:pentane) yielding the product as a clear oil (212 mg; 72.5%). ^{1}H NMR (700 MHz, $CDCl_3$, JBL622colfrac2): δ 7.309-7.369 (m, 5H), 5.079 (d, J = 12.3, 1H), 5.006 (d, J = 12.3, 1H), 4.150-4.250 (m, 2H), 3.500 (d, J = 13.1, 1H), 3.084-3.174 (m, 2H), 2.501 (d, J = 13.1, 1H), 2.376 (d, J = 14.9, 1H), 1.985 (d, J = 14.9, 1H), 1.871-1.944 (m, 2H), 1.661-1.704 (m, 1H), 1.581 (s, 3H), 1.472 (s, 3H), 1.444 (s, 3H), 1.411 (s, 3H), 1.278 (t, J = 7.1, 3H). ^{13}C NMR (700 MHz, $CDCl_3$, JBL622colfrac2): δ 204.3, 172.5, 159.3, 136.1, 128.6, 128.4, 128.2, 67.1, 61.7, 61.0, 59.3, 57.4, 55.1, 47.2, 37.8, 35.1, 31.0, 30.3, 30.1, 28.8, 14.2, 6.3. HR EI-MS (JBL622colfrac2) *m/z*: calculated for $^{12}C_{24}{}^{1}H_{34}{}^{14}N^{16}O_5{}^{127}I$ $[M]^+$ calculated 543.1482 , found 543.1486 (0.8 ppm).

1-Benzyl 4-ethyl 4-(4-ethoxy-4-oxobutyl)-2,2,7,7-tetramethyl-5-oxoazepane-1,4-dicarboxylate (85)

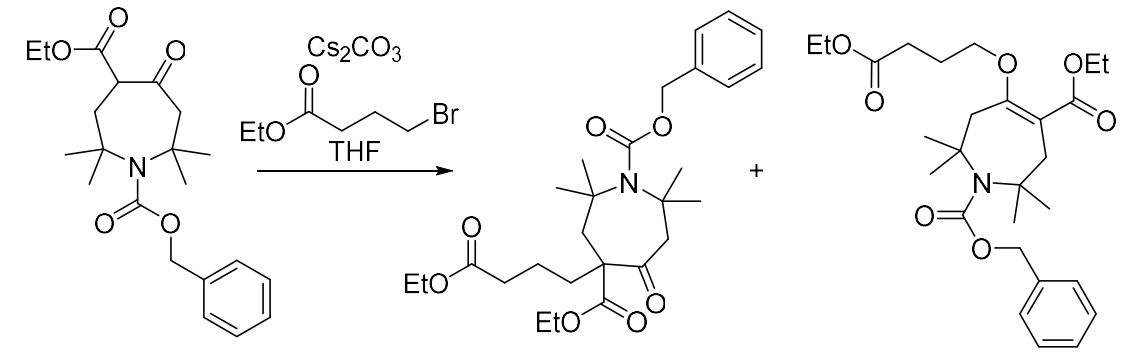

Molecular Weight: 375.47

Molecular Weight: 489.61

Run	SM (g)	Cs_2CO_3 (g)	Ethyl 4-bromo-butyrate (g)	THF (mL)	TM (g)	Yield (%)	TM label
JBL690	0.430	0.392	0.504	10[a]	0.125	22.3	JBL690colfrac2
JBL731	1.14	1.1	1.02	25	0.90	60.4	JBL731colfrac2

[a] Used DMF as solvent

JBL731: **78** (JBL266colf7, 1.14 g; 3.04 mmol) was transferred to a Schlenk with a spin bar and sealed. The Schlenk vessel was then evacuated under high vacuum, then filled with N_2 three times. THF (distilled, 25 mL) was then transferred to the Schlenk via syringe under N_2. The solution was then cooled to 0°C, and then Cs_2CO_3 (dried under vacuum overnight, 1.1 g; 3.4 mmol; 1.11 equiv.) was added to the Schlenk under N_2 with stirring. The suspension was stirred for 15 minutes at 0°C. Then (1.02 g, 5.243 mmol., 1.7 equiv.) was added via syringe under N_2 to the stirred solution. The solution was then allowed to warm to room temperature and refluxed for 18 hours.

The reaction mixture was transferred to a RBF with EtOAc and evaporated. $CHCl_3$ was added and then the suspension was filtered, collecting the filtrate. The filtrate was evaporated and dried with Na_2SO_4 and then evaporated. The crude material was then subjected to column chromatography (silica; 10% EtOAc:Pentane) yielding the product as a clear oil (900 mg; 60.4%).

^{1}H NMR (700 MHz, $CDCl_3$, JBL690coltube28): δ 7.309-7.353 (m, 5H), 5.0784 (d, J = 12.6, 1H), 5.012 (d, J = 12.6, 1H), 4.197 (dq, 2H), 4.106 (q, J = 7.0, 2H), 3.465 (d, J = 12.6, 1H), 2.514 (d, J = 13.3, 1H), 2.389 (d, J = 14.7, 1H), 2.246-2.284 (m, 2H), 1.9825 (d, J = 14.7, 1H) 1.868-1.972 (m, 1H), 1.581-1.621 (m, 2H), 1.580 (s, 3H), 1.558 (m, 1H), 1.467 (s, 3H), 1.440 (s, 3H), 1.413 (s, 3H), 1.230-1.277 (m, 6H). ^{13}C NMR (700 MHz, $CDCl_3$, JBL690coltube28): δ 204.3, 173.3, 172.5, 159.3, 136.2, 128.6, 128.4, 128.2, 67.1, 61.6, 61.4, 60.4, 59.4, 57.5, 55.2, 47.0, 36.3, 35.1, 34.6, 31.0, 30.3, 30.2, 20.2, 14.4, 14.2.

O-alkylated side product: ^{1}H NMR (700 MHz, $CDCl_3$, JBL690coltube38): δ 7.302-7.373 (m, 5H), 5.103 (s, 2H), 4.199 (q, J = 7.0, 2H), 4.125 (q, J = 12.6, 2H), 3.912 (t, J = 6.3, 1H), 2.699 (d, J = 18.9, 4H), 2.474 (t, J = 7.7, 2H), 1.978 (quint., J = 7.0, 2H), 1.528 (s, 6H), 1.468 (s, 6H), 1.288 (t, J = 7.0, 3H), 1.257 (t, J = 12.6, 3H). ^{13}C NMR (700 MHz, $CDCl_3$, JBL690coltube38): δ 173.3, 167.5, 162.8, 158.0, 136.7, 128.6, 128.4, 128.0, 108.9, 69.2, 66.9, 60.6, 60.5, 60.4, 59.3, 46.4, 43.5, 30.6, 30.2, 30.0, 25.4, 14.5, 14.4.

2.4.4 Outcomes of the Dowd-Beckwith one carbon Ring homologation of the protected 7-membered alkylated keto-ester

1-Benzyl 4-ethyl 2,2,8,8-tetramethyl-6-oxoazocane-1,4-dicarboxylate (81)

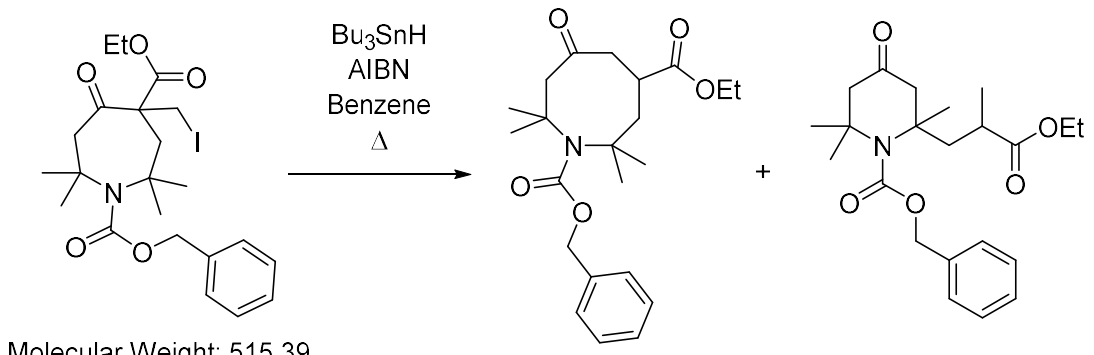

Molecular Weight: 515.39

Molecular Weight: 389.49

Run	SM (g)	Bu_3SnH (mg)	AIBN (mg)	Benzene (mL)	TM (mg)	Yield (%)	TM label
JBL648	0.029	0.018	0.0028	50	16.2cr	N/A	JBL655colfrac5 (mixture of ring contraction and expansion)
JBL673	0.200	146.9	19.1	100	122cr	N/A	JBL673colfrac2 (mixture of TM and impurities)
JBL686	1.11	808	106	555	94	11.2	JBL686colfrac3
JBL710	0.360	265	35.0	120	33	12.5	JBL733colfrac4
JBL742	0.500	425	56.0	120	240	29.5	JBL743colfrac3
JBL743	0.580	510	67.2	120			

JBL743: **79** (JBL730colfrac2, 580 mg; 1.12 mmol) was transferred to a 2-necked 500 mL RBF with a stir bar and fitted with a reflux condenser and sealed with septum. It was then evacuated under high vacuum, then filled with Ar three times and placed under Ar balloon. Benzene (distilled, then degassed via three freeze-pump-thaw cycles and then placed under Ar; 80 mL) was added to the vessel under Ar using a syringe.

In separate Schlenk vessel AIBN (recrystallized, 56 mg, 0.409 mmol, 0.35 equiv.) was placed in a Schlenk vessel and evacuated under high vacuum and filled with Ar three times. Benzene (distilled, then degassed via three freeze-pump-thaw cycles and then placed under Ar; 40 mL) was then transferred to the Schlenk via syringe under Ar. $SnBu_3H$ (510 mg, 1.75 mmol, 1.5 equiv.) was then added to the AIBN solution under Ar. The resulting solution was degassed via three freeze-pump-thaw cycles and placed under Ar. This solution was transferred to a syringe and added via syringe pump over 48 hours to the solution in 2-necked RBF at 85°C.

The reaction mixture was transferred to a RBF with diethyl ether and evaporated. The crude material was then subjected to column chromatography (10% K_2CO_3:silica; 8% Et_2O:1% EtOAc:pentane) yielding the product as a clear oil (240 mg; combined yield with JBL742: 29.5%). Other byproducts isolated include the ring contraction product and direct reduction product.

Ring expansion product: ^{1}H NMR (700 MHz, $CDCl_3$, JBL686coltube38): δ 7.265-7.376 (m, 5H), 5.190 (d, J = 12.4, 1H), 4.991 (d, J = 12.4, 1H), 4.156 (m, 2H), 3.2233 (d, J = 12.1, 1H), 3.014 (t, J = 5.0, 1H), 2.999 (t, J = 5.3, 1H), 2.660 (d, J = 8.6, 1H), 2.463 (d, J = 12.1, 1H), 2.103 (dd, J = 7.5, 1H), 1.996 (dd, J = 6.8, 1H), 1.737 (t, J = 5.6, 1H), 1.479 (s, 3H), 1.425 (s, 3H), 1.413 (s, 3H), 1.349 (s, 3H), 1.257 (t, J = 7.1, 3H). ^{13}C NMR (700 MHz, $CDCl_3$, JBL686coltube38): δ 210.8, 174.7, 160.4, 136.0, 128.7, 128.4, 128.3, 67.4, 61.2, 58.9, 58.7, 55.9, 44.9, 41.7, 37.3, 33.9, 30.9, 30.8, 30.3, 14.3.

Ring Contraction side-product: ^{1}H NMR (700 MHz, $CDCl_3$, JBL710coltube86): δ 7.329-7.409 (m, 5H), 5.211 (d, J = 11.9, 1H), 5.081 (d, J = 11.9, 1H), 4.099 (q, J = 7.0,

2H), 4.106 (q, J = 7.0, 2H), 2.683 (d, J = 18.2, 1H), 2.629 (d, J = 18.2, 1H), 2.548 (d, J = 18.9, 1H), 2.385-2.447 (m, 1H), 2.341 (d, J = 17.5, 1H), 2.230 (d, J = 15.4, 1H), 2.050-2.125 (m, 1H), 1.554 (s, 3H), 1.501 (s, 3H), 1.480 (s, 3H), 1.434 (s, 3H), 1.228 (t, 3H), 1.035 (d, J = 7.0, 3H). ^{13}C NMR (700 MHz, $CDCl_3$, JBL710coltube86): δ 208.1, 177.3, 156.3, 136.4, 128.7, 128.5, 128.3, 67.0, 60.7, 59.9, 56.8, 53.4, 50.4, 44.3, 36.0, 31.4, 29.3, 29.0, 20.1, 14.3. ^{15}N NMR from ^{1}H—^{15}N HMBC (700 MHz, $CDCl_3$, JBL710coltube86): δ 81.0.

2.4.5 Deprotection and attempts of oxidation of 8-membered keto-ester

Ethyl 2,2,8,8-tetramethyl-6-oxoazocane-4-carboxylate (87)

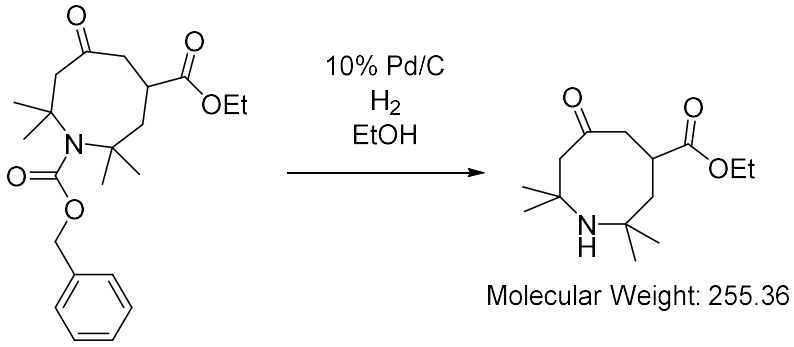

Molecular Weight: 389.49

Molecular Weight: 255.36

Run	SM (mg)	10% Pd/C (mg)	MeOH (mL)	TM (mg)	Yield (%)	TM label
JBL657	4.0	0.309	0.05		N/A	JBL657crude
JBL677	40	10	1	12.3	N/A	JBL677pTLCfrac3-5
JBL679	55	15	2.0	16.4	N/A	JBL679colfrac2
JBL688	84.6	20	0.275	4.6	42	JBL688coltub18-21

Pd/C (10%, 10 mg) was placed in a vial with a stir bar and sealed with a septum. The vial was then evacuated and a solution of **81** (44.7 mg, 0.1075 mmol) in MeOH (1

mL) was added via syringe. A balloon of H_2 was then placed on the vial. The reaction was allowed to stir for 8 hours. The reaction mixture was diluted with MeOH and filtered over Celite and the vial and Celite pad were washed with EtOAc. The filtrate was evaporated leaving a crude oil. The oil was purified via column chromatography (silica, 8-10% MeOH:DCM) giving a pure fraction (2.3 mg), and a mix of other fractions with unknown compounds. Unknown if this sample is intended TM, Proton peak at 3.120 doesn't make sense. ^{1}H NMR (700 MHz, $CDCl_3$, JBL688coltube18-21): δ 4.095-4.139 (m, 2H), 3.120 (s, 3H), 2.988 (m, 1H), 2.730-2.870 (m, 4H), 1.877 (m, 1H), 1.546 (m, 1H), 1.470 (s, 3H), 1.447 (s, 3H), 1.252 (t, J = 7.3, 3H), 1.181 (s, 3H), 1.158 (s, 3H). ^{13}C NMR (700 MHz, $CDCl_3$, JBL688coltube18-21): δ 209.8, 175.9, 74.5, 61.0, 53.2, 50.6, 49.4, 46.8, 42.0, 36.5, 27.1, 26.7, 25.2, 24.6, 14.3.

2.4.6 Attempts of Dowd-Beckwith 3-carbon ring expansion of protected 7-membered alkylated keto-ester

1-Benzyl 4-ethyl 2,2,10,10-tetramethyl-8-oxoazecane-1,4-dicarboxylate and 1-benzyl 4-ethyl 5-ethyl-2,2,8,8-tetramethyl-6-oxoazocane-1,4-dicarboxylate (83)

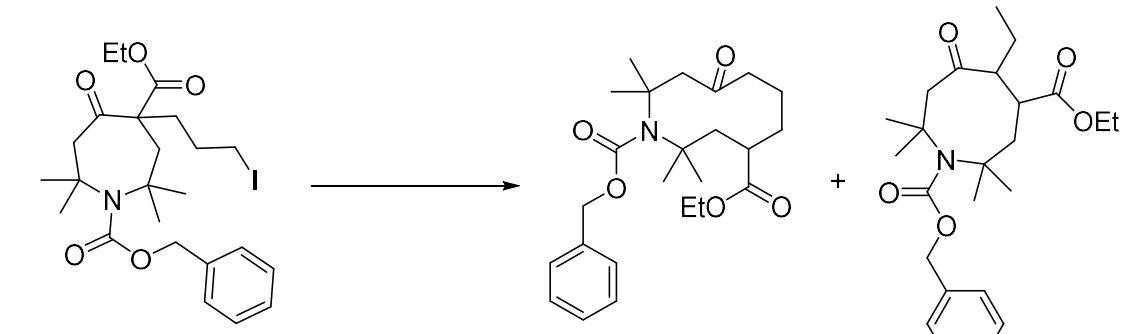

Molecular Weight: 543.44

Molecular Weight: 417.55

Run	SM (mg)	Bu_3SnH (mg)	AIBN (mg)	Benzene (mL)	TM (mg)	Yield (%)	TM label
JBL624	15.0	12.62	0.90	13	No Reaction-recovered SM		
JBL626	4.0	6.54	0.446	3.5	No Reaction-recovered SM		
JBL631	2.0	3.2	0.25	1	Only direct reduction product		
JBL632	2.0	3.2	0.25	1	Only direct reduction product		
JBL633	4.0	6.43	0.485	3.5	Partial reaction, new product in crude NMR		
JBL634	15.0	12.1	1.0	13	No reaction-need to use fresh AIBN/$SnBu_3H$ mixture		
JBL635	15.0	12.1	1.0	13	Partial reaction, new product in crude NMR, purification failed		
JBL638	35	28.11	2.11	30	Partial reaction, new product in crude NMR, purification failed		
JBL643[a]	15	20.3	13.5	15	Partial reaction, new product in crude NMR, purification failed		
JBL645[a]	15	8.24	13.61	2	No Reaction-Recovered SM		
JBL647	45	36.2	2.72	39	No Reaction-Recovered SM		
JBL649	42	32.8	2.5	30	5	15.6	JBL656colfrac5
JBL662	64	50	3.8	45	10.1	20.6	JBL662colfrac5

JBL667	200	156	15	150	86.8	N/A	JBL667colfr3(impure)
JBL670	700	546	52.5	540	104	19.3	JBL670colfrac3-4
[a] Used TTMS instead of $SnBu_3H$; toluene instead of benzene							

JBL743: Compound (JBL665colfrac2, 700 mg; 1.29 mmol) was transferred to a 2-necked 1 L RBF with a stir bar and fitted with a reflux condenser and sealed with septum. It was then evacuated under high vacuum, then filled with Ar three times and placed under Ar balloon. Benzene (distilled, then degassed via three freeze-pump-thaw cycles and then placed under Ar; 480 mL) was added to the vessel under Ar using a syringe.

In separate Schlenk vessel AIBN (recrystallized, 52.5 mg, 0.320 mmol, 0.25 equiv.) was placed in a Schlenk vessel and evacuated under high vacuum and filled with Ar three times. Benzene (distilled, then degassed via three freeze-pump-thaw cycles and then placed under Ar; 60 mL) was then transferred to the Schlenk via syringe under Ar. $SnBu_3H$ (546 mg, 1.87 mmol, 1.5 equiv.) was then added to the AIBN solution under Ar. The resulting solution was degassed via three freeze-pump-thaw cycles and placed under Ar. This solution was transferred to a syringe and added via syringe pump over 56 hours to the solution in 2-necked RBF at 85°C.

The reaction mixture was transferred to a RBF with diethyl ether and evaporated. The crude material was then subjected to column chromatography (10% K_2CO_3:silica, 10% Et_2O:2.5% EtOAc:pentane) yielding the side product as a white oily solid (104.7 mg; 29.5%).

^1H NMR (700 MHz, $CDCl_3$, JBL667colfrac2pTLCfupper): δ 7.312-7.386 (m, 5H), 5.235 (d, J = 12.3, 1H), 5.052 (d, J = 12.3, 1H), 4.089 (q, J = 6., 2H), 3.330 (d, J =

14.354, 1H), 2.683 (t, *J* = 6.9, 1H), 2.3883 (s, 1H), 2.319 (d, *J* = 14.4, 1H), 1.985 (q, *J* = 7.4, 2H), 1.592 (s, 3H), 1.517 (s, 3H), 1.511 (s, 3H), 1.456 (s, 3H), 1.394 (s, 3H), 1.231 (t, *J* = 7.1, 3H), 0.957 (t, *J* = 7.3, 3H). ^{13}C NMR (700 MHz, $CDCl_3$, JBL667colfrac2pTLCfupper): δ 209.1, 174.8, 157.1, 136.3, 128.6, 128.4, 128.2, 66.9, 61.3, 61.0, 57.9, 56.8, 54.9, 46.9, 35.2, 31.2, 30.2, 29.5, 23.4, 21.3, 14.2, 14.1.

Ethyl 5-ethyl-2,2,8,8-tetramethyl-6-oxoazocane-4-carboxylate (88)

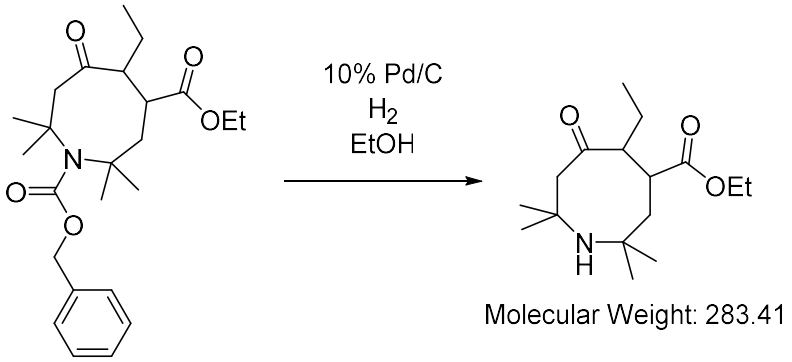

Molecular Weight: 417.55

Molecular Weight: 283.41

Run	SM (mg)	10% Pd/C (mg)	MeOH (mL)	TM (mg)	Yield (%)	TM label
JBL671	20	1.5	0.25	3.0	N/A	JBL671pTLCf2 (impurities present)
JBL676	44.7	10	1.0	2.3	3.2	JBL693coltub5 (pure)
JBL678	60	15	1.5	N/A	N/A	JBL693otherfracs

JBL676: Pd/C (10%, 10 mg) was placed in a vial with a stir bar and sealed with a septum. The vial was then evacuated and a solution of **83** (44.7 mg, 0.1075 mmol) in MeOH (1 mL) was added via syringe. A balloon of H_2 was then placed on the vial. The reaction was allowed to stir for 8 hours. The reaction mixture was diluted with MeOH and filtered over Celite and the vial and Celite pad were washed with EtOAc. The filtrate

was evaporated leaving a crude oil. The oil was purified via column chromatography (silica, 10% Acetone:pentane) giving one pure fraction as a white solid (2.3 mg, and a mix of other fractions with unknown compounds.

^{1}H NMR (700 MHz, $CDCl_3$, JBL693coltub5): δ 4.131 (q, J = 7.1, 2H), 2.704-2.730 (m, 2H), 2.301 (d, J = 11.8, 1H), 2.234 (d, J = 11.8, 1H), 1.403-1.450 (m, 1H), 1.330-1.390 (m, 1H), 1.2755 (t, J = 7.1, 3H), 1.252 (m, 2H), 1.226 (s, 3H), 1.221 (s, 3H), 1.161 (s, 3H), 1.095 (s, 3H), 0.877 (t, J = 7.3, 3H). ^{13}C NMR (700 MHz, $CDCl_3$, JBL693coltub5): δ 211.6, 175.8, 62.7, 60.7, 59.1, 55.9, 54.2, 43.6, 34.2, 32.3, 32.2, 31.9, 26.9, 20.4, 14.2, 14.0.

Ethyl 5-ethyl-2,2,8,8-tetramethyl-6-oxoazocane-4-carboxylate-N-oxyl radical (89)

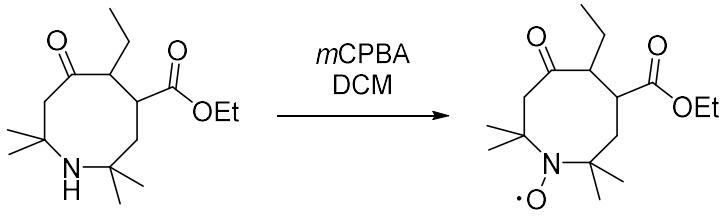

Molecular Weight: 283.41 Molecular Weight: 298.40

Run	SM (mg)	*m*-CPBA (mg)	DCM (mL)	TM (mg)	Yield (%)	Spin Concentration (%)	TM label
JBL680	10	12.9	0.275	1.5	14	13.3	JBL680coltub3
				3.0	29	10	JBL680coltub4
JBL704[a]	1.6	N/A	N/A	1.5	N/A	24	JBL704crude
JBL706[a]	6.6	N/A	N/A	0.64	N/A	4.2	JBL707pTLCf1
				0.86		37.3	JBL707pTLCf1
				0.60		14.8	JBL707pTLCf1

[a] Attempted using alternate $NaWO_4$ procedure, but unable to obtain product with spin concentration

greater than 30%

JBL680: **88** (JBL676pTLCf2, 10 mg, 0.036 mmol) was dissolved in DCM (0.075 mL) and cooled to 0°C with stirring in a RBF. Recrystallized *m*-CPBA (12.9 mg, 0.0747 mmol, 2.1 equiv.) was dissolved in DCM (0.2 mL) and added dropwise to the RBF, the solution was stirred for 20 minutes at 0°C , before being allowed to warm up to room temperature over 2 hours. The solid was filtered off and washed with DCM. The filtrate was washed with sat. $NaHCO_3$ (3 x 20 mL), followed by sat. NaCl (20 mL). The organic layer was collected and dried over $NaSO_4$, filtered and evaporated giving an orange oil. This was purified via column chromatography (10-20% EtOAc:pentane gradient). Fractions were checked via EPR, nitroxide signal was present but spin concentration less than 13% for the two fractions of interest.

2.4.7 Attempts of Nucleophilic 3-carbon ring expansion of protected 7-membered alkylated keto-ester

1-benzyl 4,7-diethyl 2,2,10,10-tetramethyl-8-oxoazecane-1,4,7-tricarboxylate (84)

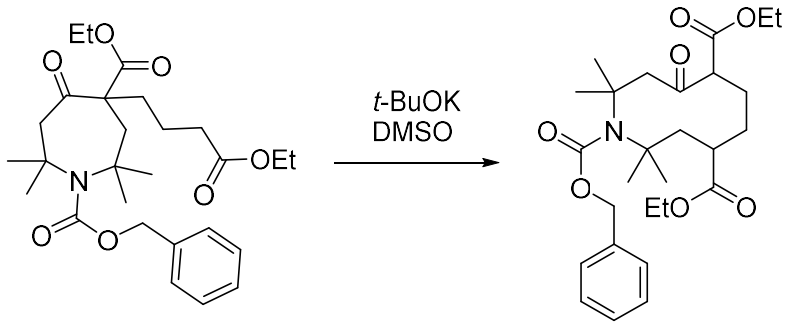

Molecular Weight: 489.61

Molecular Weight: 489.61

Run	SM (mg)	KO*t*Bu (mg)	DMSO (mL)	Temp (°C)	Time (hr)	TM (mg)	Yield (%)	TM label
JBL724	125	35	1.65	25	12	No Reaction, recovered SM		

JBL725	65	15.71	0.85	40	24	No Reaction, recovered SM		
JBL728	65	22	1	70	10	Mostly SM, but some new material forming		
JBL732	40	23	0.6	70	84	N/A	N/A	JBL732coltub9-10
JBL734	100	57.1	1.5	70	84			

JBL734: Modifying a literature procedure[93], **85** (JBL731colfrac2, 100.0 mg; 0.2045 mmol) was transferred to a Schlenk with a spin bar then evacuated under high vacuum, then filled with N_2 three times. In another Schlenk vessel, KO*t*-Bu (57 mg, 0.5112 mmol, 2.5 equiv.) was added and then the Schlenk was then evacuated under high vacuum, then filled with N_2 three times. DMSO (distilled, 1.0 mL) was then transferred to the Schlenk with KO*t*-Bu via syringe under N_2. DMSO (distilled, 0.5 mL) was then transferred to the Schlenk with SM and that solution was then added via syringe to the Schlenk with dissolved KO*t*-Bu. The suspension was stirred for 84 hours at 70°C. The solution was cooled to

The reaction mixture was transferred to a RBF with EtOAc and evaporated. The suspension was then diluted with water and placed in a separatory funnel and extracted with diethyl ether. The aqueous layer was then transferred into another separatory funnel with diethyl ether, leaving the previous diethyl ether layer in the preceding funnel. This same process was repeated for a total of 5 extractions. Water was then added to the first separatory funnel containing the first diethyl ether extract. The aqueous layer was then, transferred to the remaining separatory funnels sequentially. This process was repeated three more times. Finally, all the organic layers were combined and dried with Na_2SO_4 and then evaporated. The crude material was then subjected to column chromatography (silica; 20% EtOAc:EtOAc) yielding a fraction of interest, but unable to characterize.

2.5 References

[1] Tebben, L.; Studer, A. Nitroxides: applications in synthesis and in polymer chemistry. *Angew. Chem. Int. Ed. Engl*., **2011** *50*, 5034–5068.

[2] Rajca, A.; Wang, Y.; Boska, M.; Paletta, J. T.; Olankitanit, A.; Swanson, M. A.; Mitchell, D. G.; Eaton, S. S.; Eaton, G. R.; Rajca, S.; Organic radical contrast agents for magnetic resonance imaging. *J. Am. Chem. Soc.,* **2012**, *134*, 15724–15727.

[3] Fremy, E. Sur un nouvelle série d'acides formés d'oxygène, de soufre, d'hydrogène et de d'azote. *Ann. Chim. Phys.,* **1845**, *15*, 408-488.

[4] Piloty, O.; Schwerin, B. G. Ueber die Existenz von Derivaten des vierwerthigen Stickstoffs. *Chem. Ber.,* **1901**, *34*, 2354-2367.

[5] Lebedev, O. L.; Kazaranzovsky, S. N. Catalytic oxidation of aliphatic amines with hydrogen peroxide. *Trud. Khim. Technol.,* **1959**, *2*, 649-665.

[6] Lajzérowicz-Bonneteau, J. Structure du radical nitroxyde tétraméthyl-2,2,6,6 piperidinol-4 oxyle-1. *Acta. Cryst.,* **1968**, *B24*, 196-199.

[7] Gange, D. M.; Kallel, E. A. The structure and conformation of hydroxylamine and its methylated derivatives. *J. Chem. Soc. Chem. Commun.,* **1992**, 824-825.

[8] Percino, M. J.; Cerón, M.; Soriano-Moro, G.; Pacheco, J. A.; Castro, M. E.; Chapela, V. M.; Bonilla-Cruz, J.; Saldivar-Guerra, E. 2,2,6,6-Tetramethyl-1-oxopiperidinetribromide and two forms of 1-hydroxy-2,2,6,6-tetramethylpiperidinium bromide salt: Syntheses, crystal structures and theoretical calculations. *J. Mol. Struct.,* **2016**, *1103*, 254-264.

[9] Giguère, P. A.; Liu, J. D. Infrared Spectrum, Molecular Structure, and Thermodynamic Functions of Hydroxylamine. *Can. J. Chem.,* **1952**, *30*, 948-962.

[10] Rintoul, L.; Micallef, A. S.; Bottle, S. E. The vibrational group frequency of the N–O stretching band of nitroxide stable free radicals. *Spect. Acta,* **2008**, *70*, 713-717.

[11] Morat, C.; Rassat, A. Nitroxydes—XLVI Determination de la frequence d'elongation no dans des radicaux libres nitroxydes piperidiniques. *Tetrahedron,* **1972**, *28*, 735-740.

[12] Soule, B. P.; Hyudo, F.; Matsumoto, K.; Simone, N. L.; Cook, J. A.; Krishna, M. C.; Mitchell, J. B. Therapeutic and Clinical Applications of Nitroxide Compounds. *Antioxid. Redox. Signal.*, **2007**, *9*, 1731-1743.

[13] Haugland, M. M.; Lovett, J. E.; Anderson, E. A. Advances in the Synthesis of Nitroxide Radicals for Use in Biomolecule Spin Labeling. *Chem. Soc. Rev.,* **2018**, *47*, 668-680.

[14] Prescott, C.; Bottle, S. E. Biological Relevance of Free Radicals and Nitroxides. *Cell Biochem. Biophys.,* **2017**, *75*, 227-240.

[15] Matsumoto, K.; Krishna, M. C.; Mitchell, J. B. Novel Pharmacokinetic Measurement Using Electron Paramagnetic Resonance Spectroscopy and Simulation of *in Vivo* Decay of Various Nitroxyl Spin Probes in Mouse Blood. *J. Pharmacol. Exp. Ther.,* **2004**, *310*, 1076–1083.

[16] Kuppusamy, P.; Li, H.; Ilangovan, G.; Cardounel, A. J.; Zweier, J. L.; Yamada, K.; Krishna, M. C.; Mitchell, J. B. Noninvasive Imaging of Tumor Redox Status and Its Modifcation by Tissue Glutathione Levels. *Cancer Res.,* **2002**, *62*, 307–312.

[17] Yamada, K.; Inoue, D.; Matsumoto, S.; Utsumi, H. *In Vivo* Measurement of Redox Status in Streptozotocin-Induced Diabetic Rat Using Targeted Nitroxyl Probes. *Antioxid. Redox Signal.,* **2004**, *6*, 605-611.

[18] Kasazaki, K.; Yasukawa, K.; Sano, H.; Utsumi, H. Non-invasive Analysis of Reactive Oxygen Species Generated in NH_4OH-induced Gastric Lesions of Rats using a 300 MHz *In Vivo* ESP Technique. *Free Radic. Res.,* **2003**, *37*, 757-766.

[19] Liu, S.; Timmins, G. S.; Shi, H.; Gasparovic, C. M.; Liu, K. J. Application of *in vivo* EPR in brain research: monitoring tissue oxygenation, blood flow, and oxidative stress. *NMR Biomed.,* **2004**, *17*, 327-324.

[20] Yokoyama, H.; Itoh, O.; Aoyama, M.; Obara, H.; Ohya, H.; Kamada, H. *In vivo* EPR imaging by using an acyl-protected hydroxylamine to analyze intracerebral oxidative stress in rats after epileptic seizures. *Magn. Reson. Imaging,* **2000**, *18*, 875-879.

[21] Dikalov, S.; Fink, B.; Skatchkov, M.; Bassenge, E. Comparison of Glyceryl Trinitrate-induced with Pentaerythrityl Tetranitrate-induced *in vivo* Formation of Superoxide Radicals: Effect of Vitamin C. *Free Radic. Biol. Med.,* **1999**, *27*, 170-176.

[22] Nguyen, H. V.-T.; Detappe, A.; Gallagher, N. M.; Zhang, H.; Harvey, P.; Yan, C.; Mathieu, C.; Golder, M. R.; Jiang, Y.; Ottaviani, M. F.; Jasanoff, A.; Rajca, A.; Ghobrial, I.; Ghoroghchian, P. P.; Johnson, J. A. Triply Loaded Nitroxide Brush-Arm Star Polymers Enable Metal-Free Millimetric Tumor Detection by Magnetic Resonance Imaging. *ACS Nano.,* **2018**, *12*, 11343-11354.

[23] Hansen, K.-A.; Blinco, J. P. Nitroxide Radical Polymers—A Versatile Material Class for High-Tech Applications. *Polym. Chem.*, **2018**, *9*, 1479-1516.

[24] Kocherginsky, N.; Swartz. H. M.; *Nitroxide Spin Labels: Reactions in Biology and Chemistry*; CRC Press: Boca Raton, 1995.

[25] Amar, M.; Bar, S.; Iron, M. A.; Toledo, H.; Tumanskii, B.; Shimon, L. J. W.; Botoshansky, M.; Fridman, N.; Szpilman, A. M. Design Concept for α-Hydrogen-Substituted Nitroxides. *Nat. Commun.,* **2015**, *6*, 6070.

[26] Couet, W. R.; Brasch, R. C.; Sosnovsky, G.; Lukszo, J.; Prakash, I.; Gnewuch, C. T.; Tozer, T. N. Influence of Chemical Structure of Nitroxyl Spin Labels on their Reduction by Ascorbic Acid, *Tetrahedron*, **1985**, *41*, 1165-1172.

[27] Bielski, B. H. J.; Allen, A. O.; Schwarz, H. A. Mechanism of the disproportionation of ascorbate radicals. *J. Am. Chem. Soc.,* **1981**, *103*, 3516-3518.

[28] Bobko, A. A.; Kirilyuk, I. A.; Grigor'ev, I. A.; Zweier, J. L.; Khramtsov, V. V. Reversible reduction of nitroxides to hydroxylamines: Roles for ascorbate and glutathione. *Free Radical Biol. Med.,* **2007**, *42*, 404-412.

[29] Paletta, J. T.

[30] Glebska, J.; Gwozdnzinski, K. Oxygen-Dependent Reduction of Nitroxides by Ascorbic Acid and Glutathione. An EPR Study. *Curr. Topics Biophys.,* **1998**, *22*, 75-82.

[31] Rossi, R.; Milzani, A.; Dalle-Donne, I.; Giustarini, D.; Lusini, L.; Colombo, R.; Simplicio, P. D. Blood Glutathione Disulfide: *In Vivo* Factor or in Vitro Artifact. *Clin. Chem.,* **2002**, *48*, 742-753.

[32] Bradley, D. W.; Maynard, J. E.; Emery, G. Comparison of Ascorbic Acid Concentrations in Whole Blood Obtained by Venipuncture or by Finger Prick. *Clin. Chem.,* **1972**, *18*, 968-970.

[33] Bradley, D. W.; Maynard, J. E.; Webster, H. Plasma and Whole Blood Concentrations of Ascorbic Acid in Patients Undergoing Long-term Hemodialysis. *A. J. C. P.,* **1973**, *59*, 145-147.

[34] Paletta, J. T.; Pink, M.; Foley, B.; Rajca, S.; Rajca, A. Synthesis and Reduction Kinetics of Sterically Shielded Pyrrolidine Nitroxides. *Org. Lett.,* **2012**, *14*, 5322-5325

[35] Wang, Y.; Paletta, J. T.; Berg, K.; Reinhart, E.; Rajca, S.; Rajca, A. Synthesis of Unnatural Amino Acids Functionalized with Sterically Shielded Pyrroline Nitroxides. *Org. Lett.,* **2014**, *16*, 5298-5300.

[36] Kirilyuk, I. A.; Bobko, A.A.; Grigor'ev, I. A.; Khramtsov, V. V. Synthesis of tetraethyl substituted pH-sensitive nitroxides of imidazole series with enhanced stability towards reduction. *Org. Biomol. Chem.,* **2004**, *2*, 1025-1030.

[37] Kirilyuk, I. A.; Bobko, A.A.; Semenov, S. V; Komarov, D. A.; Irtegova, I. G; Grigor'ev, I. A.; Bagryanskaya, E. Effect of sterical shielding on the redox properties of imidazoline and imidazolidine nitroxides. *J. Org. Chem.,* **2015**, *80*, 9118-9125.

[38] Marx, L.; Chiarelli, R.; Guiberteau, T.; Rassat, A. A comparative study of the reduction by ascorbate of 1,1,3,3-tetraethylisoindolin-2-yloxyl and of 1,1,3,3-tetramethylisoindolin-2-yloxyl. *J. Chem. Soc., Perkin Trans. 1,* **2000**, *8,* 1181–1182.

[39] Yamasaki T.; Mito F.; Ito Y.; Pandian, S.; Kinoshita, Y.; Nakano, K.; Murugesan, R.; Sakai, K.; Utsumi, H.; Yamada, K.-i. Structure—reactivity relationship of piperidine nitroxide: electrochemical, ESR and computational studies. *J. Org. Chem.,* **2011**, *76*. 435-440.

[40] Morris, S.; Sosnovsky, G.; Hui, B.; Huber, C. O.; Rao, N. U. M.; Swartz, H. M. Chemical and Electrochemical Reduction Rates of Cyclic Nitroxides (Nitroxyls). *J. Pharm. Sci.,* **1991**, *80*, 149-152.

[41] Huang, S.; Zhang, H.; Paletta, J. T.; Rajca, S.; Rajca, A. Reduction kinetics and electrochemistry of tetracarboxylate nitroxides. *Free Rad. Res.*, **2018**, *52*, 327-334.

[42] Huang, S.; Paletta, J. T.; Elajaili, H.; Huber, K.; Pink, M.; Rajca, S.; Eaton, G. R.; Eaton, S. S.; Rajca, A. Synthesis and electron spin relaxation of tetracarboxylate pyrroline nitroxides. *J. Org. Chem*., **2017**, *82*, 1538-1544.

[43] Brown, H. C.; Fletcher, R. S.; Johannesen, R. B. I-Strain as a Factor in the Chemistry of Ring Compounds. *J. Am. Chem. Soc.,* **1951**, *73*, 212-221.

[44] Schneider, H.-J.; Schmidt, G.; Thomas, F. Alicyclic Reaction Mechanisms. 6. Strain-Reactivity Relations as a Tool for the Localization of Transition States. Equilibria, Solvolysis and Redox Reactions of Substituted Cycloalkanes. *J. Am. Chem. Soc.,* **1983**, *105*, 3556-3563.

[45] Eliel, E. L.; Wilen, S. H. Configuration and Conformation of Cyclic Molecules. *Stereochemistry of Organic Compounds*; John Wiley & Sons, Inc.: New York, NY, 1994; 769-771.

[46] Pitzer, K. S. Potential Energies for Rotations about Single Bonds. *Discuss. Faraday Soc.*, **1951**, *10*, 66-73.

[47] Audran, G.; Brémond, P.; Marque, S. R. A. Labile Alkoxyamines: Past, Present, and Future. *Chem. Commun.*, **2014**, *50*, 7921-7928.

[48] Moncelet, D.; Voisin, P.; Koonjoo, N.; Bouchaud, V.; Massot, P.; Parzy, E.; Audran, G.; Franconi, J.-M.; Thiandiere, E.; Marque; S. R. A.; Bremond. P.; Mellet, P. Alkoxyamines: Toward a New Family of Theranostic Agents against Cancer. *Molecular Pharmaceutics*, **2014**, *11*, 2412-2419.

[49] Bertin, D.; Gigmes, D.; Marque, S. R. A.; Tordo, P. Kinetic Subtleties of Nitroxide Mediated Polymerization. *Chem. Soc. Rev.,* **2011,** *40,* 2189-2198.

[50] Audran, G.; Bremond. P.; Franconi, J.-M.; Marque; S. R. A.; Massot, P.; Mellet, P.; Parzy, E.; Thiandiere, E. Alkoxyamines: A New Family of Pro-Drugs Against Cancer. Concept for Theranostics. *Org. Biomol. Chem.,* **2014,** *12,* 719-723.

[51] Johnson, D. H.; Ahmad, R.; He, G.; Samouilov, A.; Zweier, J. L. Compressed Sensing of Spatial Electron Paramagnetic Resonance Imaging. *Magn. Res. Med.*, **2013**, DOI: 10.1002/mrm.24966.

[52] Lurie, D. J.; Bussell, D. M.; Bell, L. H.; Mallard, J. R. Proton Electron Double Magnetic Resonance Imaging of Free Radical Solutions. *J. Magn. Reson.*, **1988**, *76*, 366-370.

[53] Bremond P.; Marque, S. R. A. First Proton Triggered C–ON Bond Homolysis in Alkoxyamines. *Chem. Comm.,* **2011,** *47,* 4291-4293.

[54] Bremond P.; Koita, A.; Marque, S. R. A. Pesce, V.; Roubaud, V.; Siri, D. Chemically Triggered C–ON Bond Homolysis of Alkoxyamines. Quaternization of the Alkyl Fragment. *Org. Lett.* **2012,** *14,* 358-361.

[55] Fischer, H. The Persistent Radical Effect: A Principle for Selective Radical Reactions and Living Radical Polymerizations. *Chem. Rev.*, **2001**, *101*, 3581-3610.

[56] Schulte, T.; Studer, A. New Seven- and Eight-Membered Cyclic Alkoxyamines for the Living Free Radical Polymerization. *Macromolecules*, **2003**, *36*, 3078-3084.

[57] Wetter, C.; Gierlich, J.; Knopp, C. A.; Müller, C.; Schulte, T.; Studer, A. Steric and Electronic Effects in Cyclic Alkoxyamines—Synthesis and Applications as Regulators for Controlled/Living Radical Polymerization. *Chem. Eur. J.*, **2004**, *10*, 2156-2166.

[58] Chai, Y.; Wan, Z.-L.; Wang, B.; Guo, H.-Y.; Liu, M.-L. Synthesis and *in vitro* Antibacterial Activity of 7-(4-alkoxyimino-3-amino-3-methylpiperidin-1-yl)fluoroquinolone Derivatives. *Eur. J. Med Chem*. **2009**, *44*, 4061-4069

[59] Dagonneau, M.; Kagan, E. S.; Mikhailov, V. I.; Rozantsev, E. G.; Sholle, V. D. Chemistry of Hindered Amines from the Piperidine Series. *Synthesis*, **1984**, *11*, 895-916.

[60] Sensfuβ, U.; Habicher,W. D. Synthesis of 3-Alkylated Triacetoneamine Derivatives. *J. Prakt. Chem.,* **1999**, *341*, 398-402.

[61] Rozantsev, E. G.; Dagonneau, M.; Kagan, E. S.; Mikhailov,V. I.; Sholle, V. D. Synthesis of 3-substituted Derivatives of 2,2,6,6-tetramethylpiperidine: Potential New Spin Labels. *J. Chem. Research (M),* **1979**, 2901-2909.

[62] Werchan, H. G.; Russew, R. I.; Held, P.; Schubert, H. Triacetoneamine Chemistry. I. Synthesis of Derivatives of 2,2,6,6-Tetramethyl-4-oxo-piperidine-1-carboxylic Acid and 2,2,6,6-Tetramethyl-piperidine-1-carboxylic Acid. *J. Prakt. Chem.,* **1977**, *319*, 516-521.

[63] Finney, Z. G.; Riley, T. N. 4-Anilidopiperidine Analgesics. 3. 1-Substituted 4-(Propananilido)perhydroazepines as Ring-Expanded Analogues. *J. Med. Chem.*, **1980**, *23*, 895-899.

[64] Roglans, A.; Marquet, J.; Moreno-Mañas, M. Preparation of 3-Pyrrolidone and 4-Perhydroazepinone. *Syn. Commun.*, **1992**, *22*, 1249-1258.

[65] Tai, W. T.; Warnhoff, E. W. β-Keto Esters from Reaction of Ethyl Diazoacetate with Ketones. *Can. J. Chem.*, **1964**, *42*, 1333-1340.

[66] Mock, W. L.; Hartman, M. E. Synthetic Scope of the Triethyloxonium Ion Catalyzed Homologation of Ketones with Diazoacetic Esters. *J. Org. Chem.*, **1977**, *42*, 459-465.

[67] Mock, W. L.; Hartman, M. E. Mechanism of the Triethyloxonium Ion Catalyzed Homologation of Ketones with Diazoacetic Esters. *J. Org. Chem.*, **1977**, *42*, 466-472.

[68] Pellicciari, R.; Natalini, B.; Sadeghpour, B. M.; Rosato, G. C.; Ursini, A. The Reaction of α-Diazo-β-hydroxy Esters with Boron Trifluoride. *J. Chem. Soc. Chem. Commun.*, **1993**, 1798-1800.

[69] Gauem, B. Biological Spin Labels as Organic Reagents. Oxidation of Alcohols to Carbonyl Compounds Using Nitroxyls. *J. Org. Chem.*, **1975**, *40*, 1998-2000.

[70] Cella, J. A.; Kelley, J. A.; Kenehan, E. F. Unexpected Oxidation of a Nitroxide Alcohol with *m*-Chloroperbenzoic Acid. *J. Chem. Soc. Chem. Comm.*, **1974**, 943a-943b.

[71] Cella, J. A.; Kelley, J. A.; Kenehan, E. F. Nitroxide-Catalyzed Oxidation of Alcohols using *m*-Chloroperbenzoic Acid. A New Method. *J. Org. Chem.*, **1975**, *40*, 1860-1862.

[72] Lajzérowicz-Bonneteau, J. Structure du radical nitroxyde tétraméthyl-2,2,6,6 piperidinol-4 oxyle-1. *Acta Cryst.,* **1968**, *B24*, 196-199.

[73] Gange, D. M.; Kallel, E. A. The Structure and Conformation of Hydroxylamine and its Methylated Derivatives. *J. Chem. Soc. Chem. Commun.,* **1992**, 824-825.

[74] Percino, M. J.; Cerón, M.; Soriano-Moro, G.; Pacheco, J. A.; Castro, M. E.; Chapela, V. M.; Bonilla-Cruz, J.; Saldivar-Guerra, E. 2,2,6,6-Tetramethyl-1-oxopiperidinetribromide and Two Forms of 1-hydroxy-2,2,6,6-tetramethylpiperidinium Bromide Salt: Syntheses, Crystal Structures and Theoretical Calculations. *J. Mol. Struct.,* **2016**, *1103*, 254-264.

[75] Arata, Y.; Tanaka, K.-I.; Yoshifuji, S.; Kanatomo, S. Studies on 1-Azabicyclo Compounds. XXVIII. Synthesis of 1-Methyl-perhydroazocin-5-one from Pyrrolizidine. *Chem. Pharm. Bull.* **1979**, *27*, 981-983.

[76] Dowd, P.; Choi, S.-C. Free Radical Ring-Expansion Leading to Novel Six- and Seven-membered Heterocycles. *Tetrahedron Lett.,* **1989,** *30,* 6129-6132.

[77] Dowd, P.; Choi, S.-C. Free Radical Ring-Expansion Leading to Novel Six- and Seven-membered Heterocycles. *Tetrahedron,* **1991,** *47,* 4847-4860.

[78] McNally, A.; Haffemayer, B.; Collins, B. S. L.; Gaunt, M. J. Palladium-catalysed C—H Activation of Aliphatic Amines to Give Strained Nitrogen Heterocycles. *Nature*, **2014**, *510*, 129-133.

[79] Leonard, N. J.; Oki, M. Cyclic Aminoacyloins and Aminoketones. VII. N-Aryl Substitution and Transannular Interaction between N and C_{CO}. *J. Am. Chem. Soc.*, **1955**, *77*, 6241-6244.

[80] Leonard, N. J.; Fox, R. C.; Oki, M. Cyclic Aminoacyloins. Ring-Size Limitations of Transannular Interaction between N and $C_{CO.}$ *J. Am. Chem. Soc.*, **1954**, *76*, 630-631.

[81] Leonard, N. J.; Oki, M. Cyclic Aminoacyloins. III. Synthesis, Properties and the Detection of Transannular Interaction between N and C_{CO}. *J. Am. Chem. Soc.*, **1954**, *76*, 5708—5714.

[82] Sutharchanadevi, M.; Murugan, R. Eight-membered Rings with One Nitrogen Atom. *Comprehensive Heterocyclic Chemistry II.,* **1996**, 403-428.

[83] Spanka, G.; Rademacher, P. Transannular Interactions of Difunctional Medium Rings. Part 3. ^{13}C and ^{17}O Nuclear Magnetic Resonance Studies on Cyclic Amino Ketones. *J. Chem. Soc. Perkin Trans. II,* **1988**, 2119-2121.

[84] Spanka, G.; Rademacher, P. Transannular Interactions of Difunctional Medium Rings. 1. n/π Interactions in Cyclic Amino Ketones and Aminoalkenes Studied by Photoelectron Spectroscopy. *J. Org. Chem.,* **1986**, *51*, 592-596.

[85] Spanka, G.; Boese, R.; Rademacher, P. Transannular Interactions of Difunctional Medium Rings. 2. Molecular Structure and Conformational Properties of 1-Alkylhexahydroazocin-5-ones. *J. Org. Chem.,* **1987**, *52*, 3362-3367.

[86] Dowd, P.; Zhang, W. Free Radical-Mediated Ring Expansion and Related Annulations. *Chem. Rev.,* **1993,** *93,* 2091-2115.

[87] Dowd, P.; Choi, S.-C. A New Tri-*n*-butyltin Hydride Based Rearrangement of Bromomethyl β-Keto Esters. A Synthetically Useful Ring Expansion to γ-Keto Esters. *J. Am. Chem. Soc.* **1987,** *109,* 3493-3494.

[88] Dowd, P.; Choi, S.-C. Free Radical Ring Expansion by Three and Four Carbons. *J. Am. Chem. Soc.,* **1987,** *109,* 6548-6549.

[89] Beckwith, A. L. J.; O'Shea, D. M.; Westwood, S. W. Rearrangement of Suitably Constituted Aryl, Alkyl, or Vinyl Radicals by Acyl or Cyano Group Migration. *J. Am. Chem. Soc.,* **1988**, *110*, 2565-2575.

[90] Sugi, M.; Togo, H. Environmentally Friendly TPDS-mediated Free Radical Ring Expansion of α-Haloalkyl Cyclic β-Keto Esters. *Tetrahedron*, **2002**, *58*, 3171-3175.

[91] Sugi, M.; Sakuma, D.; Togo, H. Zinc- and Indium-Mediated Ring-Expansion Reaction of α-Halomethyl Cyclic β-Keto Esters in Aqueous Alcohol. *J. Org. Chem.*, **2003**, *66*, 7629-7633.

[92] Harrowven, D. C.; Curran, D. P.; Kostiuk, S. L.; Wallis-Guy, J. L.; Whiting, S.; Stenning, K. J.; Tang, B.; Packard, E.; Nanson, L. Potassium Carbonate—Silica: A Highly Effective Stationary Phase for the Chromatographic Removal of Organotin Impurities. *Chem. Commun.,* **2010,** ***46,*** 6335-6337.

[93] Xie, Z.-F.; Sakai, K. Construction of Medium and Large-Sized Cyclic β-Keto Esters (or Nitriles) via One-Pot Three Carbon Ring Expansion of Carbocyclic β-Keto Esters and Its Application to the Syntheis of (-)-Muscone. *J. Org. Chem.,* **1990**, *55*, 820-826.

[94] Nortcliffe, A.; Moody, C. J. Seven-Membered Ring Scaffolds for Drug Discovery: Access to Functionalised Azepanes and Oxepanes through Diazocarbonyl Chemistry., *Bioorg. Med. Chem.*, **2015**, *23*, 2730-2735.

APPENDIX A

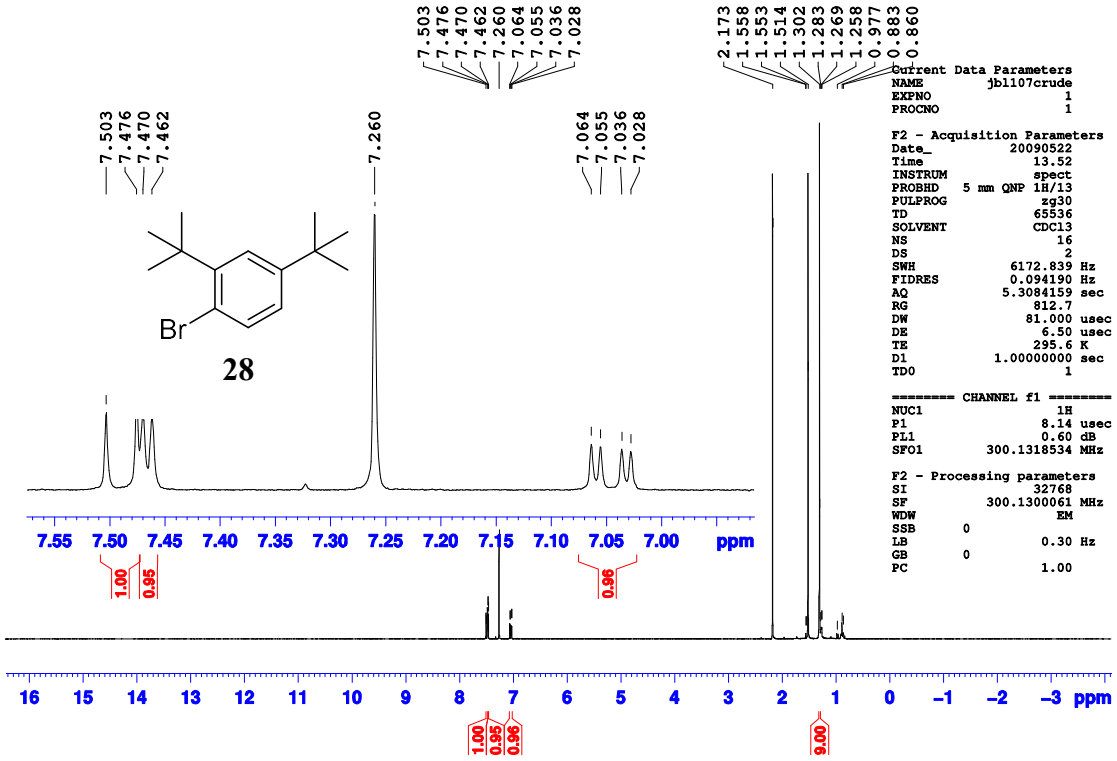

Figure A-1. ^{1}**H NMR of (400 MHz, $CDCl_3$) spectrum of 28 (JBL107crude).**

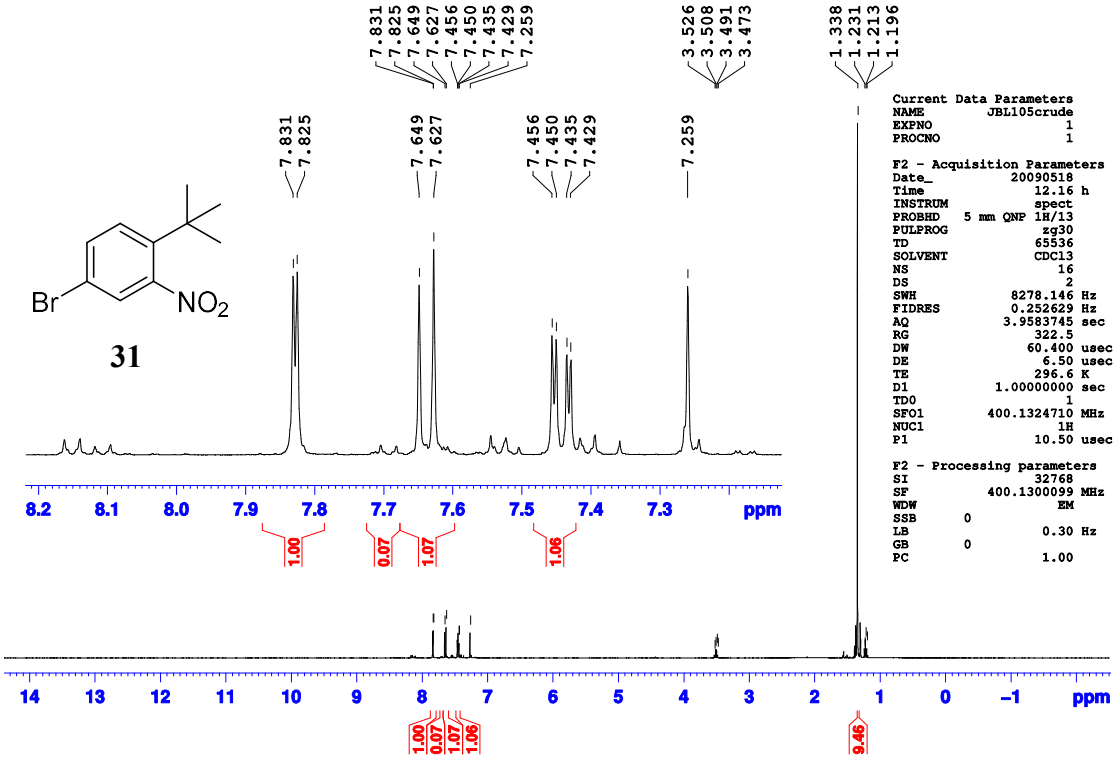

Figure A-2. ^{1}**H NMR of (400 MHz, $CDCl_3$) spectrum of 31 (JBL105crude).**

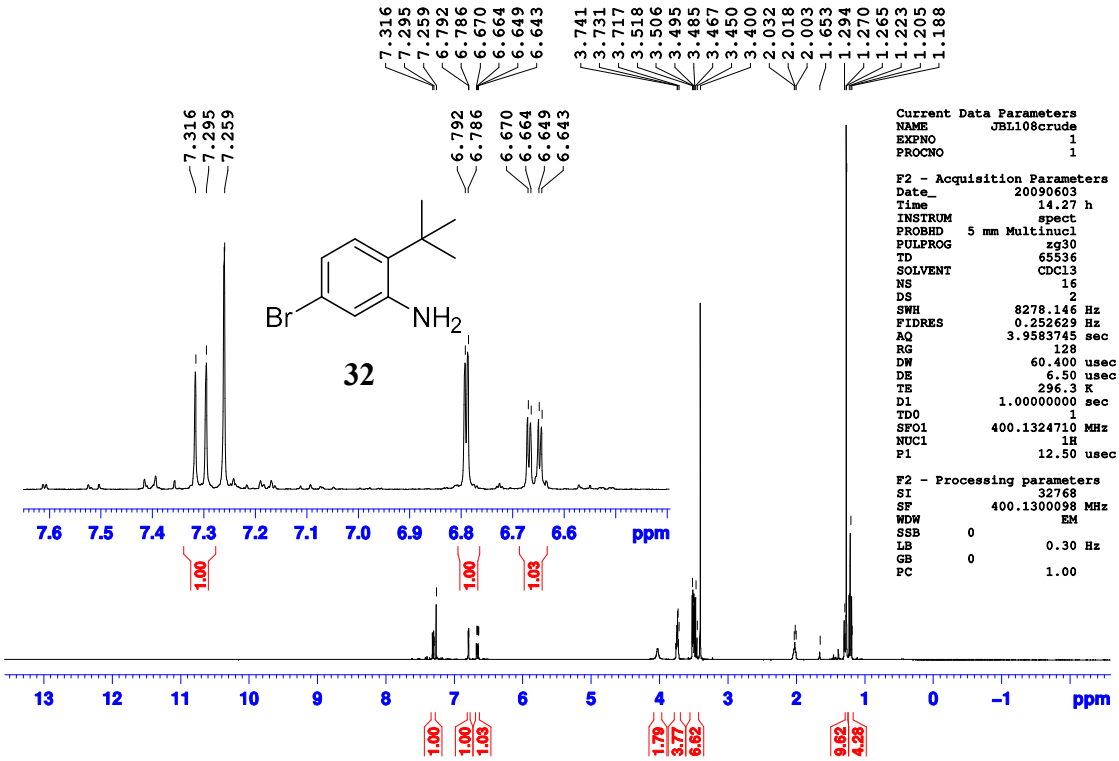

Figure A-3. ^{1}H NMR of (400 MHz, $CDCl_3$) spectrum of 32 (JBL108crude).

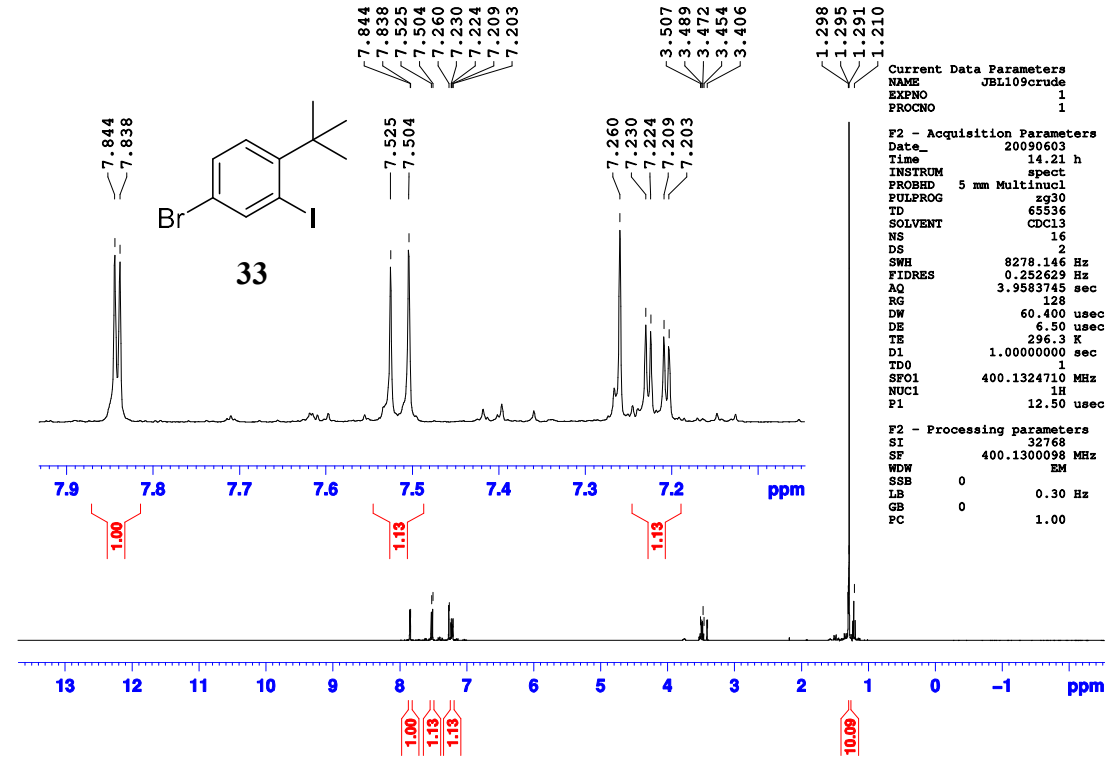

Figure A-4. ^{1}H NMR of (400 MHz, $CDCl_3$) spectrum of 33 (JBL109crude).

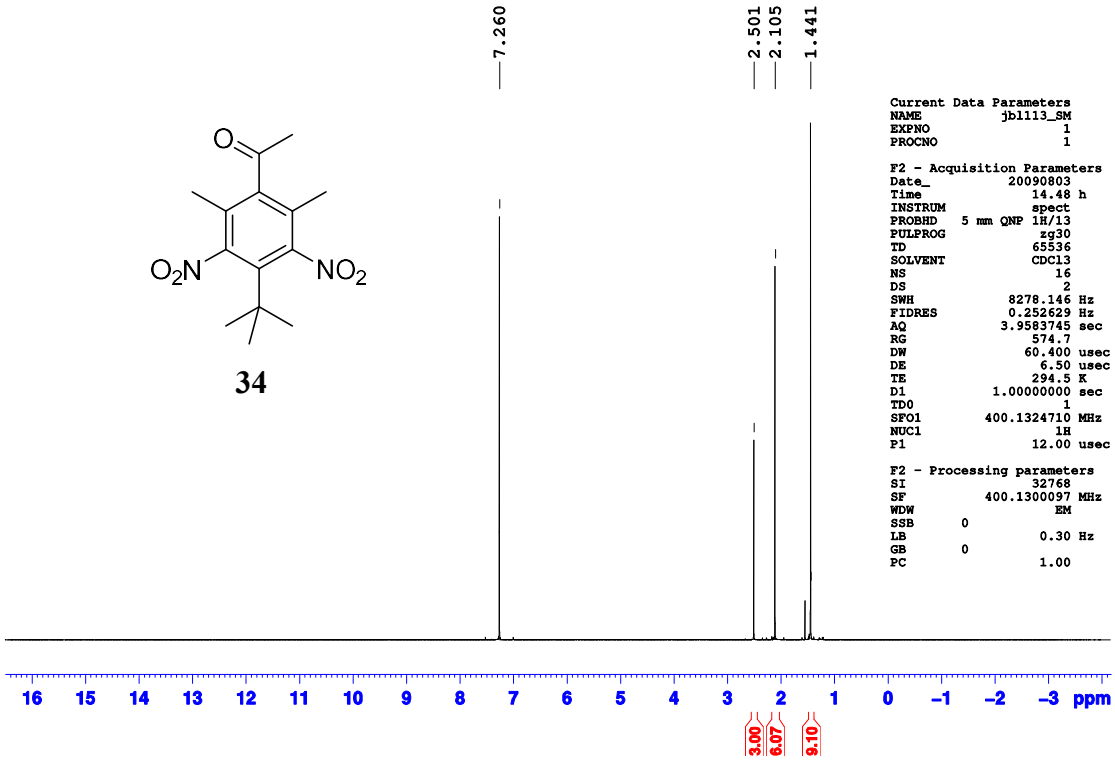

Figure A-5. ^{1}H NMR of (400 MHz, $CDCl_3$) spectrum of 34 (JBL113SM).

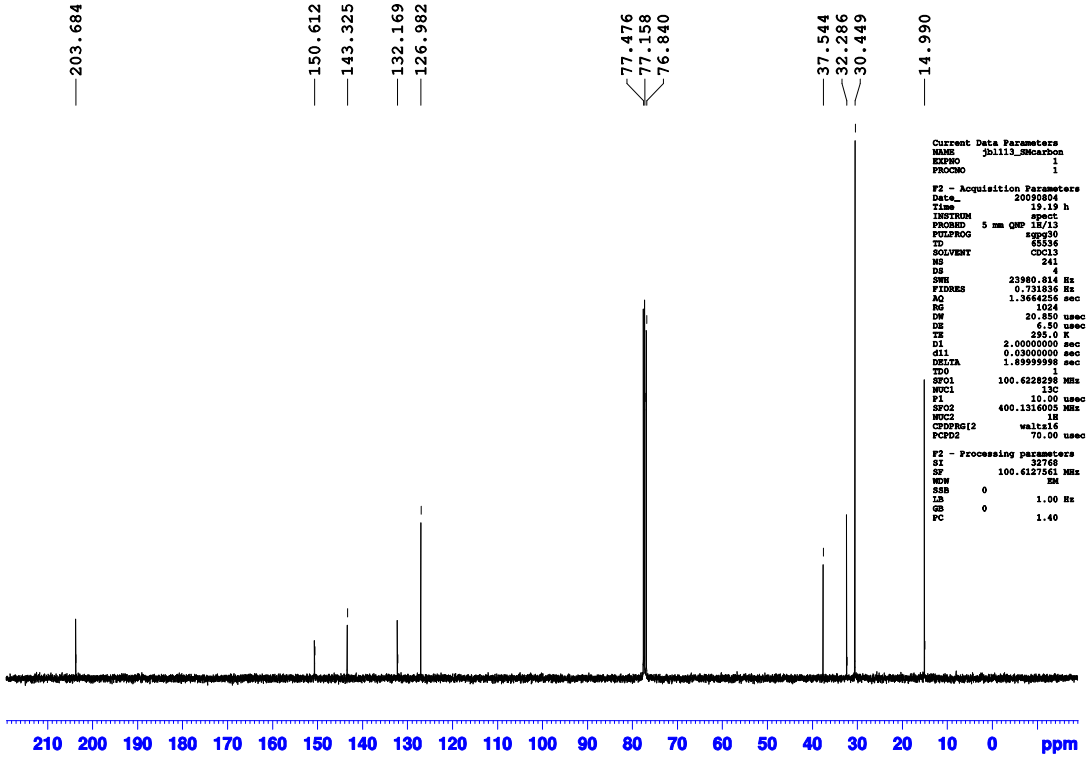

Figure A-6. ^{13}C NMR of (400 MHz, $CDCl_3$) spectrum of 34 (JBL113SM).

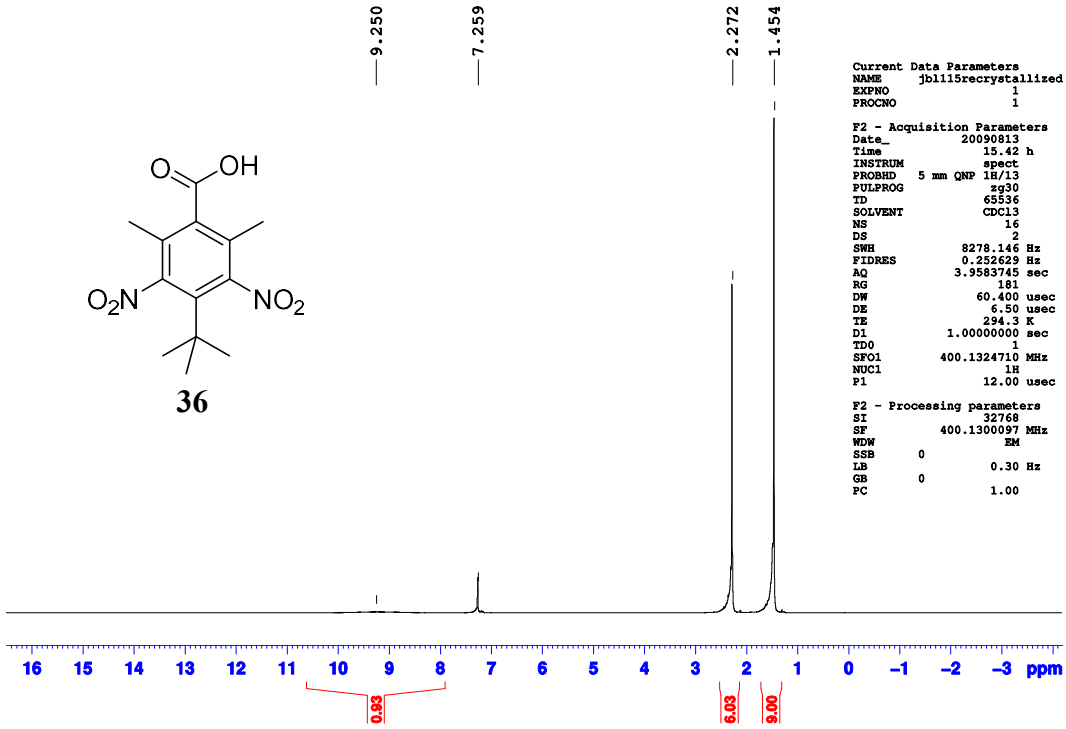

Figure A-7. ^{1}H NMR of (400 MHz, $CDCl_3$) spectrum of 36 (JBL115recryst).

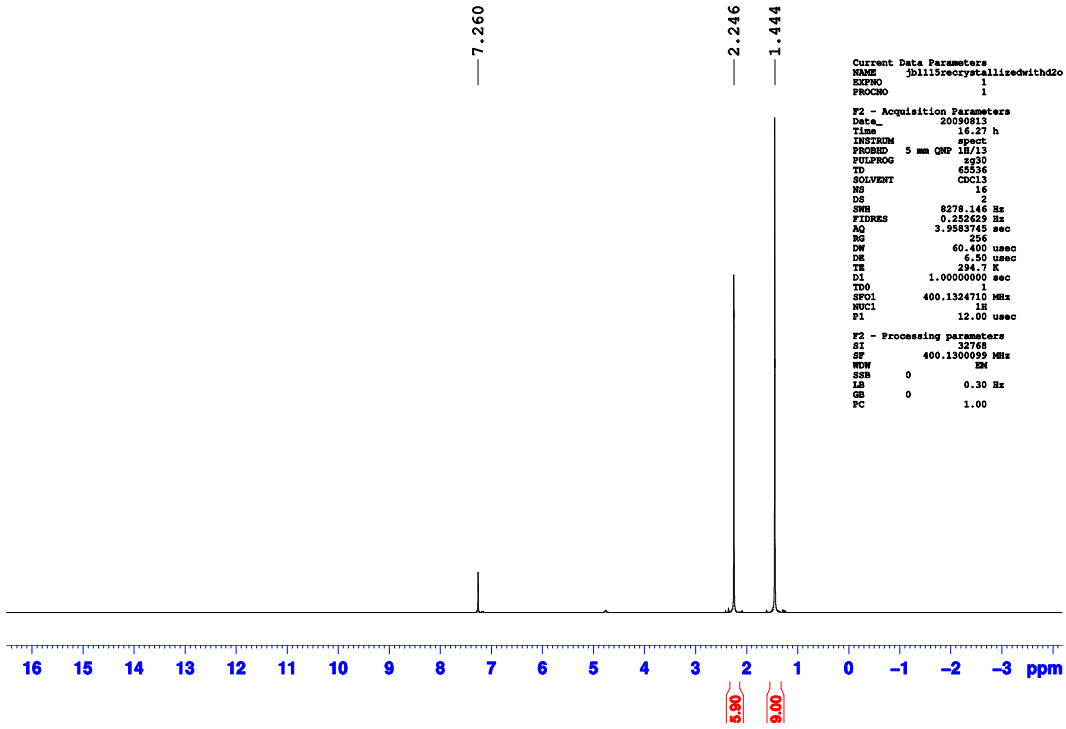

Figure A-8. ^{1}H NMR of (400 MHz, $CDCl_3$ + D_2O) spectrum of 36 (JBL115recryst).

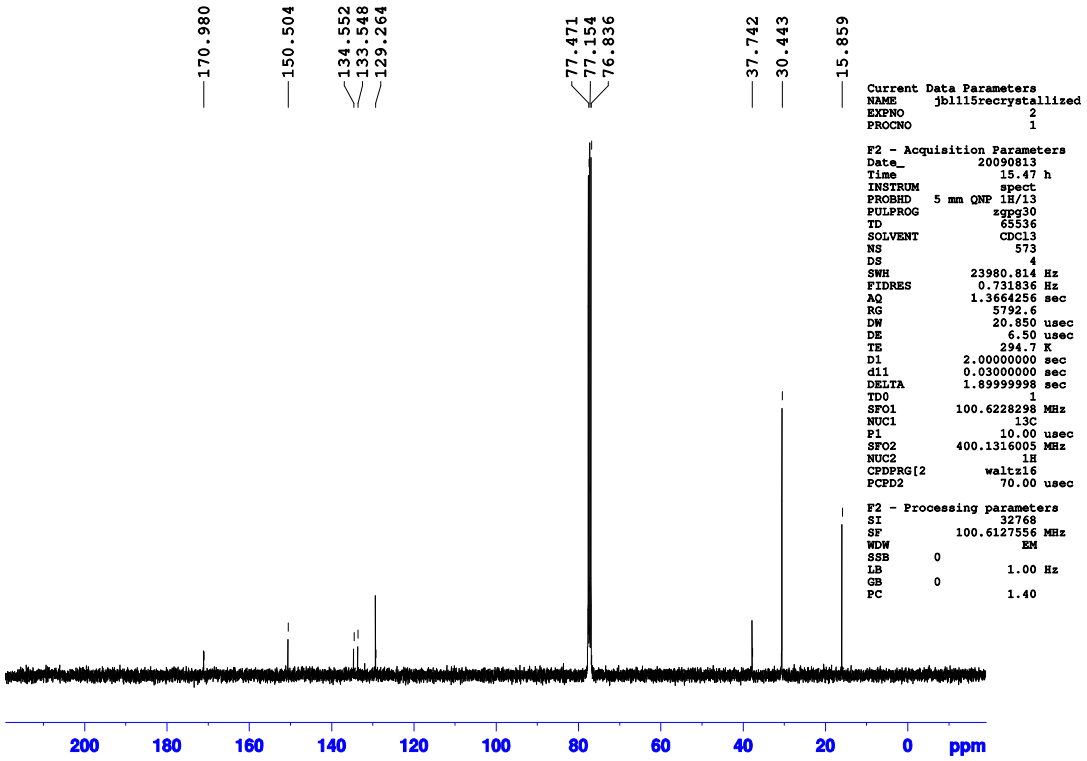

Figure A-9. ^{13}C NMR of (400 MHz, $CDCl_3$) spectrum of 36 (JBL115recryst).

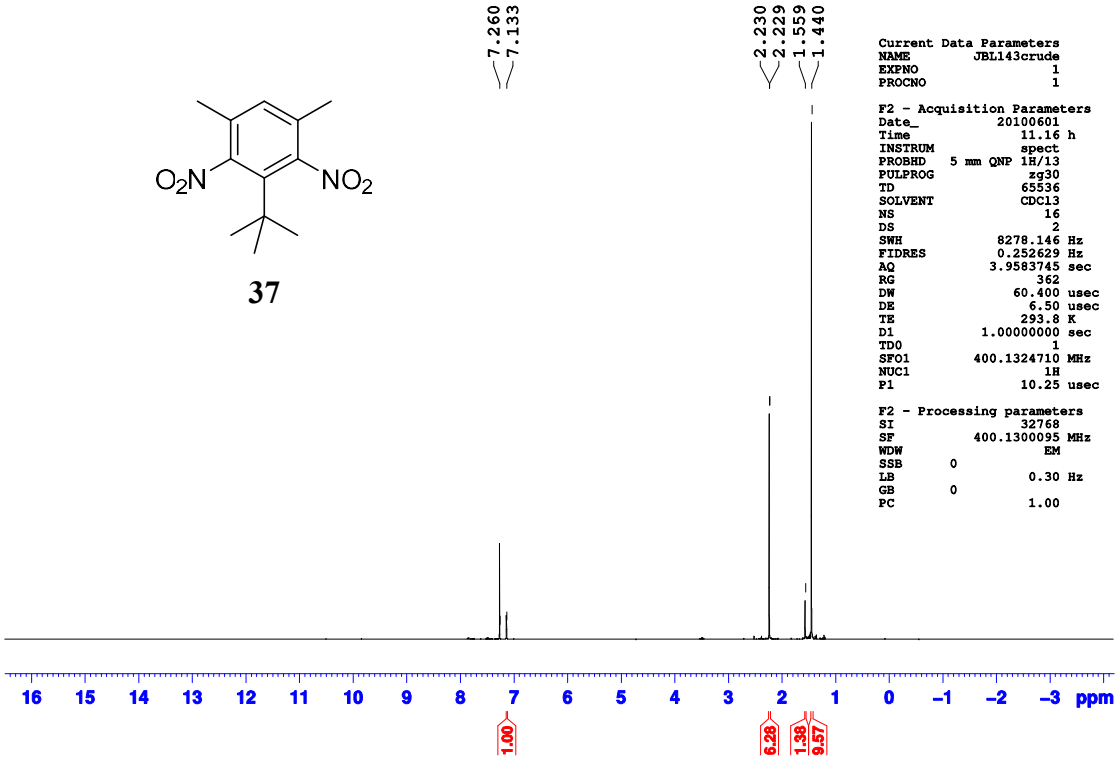

Figure A-10. ^{1}H NMR of (400 MHz, $CDCl_3$) spectrum of 37 (JBL143crude).

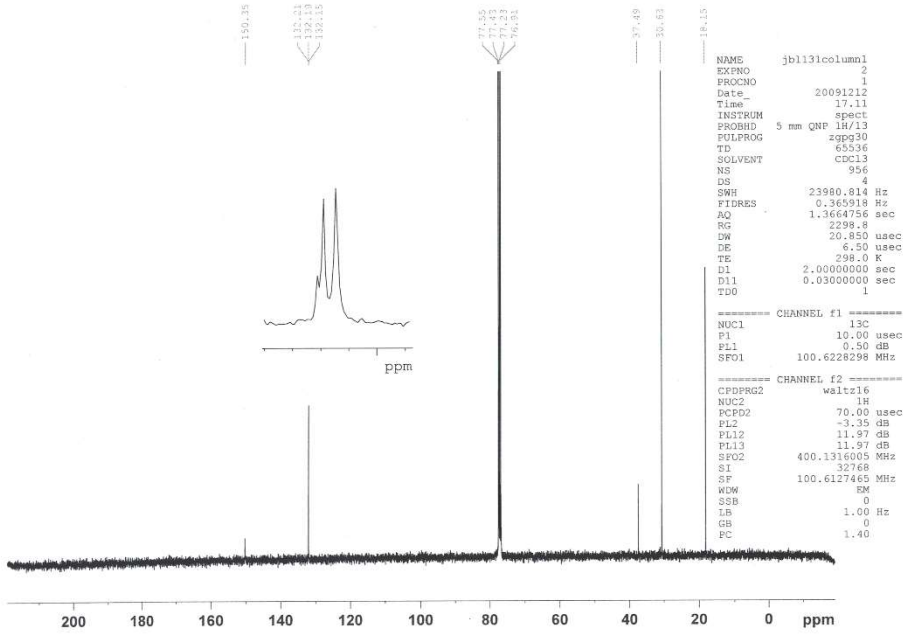

Figure A-11. ^{13}C NMR of (400 MHz, $CDCl_3$) spectrum of 37 (JBL131colfrac1).

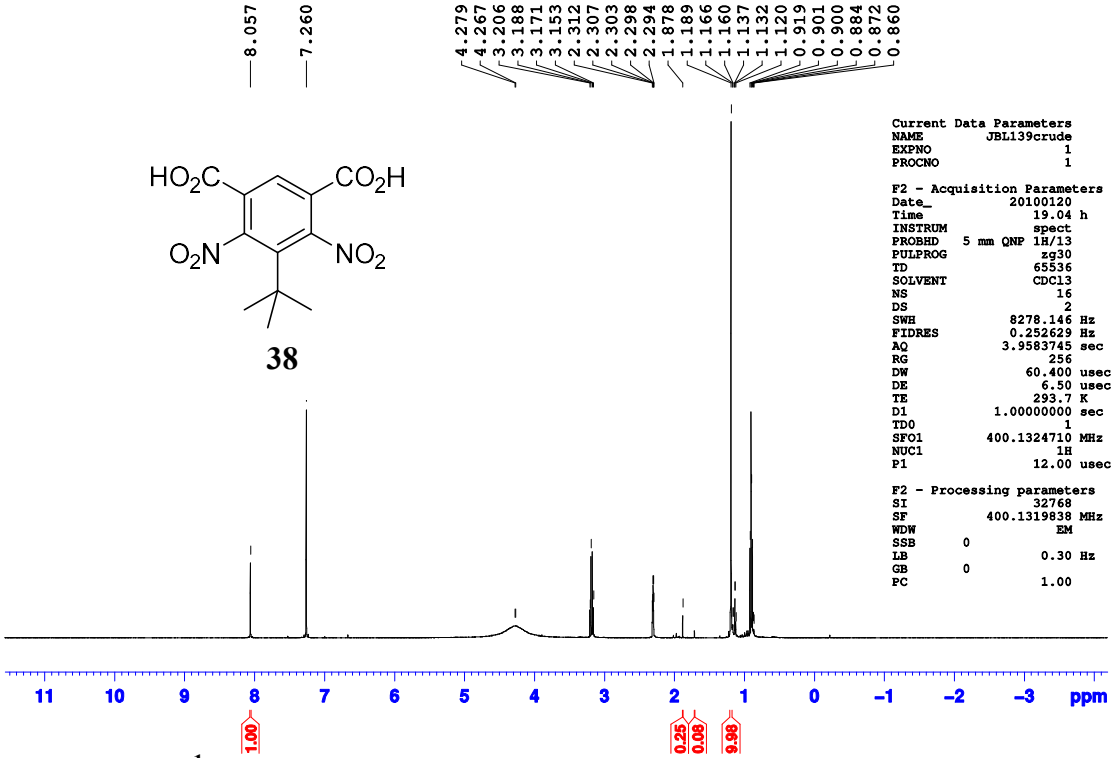

Figure A-12. ^{1}H NMR of (400 MHz, $CDCl_3$) spectrum of 38 (JBL139crude).

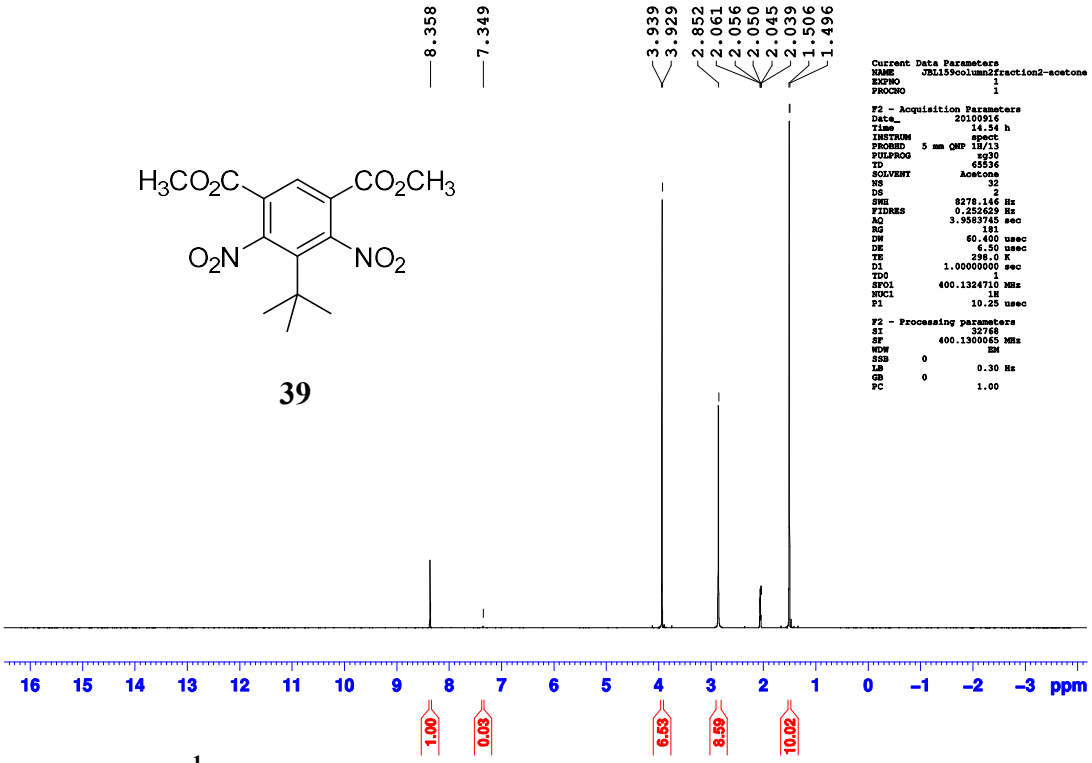

Figure A-13. ^{1}H NMR of (400 MHz, acetone-d_6) spectrum of 39 (JBL159col2fr2).

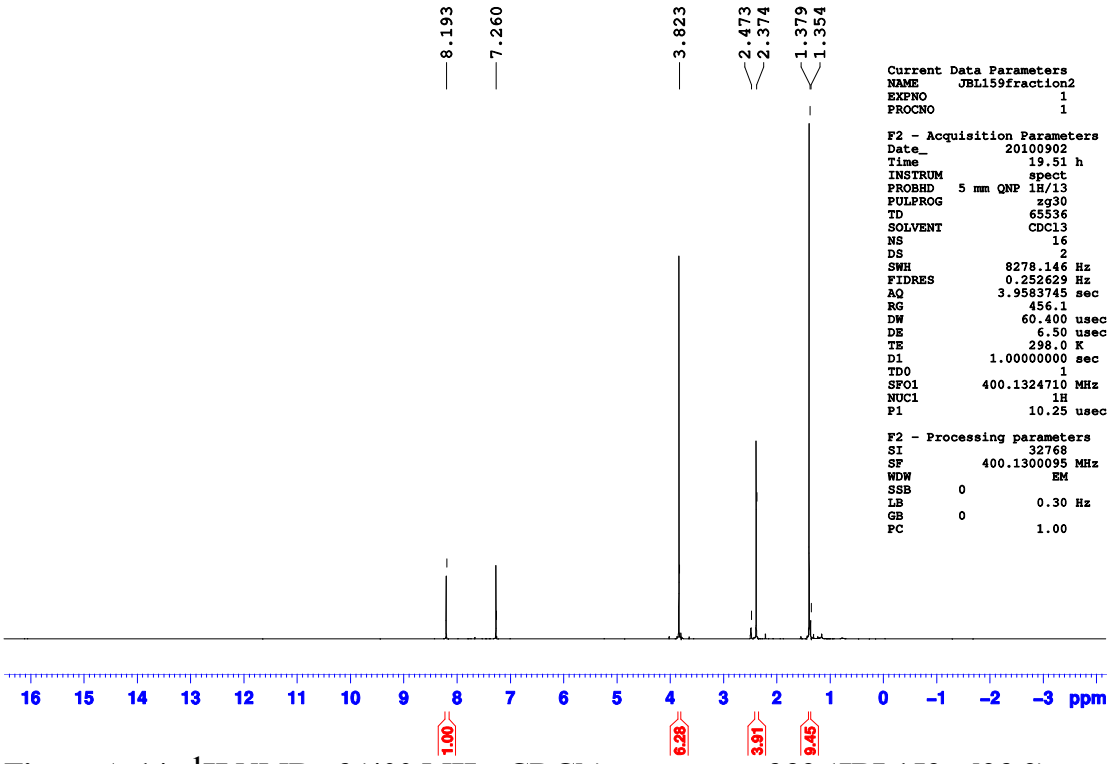

Figure A-14. ^{1}H NMR of (400 MHz, $CDCl_3$) spectrum of 39 (JBL159col2fr2).

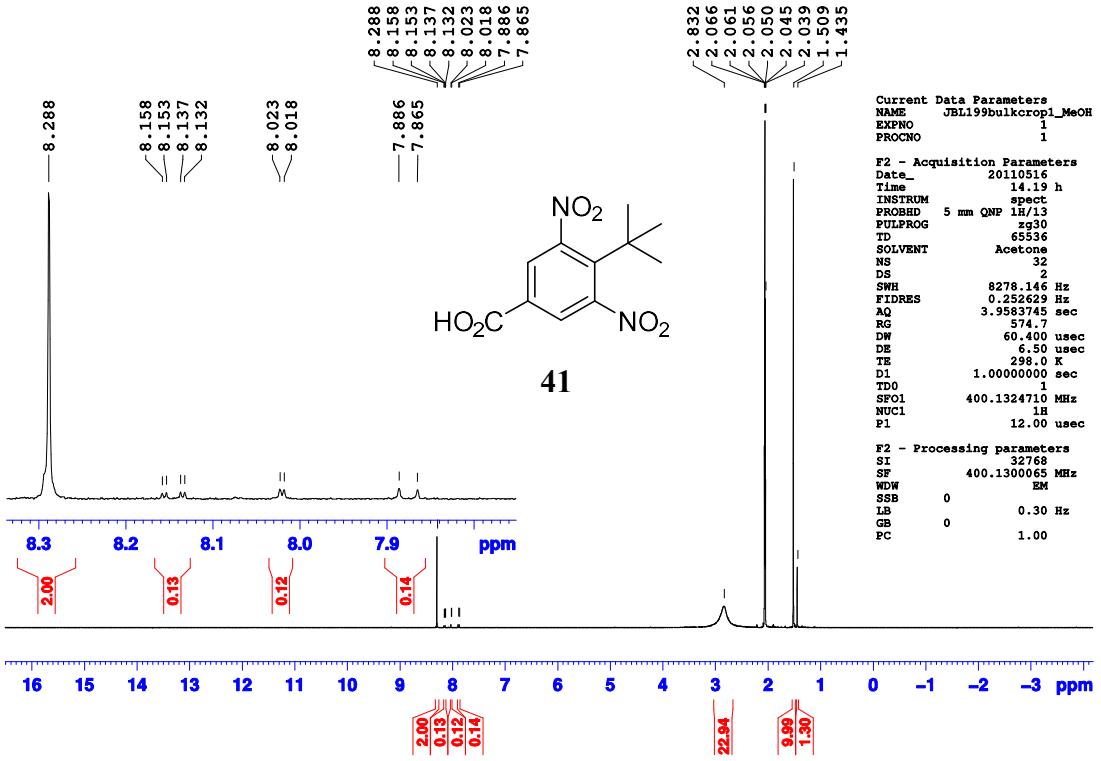

Figure A-15. ^{1}H NMR of (400 MHz, acetone-d_6) spectrum of 41 (JBL199bulkrecr1).

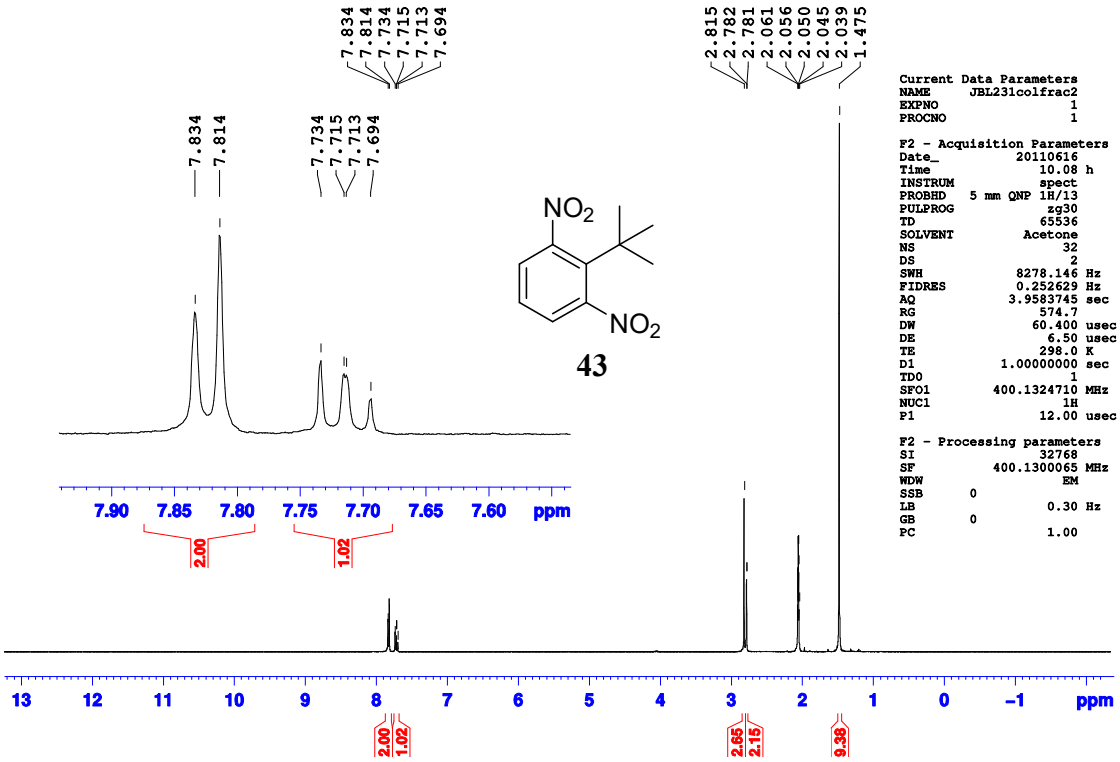

Figure A-16. ^{1}H NMR of (400 MHz, acetone-d_6) spectrum of 43 (JBL231colfrac2).

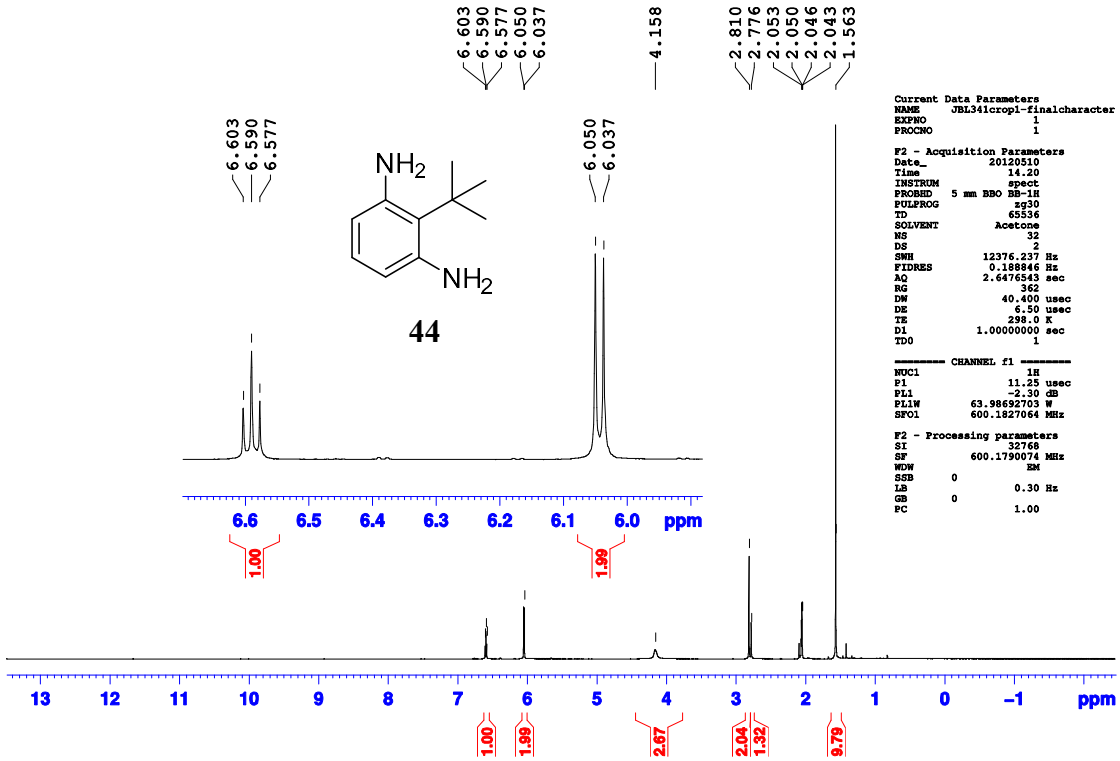

Figure A-17. ^{1}H NMR of (400 MHz, acetone-d_6) spectrum of 44 (JBL341recrystcr1).

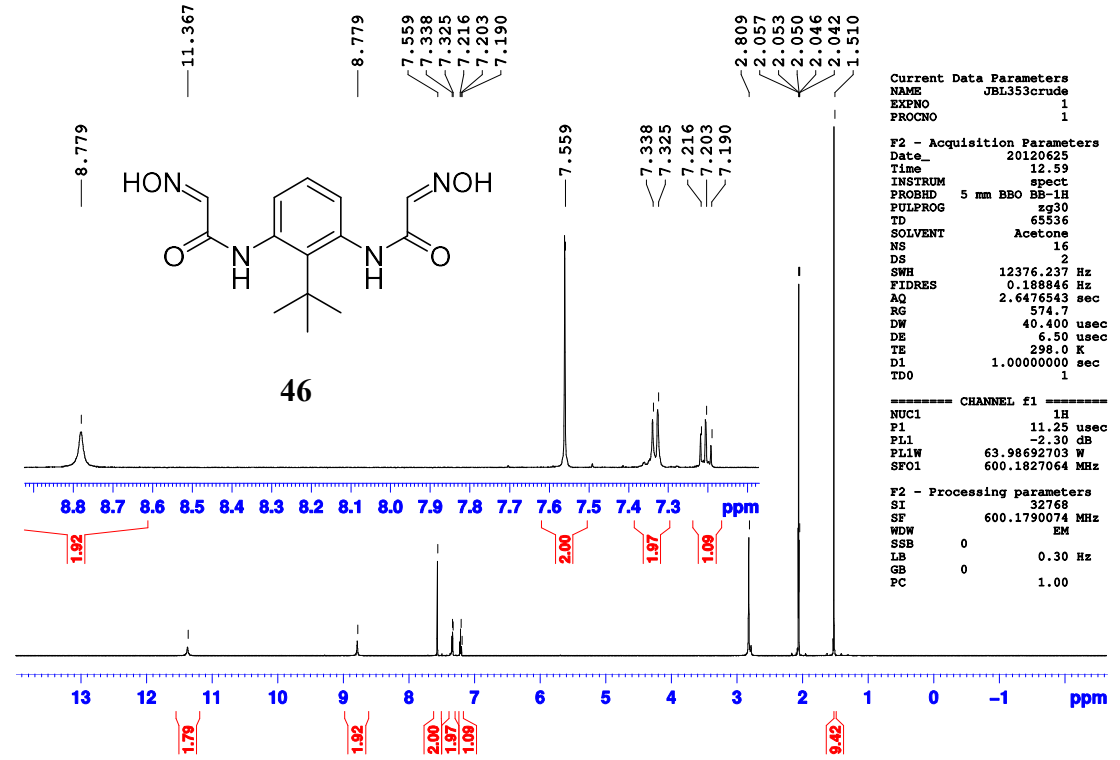

Figure A-18. ^{1}H NMR of (400 MHz, acetone-d_6) spectrum of 46 (JBL353crude).

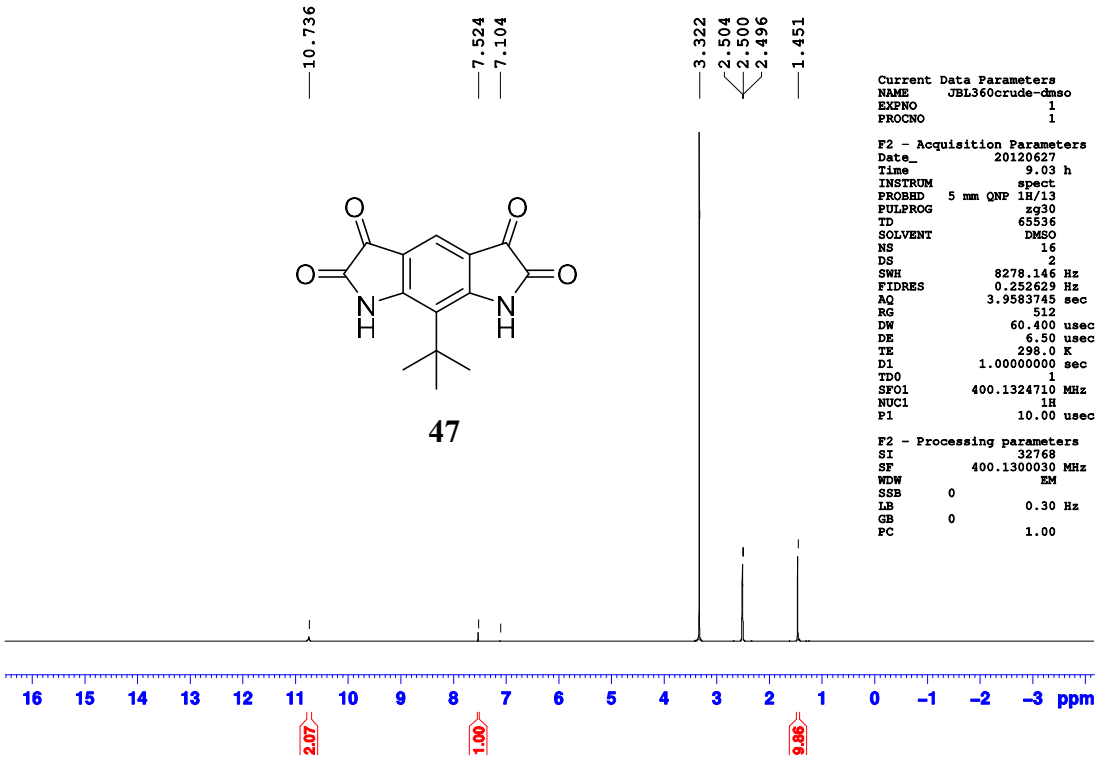

Figure A-19. ^{1}H NMR of (400 MHz, DMSO-d_6) spectrum of 47 (JBL360crude).

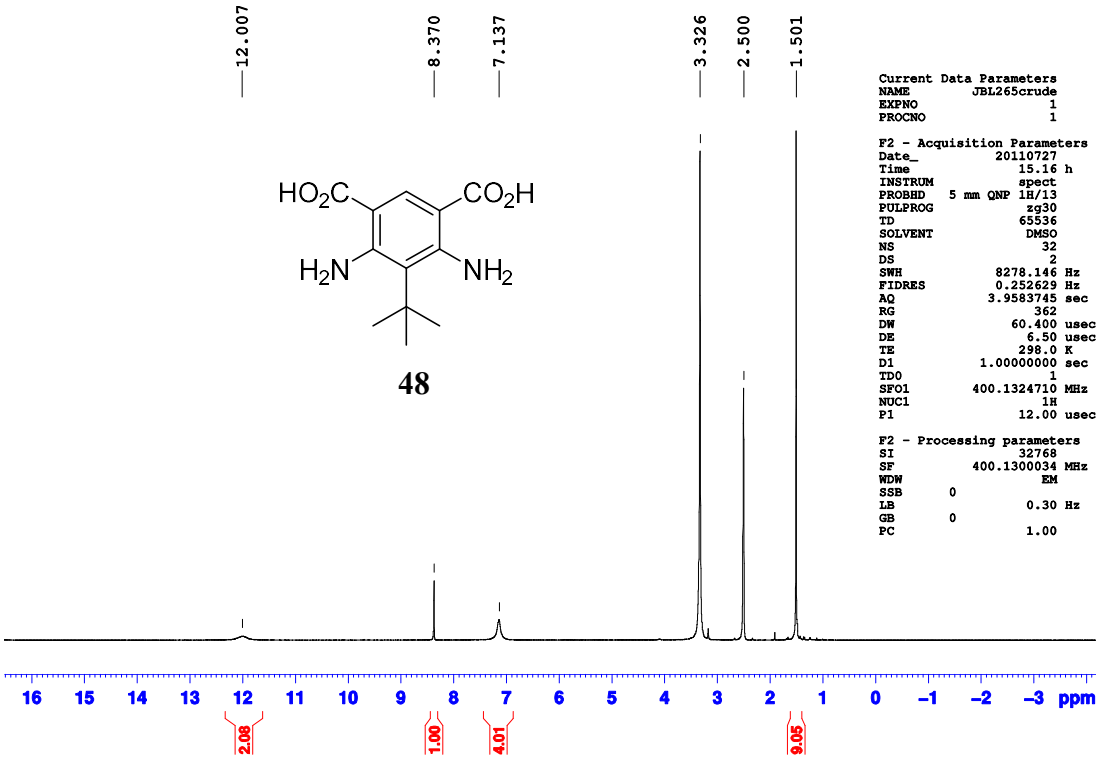

Figure A-20. ^{1}H NMR of (400 MHz, DMSO-d_6) spectrum of 48 (JBL265crude).

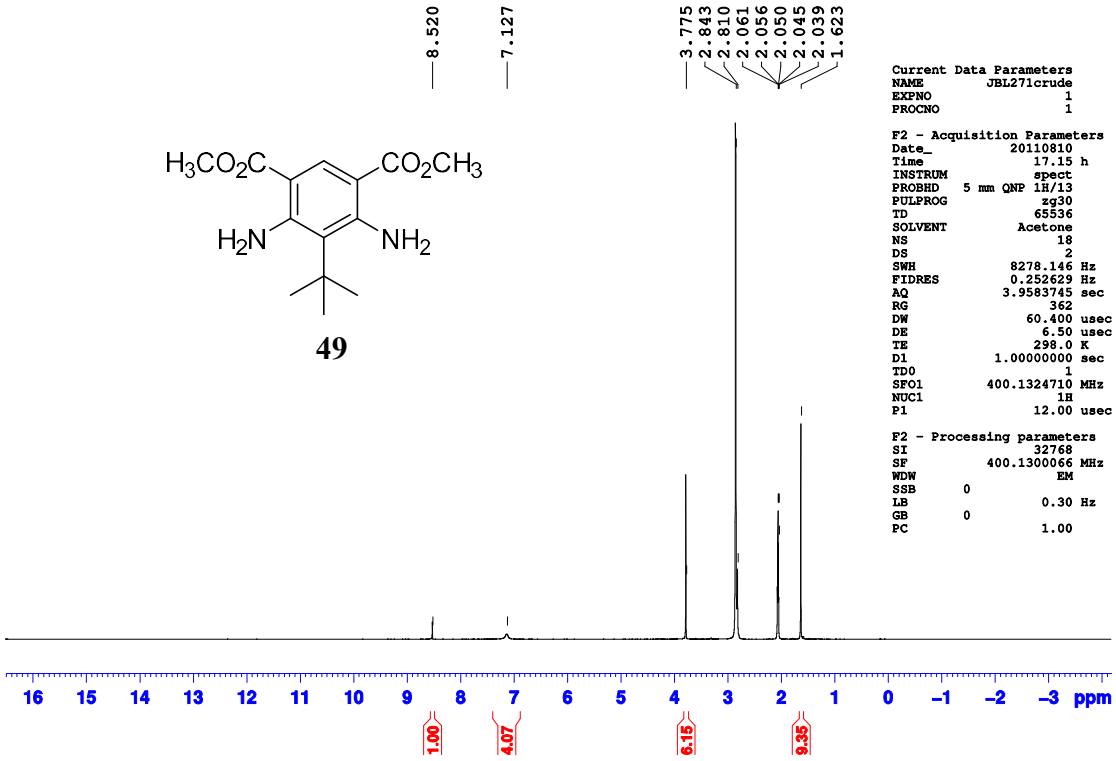

Figure A-21. ^{1}H NMR of (400 MHz, acetone-d_6) spectrum of 49 (JBL271crude).

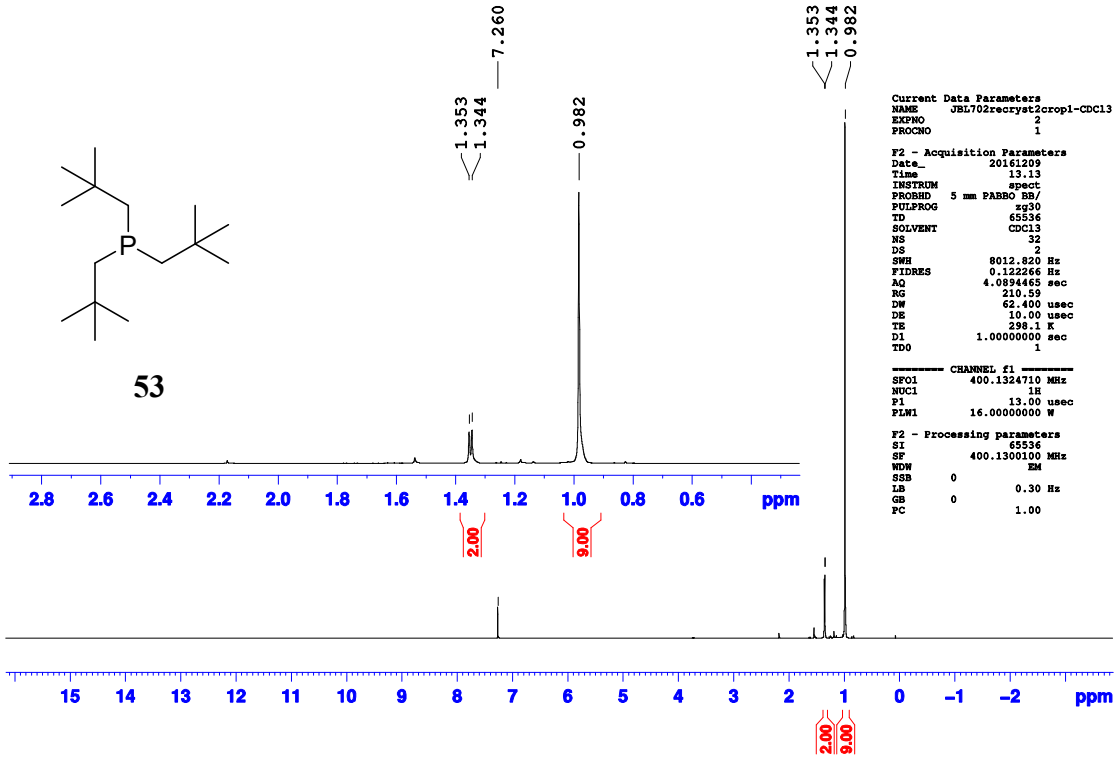

Figure A-22. ^{1}H NMR of (400 MHz, $CDCl_3$) spectrum of 53 (JBL702recryst2crop1).

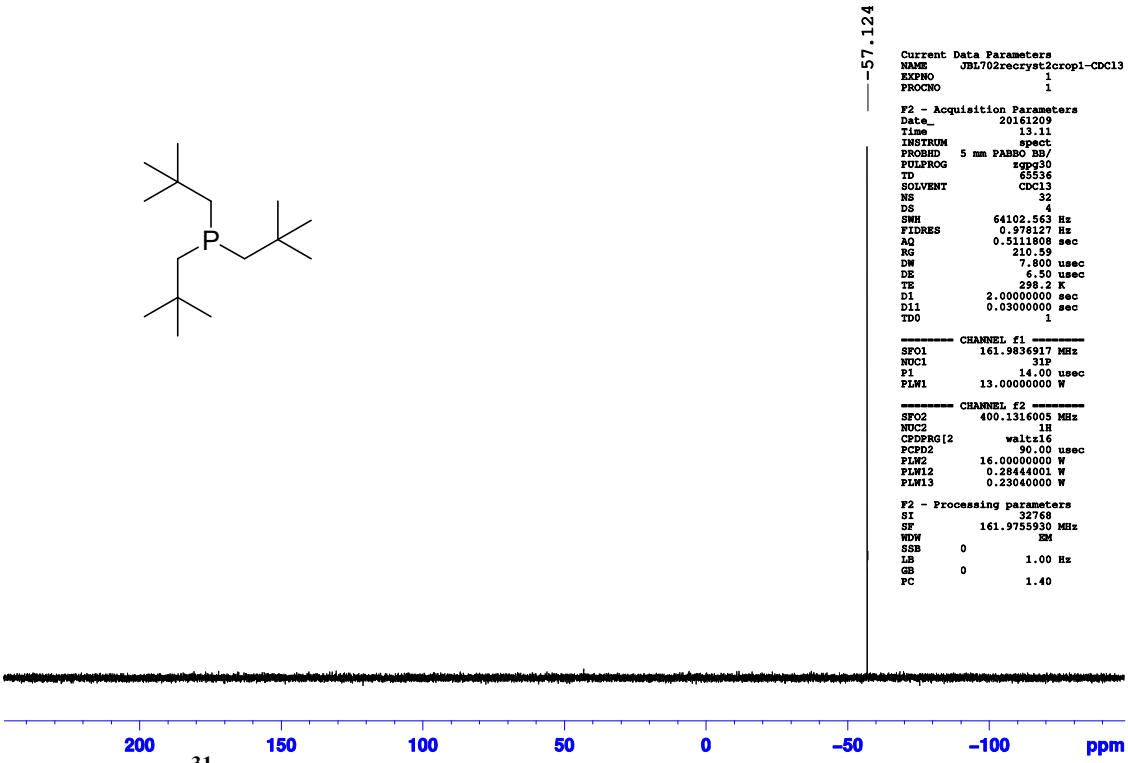

Figure A-23. ^{31}P NMR of (400 MHz, $CDCl_3$) spectrum of 53 (JBL702recryst2crop1).

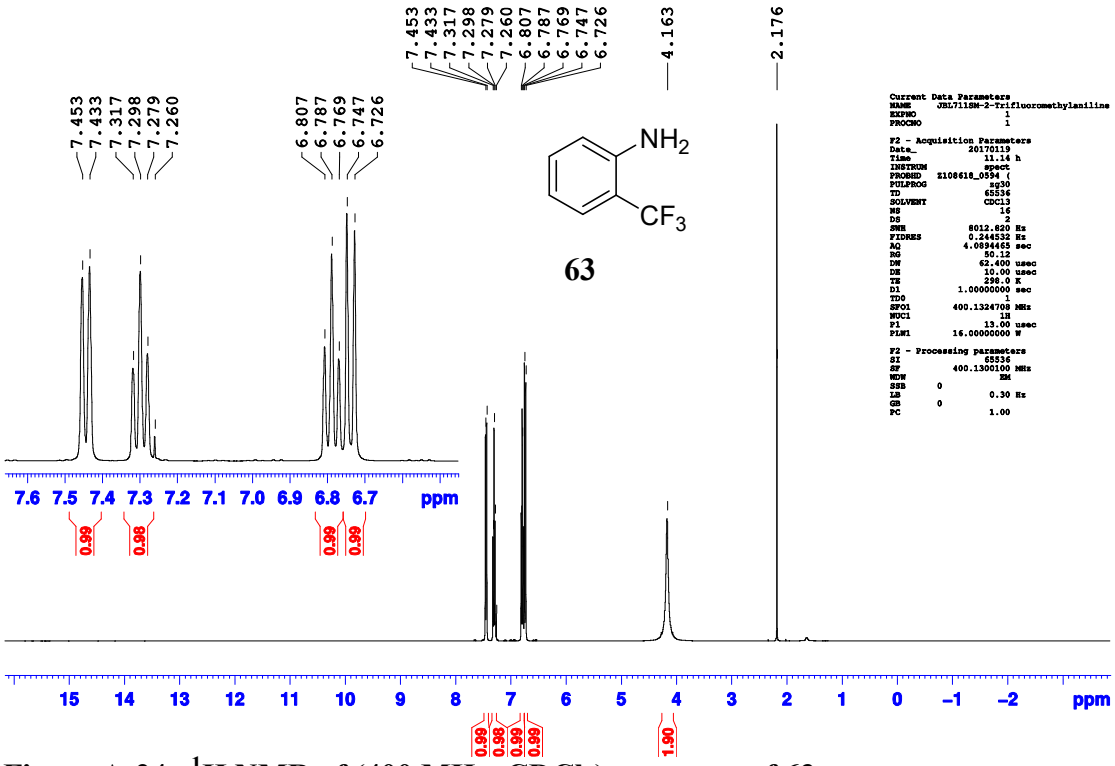

Figure A-24. ^{1}H NMR of (400 MHz, $CDCl_3$) spectrum of 63.

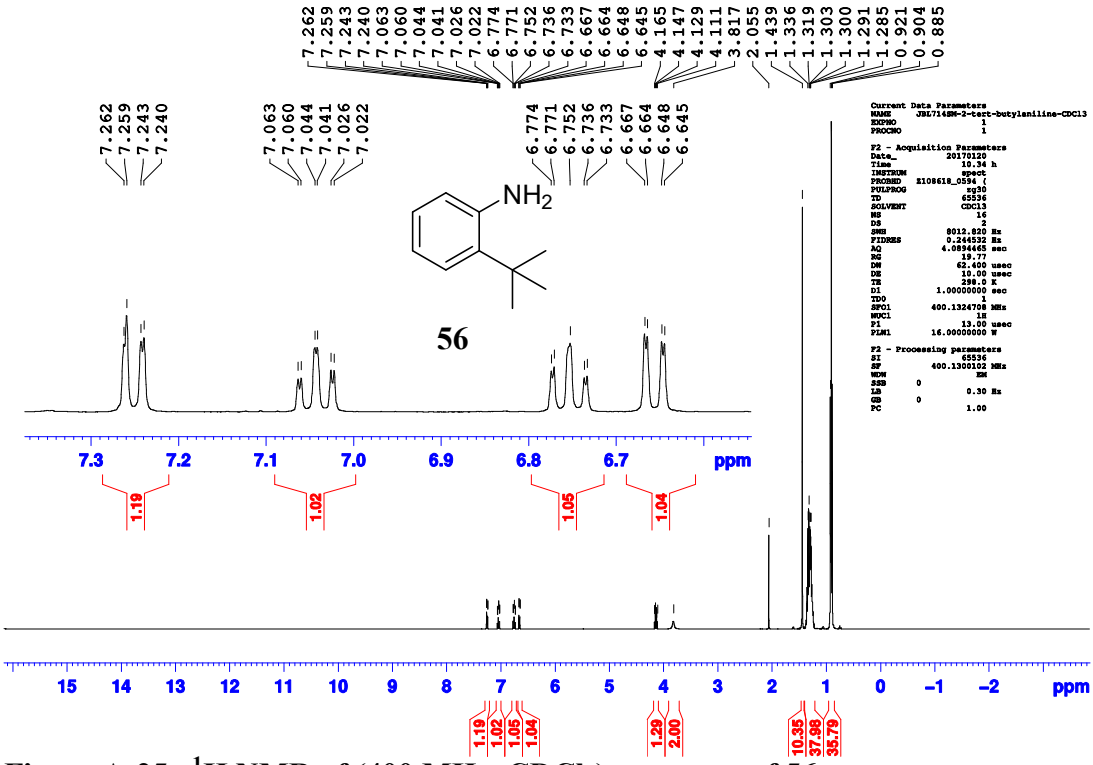

Figure A-25. ^{1}H NMR of (400 MHz, $CDCl_3$) spectrum of 56.

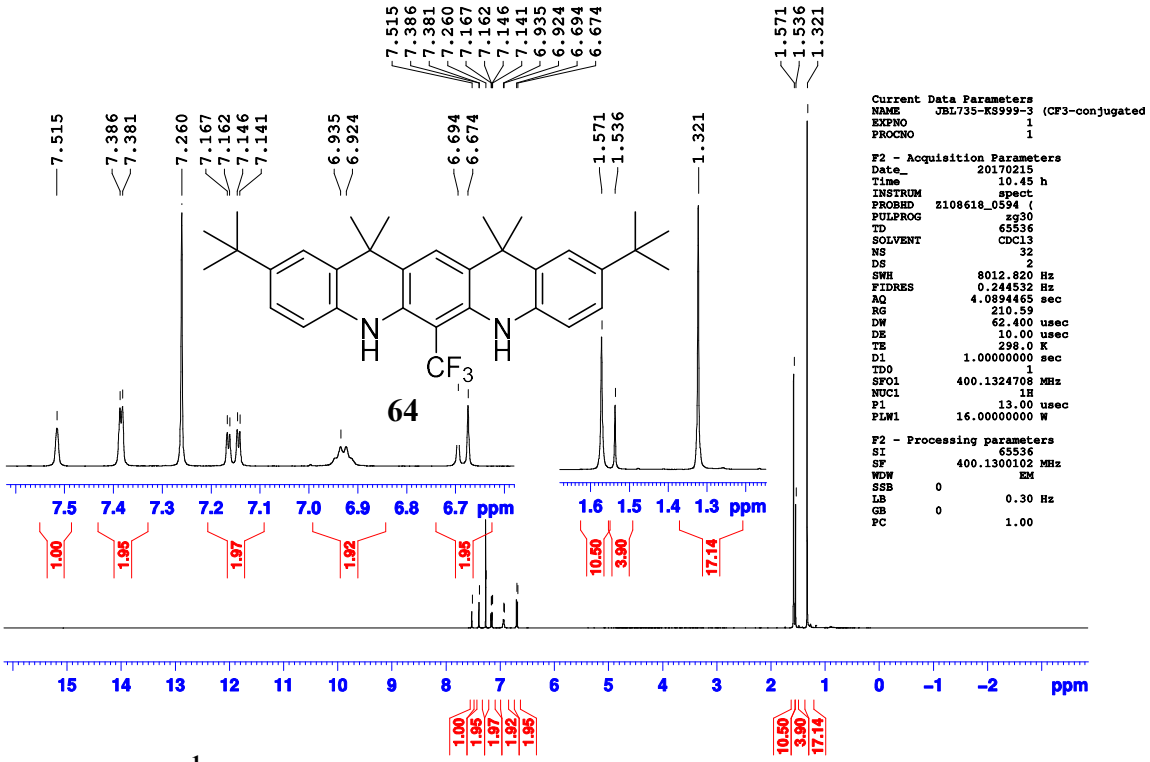

Figure A-26. ^{1}H NMR of (400 MHz, $CDCl_3$) spectrum of 64 (KS999-3).

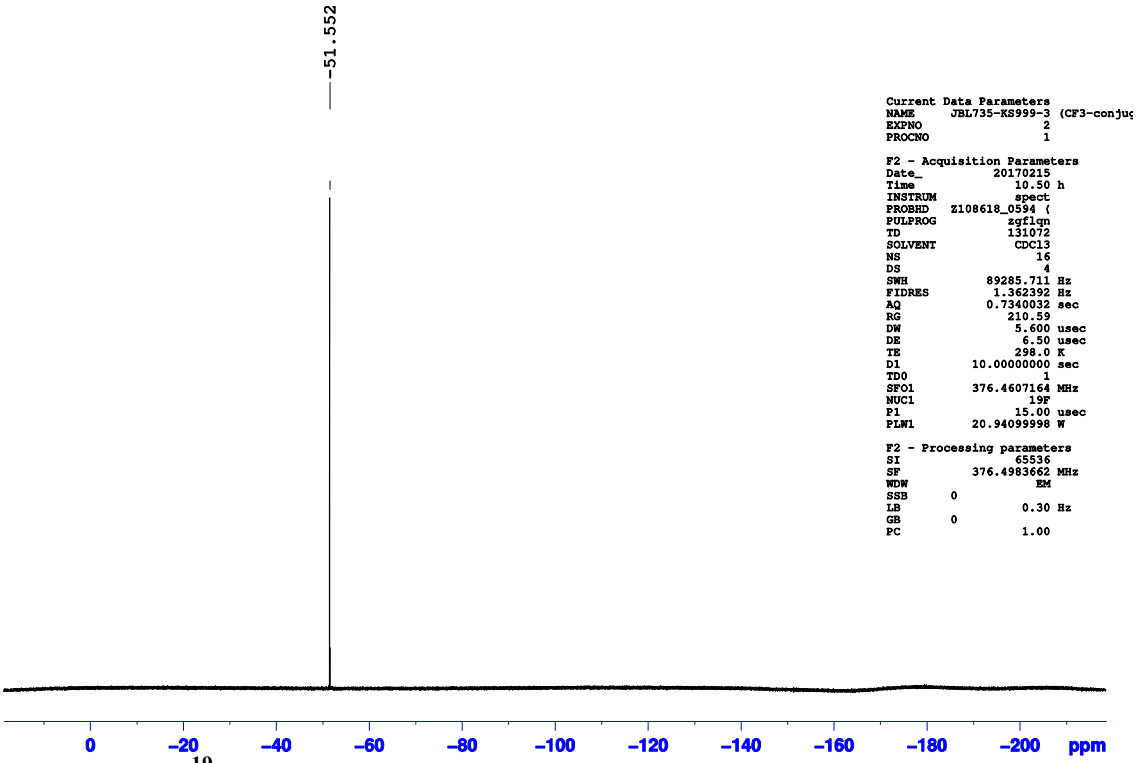

Figure A-27. ^{19}F NMR of (400 MHz, $CDCl_3$) spectrum of 64 (KS999-3).

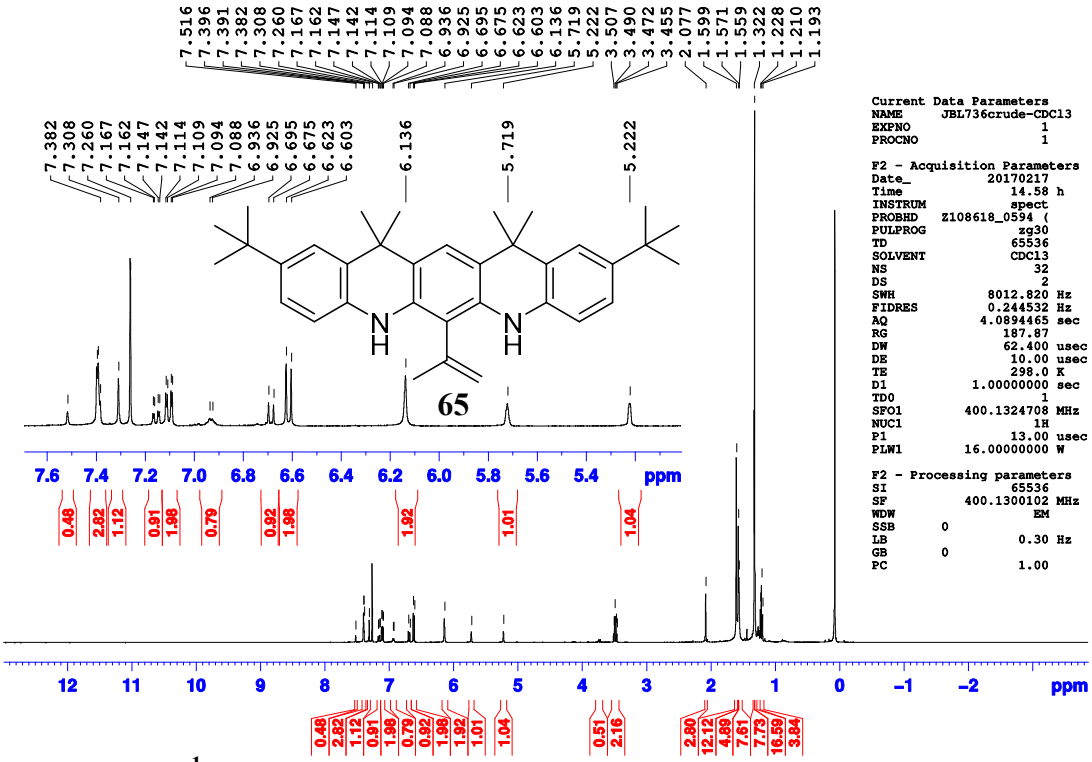

Figure A-28. ^{1}H NMR of (400 MHz, $CDCl_3$) spectrum of 65 (JBL736crude).

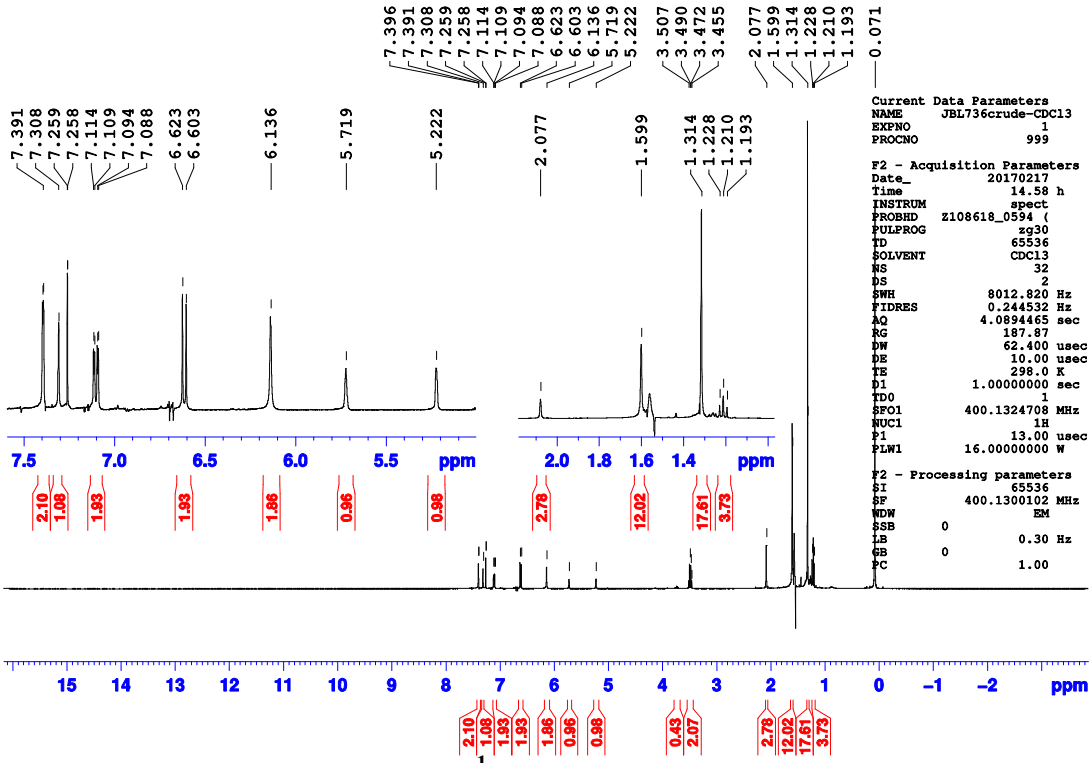

Figure A-29. SM subtracted from ^{1}H NMR of (400 MHz, $CDCl_3$) spectrum of 65 (JBL736crude).

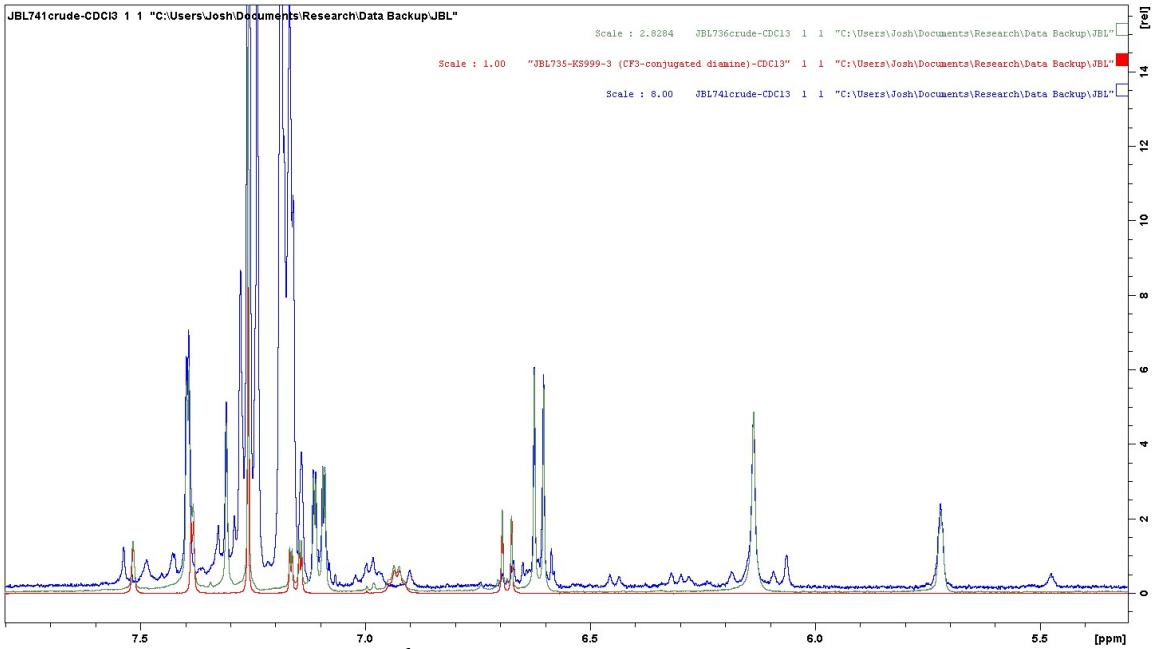

Figure A-30. Comparison of ^{1}H NMR of (400 MHz, $CDCl_3$) spectrum for Grignard vs. $AlMe_3$ Alkylation of 64 (JBL741crude and JBL736crude).

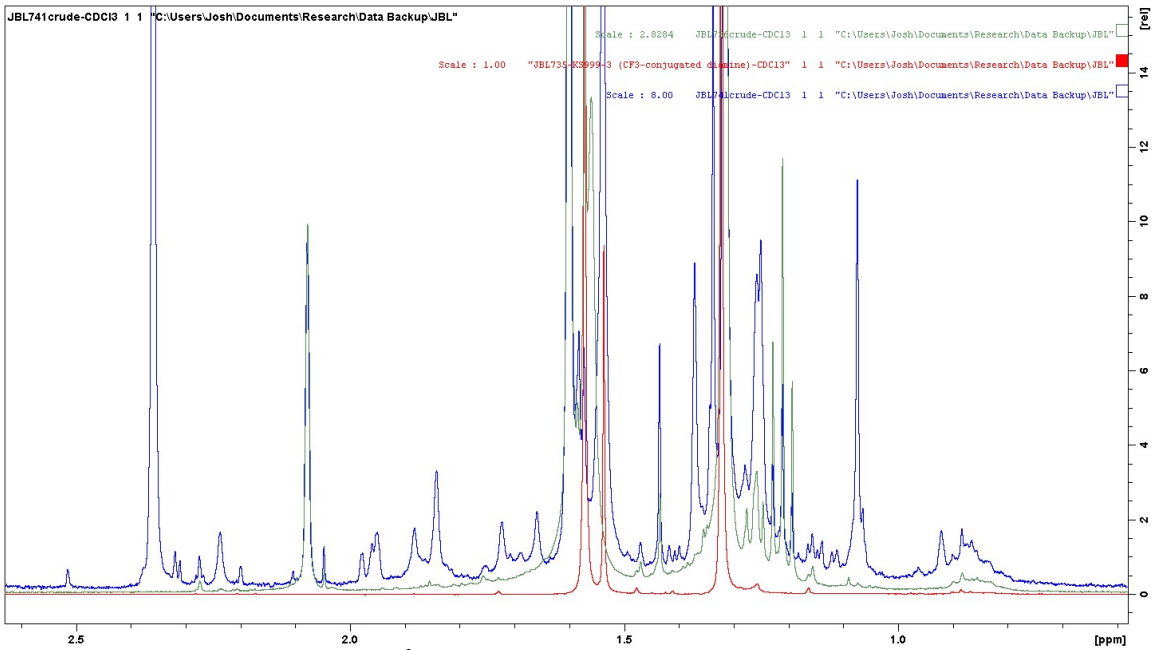

Figure A-31. Comparison of ^{1}H NMR of (400 MHz, $CDCl_3$) spectrum for Grignard vs. $AlMe_3$ Alkylation of 64 (JBL741crude and JBL736crude).

Figure A-32. ESI-MS spectrum of $AlMe_3$ reaction of 64 (JBL741crude).

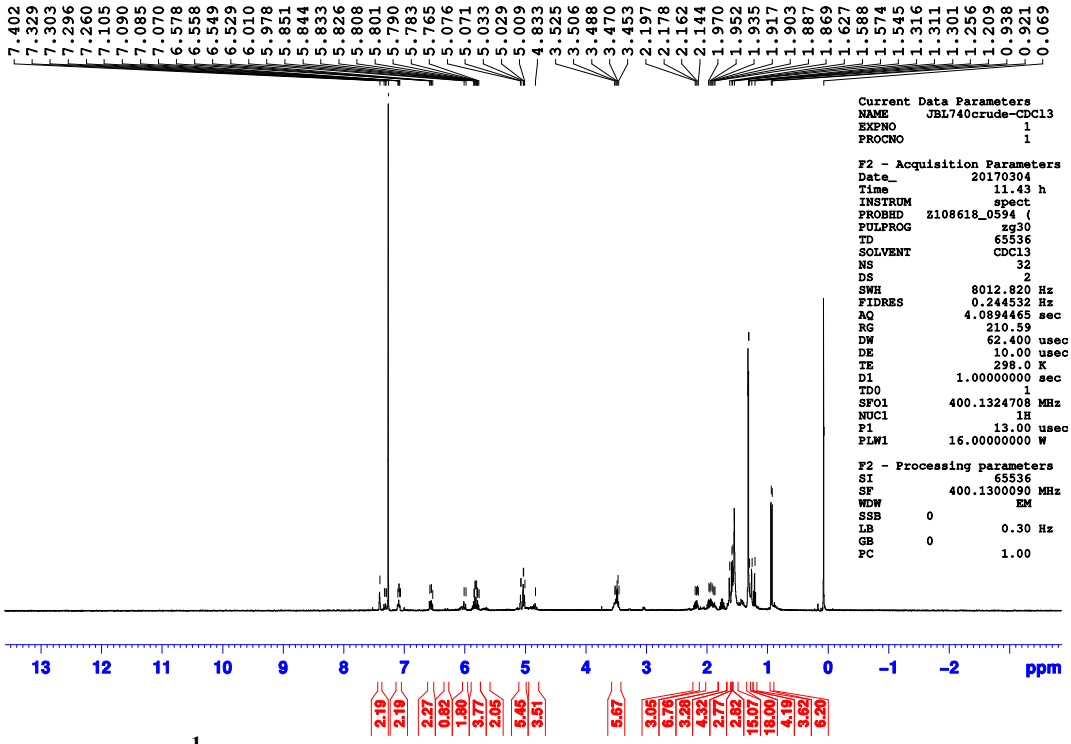

Figure A-33. ^{1}H NMR of (400 MHz, $CDCl_3$) spectrum for reaction of 64 (JBL740cr).

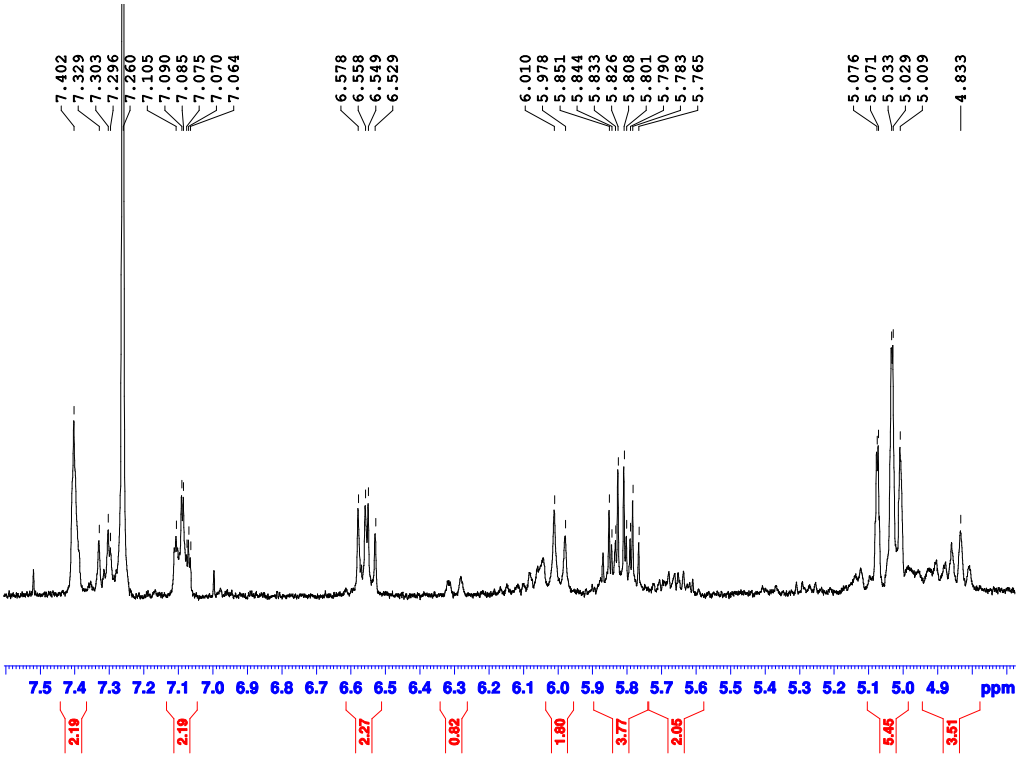

Figure A-34. Zoomed ^{1}H NMR of (400 MHz, $CDCl_3$) spectrum for reaction of 64 (JBL740cr).

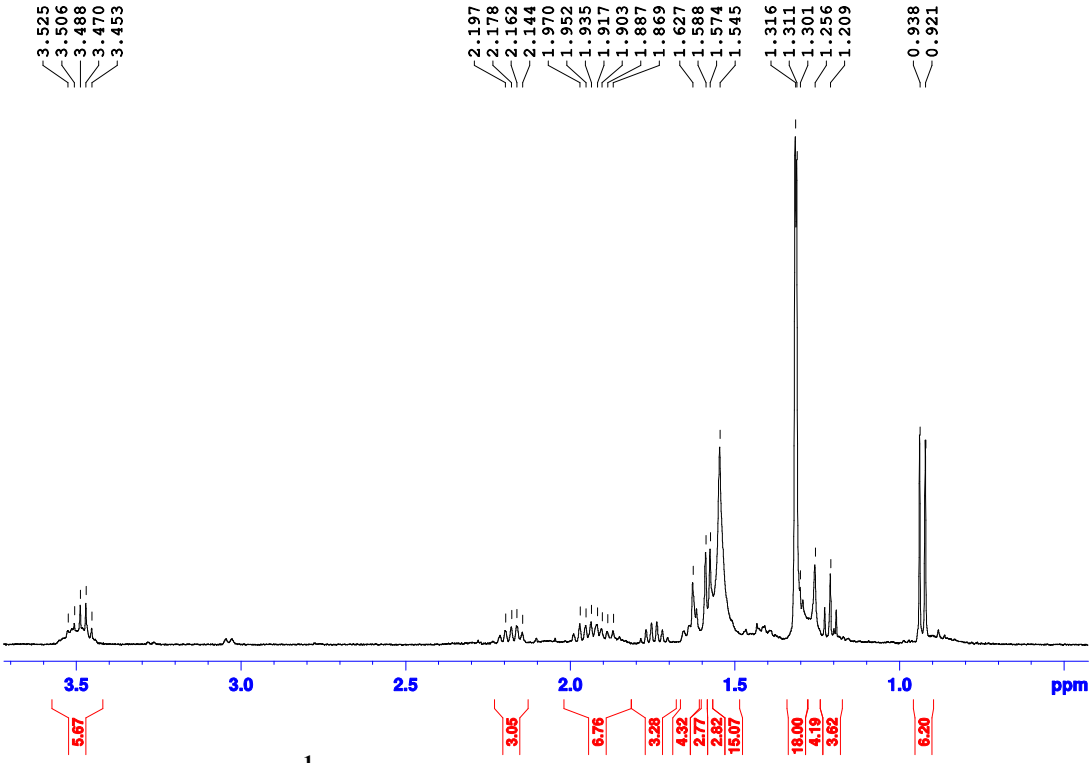

Figure A-35. Zoomed ^{1}H NMR of (400 MHz, $CDCl_3$) spectrum for reaction of 64 (JBL740crude).

Figure A-36. ESI-MS spectrum of Allyl Grignard reaction of 64 (JBL740crude).

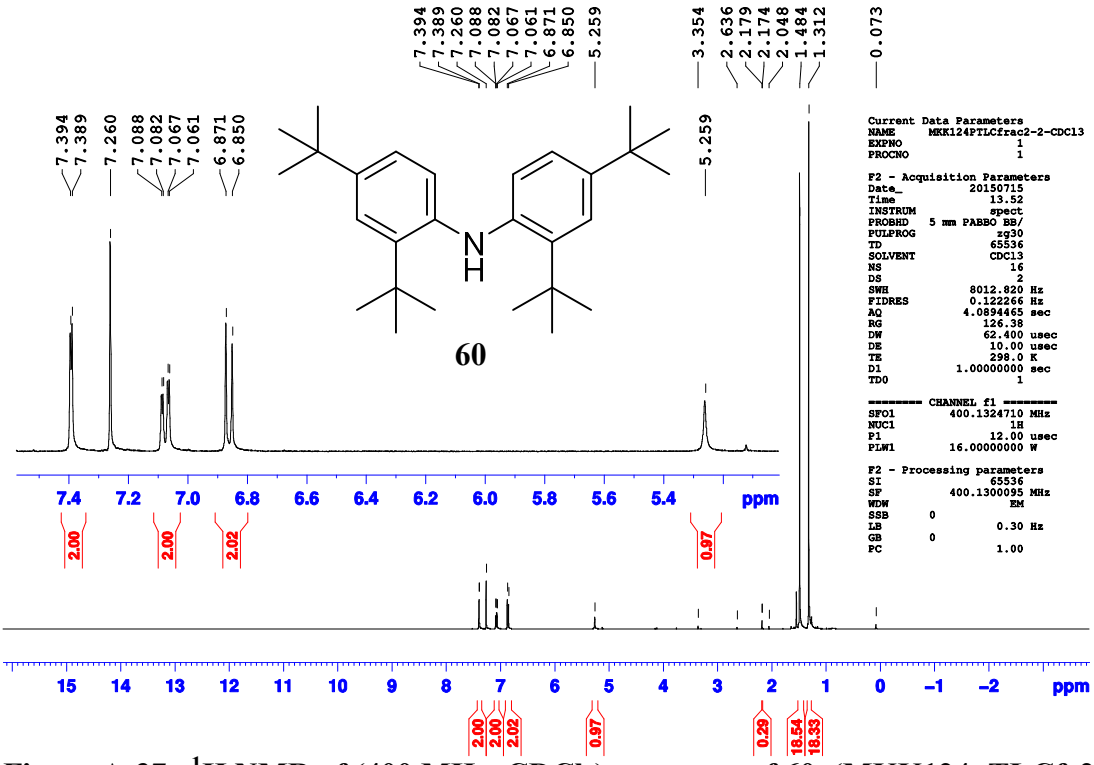

Figure A-37. ^{1}H NMR of (400 MHz, $CDCl_3$) spectrum of 60 (MKK124pTLCfr2).

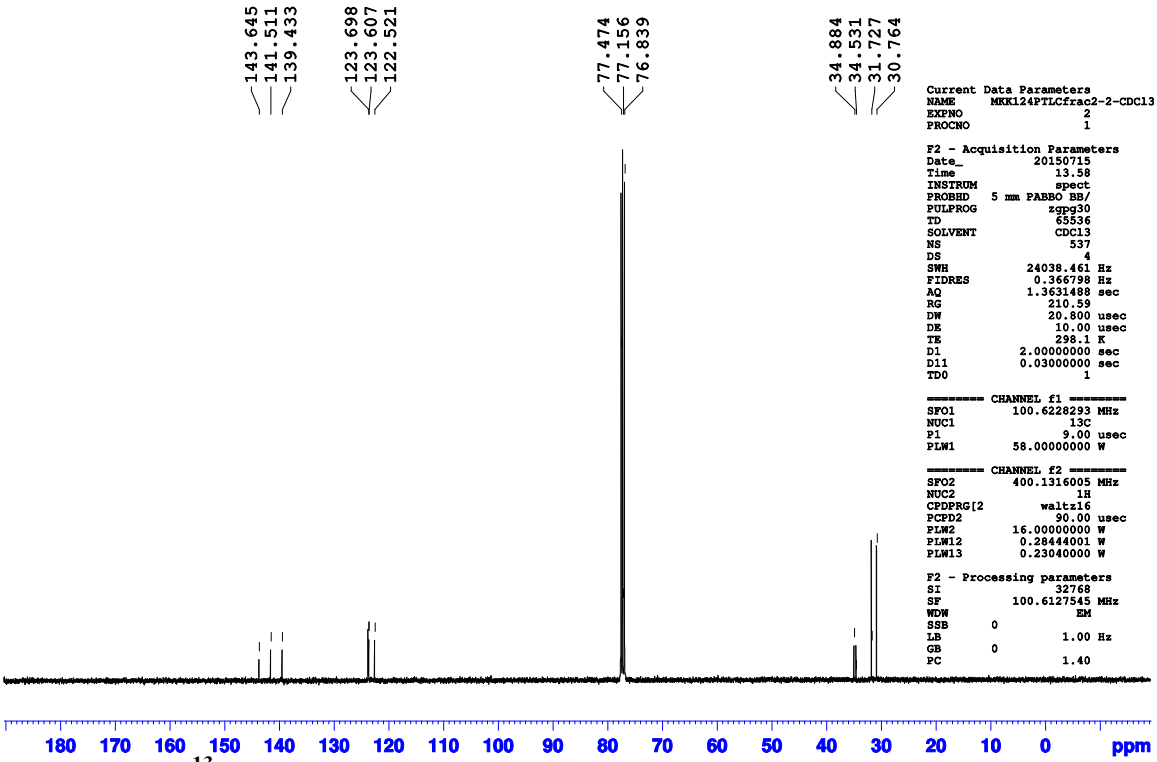

Figure A-38. ^{13}C NMR of (400 MHz, $CDCl_3$) spectrum of 60 (MKK124pTLCfr2).

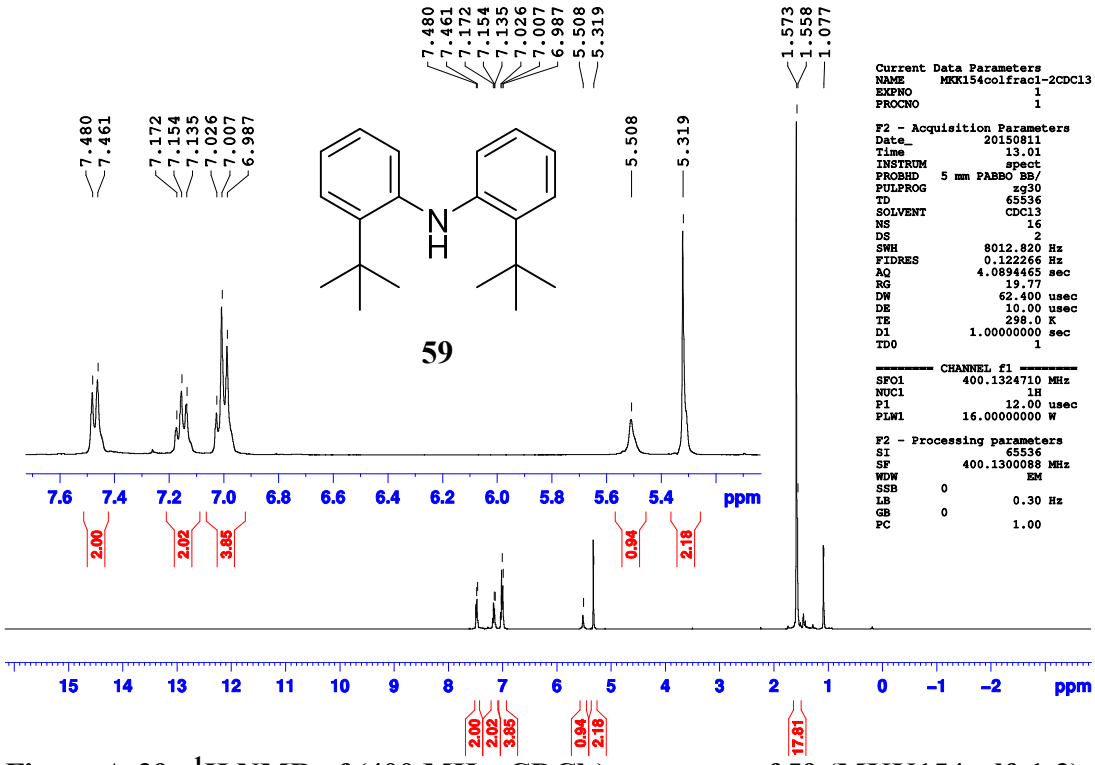

Figure A-39. ^{1}H NMR of (400 MHz, $CDCl_3$) spectrum of 59 (MKK154colfr1-2).

APPENDIX B

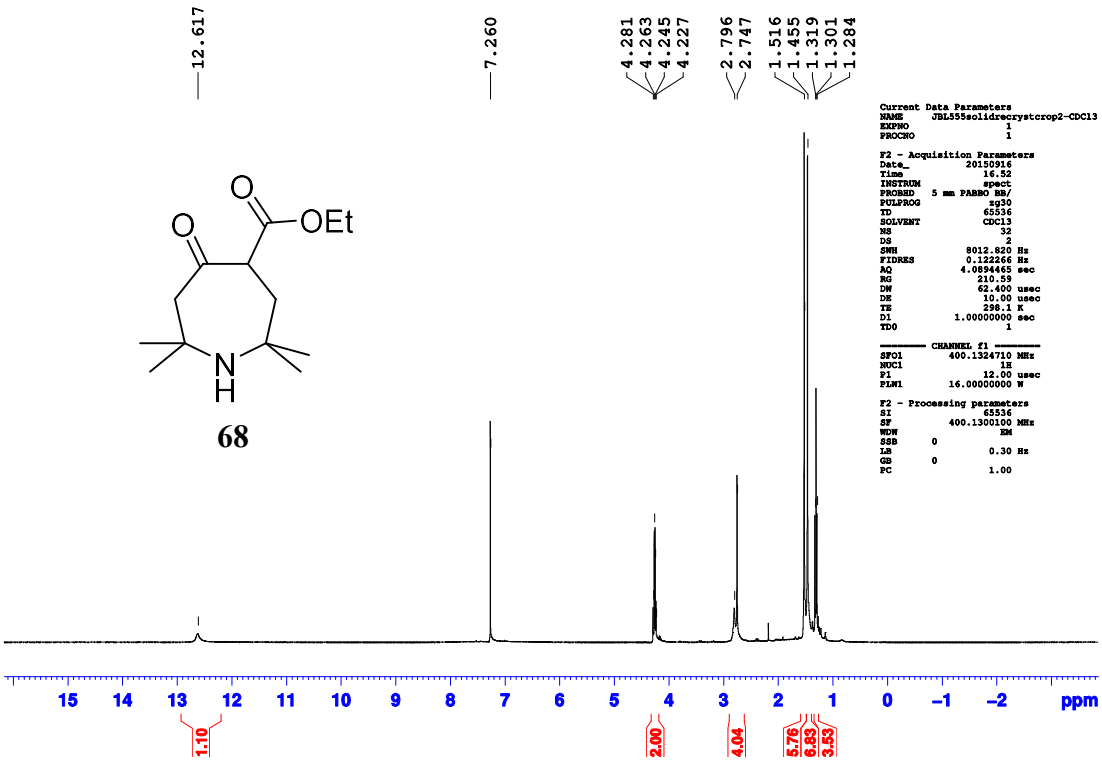

Figure B-1. ^{1}H NMR of (400 MHz, $CDCl_3$) spectrum of 68 (JBL271crude).

Figure B-2. HR ESI-MS (methanol/water) spectrum of 68 (JBL514solid).

Figure B-3. HR ESI-MS (methanol/water+NaAcetate) of 68 (JBL514solid).

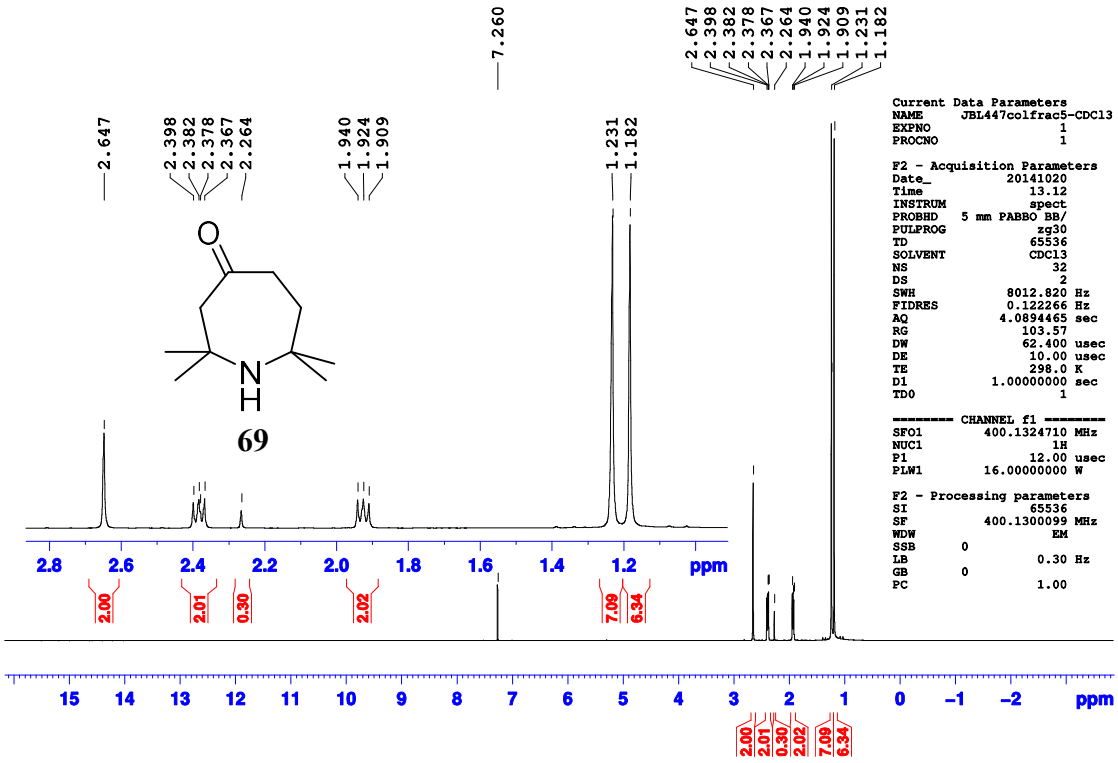

Figure B-4. ^{1}H NMR of (400 MHz, $CDCl_3$) spectrum of 69 (JBL447colfrac5).

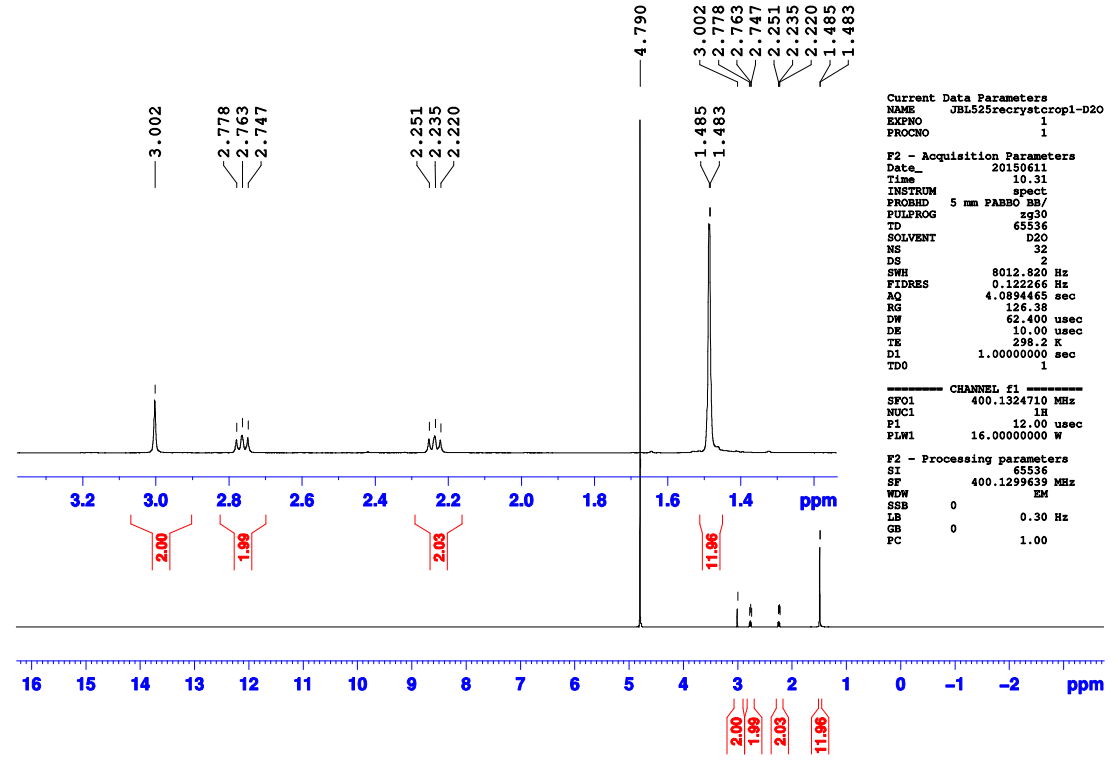

Figure B-5. ^{1}H NMR of (400 MHz, D_2O) spectrum of 69 (JBL525recyrstcr1).

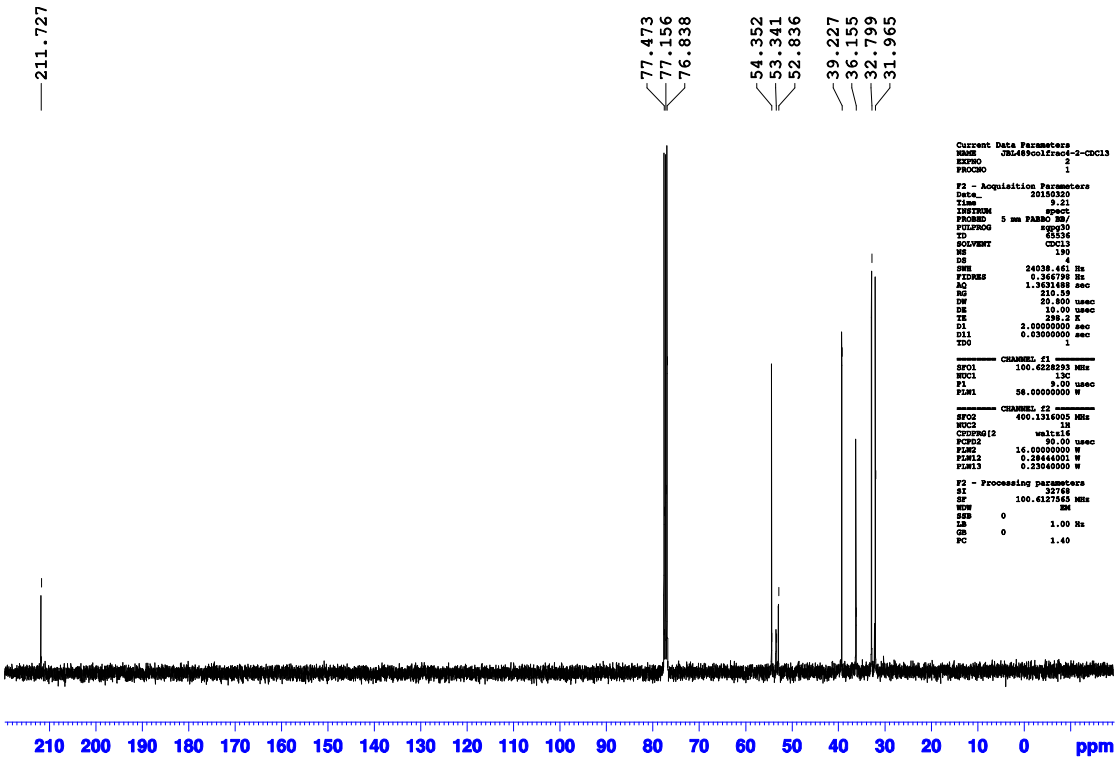

Figure B-6. ^{13}C NMR of (400 MHz, $CDCl_3$) spectrum of 69 (JBL489colfrac4).

Figure B-7. HR-EI mass spectrum of 69 (JBL489colfrac4).

Figure B-8. IR spectrum of 69 (JBL489colfrac4).

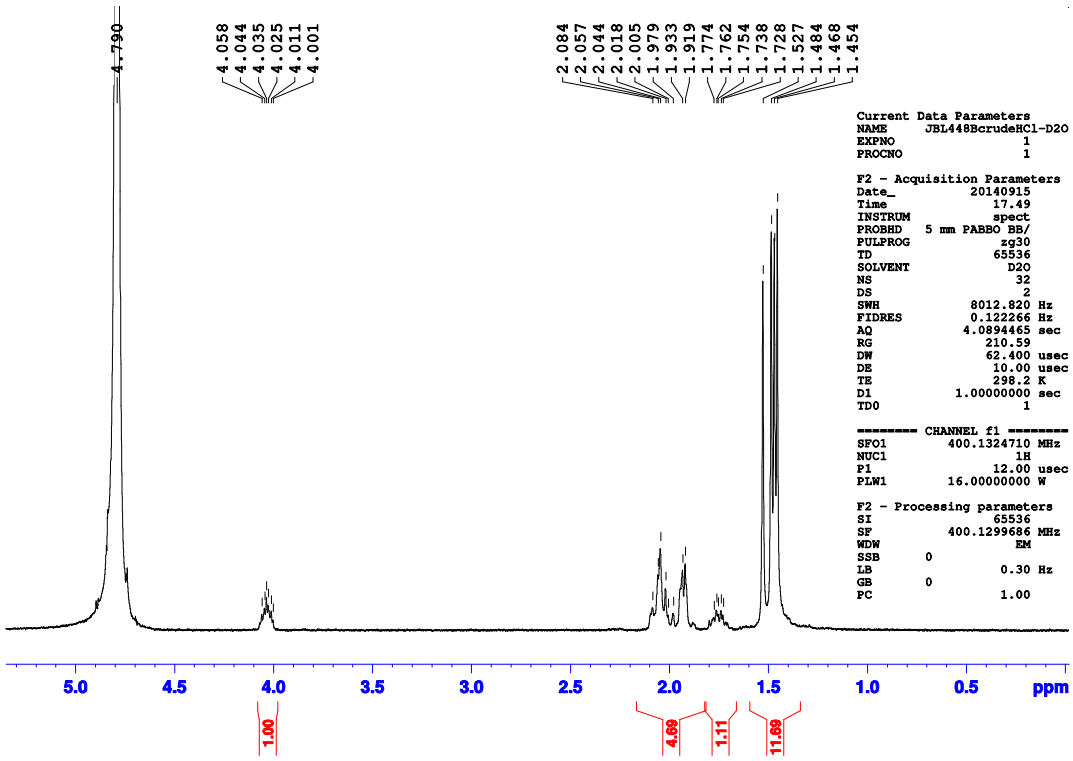

Figure B-9. ^{1}H NMR of (400 MHz, D_2O) spectrum of 72+H (JBL448BcrudeHCl).

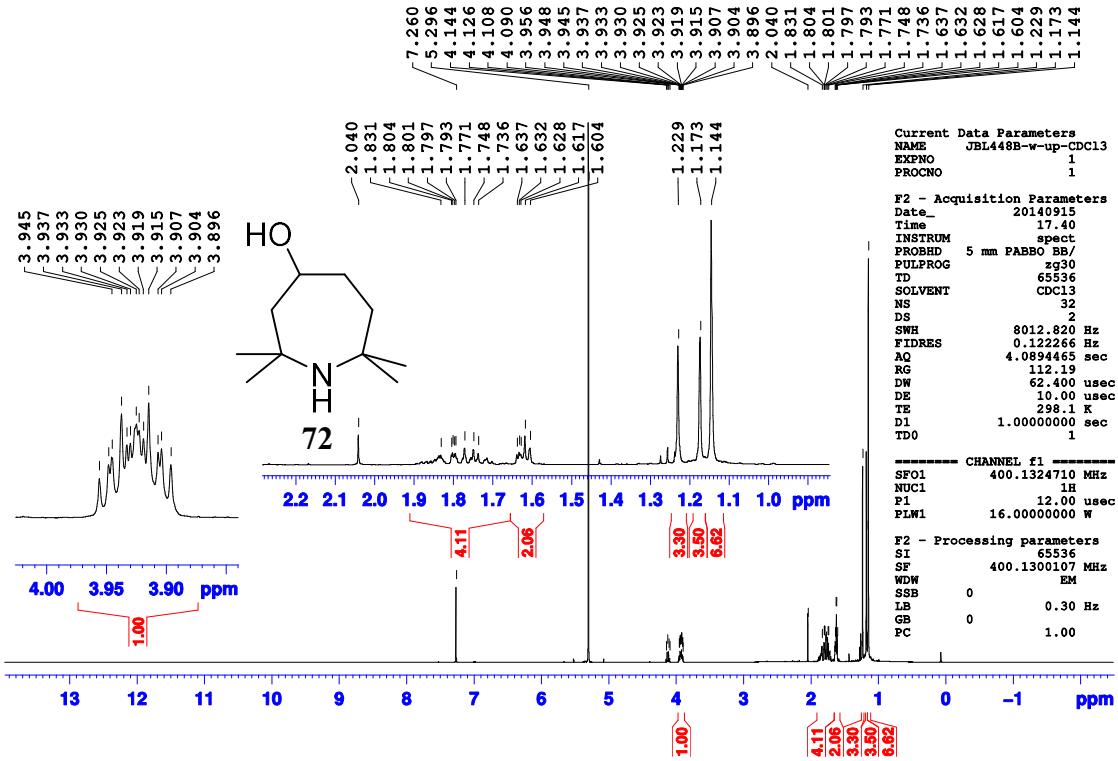

Figure B-10. ^{1}H NMR of (400 MHz, $CDCl_3$) spectrum of 72 (JBL448Bw-up).

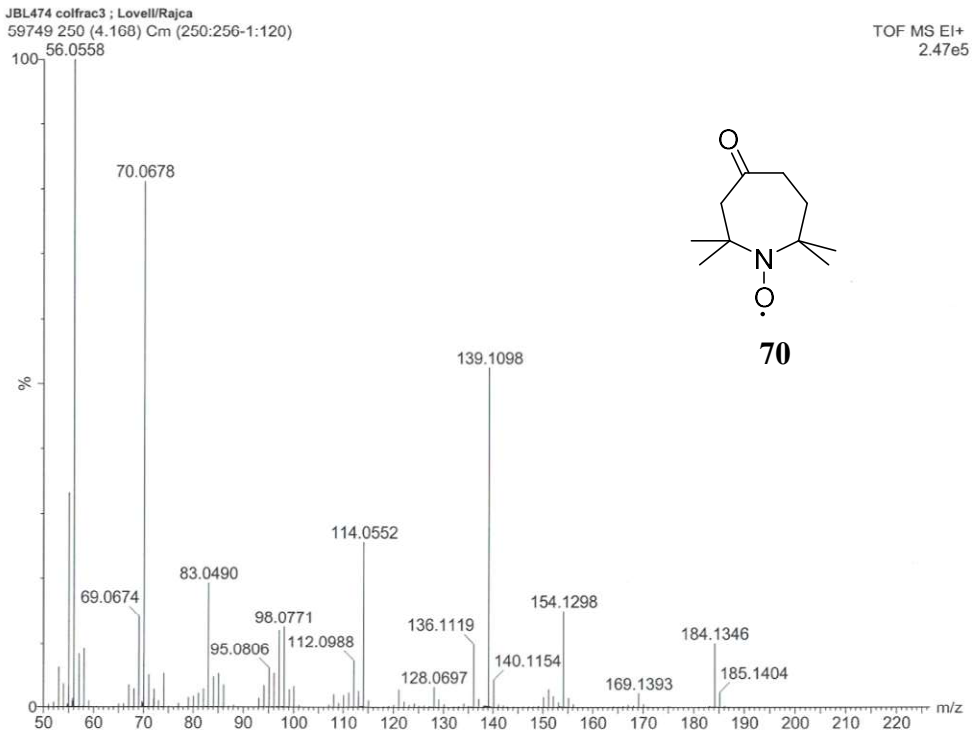

Figure B-11. HR-EI mass spectrum of 70 (JBL474colfrac3).

Figure B-12. IR spectrum of 70 (JBL474colfrac3).

Figure B-13. EPR spectrum of 70 (JBL474colfrac3).

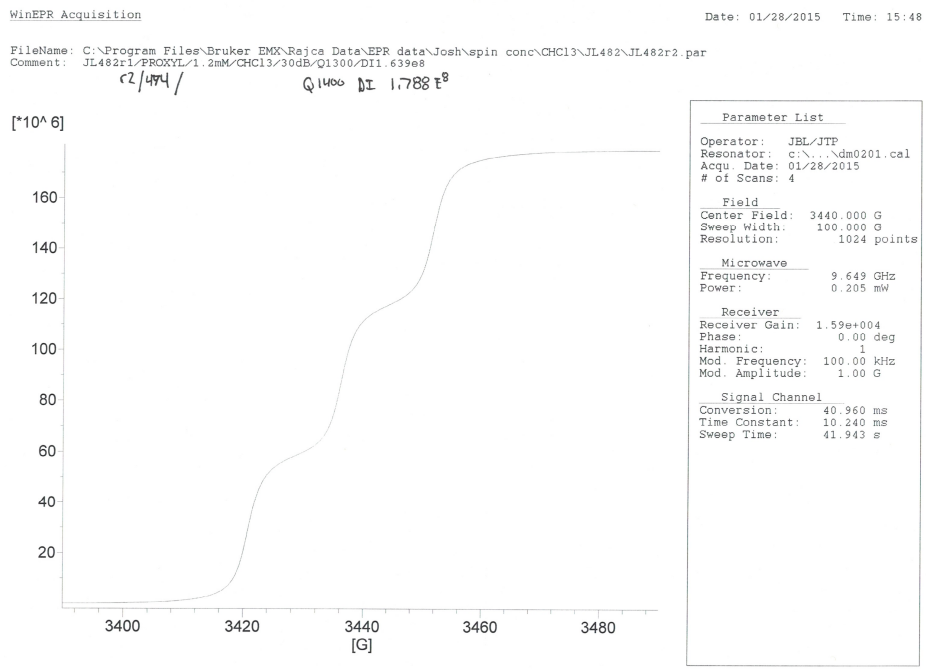

Figure B-14. EPR spectrum of 70 (JBL474colfrac3).

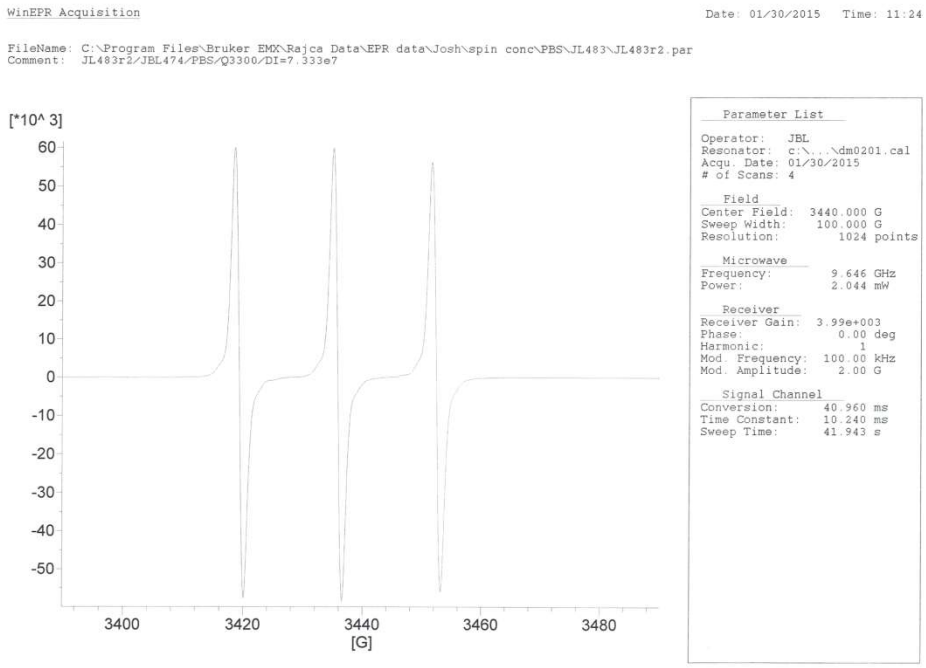

Figure B-15. EPR spectrum of 70 (JBL474colfrac3).

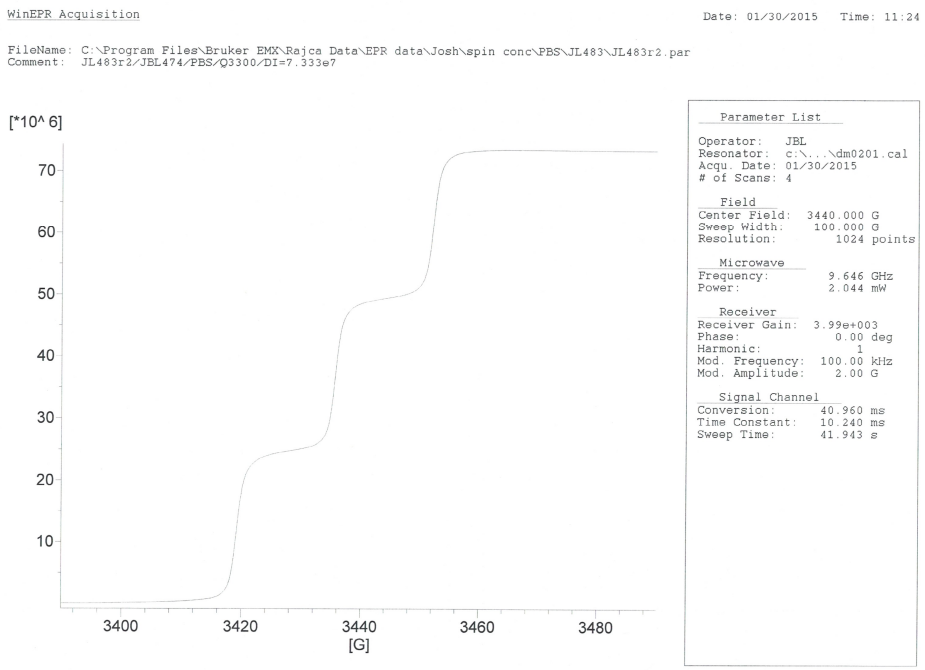

Figure B-16. EPR spectrum of 70 (JBL474colfrac3).

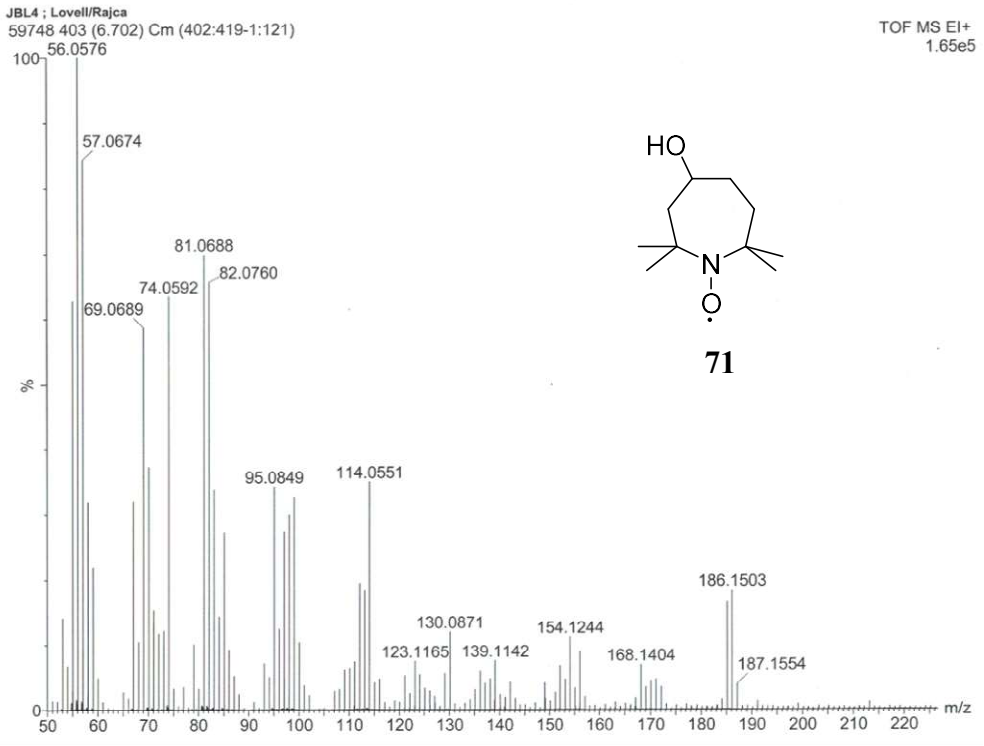

Figure B-17. HR-EI mass spectrum of 71 (JBL479colfrac2).

Figure B-18. IR spectrum of 71 (JBL479colfrac2).

Figure B-19. EPR spectrum of 71 (JBL479colfrac2).

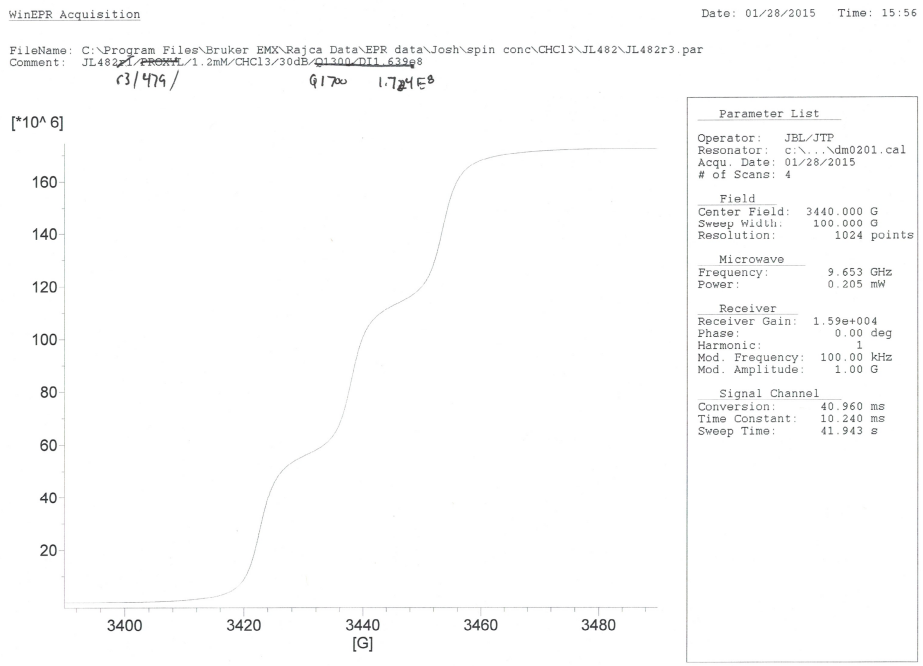

Figure B-20. EPR spectrum of 71 (JBL479colfrac2).

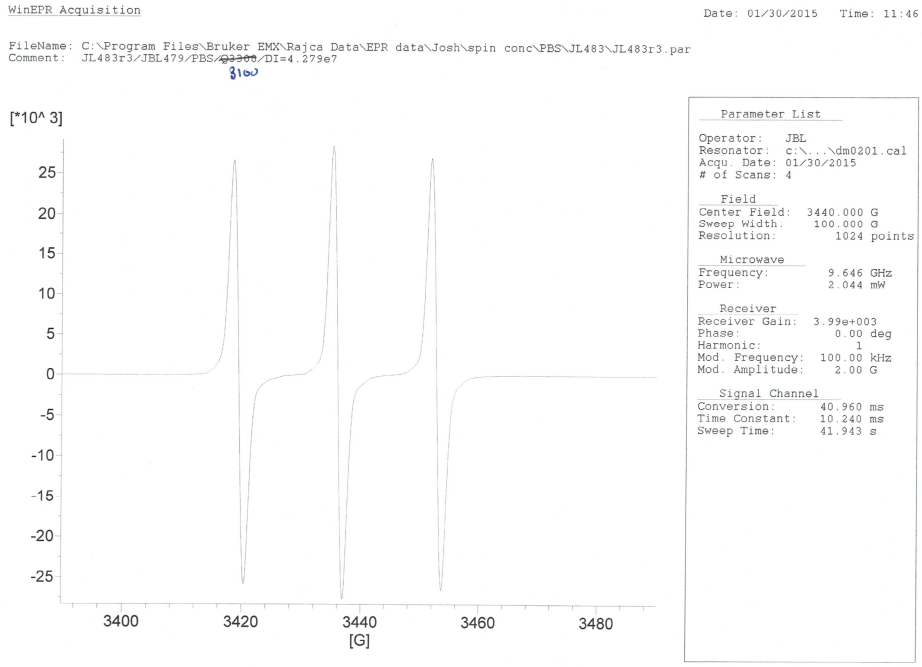

Figure B-21. EPR spectrum of 71 (JBL479colfrac2).

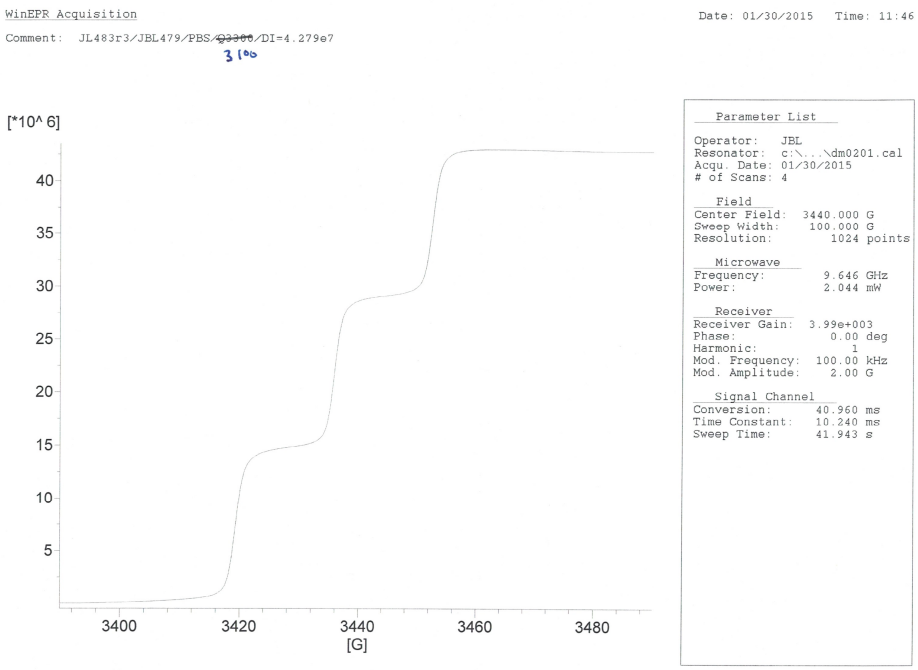

Figure B-22. EPR spectrum of 71 (JBL479colfrac2).

APPENDIX C

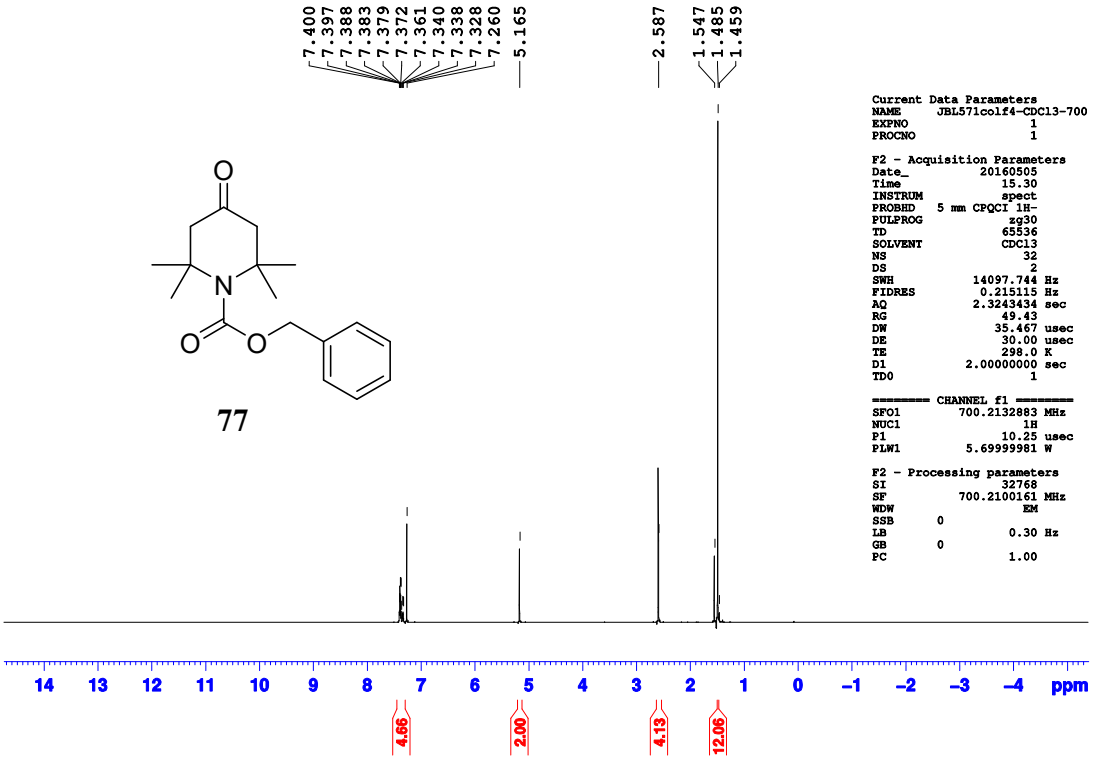

Figure C-1. ^{1}H NMR of (700 MHz, $CDCl_3$) spectrum of 77 (JBL571colf4).

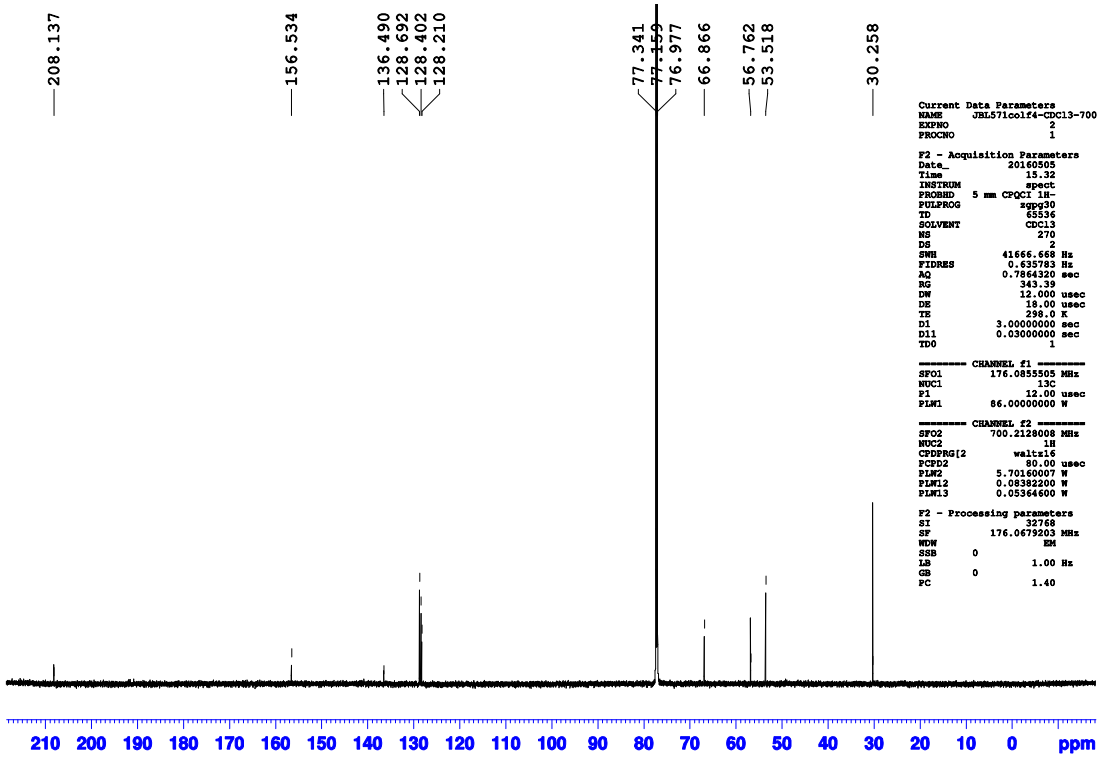

Figure C-2. ^{13}C NMR of (700 MHz, $CDCl_3$) spectrum of 77 (JBL571colf4).

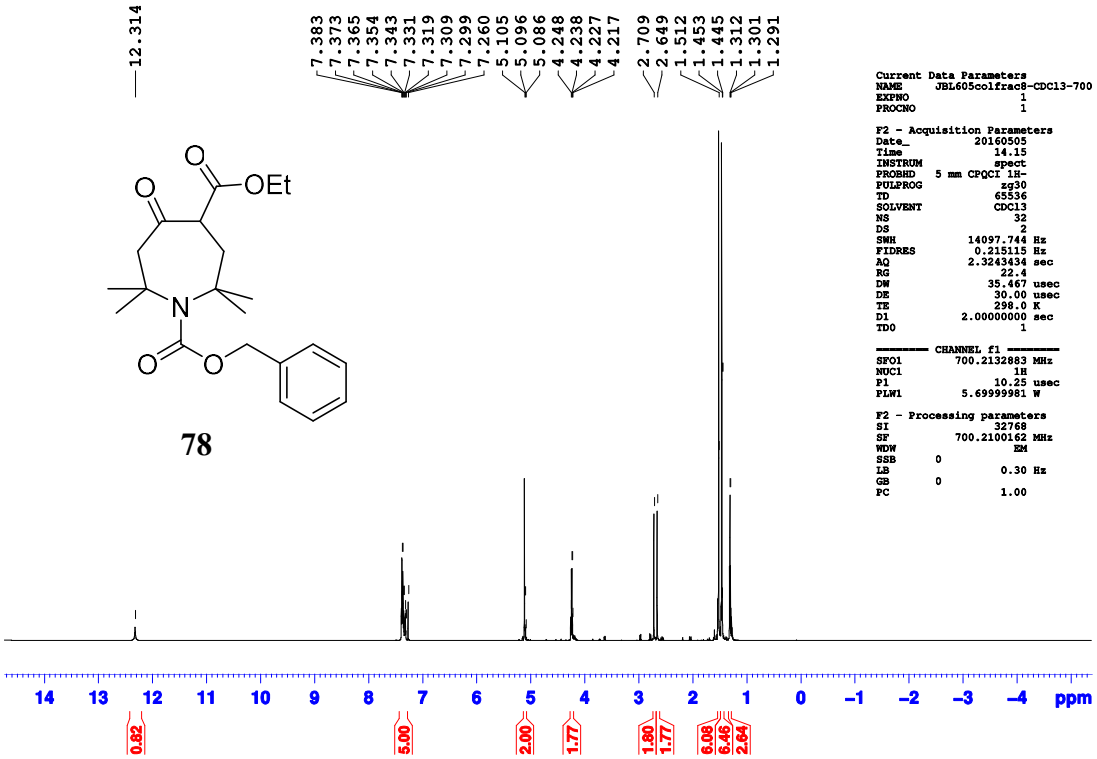

Figure C-3. ^{1}H NMR of (700 MHz, $CDCl_3$) spectrum of 78 (JBL605colf8).

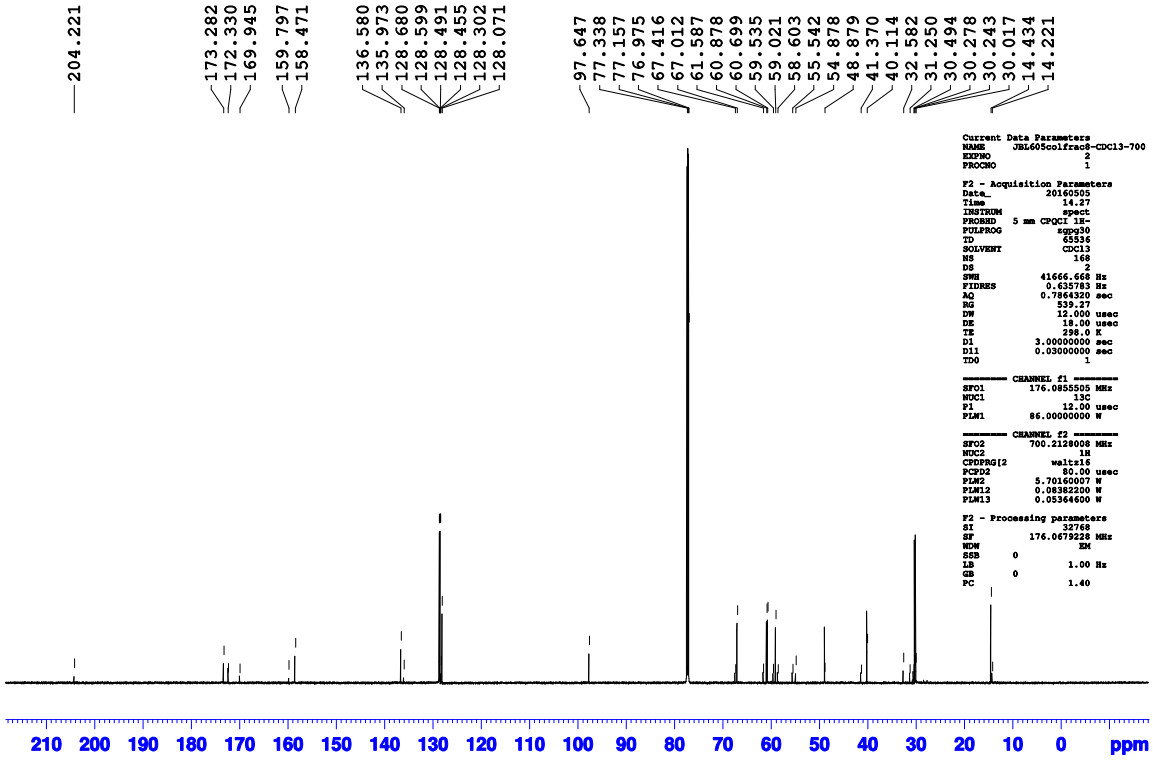

Figure C-4. ^{13}C NMR of (700 MHz, $CDCl_3$) spectrum of 78 (JBL605colf8).

Figure C-5. 2-D ^{1}H—^{13}C HSQC and HMBC NMR of (700 MHz, $CDCl_3$) spectrum of 78 (JBL605colf8).

Figure C-6. 2-D ^{1}H—^{13}C HSQC and HMBC NMR of (700 MHz, $CDCl_3$) spectrum of 78 (JBL605colf8).

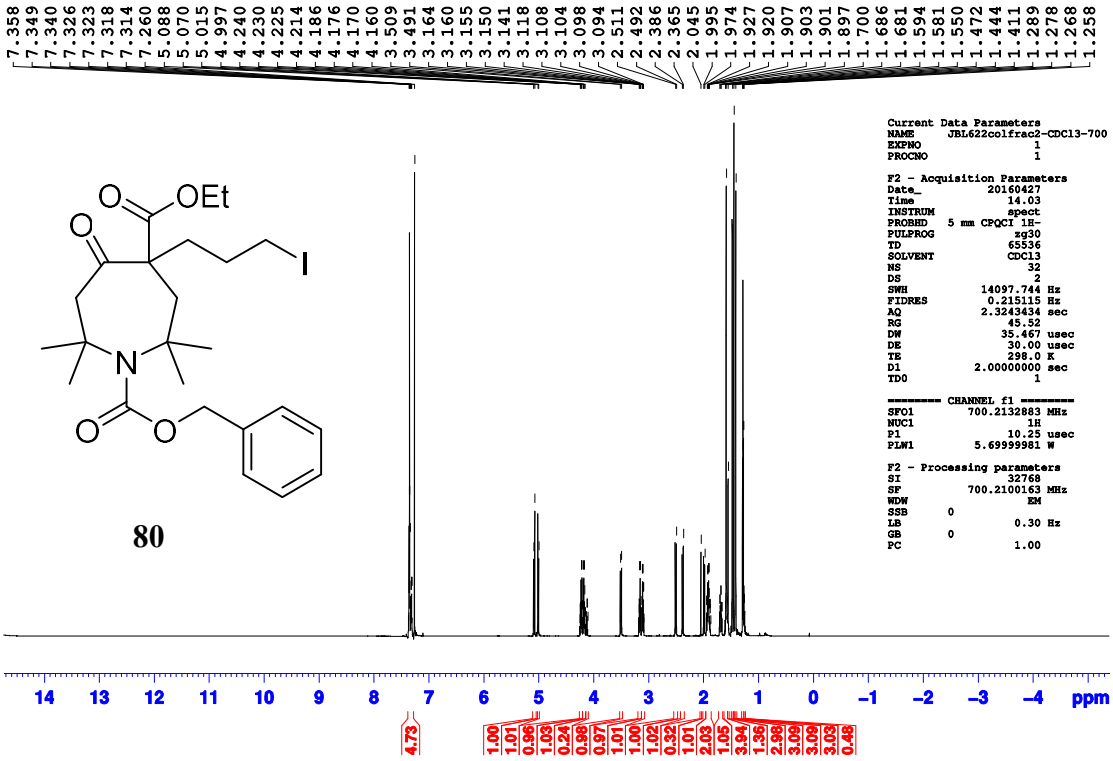

Figure C-7. ^{1}H NMR of (700 MHz, $CDCl_3$) spectrum of 80 (JBL622colf2).

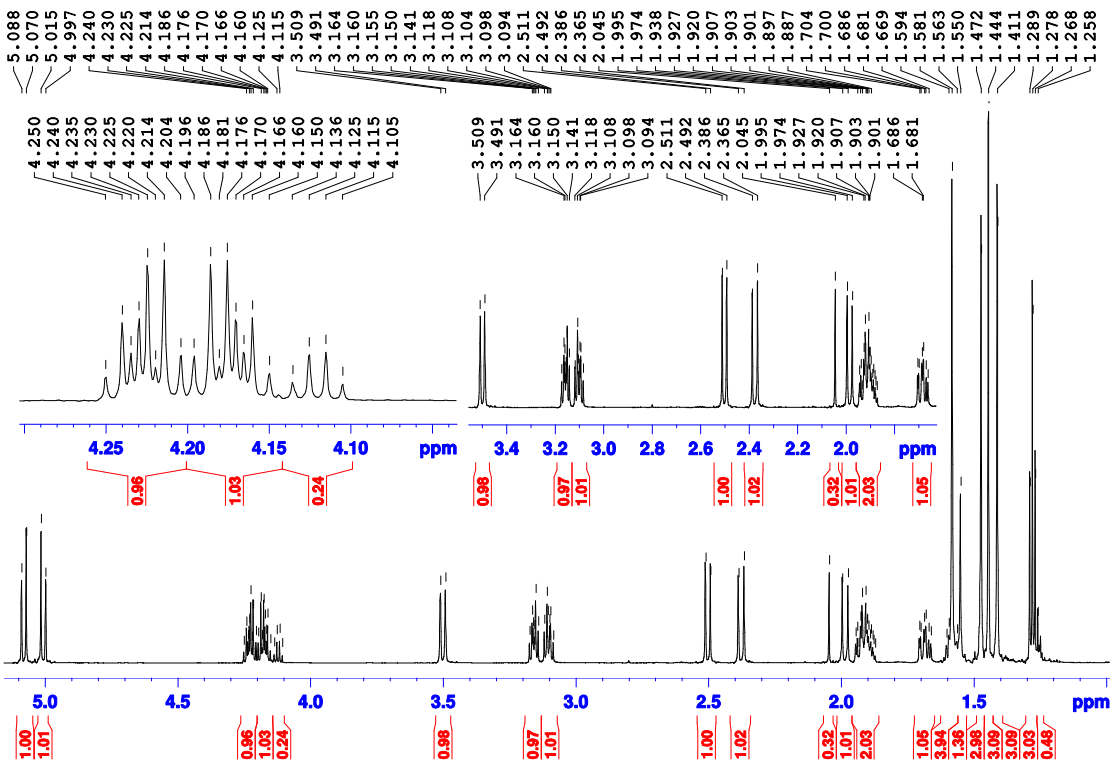

Figure C-8. ^{1}H NMR of (700 MHz, $CDCl_3$) spectrum of 80 (JBL622colf2).

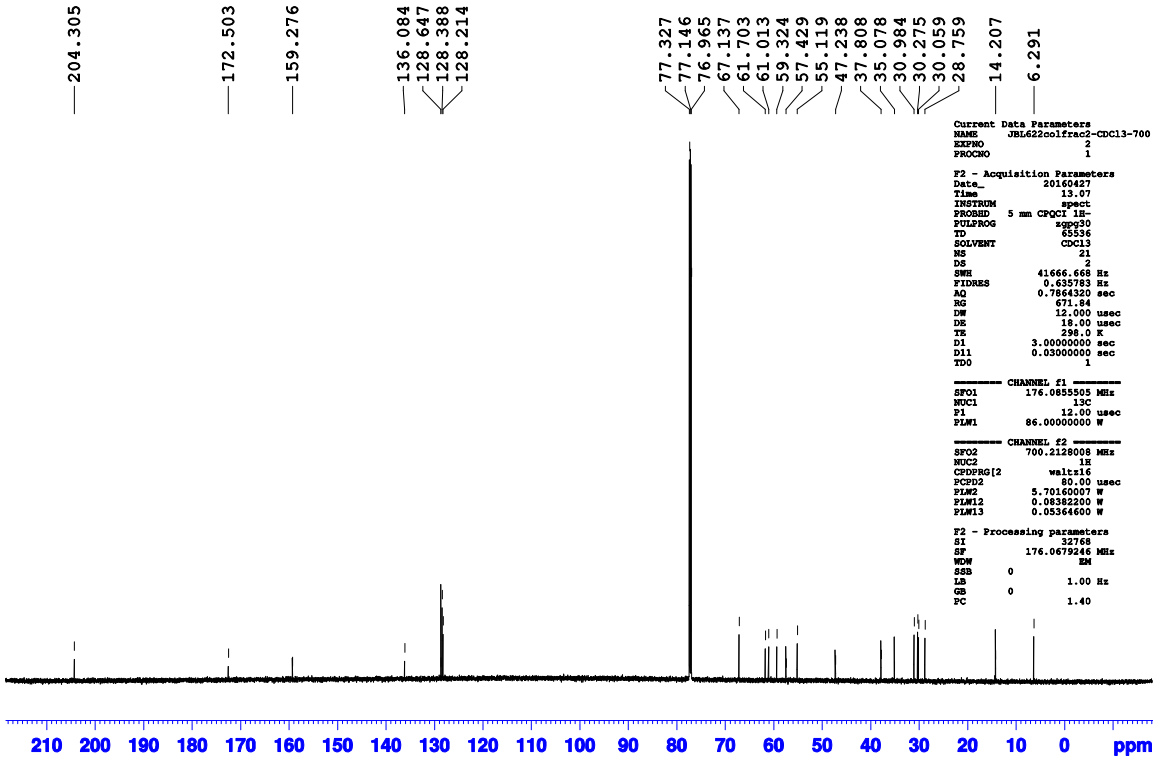

Figure C-9. ^{13}C NMR of (700 MHz, $CDCl_3$) spectrum of 80 (JBL622colf2).

Figure C-10. 2-D ^{1}H—^{1}H COSY NMR of (700 MHz, $CDCl_3$) spectrum of 80 (JBL622colf2).

Figure C-11. 2-D ^{1}H—^{13}C HSQC and HMBC NMR of (700 MHz, $CDCl_3$) spectrum of 80 (JBL622colf2).

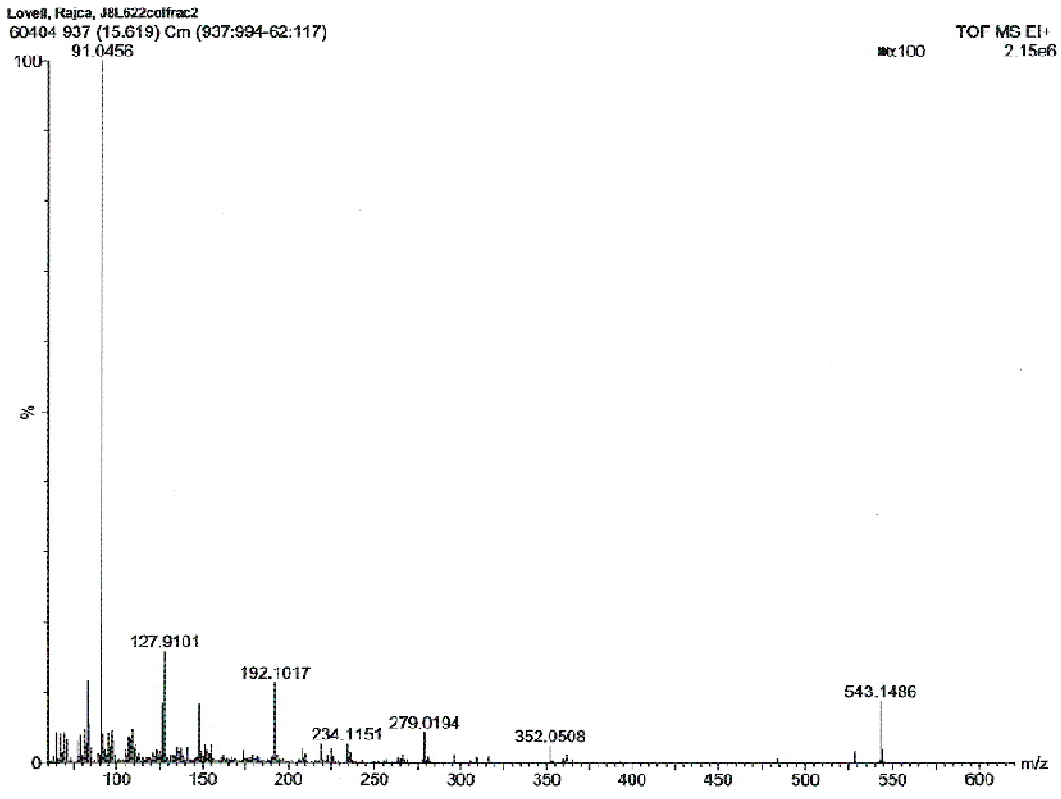

Figure C-12. HR-EI mass spectrum of 80 (JBL622colf2).

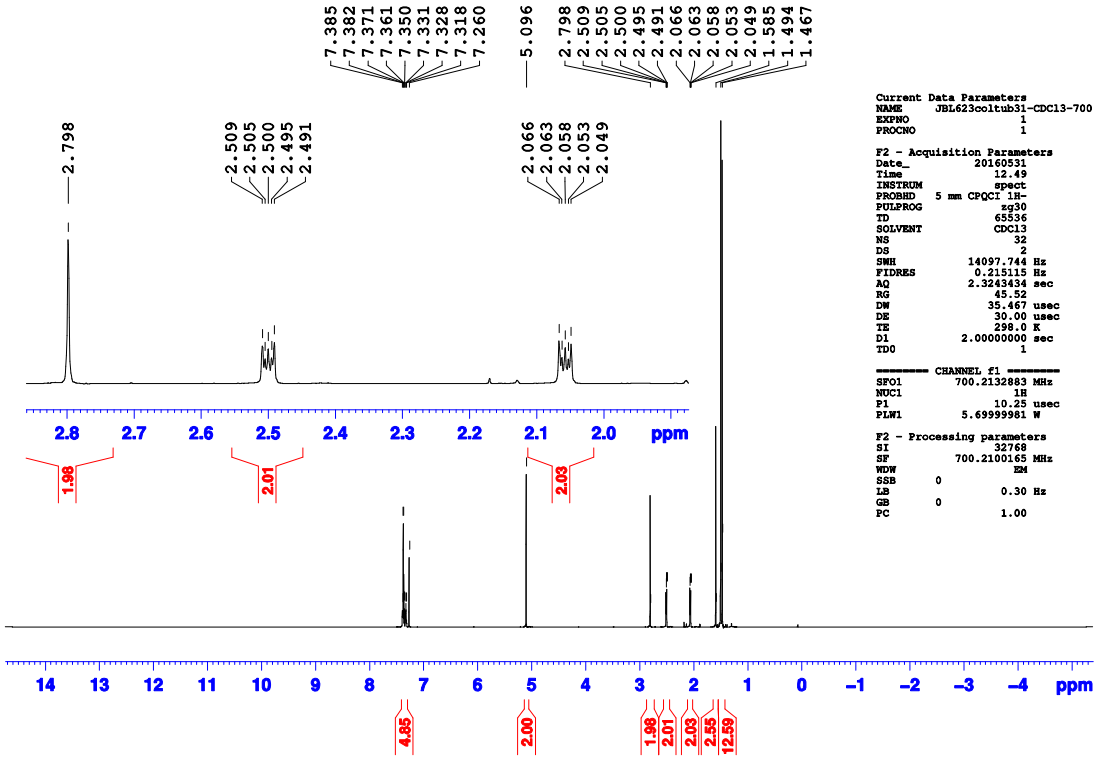

Figure C-13. ^{1}H NMR of (700 MHz, $CDCl_3$) spectrum of 86 (JBL623coltube31).

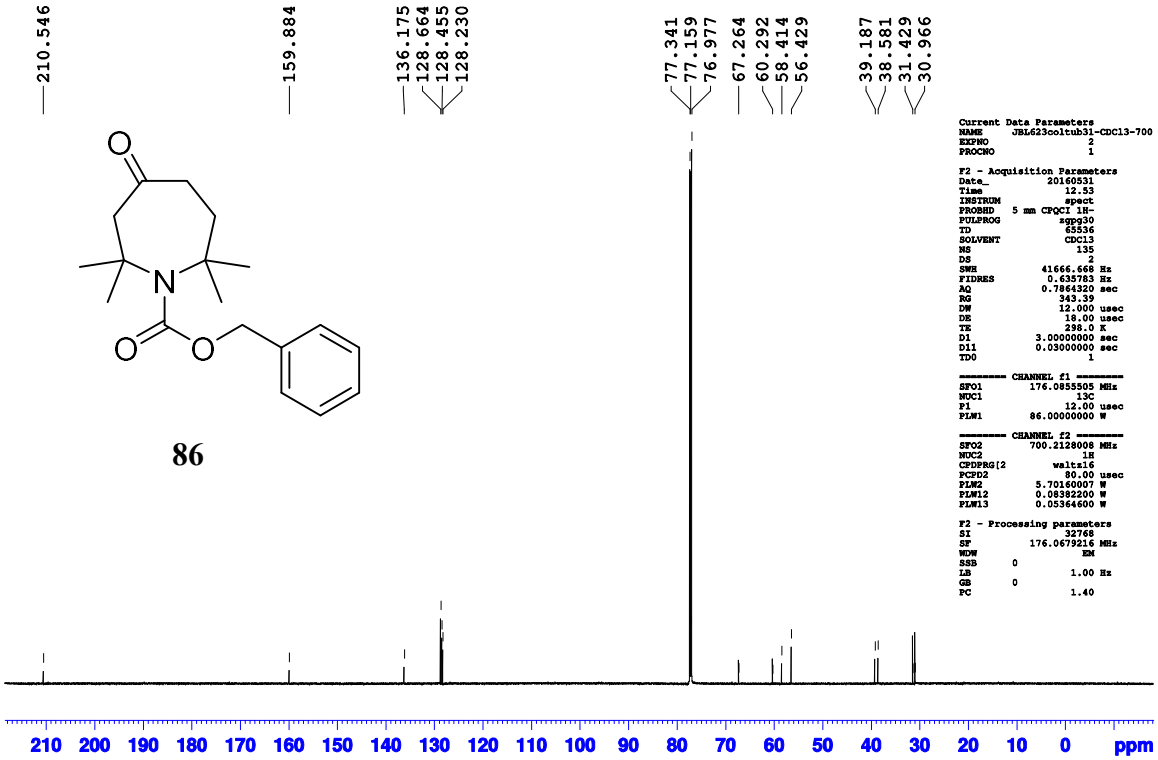

Figure C-14. ^{13}C NMR of (700 MHz, $CDCl_3$) spectrum of 86 (JBL623coltube31).

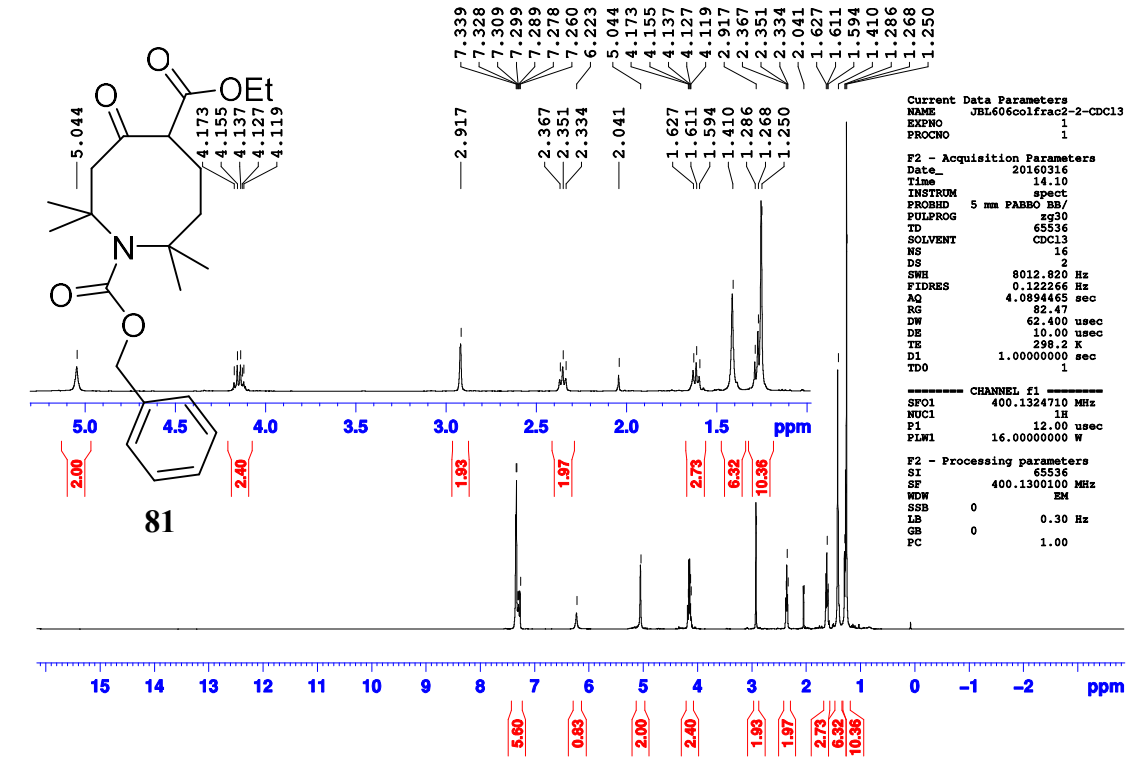

Figure C-15. ^{1}H NMR of (700 MHz, $CDCl_3$) spectrum of 81 (JBL606colfrac2).

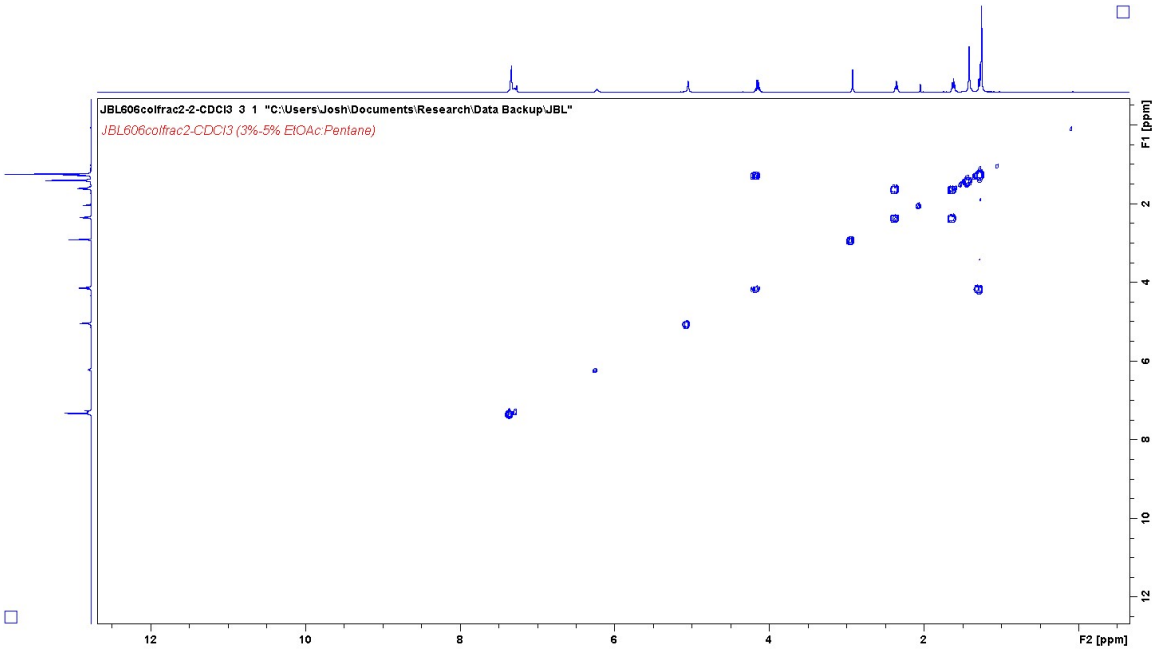

Figure C-16. 2-D ^{1}H—^{1}H COSY NMR of (700 MHz, $CDCl_3$) spectrum of 81 (JBL606colfrac2).

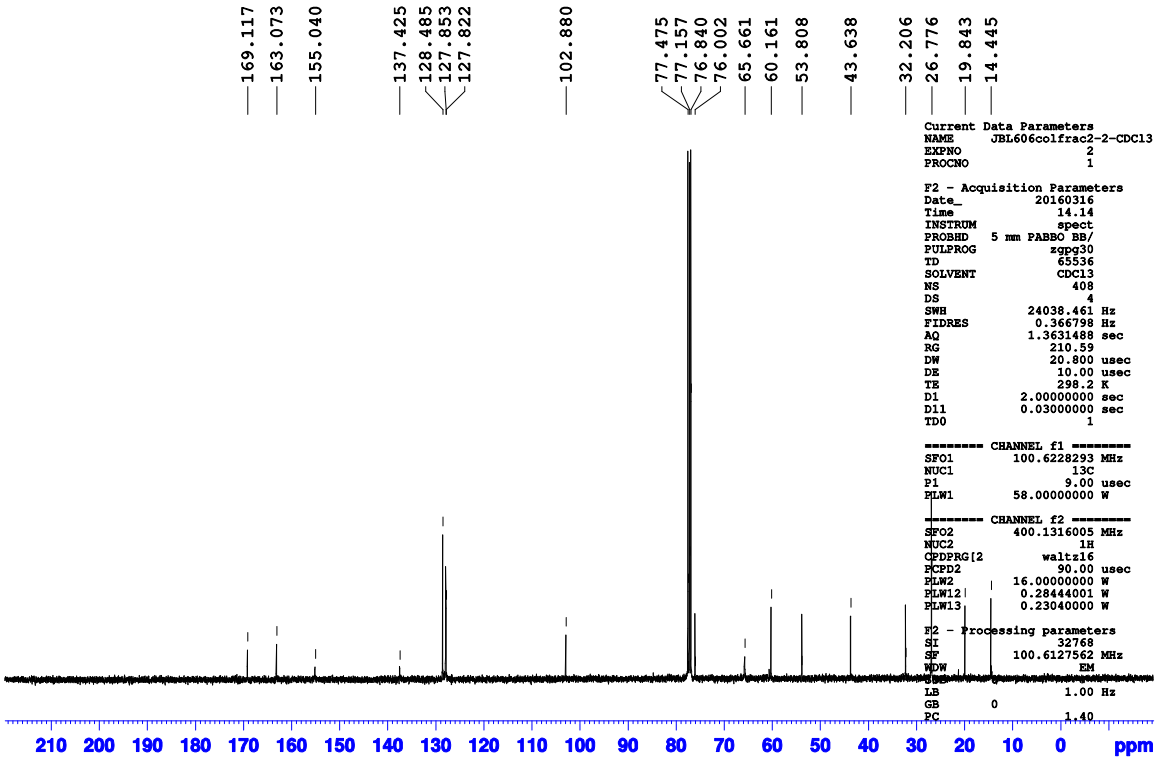

Figure C-17. ^{13}C NMR of (700 MHz, $CDCl_3$) spectrum of 81 (JBL606colfrac2).

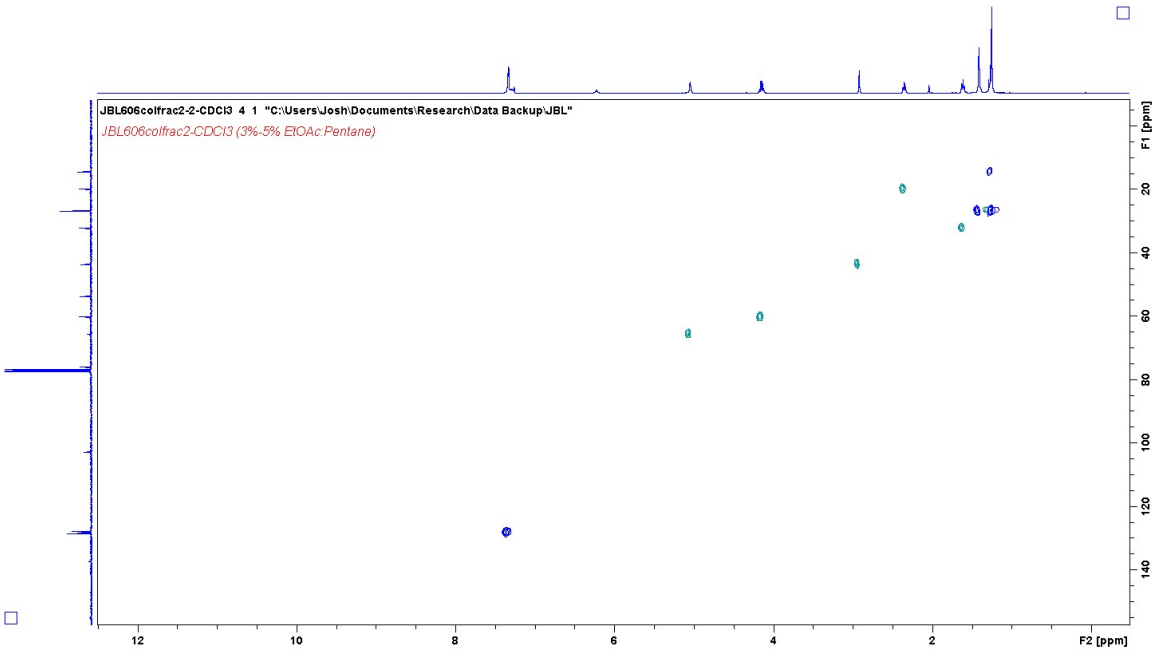

Figure C-18. 2-D ^{1}H—^{13}C HSQC NMR of (700 MHz, $CDCl_3$) spectrum of 81 (JBL606colfrac2).

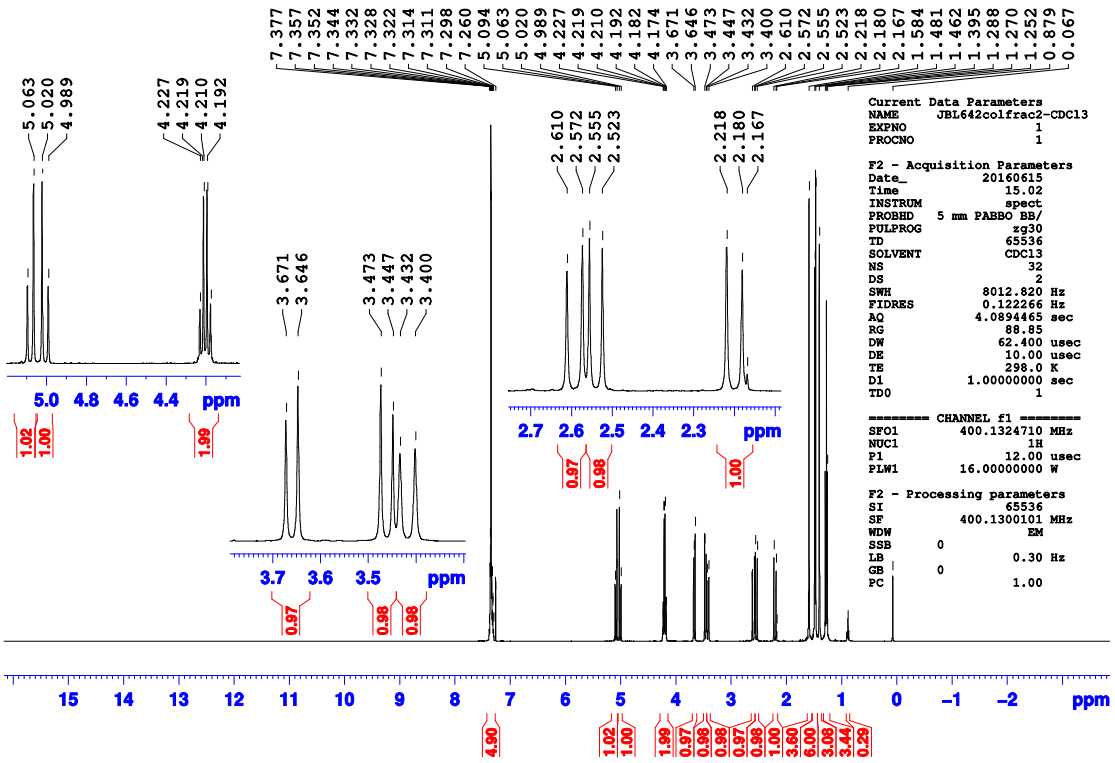

Figure C-19. ^{1}H NMR of (700 MHz, $CDCl_3$) spectrum of 79 (JBL642colfrac2).

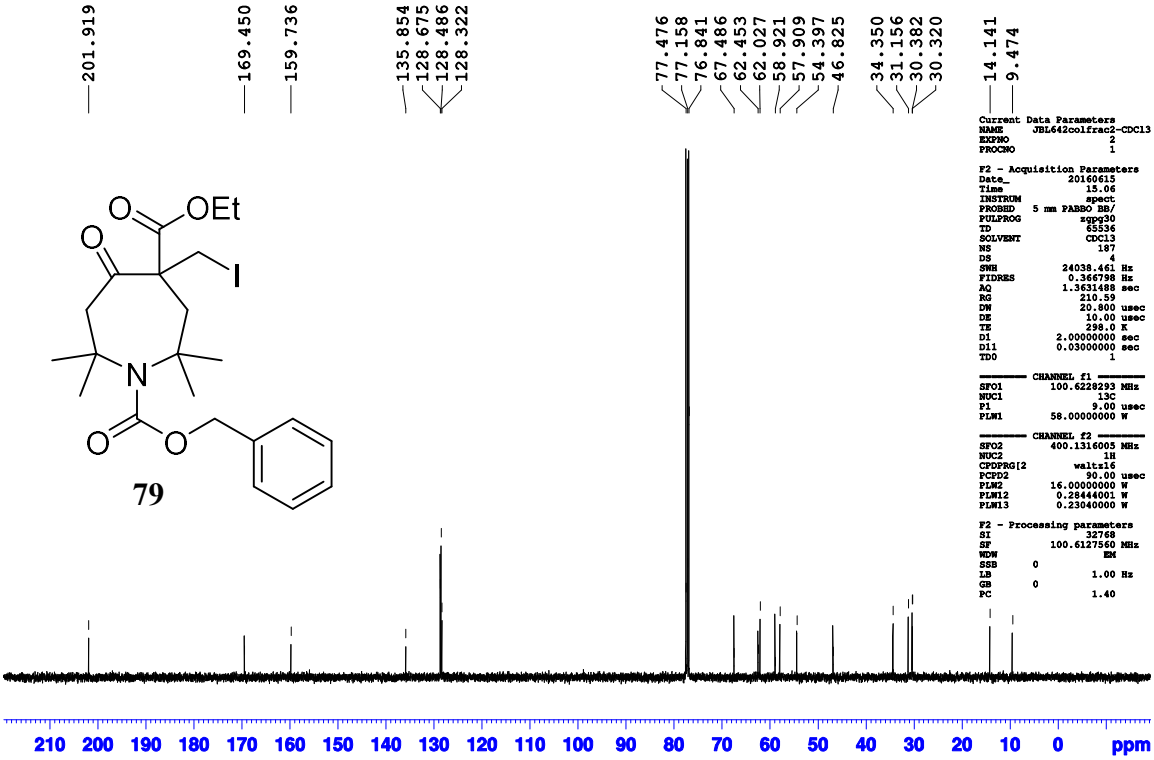

Figure C-20. ^{13}C NMR of (700 MHz, $CDCl_3$) spectrum of 79 (JBL642colfrac2).

Figure C-21. 2-D $^{1}H—^{1}H$ COSY NMR of (700 MHz, $CDCl_3$) spectrum of 79 (JBL642colfrac2).

Figure C-22. 2-D $^{1}H—^{13}C$ HSQC NMR of (700 MHz, $CDCl_3$) spectrum of 79 (JBL642colfrac2).

Figure C-23. 2-D ^{1}H—^{13}C HSQC NMR of (700 MHz, $CDCl_3$) spectrum of 79 (JBL642colfrac2).

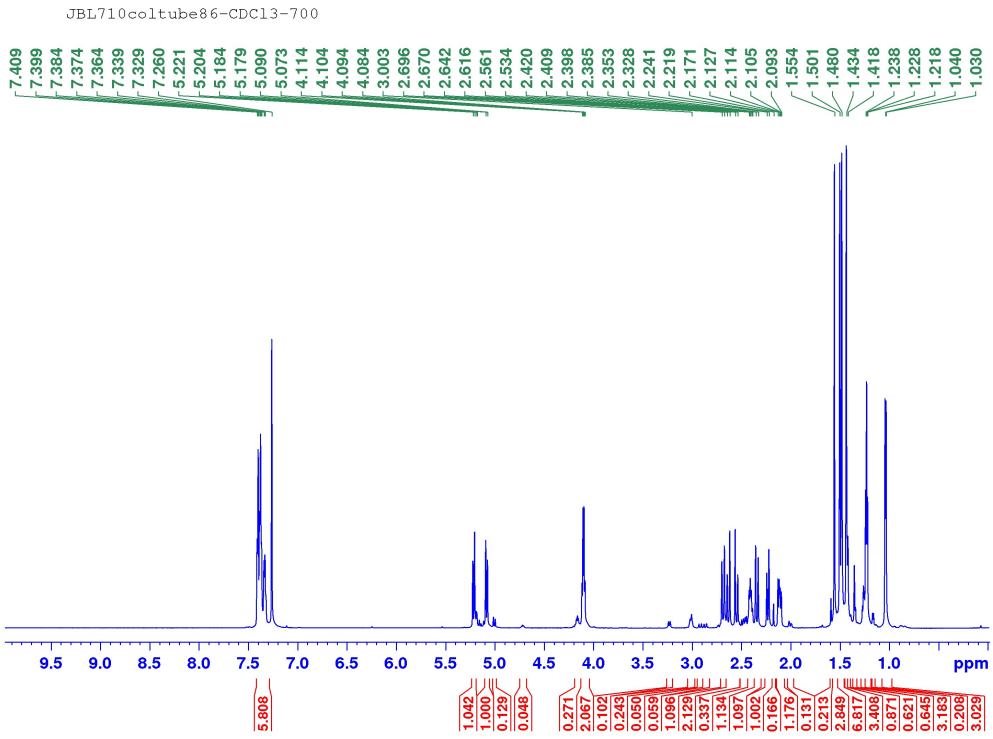

Figure C-24. ^{1}H NMR of (700 MHz, $CDCl_3$) spectrum of 82 (JBL710coltub86).

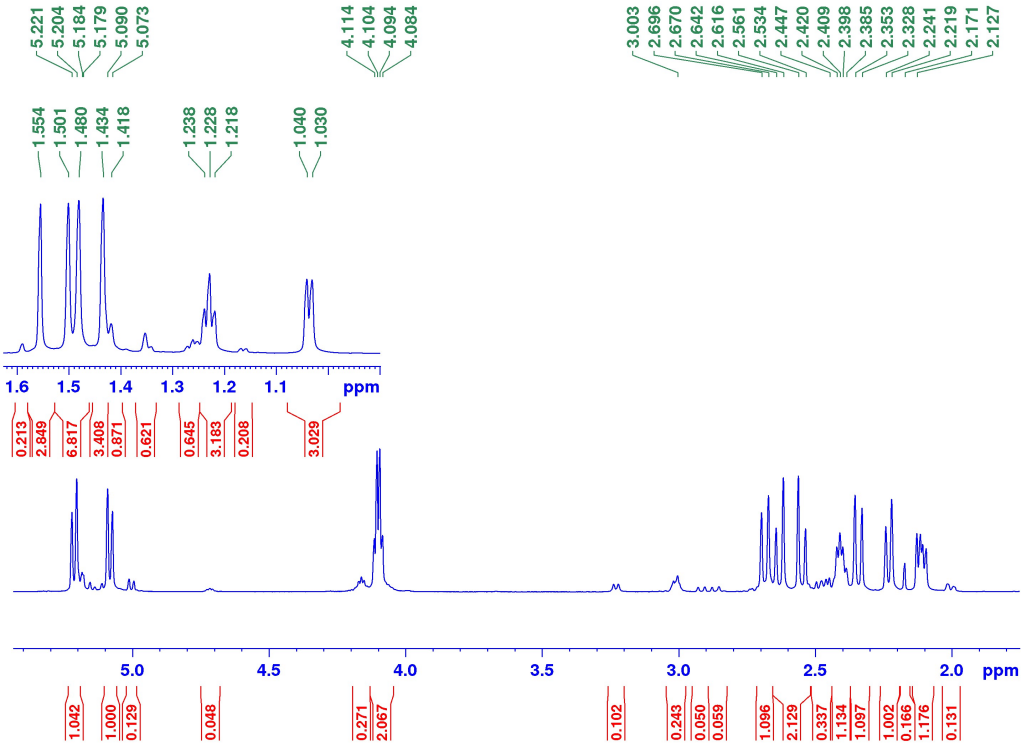

Figure C-25. ^{1}H NMR of (700 MHz, $CDCl_3$) spectrum of 82 (JBL710coltub86).

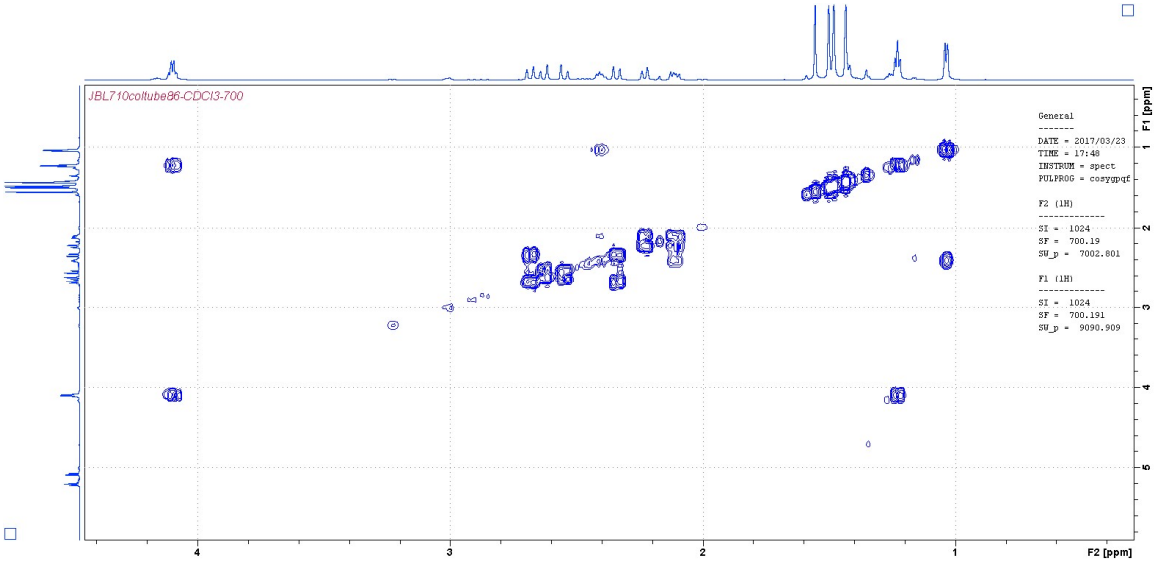

Figure C-26. 2-D ^{1}H—^{1}H COSY of (700 MHz, $CDCl_3$) spectrum of 82 (JBL710coltub86).

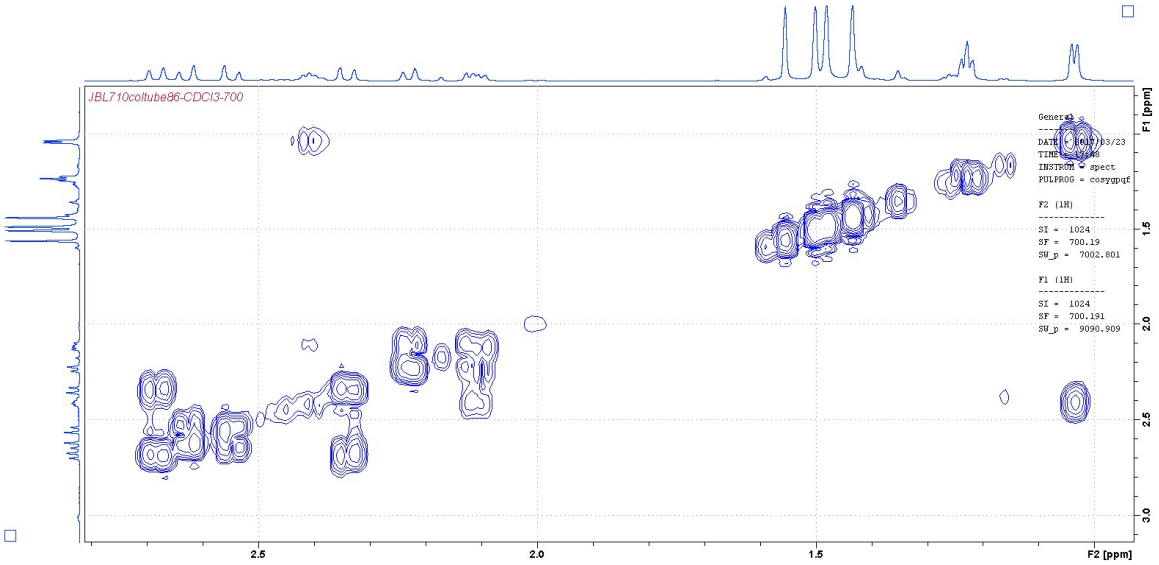

Figure C-27. 2-D ^{1}H—^{1}H COSY of (700 MHz, $CDCl_3$) spectrum of 82 (JBL710coltub86).

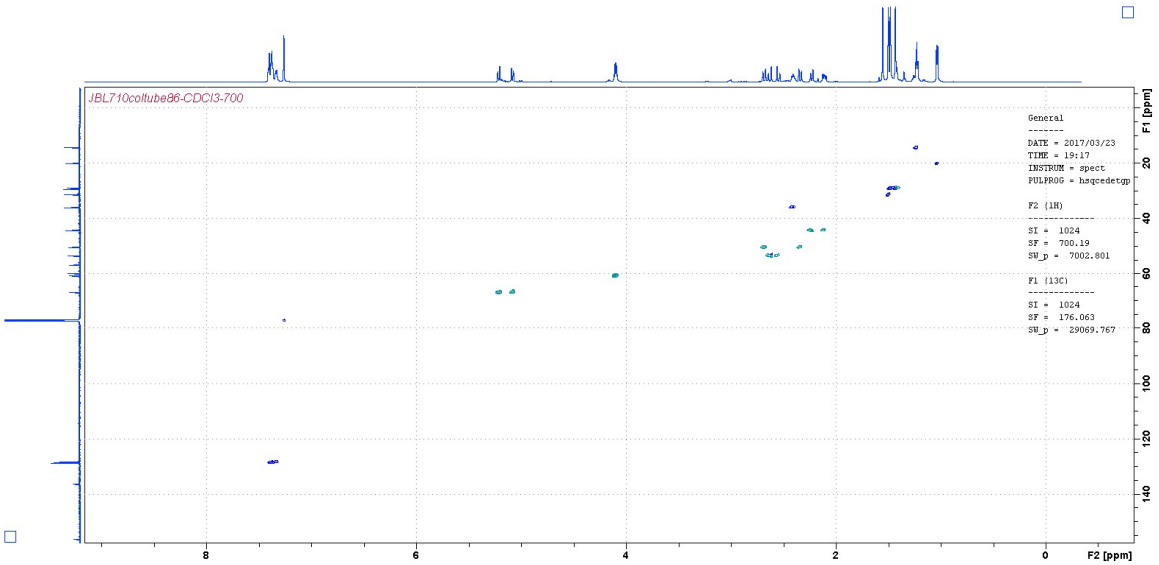

Figure C-28. 2-D ^{1}H—^{13}C HSQC of (700 MHz, $CDCl_3$) spectrum of 82 (JBL710coltub86).

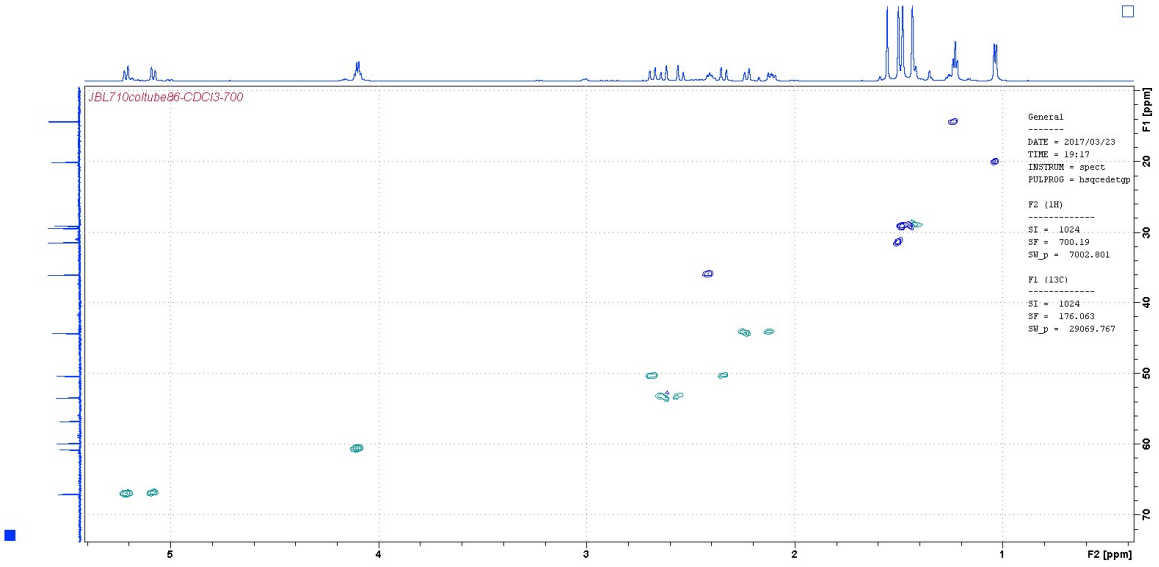

Figure C-29. 2-D ^{1}H—^{13}C HSQC of (700 MHz, $CDCl_3$) spectrum of 82 (JBL710coltub86).

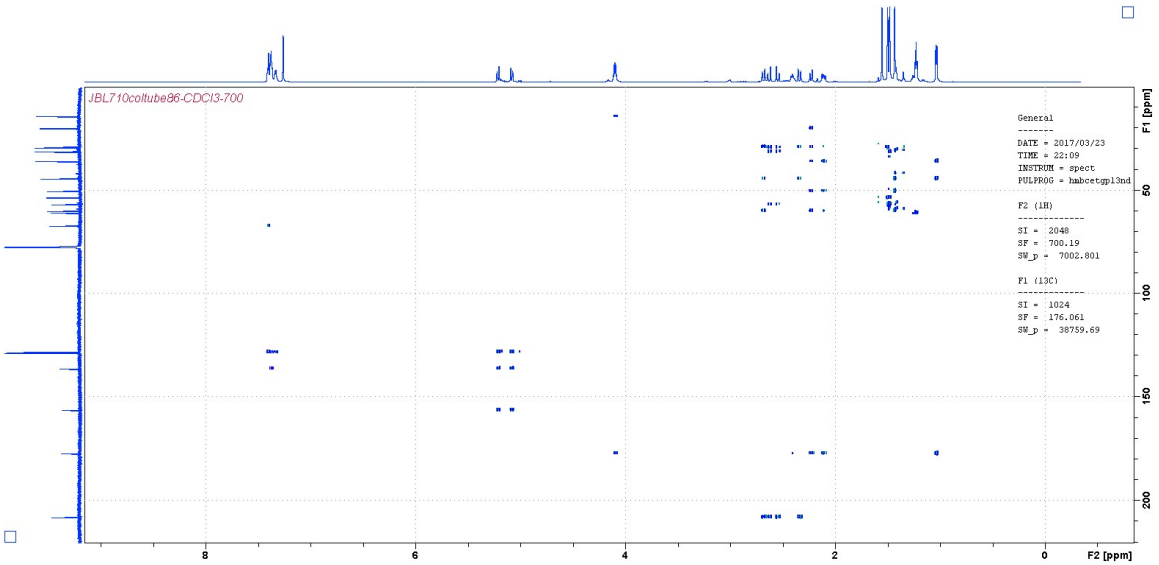

Figure C-30. 2-D ^{1}H—^{13}C HMBC of (700 MHz, $CDCl_3$) spectrum of 82 (JBL710coltub86).

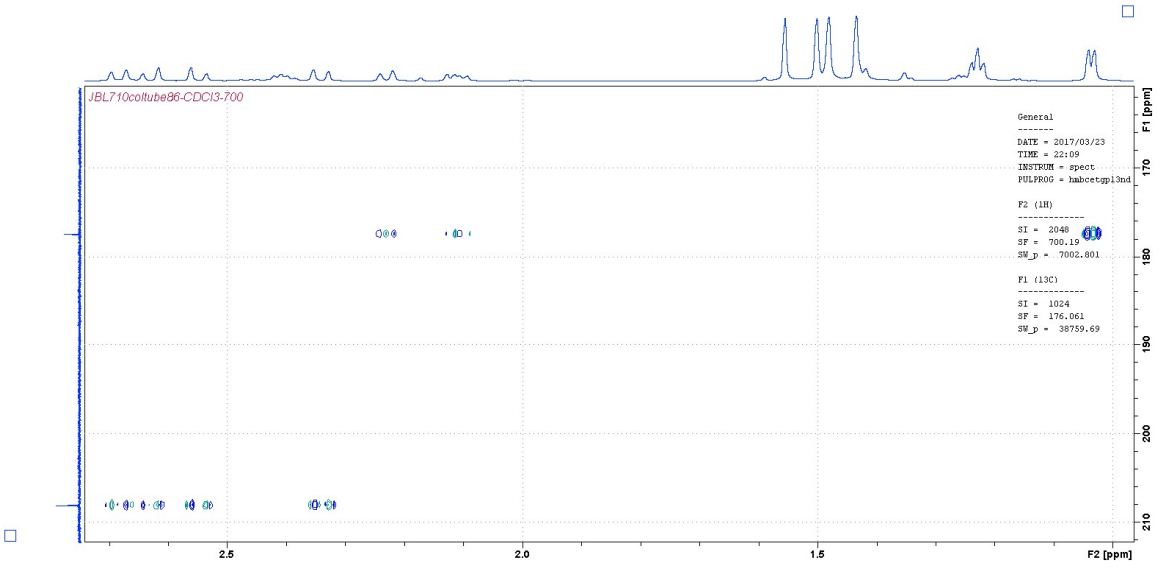

Figure C-31. 2-D ^{1}H—^{13}C HMBC of (700 MHz, $CDCl_3$) spectrum of 82 (JBL710coltub86).

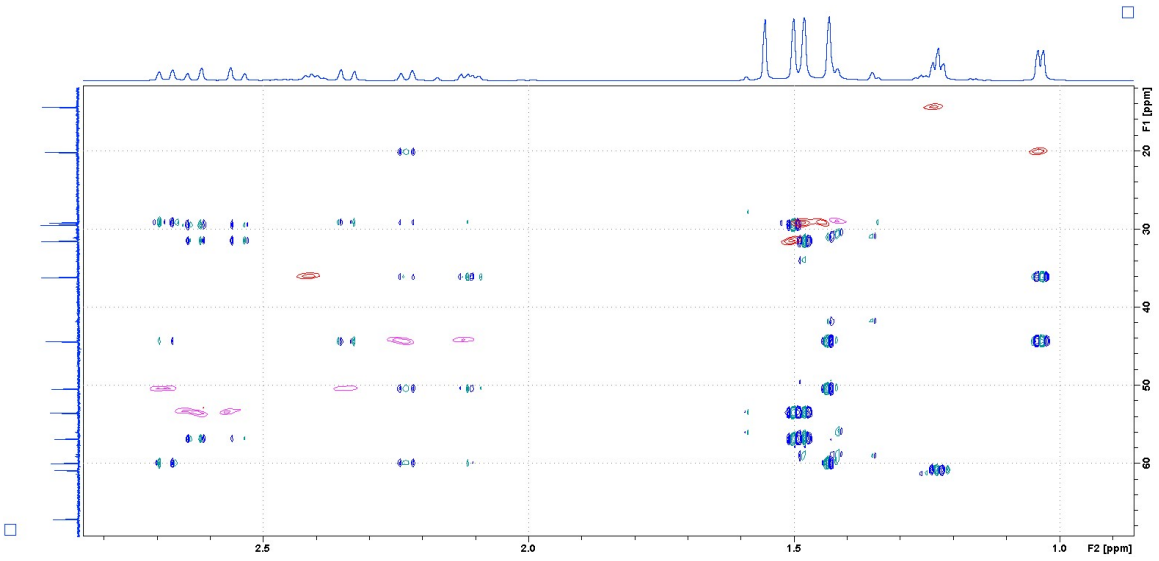

Figure C-32. 2-D ^{1}H—^{13}C HSQC and HMBC of (700 MHz, $CDCl_3$) spectrum of 82 (JBL710coltub86).

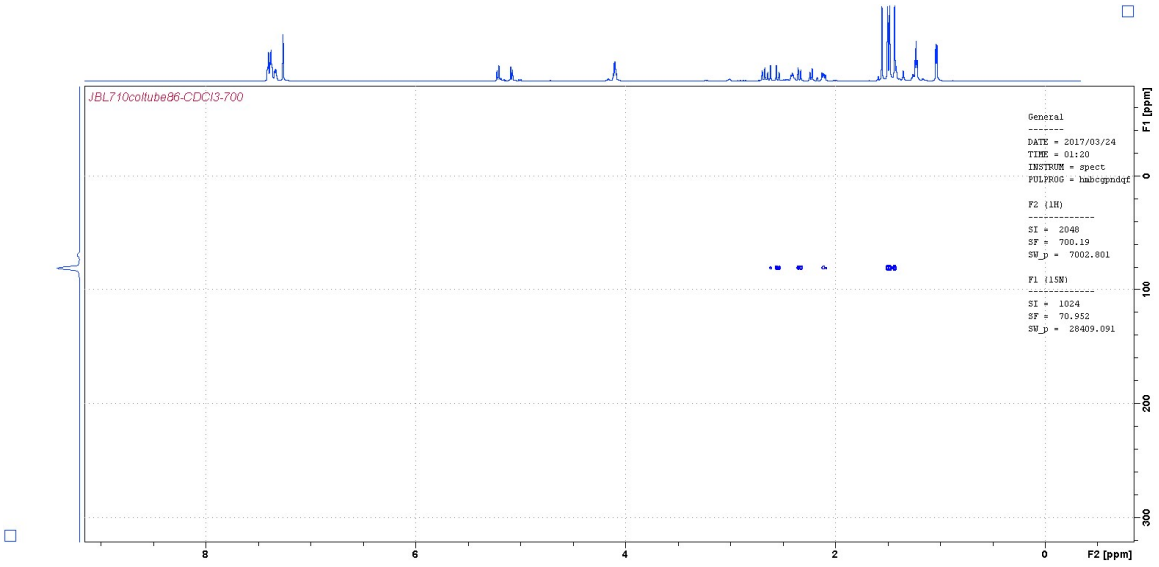

Figure C-33. 2-D ^{1}H—^{15}N HSQC of (700 MHz, $CDCl_3$) spectrum of 82 (JBL710coltub86).

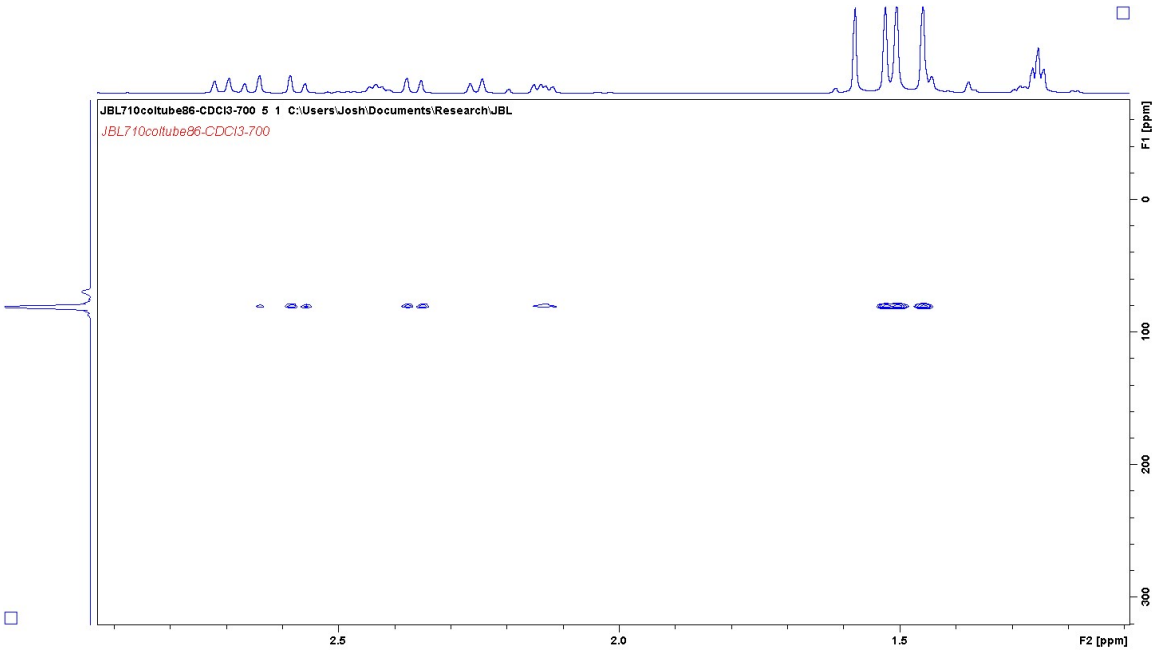

Figure C-34. 2-D ^{1}H—^{15}N HSQC of (700 MHz, $CDCl_3$) spectrum of 82 (JBL710coltub86).

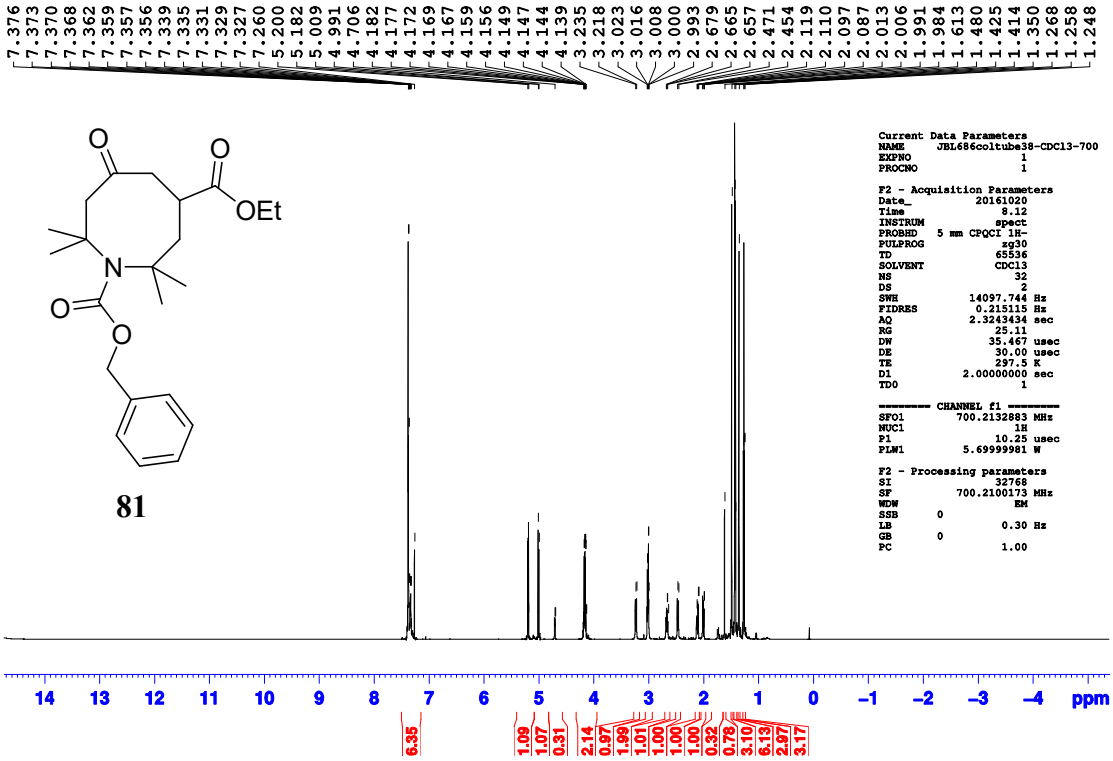

Figure C-35. ^{1}H NMR of (700 MHz, $CDCl_3$) spectrum of 81 (JBL686coltub38).

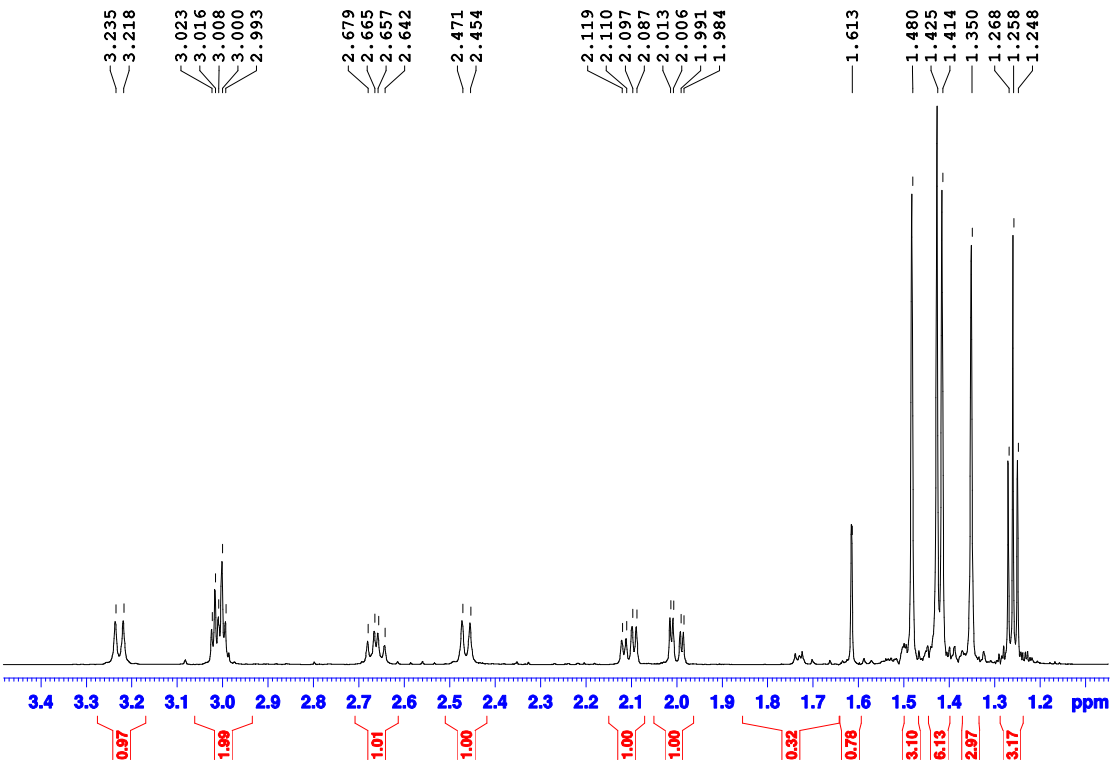

Figure C-36. ^{1}H NMR of (700 MHz, $CDCl_3$) spectrum of 81 (JBL686coltub38).

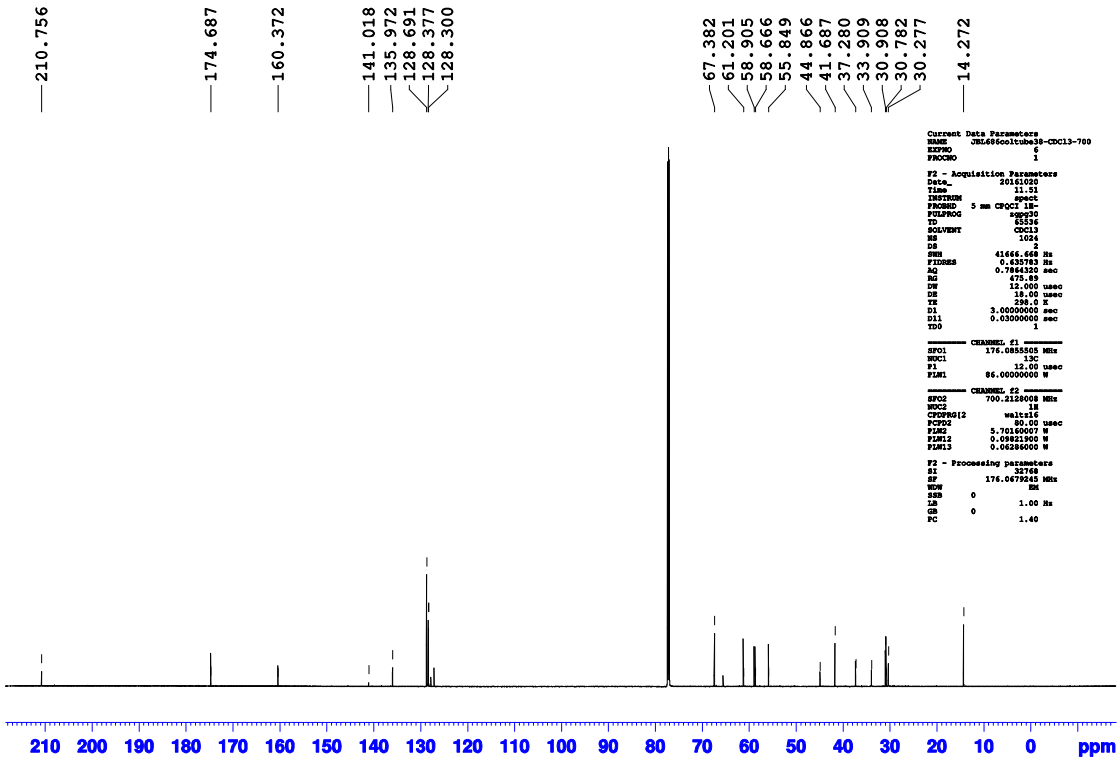

Figure C-37. ^{13}C NMR of (700 MHz, $CDCl_3$) spectrum of 81 (JBL686coltub38).

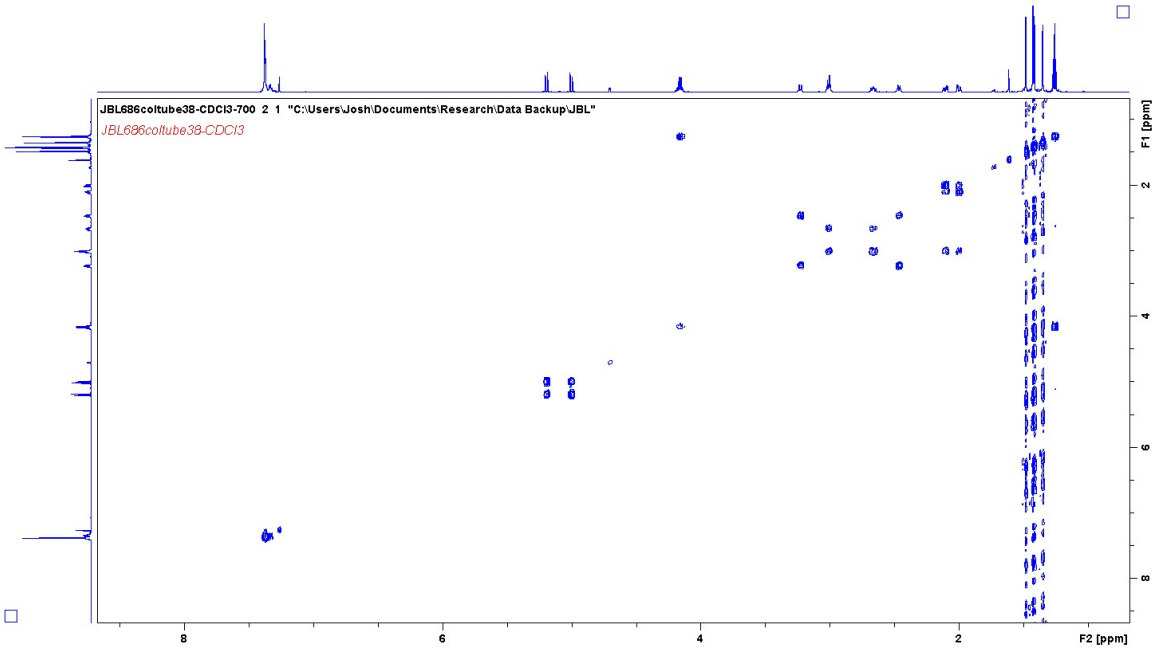

Figure C-38. ^{1}H NMR of (700 MHz, $CDCl_3$) spectrum of 81 (JBL686coltub38).

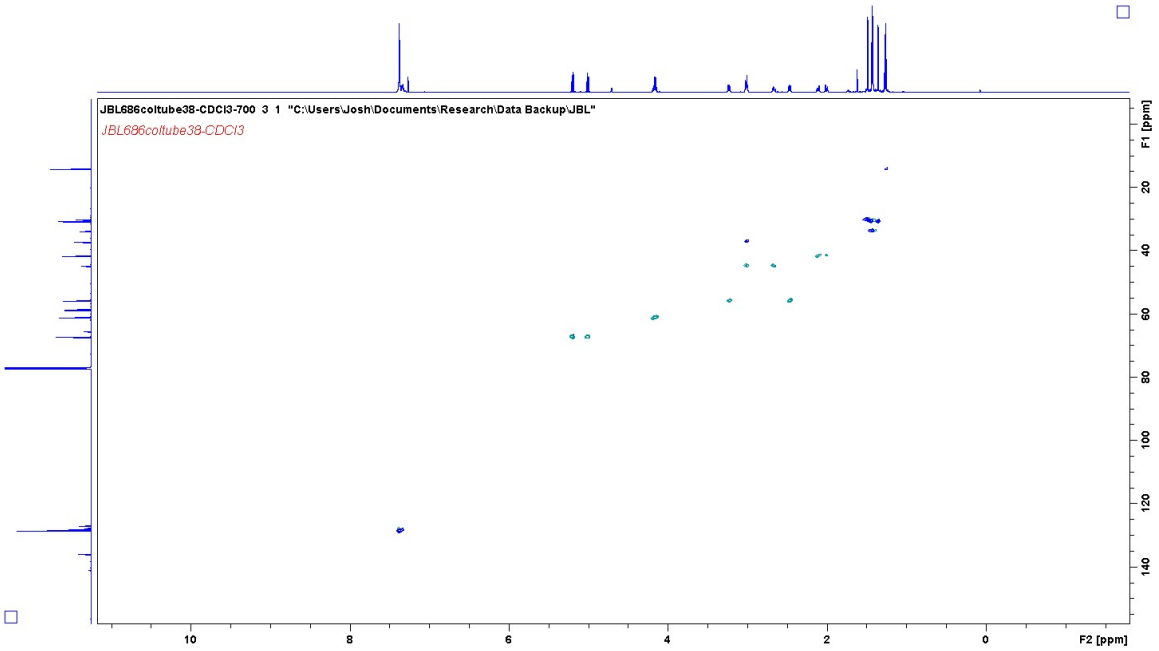

Figure C-39. 2-D ^{1}H—^{13}C HSQC of (700 MHz, $CDCl_3$) spectrum of 81 (JBL686coltub38).

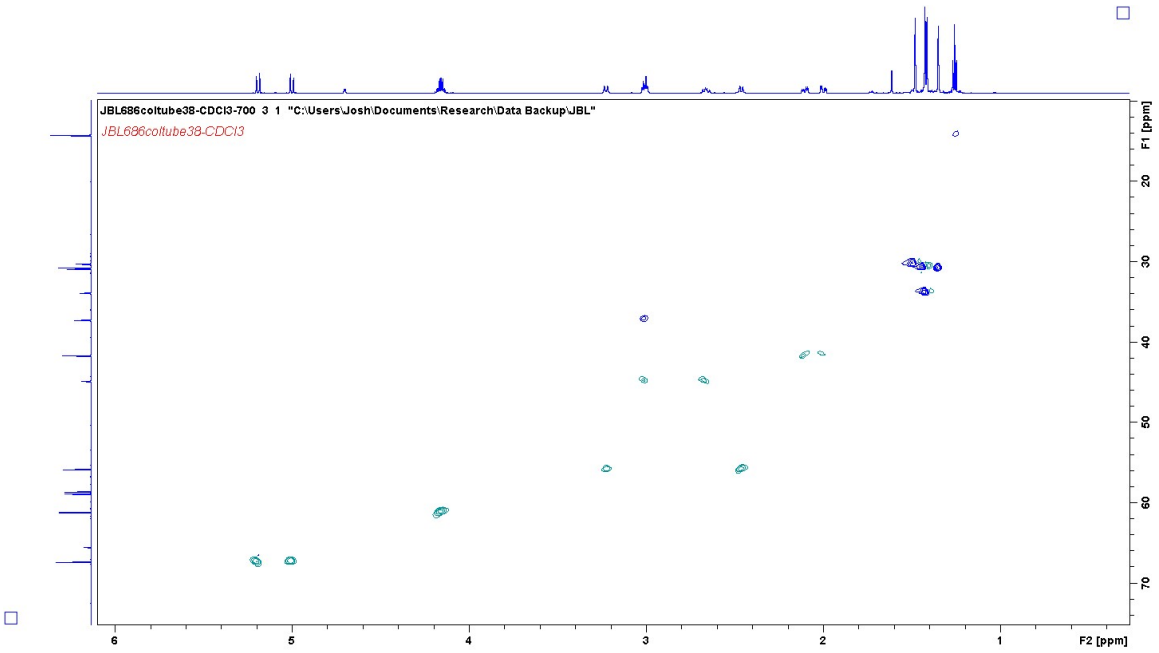

Figure C-40. 2-D ^{1}H—^{13}C HSQC of (700 MHz, $CDCl_3$) spectrum of 81 (JBL686coltub38).

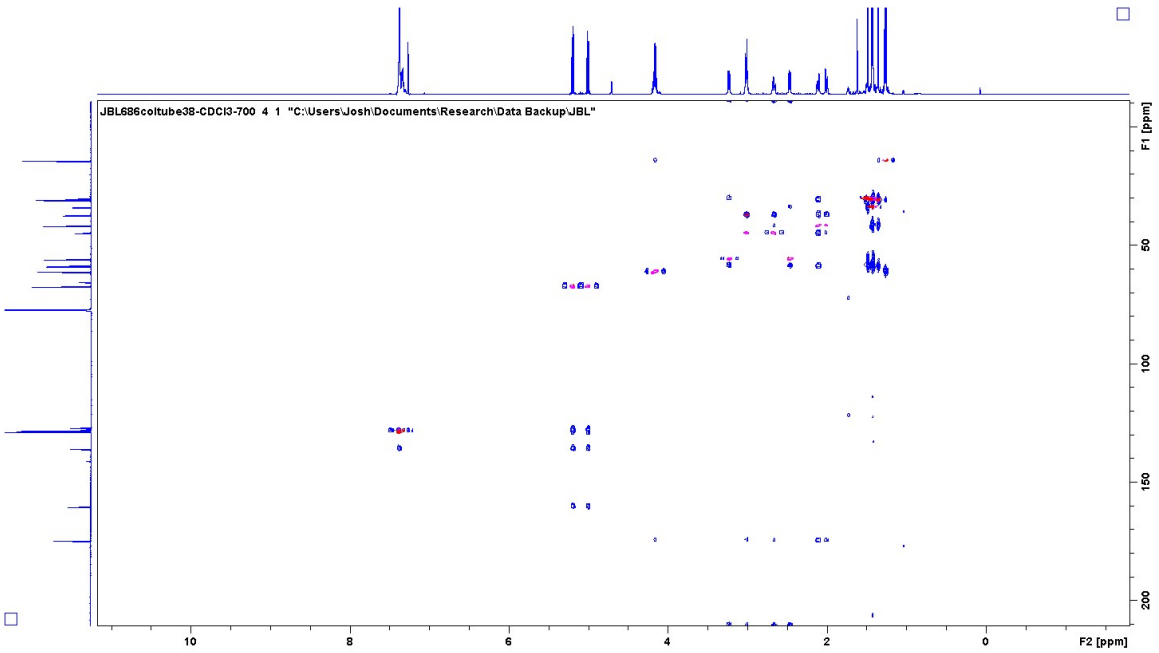

Figure C-41. 2-D ^{1}H—^{13}C HSQC and HMBC of (700 MHz, $CDCl_3$) spectrum of 81 (JBL686coltub38).

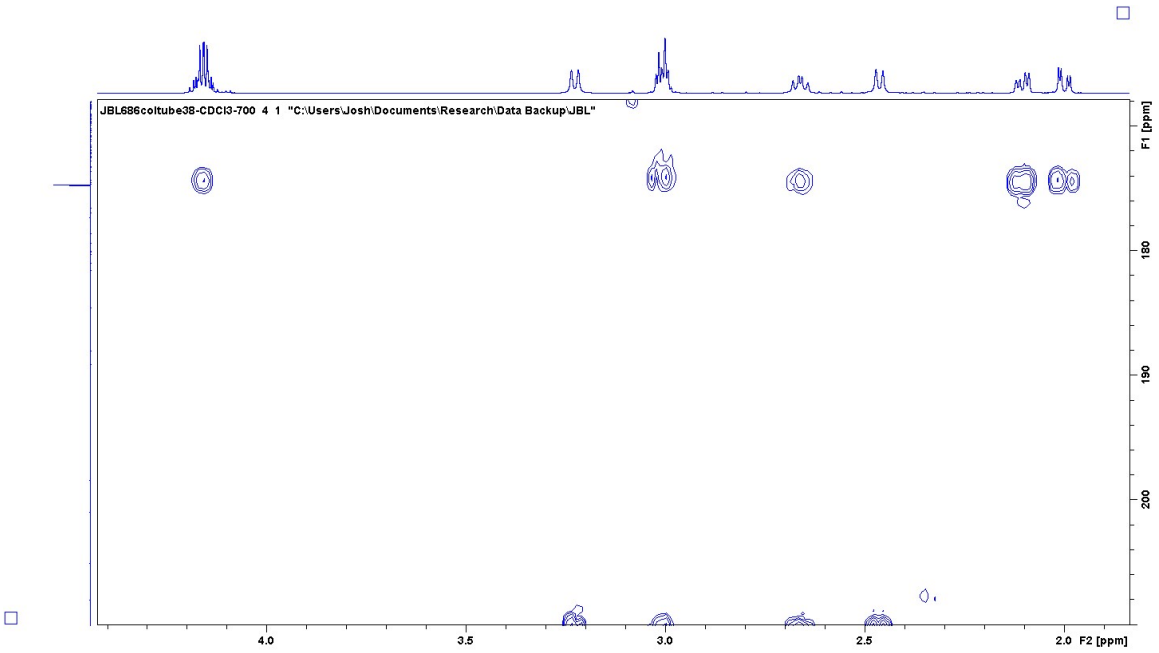

Figure C-42. 2-D ^{1}H—^{13}C HMBC of (700 MHz, $CDCl_3$) spectrum of 81 (JBL686coltub38).

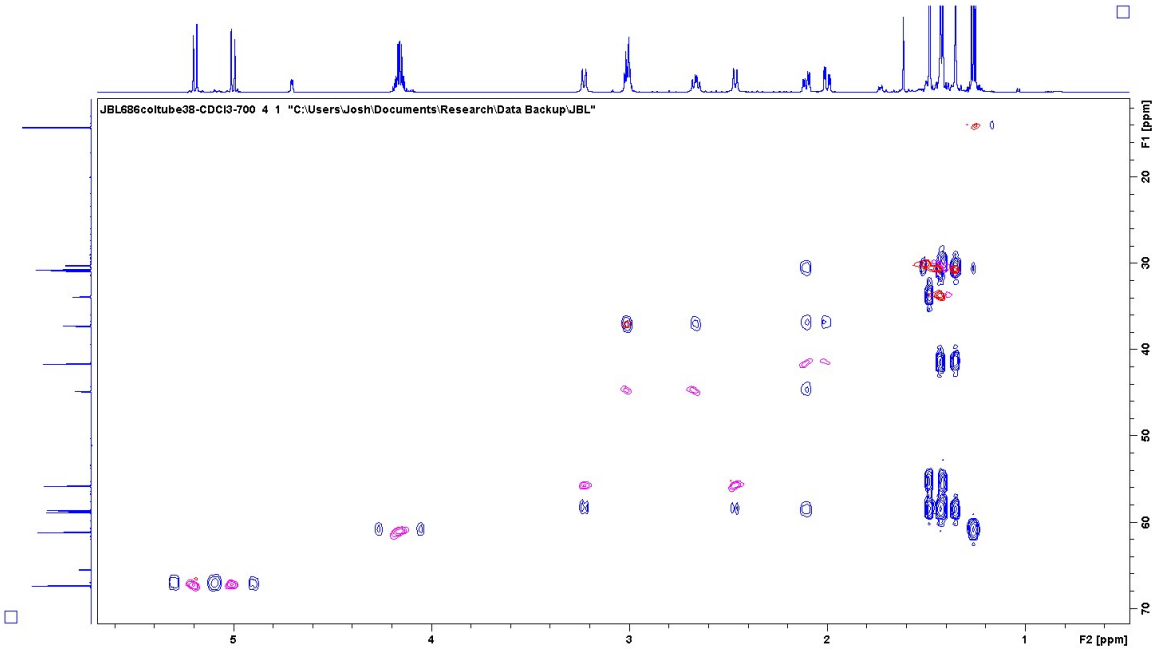

Figure C-43. 2-D ^{1}H—^{13}C HSQC and HMBC of (700 MHz, $CDCl_3$) spectrum of 81 (JBL686coltub38).

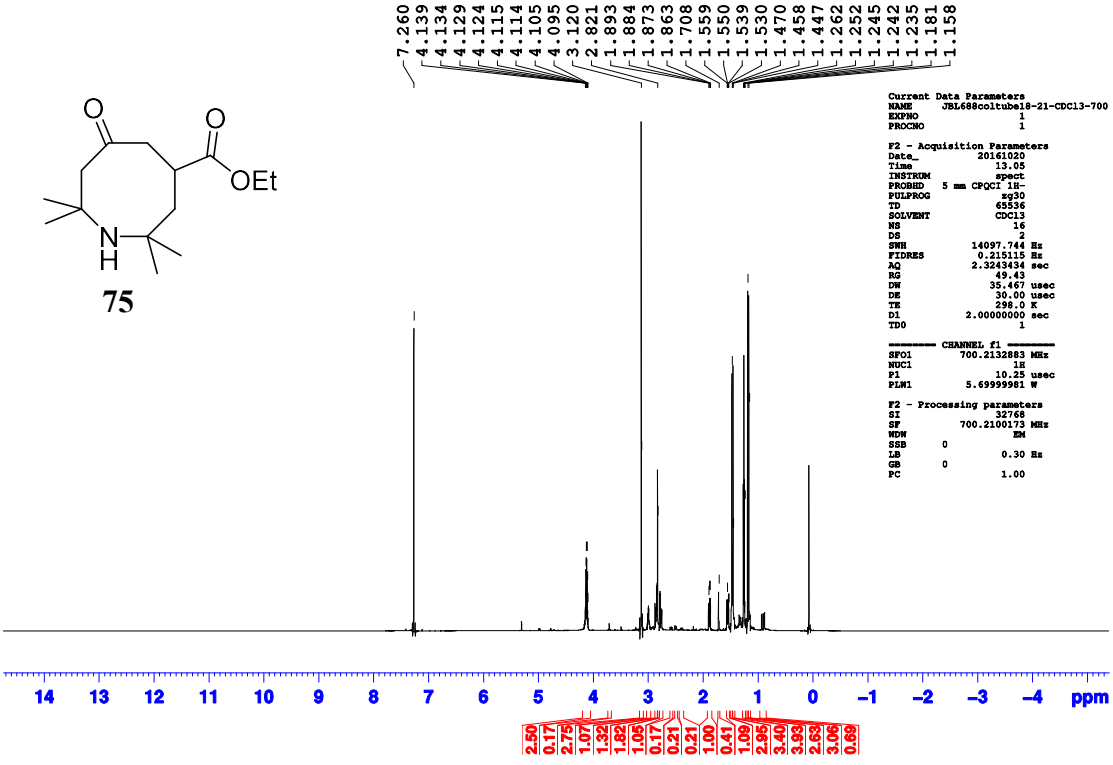

Figure C-44. ^{1}H NMR of (700 MHz, $CDCl_3$) spectrum of 75 (JBL688coltub18-21).

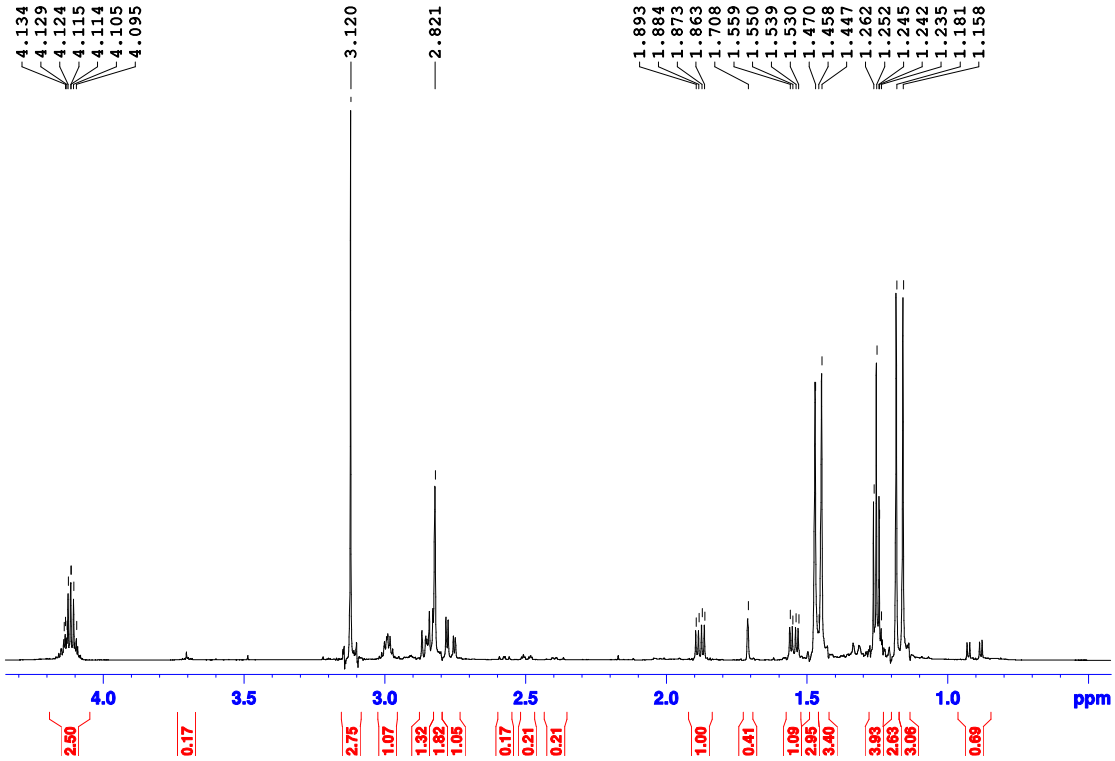

Figure C-45. ^{1}H NMR of (700 MHz, $CDCl_3$) spectrum of 75 (JBL688coltub18-21).

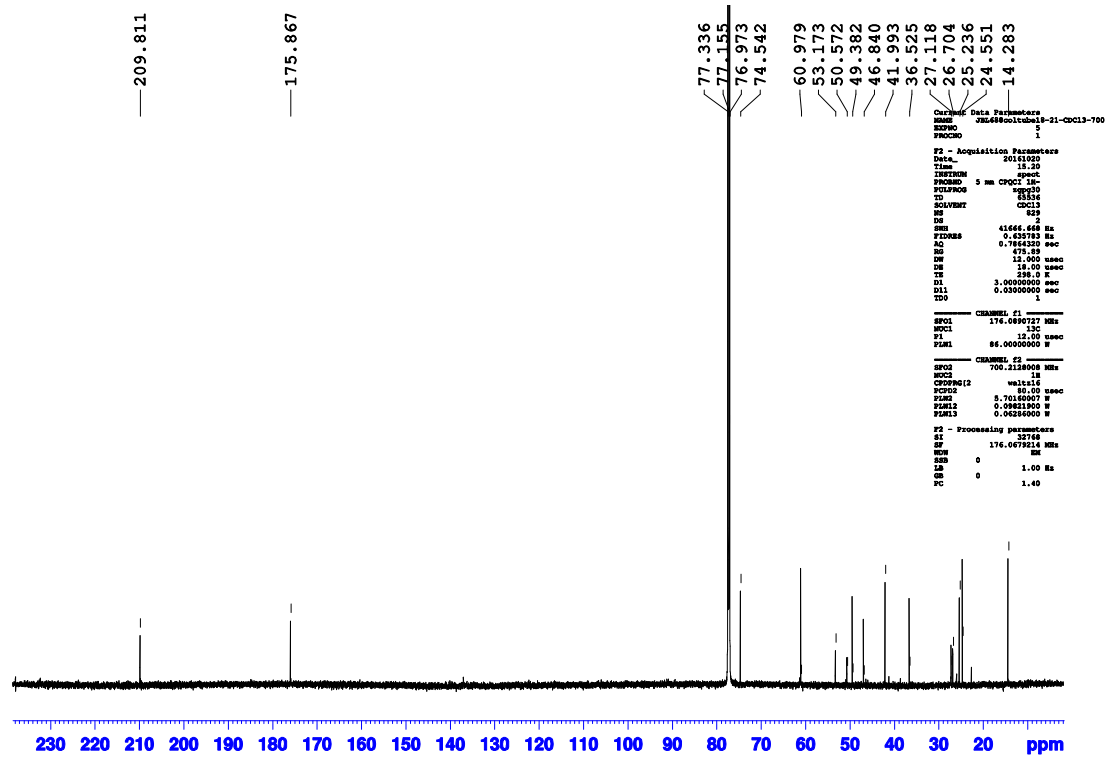

Figure C-46. ^{13}C NMR of (700 MHz, $CDCl_3$) spectrum of 75 (JBL688coltub18-21).

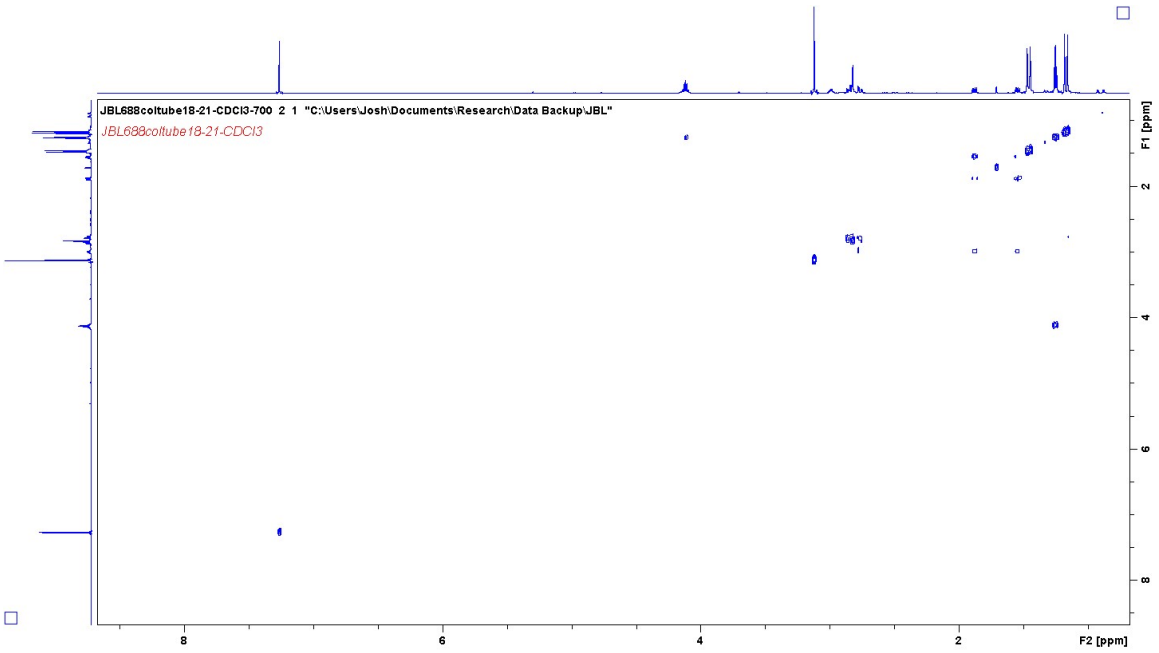

Figure C-47. ^{1}H NMR of (700 MHz, $CDCl_3$) spectrum of 75 (JBL688coltub18-21).

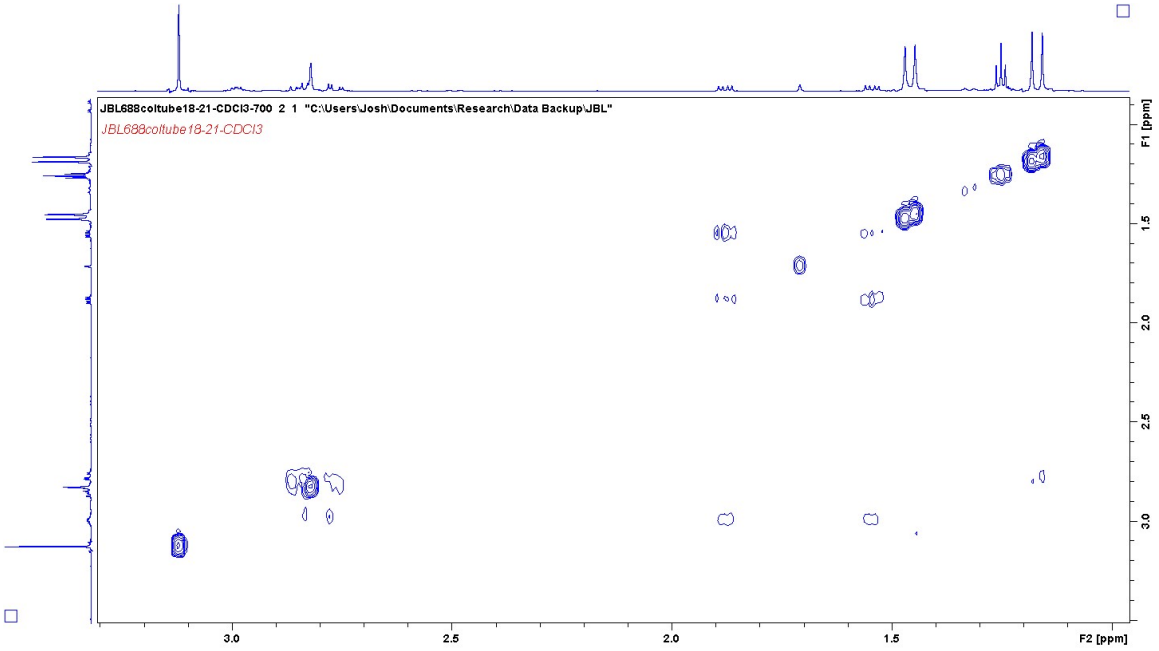

Figure C-48. ^{1}H NMR of (700 MHz, $CDCl_3$) spectrum of 75 (JBL688coltub18-21).

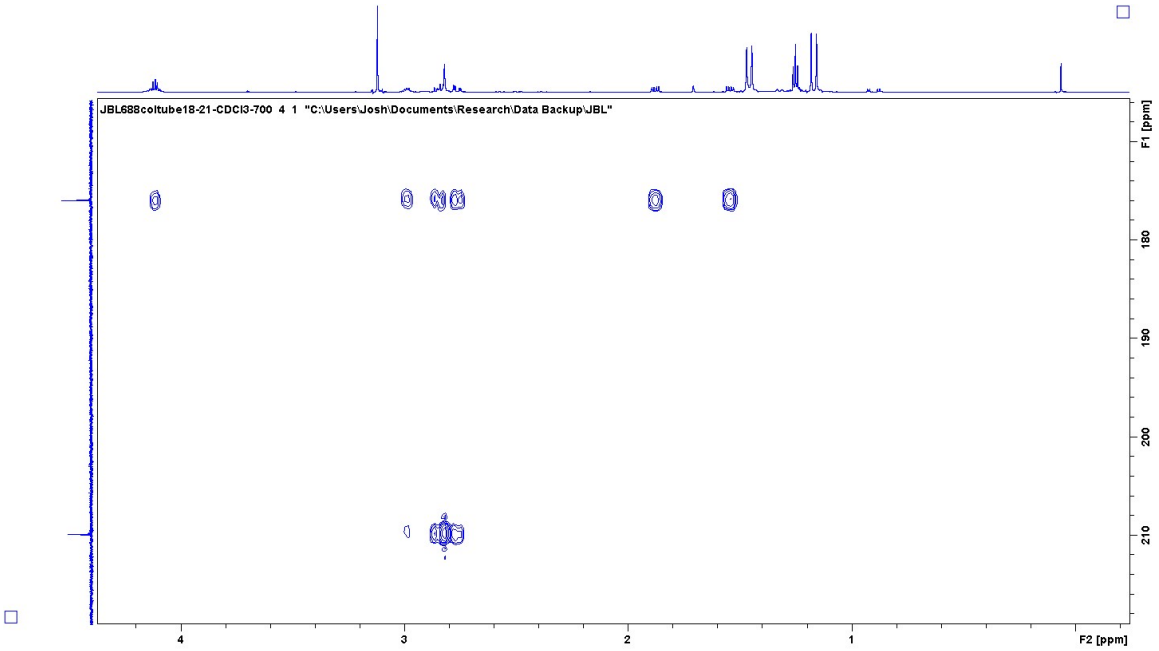

Figure C-49. 2-D ^{1}H—^{13}C HMBC of (700 MHz, $CDCl_3$) spectrum of 75 (JBL688coltub18-21).

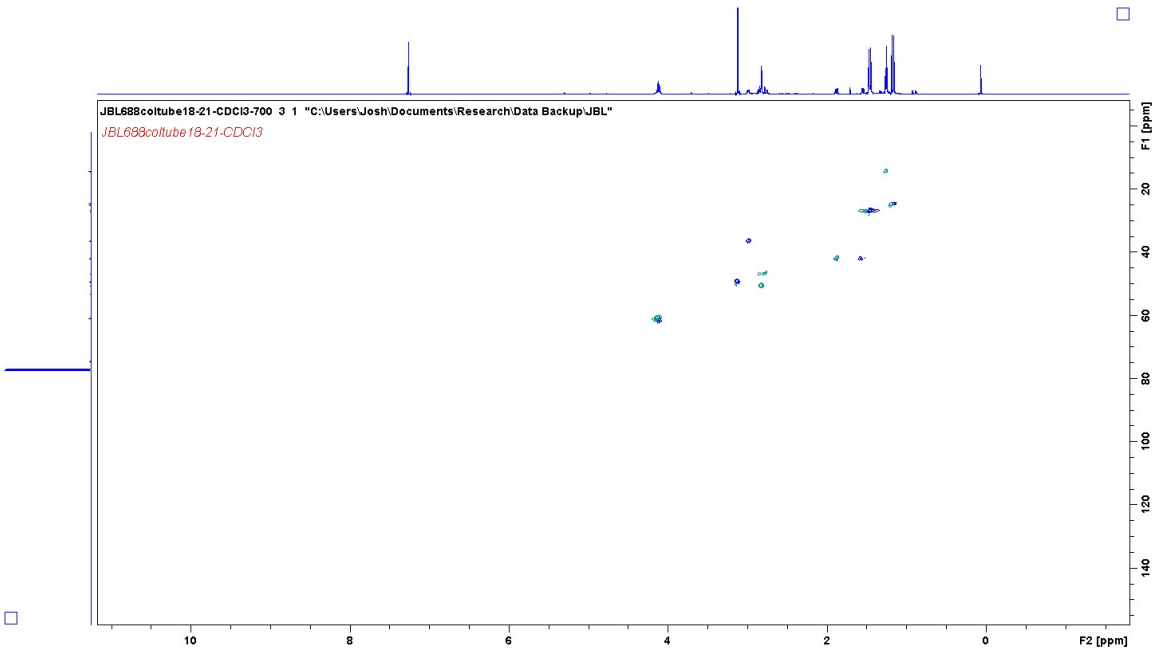

Figure C-50. 2-D ^{1}H—^{13}C HSQC of (700 MHz, $CDCl_3$) spectrum of 75 (JBL688coltub18-21).

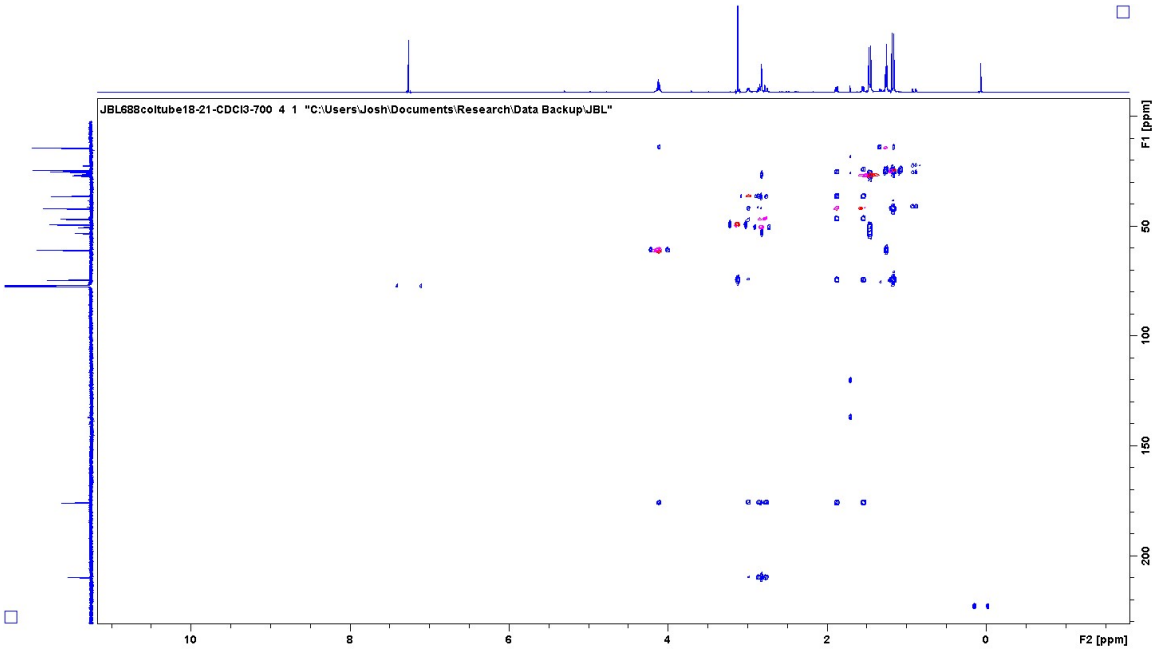

Figure C-51. 2-D ^{1}H—^{13}C HSQC and HMBC of (700 MHz, $CDCl_3$) spectrum of 75 (JBL688coltub18-21).

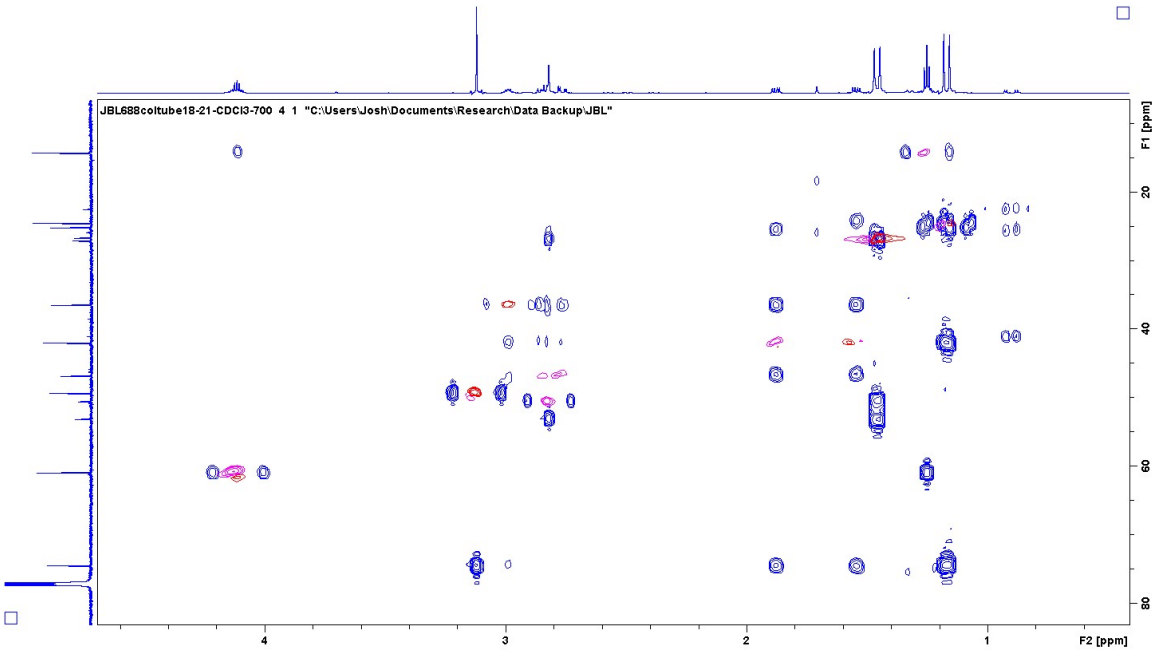

Figure C-52. 2-D ^{1}H—^{13}C HSQC and HMBC of (700 MHz, $CDCl_3$) spectrum of 75 (JBL688coltub18-21).

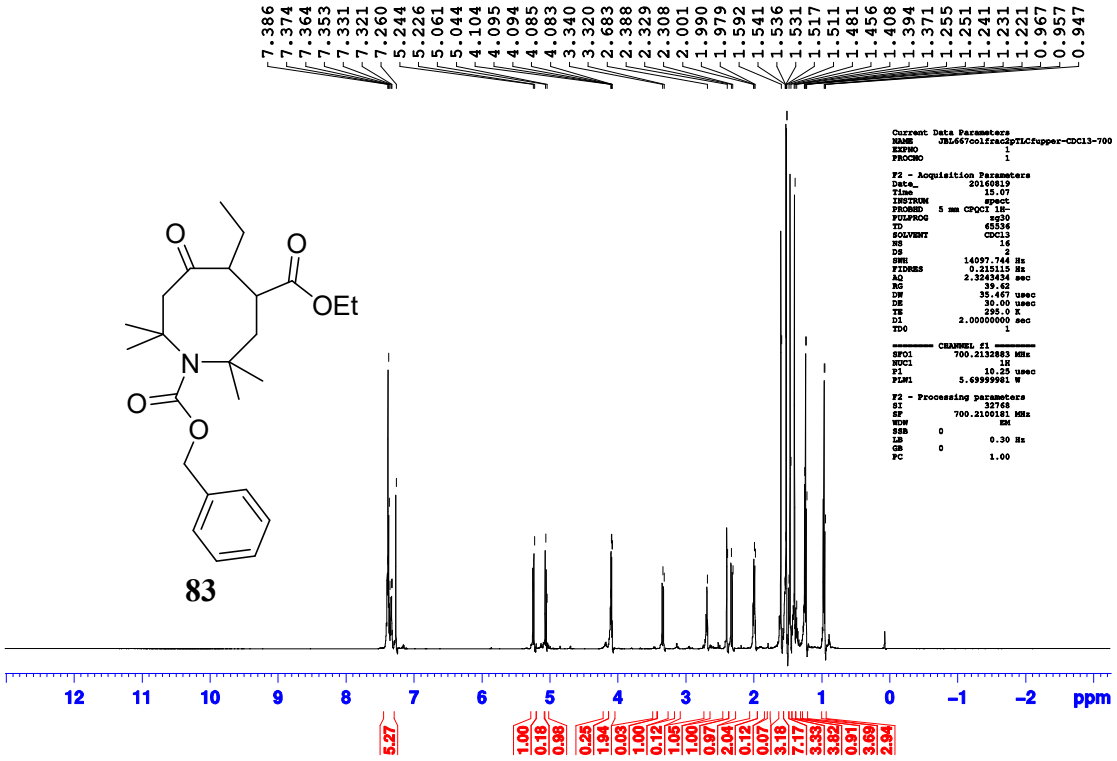

Figure C-53. ^{1}H NMR of (700 MHz, $CDCl_3$) spectrum of 83 (JBL667cf2pTLCup).

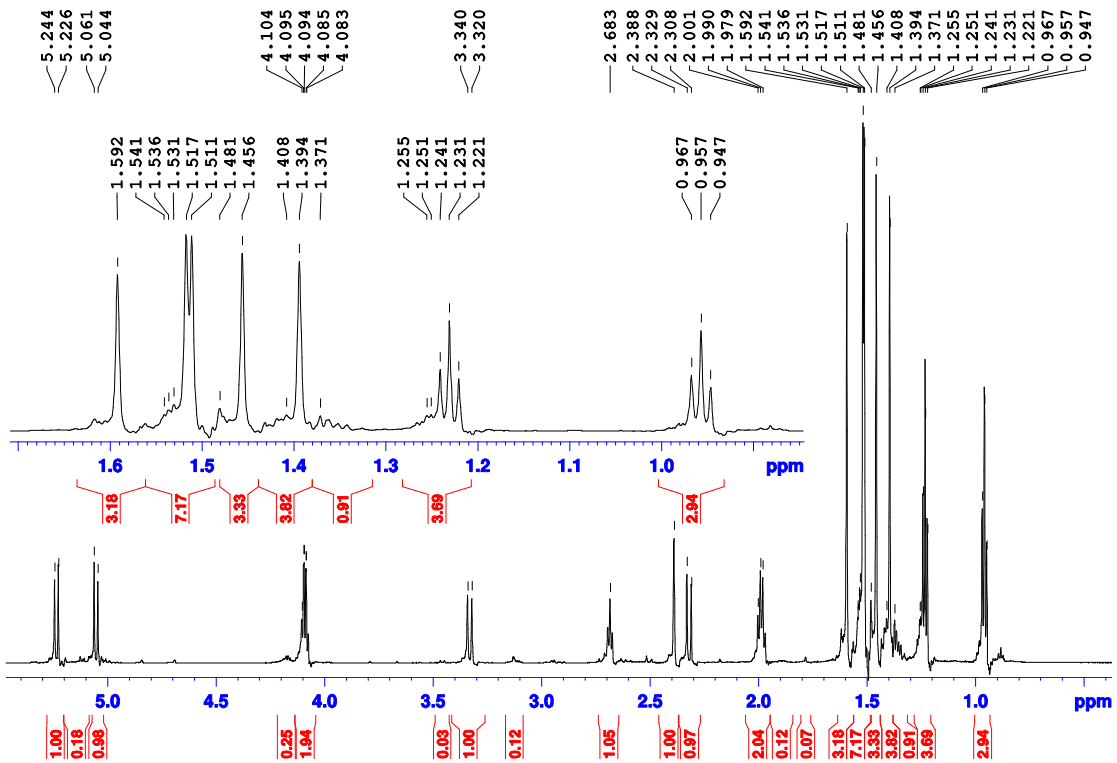

Figure C-54. ^{1}H NMR of (700 MHz, $CDCl_3$) spectrum of 83 (JBL667cf2pTLCup).

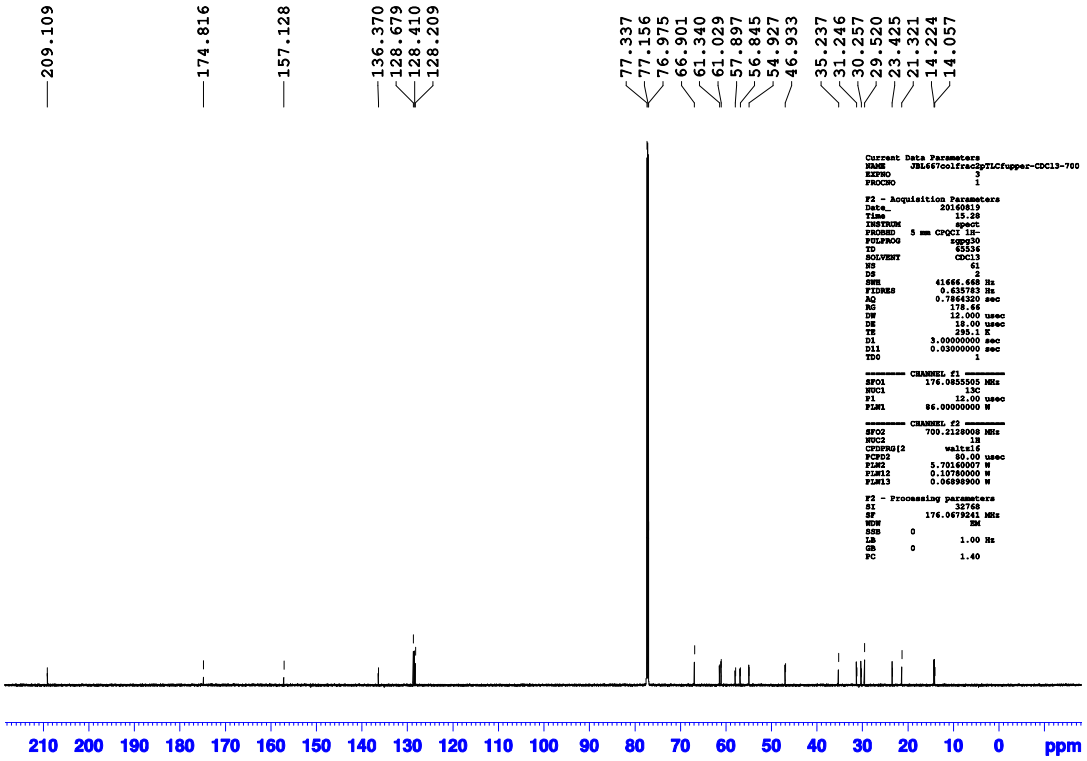

Figure C-55. ^{13}C NMR of (700 MHz, $CDCl_3$) spectrum of 83 (JBL667cf2pTLCup).

Figure C-56. 2-D ^{1}H—^{13}C HSQC of (700 MHz, $CDCl_3$) spectrum of 83 (JBL667cf2pTLCup).

Figure C-57. 2-D ^{1}H—^{13}C HSQC of (700 MHz, $CDCl_3$) spectrum of 83 (JBL667cf2pTLCup).

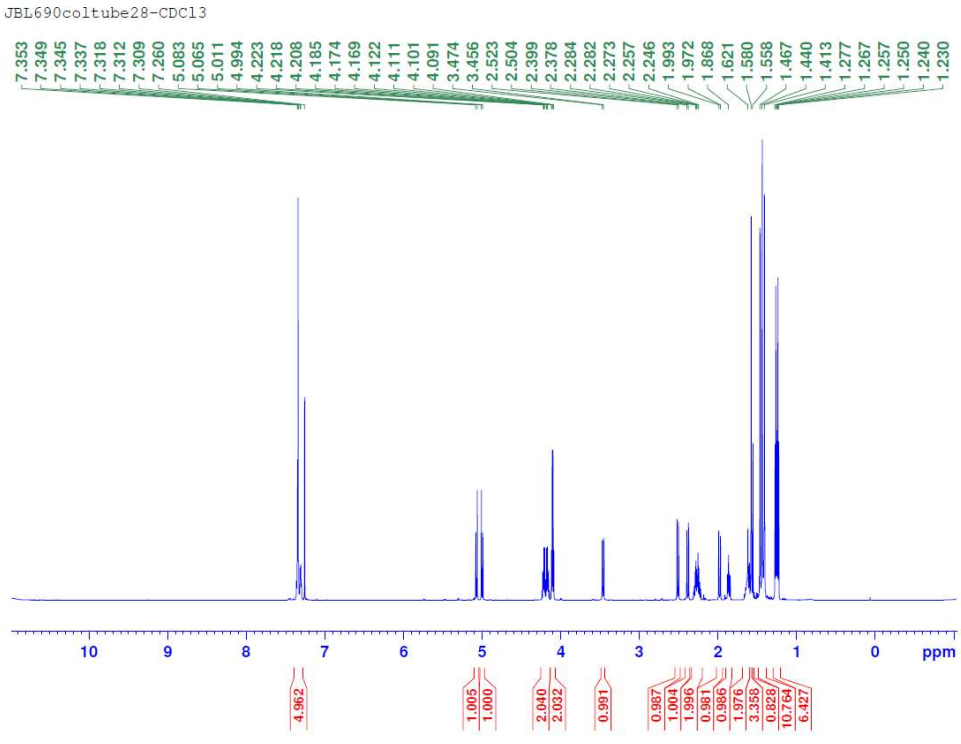

Figure C-58. ^{1}H NMR of (700 MHz, $CDCl_3$) spectrum of 85 (JBL690coltub28).

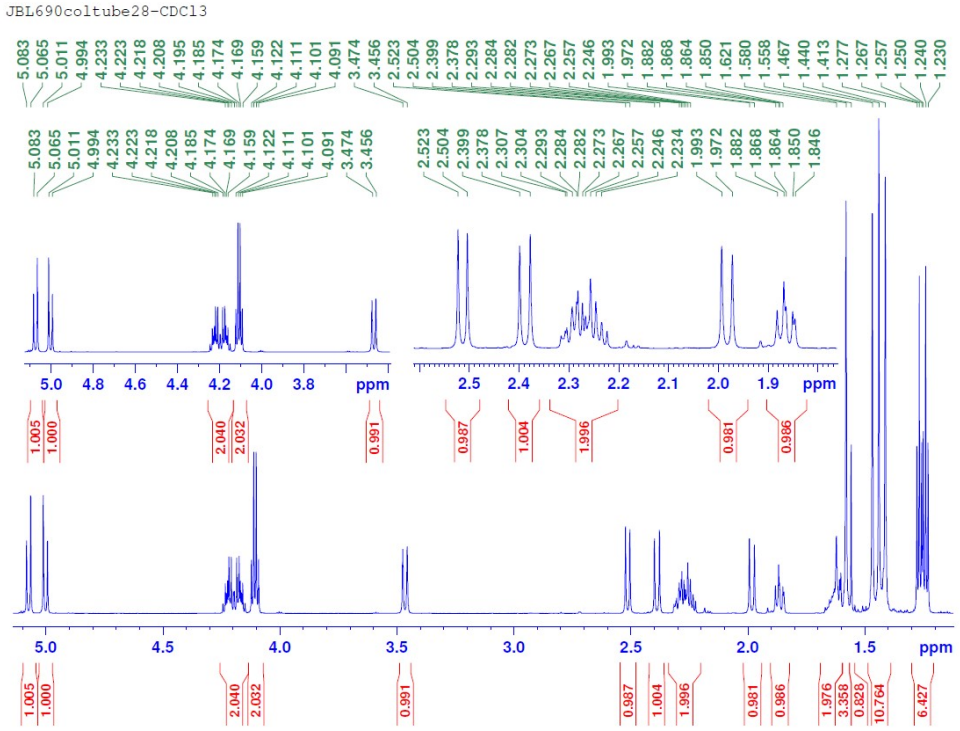

Figure C-59. ^{1}H NMR of (700 MHz, $CDCl_3$) spectrum of 85 (JBL690coltub28).

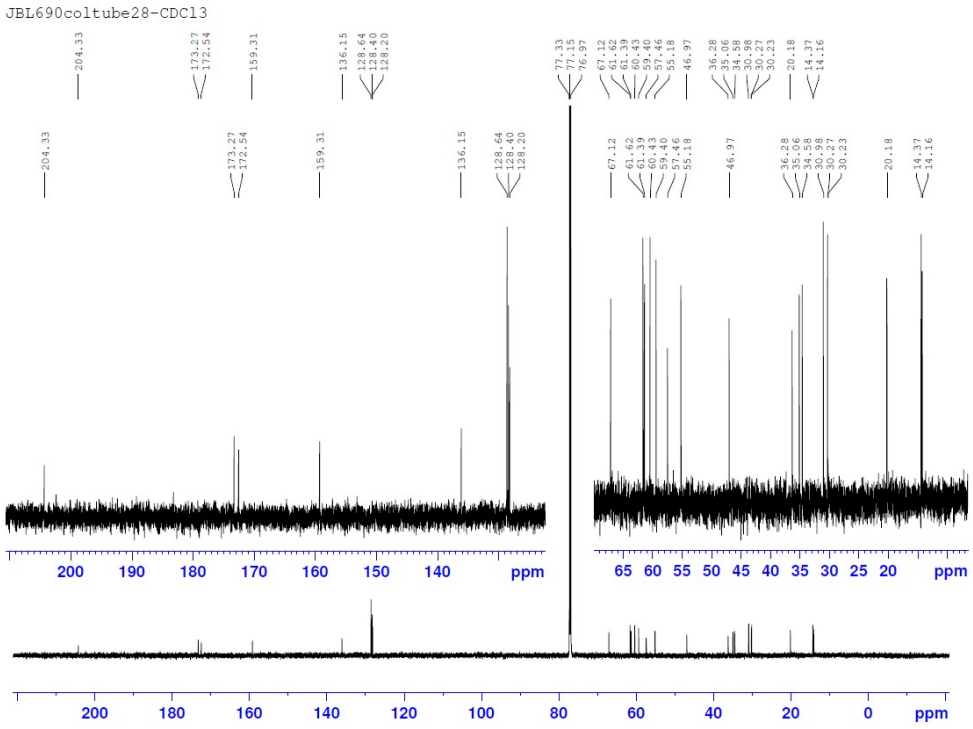

Figure C-60. ^{13}C NMR of (700 MHz, $CDCl_3$) spectrum of 85 (JBL690coltub28).

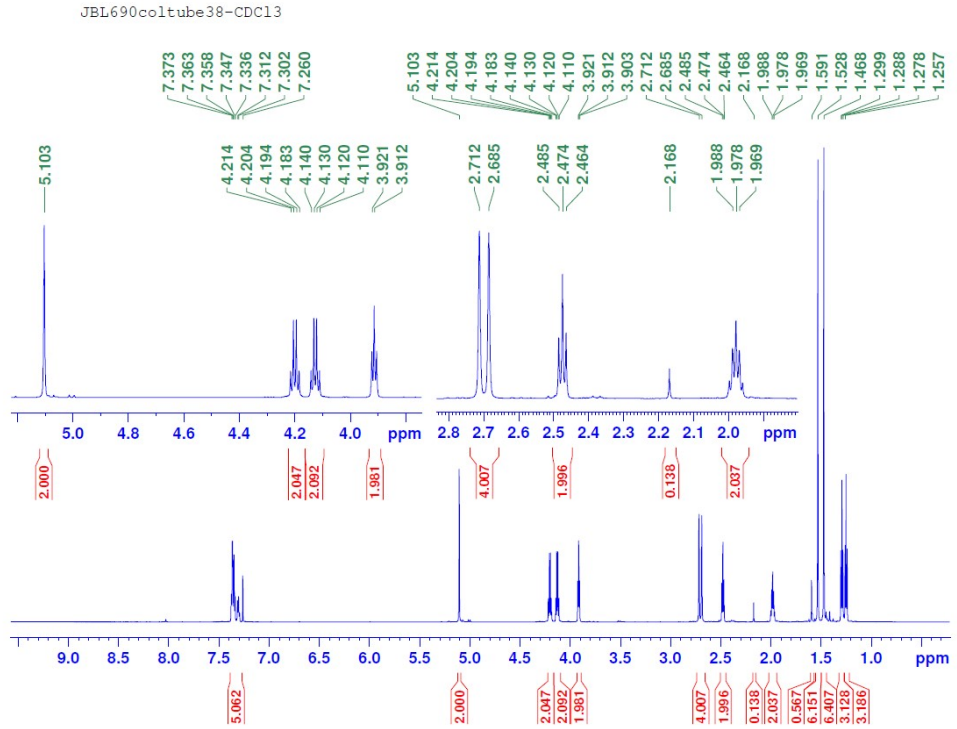

Figure C-61. ^{1}H NMR of (700 MHz, $CDCl_3$) spectrum (JBL690coltub38).

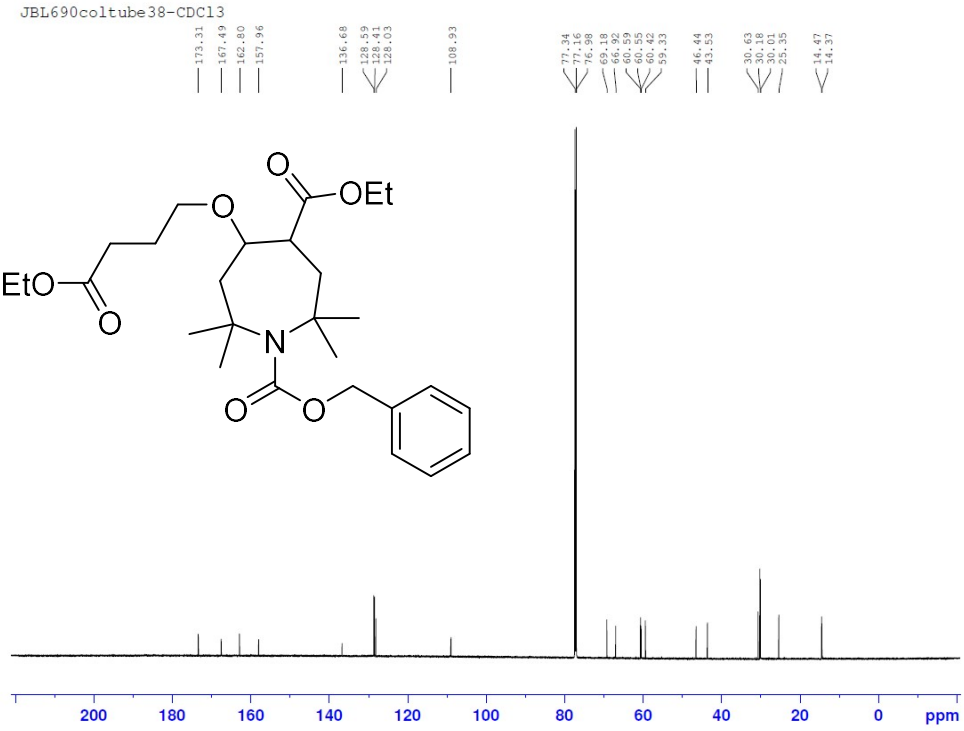

Figure C-62. ^{1}H NMR of (700 MHz, $CDCl_3$) spectrum (JBL690coltub38).